

Some pages of this thesis may have been removed for copyright restrictions.

If you have discovered material in Aston Research Explorer which is unlawful e.g. breaches copyright, (either yours or that of a third party) or any other law, including but not limited to those relating to patent, trademark, confidentiality, data protection, obscenity, defamation, libel, then please read our [Takedown policy](#) and contact the service immediately (openaccess@aston.ac.uk)

THE ROLE OF PROTEIN OXIDATION IN AGEING & DISEASE

SABAH PASHA

Doctor of Philosophy

ASTON UNIVERSITY

Sept 2015

© Sabah Pasha, 2015

Sabah Pasha asserts her moral right to be identified as the author of this thesis

The copy of the thesis has been supplied on condition that anyone who consults it is understood to recognise that its copyright rests with its author and that no quotation from the thesis and no information derived from it may be published without appropriate permission or acknowledgement.

Thesis summary

Ageing is a natural phenomenon of the human lifecycle, yet it is still not understood what causes the deterioration of the human body near the end of the lifespan. One popular theory is the Free Radical Theory of Ageing, which proposes that oxidative damage to biomolecules causes ageing of tissues. The ageing population is affected by many chronic diseases. This study focused on sarcopenia (muscle loss in ageing) and obesity as two models for comparison of oxidative damage in muscle proteins in mice. The aim of the study was to develop advanced mass spectrometry methods to detect specific oxidative modifications to mouse muscle proteins, including oxidation, nitration, chlorination, and carbonyl group formation, but western blotting was also used to provide complementary information on the oxidative state of proteins from aged and obese muscle. Mass spectrometry proved to be a powerful tool, enabling identification of the types of modifications present, the sites at which they were present and percentage of the peptide populations that were modified. Targeted and semi-targeted mass spectrometry methods were optimised for the identification and quantitation of the oxidised residues in muscle proteins. The development of the quantitative methods enabled comparisons of mass spectrometry instruments. Both the Time of Flight and QTRAP systems showed advantages of using the different mass analysers to quantify oxidative modifications. Several oxidised residues were characterised and quantified in both the obese and sarcopenic models, and higher levels of oxidation were found compared to their control counterparts. Residues found to be oxidised were oxidation of proline, tyrosine and tryptophan, dioxidation of methionine, allysine and nitration of tyrosine. However quantification was performed on methionine dioxidation and cysteine trioxidation containing residues in SERCA. The combination of measuring residue susceptibility and functional studies could contribute to understanding the overall role of oxidation in ageing and obesity.

Key words: Mass Spectrometry (MS), Oxidative Post-Translational Modifications (OxPTMs), Muscle Proteomics, Sarcopenia, Obesity

Acknowledgements

I would first and foremost like to thank my supervisors Dr Corinne Spickett and Prof. Andrew Pitt for initially providing me the opportunity to do a PhD, their guidance through the PhD, their patience with me and the immeasurable amount of knowledge and advice they have imparted that has enabled me to grow into a slightly more confident researcher who has a new found love for the field.

The time spent with the group has helped me come out of my shell and become comfortable with taking positions of responsibility. I am very fortunate to have met everyone who had entered and departed from the group. I've met wonderful people during my PhD and wish them all the best in their future endeavours.

I would also like to point out two individuals who have taught me so much and given me lots of advice throughout my PhD. Thank you Dr Ana Reis for teaching me about mass spectrometry and the art of handling stressful situations. I would also like to thank Dr Karina Tveen Jensen who has supported my individuality, helped with troubleshooting and also supported me through the tough times. You both were amazing postdocs who showed me very different views of approaching life.

The courage to overcome the difficulties of juggling a job and writing a thesis was strengthened by my friends and colleagues at the University of Birmingham. Thank you to everyone who comforted me during the tough times but most of all, thank you to Dr Melissa Grant for being so understanding and helping me realise that I am more capable than I give myself credit for.

A special thank you to Prof. Malcolm Jackson and Dr Kasia Whysall from the University of Liverpool for kindly providing the gastrocnemius samples required for ageing study and Dr Steve Russell for allowing me to work with the muscle samples from the ob/ob mice in the obesity study.

And lastly, I would like to thank my family and friends for without their huge support I would not have been able to accomplish this feat. Thank you for everything and sorry for the hardships of dealing with my constant fear that I was never good enough but please know that I appreciated the guidance and reassurance that you all had provided.

Thank you.

Contents

Thesis summary	2
Acknowledgements	3
List of Abbreviations	6
List of figures	9
List of tables	12
General introduction	13
1.1. Ageing, inflammation and the skeletal muscle	14
1.2. How oxidants are produced in the body	19
1.3. Protein oxidation	20
1.4. Oxidation of amino acid residues by different oxidants	25
1.5. Mass spectrometry	30
1.6. Protein oxidation in skeletal muscle	39
1.7. Aim of project	47
Materials & Methods	48
2.1. Materials	49
2.2. Sarcoplasmic reticulum preparation from mouse hind leg skeletal muscle	50
2.3. Protein concentration determination of sarcoplasmic reticulum	50
2.4. Assay of SERCA specific activity through free phosphate release	51
2.5. Oxidant treatment of sarcoplasmic reticulum extracted samples	51
2.6. 10% sodium dodecyl sulphate polyacrylamide gel electrophoresis (SDS-PAGE)	52
2.7. Western blotting using anti-SERCA, anti-calsequestrin, anti-nitrotyrosine and anti-nitrosothiol antibodies	53
2.8. Oxyblotting using anti-DNP antibody	54
2.9. In-gel tryptic digestion of desired excised bands of SR sample	54
2.10. Settings for QToF system.....	55
2.11. Settings for QTRAP system.....	56
2.12. Data analysis	57
2.13. Online software	59
Development of mass spectrometry methods for the identification and quantification of oxidised proteins in muscle	60
3.1. Introduction	61
3.2. Results.....	63
3.3. Discussion.....	102
Identification and quantification of oxPTMs in muscle proteins of an obese model .	109

4.1. Introduction	110
4.2. Results	112
4.3. Discussion.....	133
Identification and quantification of oxidised proteins in the muscle of aged mice and comparisons to the obese model	140
5.1. Introduction	141
5.2. Results.....	144
5.3. Discussion.....	155
General discussion	159
6.1. Summary of findings	160
6.2. Future work	163
6.3. Final conclusions.....	166
References	168
Supplementary material	185

List of Abbreviations

AA	Ascorbic acid
AC	Alternating current
Ally	Allysine
ARE	Antioxidant response element
Asn	Asparagine
Asp	Aspartate
CI	Chemical ionisation
CID	Collision induced dissociation
CIY	Tyrosine chlorination
Cys	Cysteine
DC	Direct current
DDA	Data dependent acquisition
DIA	Data independent acquisition
DioxM	Methionine dioxidation
DioxW	Tryptophan dioxidation
DMBNHS	S,S'-dimethylthiobutanoylhydroxysuccinimide ester
DNPH	Dinitrophenylhydrazine
DOPA	Hydroxytyrosine
ECL	Chemiluminescent substrate
EDL	Extensor digitorum longus
ESI	Electrospray ionisation
ETD	Electron transfer dissociation
GAPDH	Glyceraldehyde-3-phosphate dehydrogenase
GELFrEE	Gel-eluted liquid fraction entrapment electrophoresis
GSH	Reduced glutathione
GSSG	Oxidised glutathione
H ₂ O ₂	Hydrogen peroxide

HCD	High energy collisional dissociation
His	Histidine
HOCl	Hypochlorous acid
HPLC	High performance liquid chromatography
IDA	Information dependent acquisition
IodoTMT	Iodoacetyl tandem mass tag
KEAP1	Kelch-like ECH-associated protein 1
Lys	Lysine
m/z	Mass to charge
MALDI	Matrix assisted laser desorption
Met	Methionine
MH	Muscle homogenate
MRM	Multiple reaction monitoring
MS	Mass spectrometry
MS/MS	Tandem mass spectrometry
MSR	Methionine sulphoxide reductase
MW	Molecular weight
NaOCl	Sodium hypochlorite
NitroY	Tyrosine nitration
NO	Nitric oxide
NOS	Nitric oxide synthase
NRF2	Nuclear factor erythroid 2-related factor 2
ONOO ⁻	Peroxynitrite
OxF	Phenylalanine oxidation
OxH	Histidine oxidation
OxM	Methionine oxidation
OxP	Proline oxidation
oxPTM	Oxidative post-translational modifications

OxW	Tryptophan oxidation
OxY	Tyrosine oxidation
PANTHER	Protein Analysis Through Evolutionary Relationships
Phe	Phenylalanine
Pro	Proline
PVDF	Polyvinylidene fluoride
Q	Quadrupole
RF	Radio frequency
RyR	Ryanodine receptor
SDS	Sodium dodecyl sulphate
SDS-PAGE	SDS-polyacrylamide gel electrophoresis
SERCA	Sarco(endoplasmic reticulum ATPase
SH	Thiol
SNO	S-nitrosothiol
SO ₂ H	Sulphinic acid
SO ₃ H	Sulphonic acid
SOH	Sulphenic acid
SR	Sarcoplasmic reticulum
TBST	Tris buffered saline with Tween 20
TIC	Total ion chromatogram
TM	Transmembrane
ToF	Time of flight
TrioxC	Cysteine trioxidation
Trp	Tryptophan
Tyr	Tyrosine
XIC	Extracted ion chromatogram
ZDF	Zucker diabetic fatty

List of figures

Figure 1.1. Labelled diagram of skeletal muscle fibre displaying the different components contributing to the structure and function of the skeletal muscle fibre

Figure 1.2. Positions of ortho-, meta-, and para-tyrosine

Figure 1.3. Structures of twelve modified amino acids searched using Mascot

Figure 1.4. Diagram detailing the workings of electrospray ionisation

Figure 1.5. Diagrams of QTRAP and ToF instruments

Figure 1.6. y and b ion fragment series

Figure 1.7. 3D crystal structure and approximate schematic of SERCA

Figure 2.1. Thermo Scientific PageRuler Plus Prestained Protein Ladder, 10 to 250 kDa

Figure 2.2. Assembly of western sandwich

Figure 2.3. Reverse phase elution profile of sample run on nanoHPLC

Figure 3.1. SDS-page gel scans of isolated SR and MH and corresponding sequence coverages of SERCA

Figure 3.2. Representative sequence coverage of SERCA attained by tryptic digestion

Figure 3.3. Comparison of sequence coverage of SERCA and other proteins in SR samples with and without surfactant

Figure 3.4. Western blot and OxyBlot with increasing protein: oxidant concentrations of HOCl oxidised SERCA from left to right

Figure 3.5. Levels of carbonyl groups in MH oxidised with peroxyntirite

Figure 3.6. Mascot assignment of MS/MS spectrum to incorrect peptide and protein

Figure 3.7. Unallocated ion present in raw MS/MS files and highlighted in *de novo* sequenced spectrum

Figure 3.8. *De novo* sequenced peptides of SERCA from HOCl oxidised SR

Figure 3.9. Quantification of NitroY in glycogen phosphorylase with protein: oxidant molar concentrations of ONOO⁻

Figure 3.10. Percentage modification of NitroY residues in 1:250 ONOO⁻ oxidised MH samples using XIC analysis

Figure 3.11. MRM quantitation of NitroY (Y281) of glycogen phosphorylase treated with varying concentrations of ONOO⁻

Figure 3.12. MRM quantification of TrioxC in SERCA peptide CLALATR in samples with varying concentrations of HOCl

Figure 3.13. Comparison of MH and SR samples for quantitation of OxM residues using the QTRAP

Figure 3.14. Comparison of QToF and QTRAP XIC transitions for NitroY and native peptides from glycogen phosphorylase

Figure 3.15. Comparisons of QToF and QTRAP XIC of SERCA peptide EVTGSIQLCR

Figure 3.16. Comparison of QTRAP and QToF MRM analysis of SERCA peptide GTAIAICR

Figure 3.17. Example from selected product ion monitoring method with XICs generated from range between 300-550 kDa

Figure 3.18. Example of product ion scan of NitroY in glycogen phosphorylase

Figure 3.19. Example of targeted MRM method using selected product ions of native, oxidised and dioxidised methionine from SERCA peptide AEIGIAMGSGTAVAK

Figure 4.1. Comparisons of muscle weight and SERCA activity in both control and ob/ob models

Figure 4.2. NitroY detection in lean & obese mice of isolated SR and muscle homogenate using western blotting

Figure 4.3. SDS-gel and immunoblot of SNOs in control and obese MH

Figure 4.4. Expedeon stained SDS-gel of isolated SR and muscle lysate from obese mouse hind legs

Figure 4.5. Classification of ob/ob muscle homogenate and isolated SR proteins into biological processes

Figure 4.6. De novo sequenced peptides in ob/ob muscle

Figure 4.7. Number of modified residues detected in discovery MS/MS of SR samples in control and obese models for SERCA

Figure 4.8. Potential unusual modification to a SERCA peptide found in an obese sample

Figure 4.9. MRM spectrum of OxW of SERCA peptide EPLISGWLFFR in obese MH

Figure 4.10. MRM spectra of TGTLTTNQMSVCK OxM & DioxM in obese sample

Figure 4.11. Quantitation of SERCA peptides in obese muscle

Figure 5.1. Indication of sarcopenia by measurements of the weight of gastrocnemius muscle and functional activity of SERCA

Figure 5.2. Oxyblot of young and aged muscle samples

Figure 5.3. Immunoblotting with anti-SNO of young and aged samples in duplicate

Figure 5.4. Gene ontology study on MS discovered proteins in aged gastrocnemius muscle in comparison to proteins from ob/ob whole muscle

Figure 5.5. De novo sequenced oxidised peptides detected by Mascot

Figure 5.6. Example of targeted MRM method using transitions of native, oxidised and dioxidised product ions from SERCA peptide AEIGIAMGSGTAVAK MS/MS fragmentation

Figure 5.7. Quantification of cysteine and methionine oxidation in SERCA of aged and young samples

Figure 6.1. Heat map of quantified oxidised residues in SERCA

List of tables

Table 2.1. Parameters used for MS/MS analysis with Mascot.

Table 3.1. OxM in control SR samples with the presence of an oxidant scavenger (exogenous methionine) and the absence of the scavenger.

Table 3.2. Top 10 protein hits of MH oxidised with HOCl at a 1:500 (protein: oxidant molar ratio) with corresponding mascot scores and sequence coverages

Table 3.3. Mascot detection of oxidised residues following treatment of SERCA with varying HOCl concentrations

Table 3.4. Mascot detection of oxidised residues following treatment of SERCA with varying ONOO⁻ concentrations

Table 3.5. Mascot detection of oxidised residues in top 5 hit proteins of 1: 250 ONOO-oxidised muscle lysate (excised band MW~100)

Table 3.6. Transition list for methionine oxidation in peptides from SERCA for the QTRAP instrument

Table 3.7. Transitions list for NitroY in glycogen phosphorylase for the QTRAP instrument

Table 3.8. Transitions list for oxidised residues in SERCA for the QTRAP instrument

Table 3.9. Transitions list for NitroY in SERCA for the QTRAP instrument

Table 3.10. Comparison of QToF and QTRAP quantitation of OxM modifications of Met452 and Met720 of SERCA

Table 3.11. Comparison of QToF and QTRAP quantitation of NitroY in glycogen phosphorylase

Table 4.1. List of modifications identified and validated in obese muscle

Table 4.2. List of modifications detected and validated by de novo sequencing in band 2 of ob/ob SR samples

Table 4.3. Identification of oxPTMs discovered in obese muscle homogenate

Table 4.4. Transition lists for the additional modifications observed in muscle samples from obese mice

Table 5.1. Table of oxidised peptides discovered utilising Mascot

Table 5.2. MRM quantitation of AEIGIAMGSGTAVAK of SERCA in aged and obese mice

Chapter 1

General introduction

The development of the world's technology and medicine has been led by the natural human curiosity to understand the complexity of life itself. From theories to comprehending the origin of life to pushing the boundaries of science to achieve goals thought to be impossible, researchers have dedicated their lives to the constant strive of obtaining answers to all questions. This project entails the beginning of answering the question: What causes us to age and deteriorate? While it is widely accepted that it is to balance the population of species, what is still yet to be understood is what the biological mechanisms that lead to this event are. In order to do so this project explored three areas: 1) the application of an existing theory to an age-related model, 2) a study to compare and differentiate between an age-related model and a relevant diseased model, and 3) the development of methods that have been optimised for a particular biological sample. The focus of this project was the proteomic analysis of the ageing muscle which was compared to an obese model to determine whether the changes with ageing were due to the ageing process or consequences of any disruption to the norm.

1.1. Ageing, inflammation and the skeletal muscle

1.1.1. The ageing process

The definition of ageing is described as the collection of changes to which genetic and environmental factors can contribute to the increasing advancement to death (Harman, 2003). As an individual grows older the accumulation of the changes in cells and tissue can lead to diseases resulting in irreversible failure of biological systems such as the heart failing to circulate blood or the kidneys failing to detoxify the blood with both leading to eventual death if not treated. On average, the world population lives to 60-65 years, however, there have been many debates on whether the chronological age is a good indicator of an individual's lifespan (Robine and Ritchie, 1991). As discussed before, the definition of ageing is the collection of changes that result to the advancement toward death. Each person is disposed to having accumulated different changes that would vary the progression of natural

death to individuals of the same chronological age. Therefore in order to define biological ageing, it would require an understanding of the underlying mechanisms as well as markers representing advanced age.

1.1.2. Theories of ageing

There have been many theories behind the process of ageing; however, it is still not known what the biological cause of this natural progression is. Many of these theories can be categorised into two groups: programmed theories and error theories. Programmed theories suggest that ageing involves a decline in the body's maintenance and protection mechanisms via changes in gene expression, whereas error theories propose that it is cumulative damage that results in ageing (Jin, 2010). One particular error theory, named the free radical theory of ageing, describes the effects of the cumulative damage oxidants. This was first suggested by Denham Harman in 1956 and later merged with the rate of living theory to propose that an increased rate of respiration would lead to an increase production of oxygen radicals and therefore speed up ageing (Beckman and Ames, 1998). One example of an alternative ageing theory is the Hayflick Limit theory which suggests that cell division is a limited process (Hayflick and Moorehead, 1961). This theory encompasses research into telomere shortening. The telomeres of a chromosome are a repetitive sequence of nucleotides that function to protect the remainder of the chromosome from truncation during cell division. Telomere shortening results from each cell division event and early studies had correlated this to lifespan whereby telomere length was significantly shorter in tissues of advanced age (Gardner *et al.* 2007; Jiang, Ju and Rudolph, 2007). Furthermore cell lifespan extension was demonstrated by lengthening telomeres (Bodnar *et al.* 1998). This was achieved by the enzyme telomerase replacing the lost telomeres of chromosomes after cell division and was further used to produce immortalised cells. Since then comparisons of multiple studies into telomere length correlation to lifespan of different tissues showed results with significant, insignificant and no correlation and ongoing debates

question whether telomere shortening is directly linked to overall lifespan (Hornsby, 2007; Mather *et al.* 2011). Another example of an alternative ageing theory is the neuroendocrine theory, first proposed by Vladimir Dilman in 1954 and further explored with Ward Dean in 1992, which states that hormone secretion and effectiveness decreases in correlation with ageing. This is also coupled with reduced hormone receptor function and has been theorised that damage to the hypothalamus is what causes the imbalance in hormones. Hormone replacement therapy has been proposed as an intervention to improve quality of life; however, other studies debate the safety and effectiveness of the therapy in which one case was shown to increase spontaneous tumour frequency with oestrogen replacement therapy (Tosato *et al.* 2007). While there are many ageing theories, this project focused on the link between oxidative damage and ageing based on the free radical theory by Denham Harman.

Many studies have shown a correlation between ageing and the increase in the presence of oxidised biomolecules (Berlett and Stadtman, 1997; Stadtman, 2006; Friguet, 2006). However, some scientists refute this theory because antioxidant treatment studies showed very little effect on the rate of ageing (Lipman *et al.*, 1998; Gutteridge and Halliwell, 2000; Parthasarathy *et al.*, 2001). On the other hand there have also been reports of evidence that transgenic animals have altered ROS levels (Liu *et al.* 2003; Hu *et al.* 2006; Lu, Ogasawara and Huang, 2007). Therefore there are some who believe oxidised biomolecules are a symptom of ageing and not the cause (Juránek and Bezek, 2005). Nevertheless, the free radical theory still stands strong and there are those who believe that this theory still has some contribution to ageing. Exploring these theories alongside the constant development of better identification technologies will enable a greater understanding of the biological mechanisms behind ageing and may unveil new information to support pre-existing theories or define new theories.

1.1.3. Skeletal muscle and sarcopenia

The maintenance of skeletal muscle is important as it contributes towards quality life. The tissue governs movement and is made of two main types of muscle fibre: slow-twitch and fast twitch muscle fibres. These can be further subdivided into slow oxidative, fast oxidative and fast glycolytic fibres. Slow twitch fibres exhibit less force in comparison to the fast twitch fibres, due to the higher abundance of myofibrils that form glycolytic fibres. Slow twitch motor units are primarily recruited as they are easier to excite and are usually used for low activities such as standing and sitting. On the other hand, more intense activities require recruitment of fast twitch motor units (Atwood, 1963; Johnson *et al.* 1972; Edgerton *et al.* 1975). Skeletal muscle contains mostly fast twitch fibres as it requires recruitment for more intense activities.



Figure 1.1. Labelled diagram of skeletal muscle fibre displaying the different components contributing to the structure and function of the skeletal muscle fibre. Diagram includes secondary zoomed image showing the t-tubule, terminal cisterna, triad and sarcoplasmic reticulum. Image taken from Wikipedia: Blausen.com staff "Blausen gallery 2014" Wikiversity Journal of Medicine.

Sarcopenia is the loss of muscle mass and function in association with ageing. Current methods of measuring sarcopenia include grip strength and endurance. While this varies from study to study, the current European consensus is measurement of sarcopenia by the combination of gait speed, grip strength and muscle mass (Cruz-Jentoft *et al.*, 2010). There are multiple factors proposed to be associated with sarcopenia; ageing, disuse, malnutrition, but there is evidence for oxidative damage correlated with ageing (Bautmans *et al.*, 2009). Oxidised biomolecules in aged tissue could potentially be used as biomarkers for age-related diseases. It is still unclear whether they causatively contribute to ageing or are consequences of the ageing process.

1.1.4. Inflammatory diseases, ageing and obesity

Inflammation is the immune systems response to pathogens, allergens, and anything deemed harmful to the host body. It can be categorised as acute or chronic and are distinguished by several traits: onset, cell dominance and tissue injury. Acute inflammation occurs rapidly and can be defined by five cardinal signs: swelling, pain, heat, redness and loss of function. Chronic inflammation on the other hand occurs more slowly than acute inflammation. Additionally, the leukocytes that are dominant in acute inflammation are macrophages and neutrophils whereas in chronic inflammation T cells, B cells, macrophages and fibroblasts are the predominant cells present. Chronic inflammation can also be coupled to fibrosis and angiogenesis following tissue destruction by increased production of oxidants, hydrolytic enzymes, and other inflammatory responses (Schmid-Schonbein, 2006; Lech and Anders, 2013). In chronic diseases such as rheumatoid arthritis, diabetes and obesity the inflammatory status is synonymous to chronic inflammation (Wong and Lord, 2004; Wellen and Hotamisligil, 2005). Detection of oxidative modifications in these chronic diseases could be due to the underlying chronic inflammation. During the progression of ageing, the elderly are inflicted with diseases such as; Parkinson's, Alzheimer's, rheumatoid arthritis, diabetes and obesity (Wellen and Hotamisligil, 2005; Filippin *et al.* 2008; Gregor and Hotamisligil,

2011; Taylor, Main and Crack, 2013; Holmes, 2013). These diseases are reported to show levels of chronic inflammation. Additionally, some of these studies have been linked to associations with oxidation.

1.2. How oxidants are produced in the body

Common oxidants generated in the human body include superoxide, hydroxyl radicals, hydrogen peroxide, nitric oxide, nitric dioxide, peroxyxynitrite, and hypochlorite. These oxidants can be produced from a variety of endogenous sources such as; mitochondria, peroxisomes, lipoxygenases, NADPH oxidase, and cytochrome P450. They can also be generated from exogenous sources such as ionising radiation and chemotherapeutics (Finkel and Holbrook, 2000). This project will focus on the effects of endogenous sources on oxidants in the body.

Mitochondria produce superoxide, hydrogen peroxide, and hydroxyl radical through incomplete oxygen metabolism. Superoxide is formed through the addition of a free electron to molecular oxygen. In turn hydrogen peroxide can be produced when superoxide is dismutated, which can be catalysed by superoxide dismutase. Reduced transition metals can react with hydrogen peroxide to produce highly reactive hydroxyl radicals. Nitric oxide synthase (NOS) is responsible for the production of the reactive nitrogen species like nitric oxide (Kirkinezos and Moraes, 2001). NADPH oxidase produces superoxide in phagocytes with the role of killing pathogens but homologues of phagocyte NADPH oxidase have been reported to be found in many organs and tissues (Bedard and Krause, 2007). Peroxisomes contain a high concentration of hydrogen peroxide-generating oxidases and have been linked to oxygen metabolism (Bonekamp *et al.*, 2009). Cytochrome P450 generates reactive oxygen species superoxide and hydrogen peroxide in the P450 catalytic cycle (Zangar *et al.*, 2004). These naturally occurring processes in the body produce reactive oxygen species but the amount generated can increase and create an oxidative stress environment, which results in oxidants modifying the surrounding biomolecules. These biomolecules include protein, lipids, and nucleic acids (Beckman and Ames, 1998).

Oxidants are involved in many cellular processes such as the electron transport system, vasodilation of blood vessels, and destruction of pathogens by phagocytes. Alongside the production of oxidants the redox homeostasis is maintained by eliminating excess oxidants via sequestering and breakdown. Superoxide dismutase is an enzyme responsible for catalysing the dismutation of superoxide to hydrogen peroxide. This can be further broken down to water and oxygen by catalase. Glutathione peroxidase can also aid in the conversion of hydrogen peroxide to oxygen via the oxidation of reduced glutathione (GSH) to oxidised glutathione (GSSG). The cycle can be reset by the conversion of GSSG to GSH with the aid of glutathione reductase (Trachootham *et al.* 2008). Nuclear factor erythroid 2-related factor 2 (NRF2) is a redox-sensitive transcription factor that regulates antioxidant genes to counteract oxidative stress. Modifications to cysteine residues of Kelch-like ECH-associated protein 1 (KEAP1) by oxidants result in conformation changes which releases NRF2 leading to activation of genes containing the antioxidant response element (ARE). Some of the antioxidant proteins transcribed by NRF2 include: glutathione peroxidase, superoxide dismutase, glutathione reductase and thioredoxin (Nguyen, Nioi and Pickett, 2009). The KEAP1/NRF2 signalling pathway has also been linked to ageing and longevity (Sykiotis and Bohmann, 2008).

1.3. Protein oxidation

Protein is oxidatively modified through exposure to oxidants interacting with the amino acid residues. The most susceptible amino acids tend to be the sulphur-containing amino acids cysteine and methionine, followed by the aromatic amino acids histidine, tyrosine, tryptophan, and proline (Griffiths, *et al.*, 2002).

Cysteine has many oxidised forms such as the disulphide, sulphenic acid (SOH), sulphinic acid (SO₂H), sulphonic acid (SO₃H), nitrosothiol (SNO), sulphenyl chloride (SCI), thiolsulfinate (RS(O)SR') and sulfenamide, sulfinamide, sulfonamide RS(O)NH₂/RS(Ox)NHR' (x=0-2) forms (Schoneich and Sharov, 2006). Most commonly,

cysteine is progressively oxidised through from the sulphenic form to the sulphinic form and then the sulphonic form. However, it is ordinarily found to form disulphide bridges which are formed when two cysteine bonds are oxidised creating a bond between the sulphur groups that contribute to protein folding (Betz, 1993). One study has proposed that HOCl oxidation forms sulphenyl, sulphanyl, and sulphonyl chlorides which decompose to sulphenic, sulphinic, and sulphonic acid or form S-N cross links with nearby lysine and arginine residues forming sulphenamide, sulphinamide, and sulphonamide (Fu *et al.*, 2002).

Methionine has two oxidative states: methionine sulfoxide (S=O) and methionine sulphone (O=S=O) (Schoneich and Sharov, 2006). Similarly to cysteine, methionine can be oxidised to the sulfoxide state, and then the sulphone state when there is an excess of radical species. While it is considered to be a common modification, it has been suggested to impact life span and is linked to the development of Alzheimer's disease when methionine sulphur reductase (MSR) function is reduced in brain tissues (Stadtman, Moskovitz and Levine, 2003).

Tyrosine also has various different oxidative forms, such as dityrosine, 2-hydroxytyrosine, 3-hydroxytyrosine (DOPA), 3-aminotyrosine, 3-nitrotyrosine, and 3-chlorotyrosine (Schoneich and Sharov, 2006). The latter two are products of reactive nitrogen species-mediated oxidation and reactive chlorine species-mediated oxidation, respectively. Additional tyrosine modifications include dityrosine and 3-aminotyrosine formation. Dityrosine is usually generated through tyrosyl radical formation (Heinecke *et al.*, 1993; Yan and Sohal, 2002). 3-aminotyrosine is a rare oxidative modification but one study has reported to have observed this modification and proposed this was a result in the reduction of nitrotyrosine (Mirzaei *et al.*, 2006).

Phenylalanine can be oxidised to tyrosine and dihydroxyphenylalanine (hydroxytyrosine/DOPA). Figure 1.2 demonstrates that oxygen can be observed at multiple points of the aromatic ring in oxidised phenylalanine producing; ortho(O)-tyrosine, meta(M)-

tyrosine, and para(P)-tyrosine, isomers of the naturally occurring L-tyrosine which makes it easier to distinguish between oxidation and mutation (Ishimitsu *et al.*, 1984). P-tyrosine is a natural metabolite of phenylalanine and therefore cannot be used as a marker of its oxidation (Hoskins and Davis, 1988). However there are studies showing oxidation of phenylalanine to O-tyrosine and M-tyrosine (Leeuwenburgh *et al.* 1997; McPherson and Turemen, 2014).

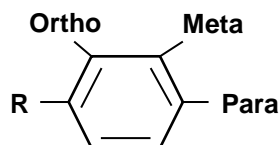


Figure 1.2. Positions of ortho-, meta-, and para-tyrosine. R group represents the remainder of the tyrosine structure.

Tryptophan oxidation products include hydroxytryptophan, nitrotryptophan, N-formylkynurenine, and kynurenine (Schoneich and Sharov, 2006). Hydroxy- and nitrotryptophan products can be in the form of more than one isomer. 2-oxo-histidine is a histidine oxidised product and hydroxyproline is a proline oxidised product (Schoneich and Sharov, 2006).

Protein carbonyl group formation can arise through many different reactions that form ketones and aldehydes. Semialdehyde amino acid formation can occur with lysine, arginine and proline residues (Stadtman and Berlett, 1991). Characterisation of the amino acid residue and the type of carbonyl modification is possible through tandem mass spectrometry analysis and searching against a sequence database (Mirzaei and Regnier, 2005). Alternatively, aldehydes can be detected through covalent labelling with nucleophilic hydrazide or hydrazine based probes, which form Schiff bases that then can be reduced to a stable carbon-nitrogen bond. An example of this method is OxyBlotting which uses 2,4-dinitrophenylhydrazine (DNPH) to react with protein carbonyls and anti-DNP antibodies to detect the modification (Levine *et al.*, 1994). There have been studies that incorporate both these SDS-gel based methods where one is immunoblotted to visualise the migration pattern of carbonyl formation on proteins and the other is stained for total protein so that

corresponding spots can be excised, digested and analysed by mass spectrometry (Yan *et al.*, 1998). In order to study a variety of modifications, the number of oxPTMs studied in this thesis research project was limited to a selected few (Fig.1.3).

The oxPTMs shown in Table 1.3 were chosen based on amino acid susceptibility to oxidation and prevalence of reported modifications in literature, which is further discussed in section 1.6. Sulphur containing amino acids methionine and cysteine are the most susceptible to oxidation due to their nucleophilic side chains when oxidised. Sulphur has six electrons in its outer shell. Two of the outer electrons have paired with the carbons on either side of sulphur in methionine or the carbon and hydrogen on either side of sulphur in the case of cysteine. The remaining four unpaired electrons in sulphur's outer shell can form double bonds with two unpaired electrons in the outer shell of oxygen. In cysteine, the first oxidation produces –SOH which is then followed by double bond formation with oxygen. This enables cysteine to have up to three oxidation states. Cysteine can also form a thiolate ion which generates a more nucleophilic form and can lead to oxidation, disulphide bridges with another cysteine or mixed disulphides (Yarnell, 2009). Aromatic amino acids; tyrosine, phenylalanine, histidine and tryptophan, are oxidised by an addition reaction to the ring resulting in oxygenation of the aromatic rings itself. Typically the aromatic amino acids have various oxidative forms depending on where the oxygenation takes place on the ring (Hawkins and Davies, 2001). To illustrate the characterisation of carbonyl formation in proteins and correlation with western blotting, allysine was also added to the variable modifications search parameters. Allysine is approximately 1 kDa smaller than its reduced form lysine and is formed by oxidative deamidation (Fan *et al.* 2009).

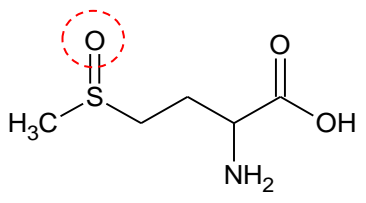
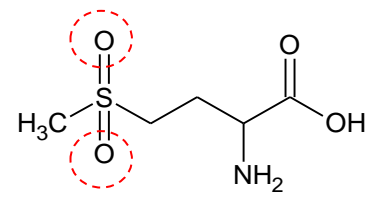
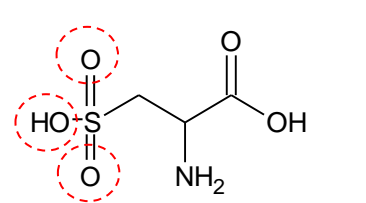
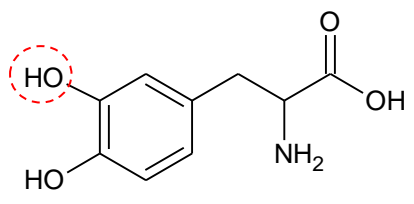
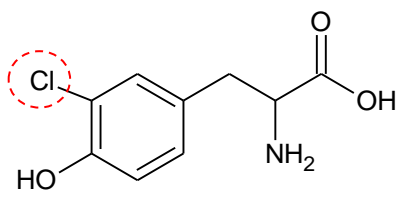
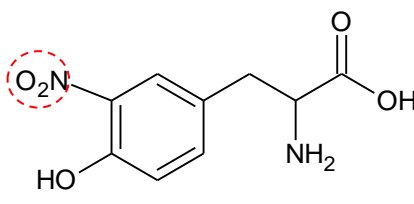
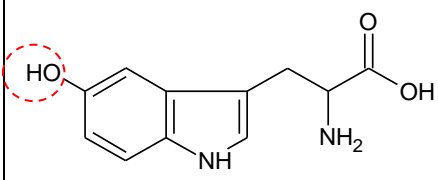
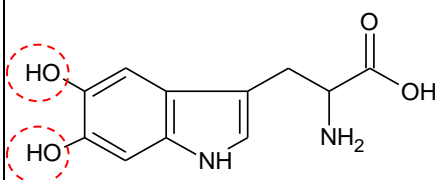
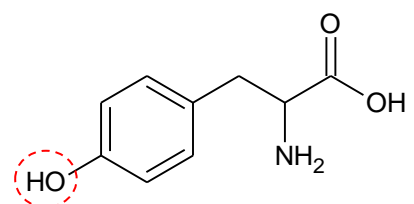
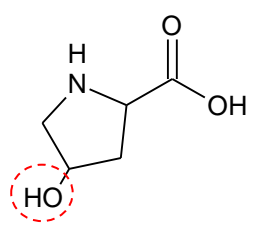
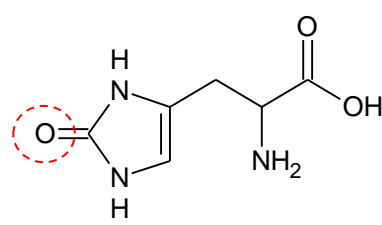
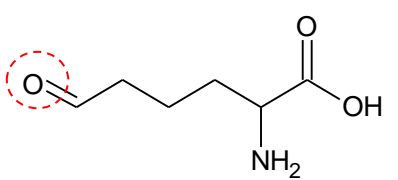
<p><u>Methionine oxidation (OxM)</u></p>  <p>Sulphoxide (+16 Da)</p>	<p><u>Methionine dioxidation (DioxM)</u></p>  <p>Sulphone (+32 Da)</p>	<p><u>Cysteine trioxidation (TrioxC)</u></p>  <p>Sulphonic acid (+48 Da)</p>
<p><u>Tyrosine oxidation (OxY)</u></p>  <p>3-Hydroxytyrosine (+16 Da)</p>	<p><u>Tyrosine chlorination (ClY)</u></p>  <p>3-Chlorotyrosine (+34 Da)</p>	<p><u>Tyrosine nitration (NitroY)</u></p>  <p>3-Nitrotyrosine (+45 Da)</p>
<p><u>Tryptophan oxidation (OxW)</u></p>  <p>5-Hydroxytryptophan (+16 Da)</p>	<p><u>Tryptophan dioxidation (DioxW)</u></p>  <p>5,6-Dihydroxytryptophan (+32 Da)</p>	<p><u>Phenylalanine oxidation (OxF)</u></p>  <p>4-Hydroxyphenylalanine (+16 Da)</p>
<p><u>Proline oxidation (OxP)</u></p>  <p>4-Hydroxyproline (+16 Da)</p>	<p><u>Histidine oxidation (OxH)</u></p>  <p>2-Oxohistidine (+16 Da)</p>	<p><u>Lysine to Allylysine (Ally)</u></p>  <p>α-Amino adipic-6-semialdehyde (-1 Da)</p>

Figure 1.3. Structures of twelve modified amino acids searched using Mascot.

*Oxidation can occur at multiple places but most commonly occurs on specified position.

1.4. Oxidation of amino acid residues by different oxidants

The oxidation of these amino acids by various oxidants has been explored in many *in vitro* and *in vivo* studies discussed below. Some oxidants have been shown to produce several oxidative products or preferential modification to certain amino acids.

1.4.1. Superoxide/Hydrogen peroxide

Superoxide is reactive towards cysteine metal centres that are redox-active (Ryan *et al.* 2010). Hydrogen peroxide is formed by superoxide dismutase but can be made into highly reactive hydroxyl radicals by the acceptance of an additional electron (Sawyer and Valentine, 1981). Hydrogen peroxide has a relatively slow reaction rate with most amino acids and is unlikely to cause efficient oxidation of proteins but it can produce more reactive oxidants such as hypochlorite through a reaction catalysed by myeloperoxidase and hydroxyl radicals by a reaction with transition metal complexes (Sysak *et al.*, 1977; Goldstein, *et al.*, 1993). Additionally, through combination of hydroxyl radicals with nitric oxide, peroxynitrite (ONOO⁻) can be formed.

1.4.2. Hypochlorous acid

Hypochlorite (HOCl) has the ability to oxidise and chlorinate biological compounds such as proteins and lipids. It is used as an antimicrobial agent generated by the enzyme myeloperoxidase in phagocytes (Harrison and Schultz, 1976). Diseases such as atherosclerosis, chronic inflammation, and some cancers are believed to be linked to the excessive production of HOCl and accumulation of tissue damage resulting from this (Hawkins, *et al.*, 2003).

The amino acids that are most susceptible to HOCl oxidation include methionine, cysteine, histidine, tryptophan, lysine, tyrosine, and arginine (Hawkins, *et al.*, 2003). HOCl is more readily reactive with sulphur-containing amino acids, cysteine and methionine, and slightly less reactive with amine and nitrogen-containing residues: histidine and lysine (Hurst *et al.*,

1991). Tryptophan oxidised by HOCl can produce the stable oxidised product 2-hydroxyindole but this is not specific to HOCl oxidation and can be formed by other radical species (Pitt and Spickett, 2008). Tyrosine, however, is able to form the chlorine-containing oxidised product 3-chlorotyrosine when attacked by HOCl, representing a specific marker for HOCl-mediated oxidation (Domigan *et al.*, 1995).

HOCl reacts with amino groups in the formation of chloramines: $R-NH_2 + HOCl \rightarrow R-NHCl + H_2O$ (Winterbourn, 1985). Chloramines are produced from the chlorination of amines of lysine and histidine residues and can also be further chlorinated by excess HOCl to generate dichloramines (Pattison and Davies, 2005). They are capable of transferring chlorine to other substrates but when other substrates are not available, chloramines stabilise themselves through hydrolysis to aldehydes (Hazen *et al.*, 1998). The formation of 3-chlorotyrosine has been proposed to occur through direct HOCl oxidation and via transfer of chlorine from chloramines (Domigan *et al.*, 1995). Lysine residues are a major site of reaction of HOCl with many proteins. Chloramine species are produced which decompose to nitrogen-centred protein radicals that induce protein backbone fragmentation and dimerisation. Low, sub-lethal doses of HOCl react with thiols and can initiate apoptosis whereas high concentrations cause rapid necrosis (Strosova *et al.*, 2009b).

1.4.3. Metal-catalysed oxidation

Hydrogen peroxide can react with reduced transition metals via the Fenton reaction to produce highly reactive hydroxyl radicals. The Fenton reaction, i.e. $Fe^{2+} + H_2O_2 \rightarrow HO^\bullet + HO^- + Fe^{3+}$, therefore leads to metal catalysed oxidation of amino acid residues of protein. It is also possible for a more efficient generation of hydroxyl radicals through the substitution of iron (Fe^{2+}) by copper (Cu^+) (Moreau, *et al.*, 1998). Other redox active transition metals that occur *in vivo* include chromium (Ti^{3+}) and cobalt (Co^{2+}). Metal-catalysed oxidation is thought to occur on both high- and low-affinity metal-binding sites of protein probably involving proline, histidine, arginine, lysine, and cysteine (Valko, *et al.*, 2006).

Metal-catalysed oxidation is found to be important in protein carbonylation and lipid peroxidation, where some amino acid residues are converted into carbonyl derivatives (Qu, *et al.*, 2011). All amino acid residues are susceptible to hydroxyl radical-mediated oxidation (Domingues, *et al.*, 2003). Whether this is through hydrogen abstraction (aliphatic amino acids), electron transfer (sulphur-containing), or addition (aromatic), hydroxyl radicals react to different amino acids in different ways (Schoneich and Sharov, 2006). Histidine, lysine, arginine, proline, methionine, and cysteine are highly susceptible to metal-catalysed oxidation compared to the other amino acids (Stadtman, 1993). Nevertheless, histidine has been reported to be particularly the most susceptible to metal-catalysed oxidation (Moreau, *et al.*, 1998). This is thought to be due to histidine being most associated with the coordination of metal ions/structural components of metal binding sites (Stadtman, 1993).

The conversion of histidine to 2-oxo-histidine is an important marker for oxidative stress. It was initially suggested that histidine was converted to aspartate (Asp) and asparagine (Asn) as products of histidine oxidation; however, it was later found that the additional product 2-oxo-histidine is also formed. The mechanism in the conversion of histidine to 2-oxo-histidine involves the reaction of HO[•] at the C-2 position of the imidazole ring and then the reduction of Cu²⁺ to Cu⁺ which then leads to deprotonation to form 2-oxo-histidine (Schoneich, 2000).

For the sulphur-containing amino acids, methionine is converted to methionine sulphoxide and cysteine is converted into mixed disulphide derivatives (Stadtman, 1990). A marker used for cysteine metal-catalysed oxidation is aminomalonic acid which is derived from unstable dehydrocysteine (Kang *et al.*, 2003). Mass spectrometry of an iron metal-catalysed oxidation showed the presence of aminomalonic acid which was proposed to be derived from the oxidative product of cysteine dehydrocysteine. Aminomalonic acid has been previously identified in human atherosclerotic plaques (Buskirk *et al.*, 1984).

Metal-catalysed oxidation systems can also result in the conversion of proline, lysine, arginine, and histidine to carbonyl derivatives (Amici, *et al.*, 1989). In the case of metal-

catalysed oxidation, protein modification is not the only result of oxidative modifications as fragmentation can also occur. Peptide bond cleavage could be the result of metal-catalysed oxidation of proline to 2-pyrrolidone (Moreau, *et al.*, 1998). Previous studies have showed that 2-pyrrolidone formation from proline oxidation was associated with cleavage of peptide bonds as acid hydrolysis to 4-aminobutyric acid was evidence of this (Berlett and Stadtman, 1997).

Other amino acids such as tyrosine and tryptophan have also been studied. The tyrosine oxidation product 3-hydroxytyrosine (Dopa) is used as a marker for hydroxyl radical-mediated oxidative stress (Qu, *et al.*, 2011). Tryptophan products of oxidation by hydroxyl radicals include 2-, 4-, 5-, 6-, 7-hydroxyl derivatives and N-formylkynurenine. The various isomers that can be formed by hydroxytryptophan are due to hydroxylation occurring at different sites in the tryptophan molecule. It is also possible through the Fenton reaction for cross-linking to occur and the formation of the tryptophan dimer (Trp-Trp) and the monohydroxytryptophan dimer (Trp-Trp-OH) (Domingues, *et al.*, 2003).

1.4.4. Nitric oxide and Peroxynitrite

Low levels of nitric oxide (NO) have shown to play an important role in inducing GSH synthesis in endothelial cells and regulate PGC-1 α expression which leads to the expression of oxidative stress protective genes (Borniquel *et al.*, 2006). NO was also found to play a role in vasodilation and neurotransmission and at higher levels it can cause oxidative damage but it is not as reactive as its secondary product peroxynitrite (Radi, 2004). Peroxynitrite (ONOO⁻) is formed through the reaction with superoxide radicals and nitric monoxide. Methionine, cysteine, tryptophan and tyrosine can be rapidly and selectively oxidised by peroxynitrite (Schoneich, *et al.*, 1999). Tryptophan is found to form nitrotryptophan at low peroxynitrite concentrations and higher peroxynitrite concentrations brings about the emergence of other oxidation products such as hydroxytryptophan, N-formylkynurenine, and

dihydroxytryptophan (Alvarez *et al.*, 1996). It was also found by the same study that nitrotryptophan yield increased at acidic pH.

Tyrosine modification to 3-nitrotyrosine is used as a marker for $\bullet\text{NO}_2$ and/or peroxynitrite oxidation (Schoneich and Sharov, 2006). One study showed that low steady-state concentrations of peroxynitrite resulted in a rise in dityrosine formation and a decline in 3-nitrotyrosine formation (Pfeiffer *et al.*, 2000). This was thought to be due to two pathways resulting in different products where high concentrations of peroxynitrite resulted in 3-nitrotyrosine formation and low concentrations formed dityrosine.

1.4.5. Measuring protein oxidation

There are a number of ways to measure protein oxidation, both using mass spectrometry and non-mass spectrometry methods. Antibodies specific for oxidative modifications, most commonly utilised in immunoblotting, can be used to determine the presence of the modification. Another immunoblotting technique involves the reaction of dinitrophenylhydrazine (DNPH) with protein carbonyls and anti-DNP antibodies to detect the modification. Although immunoblotting techniques are more sensitive than MS, it lacks the ability to pinpoint the location of the modification or be used in quantitation studies. Mass spectrometry methods involve both labelling and non-labelling methods. There are different types of tags used: isobaric, isotopic, biotinylated, etc. The biotin-switch method has been used to detect S-nitrosothiol (SNO) modifications by blocking free thiols, reducing SNOs with ascorbate, labelling with a biotin and enriching with avidin affinity capture (Jaffrey *et al.* 2001). Commercially available iodoacetyl tandem mass tag (iodoTMT) sixplex reagents have also been used for SNO MS identification and quantification. Alternatively other modifications such as lysine oxidation were labelled with the characteristic neutral loss of dimethylsulfide from modified lysine and is detected using amine-specific covalent labelling reagent: S,S'-dimethylthiobutanoylhydroxysuccinimide ester (DMBNHS) (Zhou *et al.* 2014). Although the labelling and enrichment strategy reduces the complexity of the sample, the

focus is usually on a single modification so a lot of information is lost when removing other peptides with different modifications or with a different oxidative state. On the other hand, label-free methods are amenable to the detection and quantification of multiple modifications in the same sample.

1.5. Mass spectrometry

1.5.1. Principles of mass spectrometry

Mass spectrometry (MS) uses electromagnetism to focus ions of a particular mass to generate fragmentation data that can be decoded in to structural information about the protein/s of interest. This is achieved by measuring the mass of ionised peptides which are then fragmented to create a fingerprint sequence specific to that peptide. With this information, changes in the peptide can be identified using mass shifts of the fingerprint sequence. Different types of mass spectrometers are able to generate different ion series depending on the resulting side chain cleavages that are introduced from different fragmentation methods i.e. collision induced dissociation (CID) and electron transfer dissociation (ETD) (Sobott *et al.* 2009).

1.5.2. Sample ionisation

Mass spectrometry (MS) is a technique that utilises the differences in the mass to charge ratio (m/z) of peptides and peptide fragments for protein identification as well as the detection of modifications. The charge of the peptide can be generated via different ionisation methods: electrospray ionisation (ESI), chemical ionisation (CI), matrix assisted laser desorption ionisation (MALDI), etc. ESI is a soft ionisation technique that utilises a high voltage to generate a spray of charged droplets of the sample solution and is commonly used for analysis of biomolecules in MS (Fenn *et al.*, 1989) (Fig. 1.4).

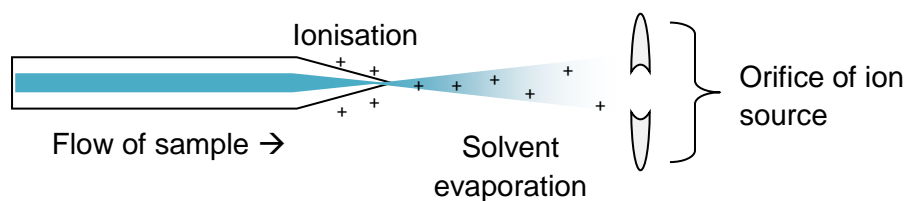


Figure 1.4. Diagram detailing the workings of electro spray ionisation. The sample flows through capillary tubing at a set rate. Once ionised, droplets are desolvated and charged particles enter the orifice of the ion source pulled by a vacuum.

1.5.3. Types of mass spectrometers

There are many different types of mass spectrometers each with different mass analysers and strengths for specific MS approaches. The two mass spectrometers outlined and used in this project are the Triple Time of Flight (ToF) and the QTRAP both from AB Sciex. Throughout the project, both these instruments utilise ESI and were coupled to high performance liquid chromatography (HPLC). Ionisation of the sample allows movement of the ions within the mass spectrometer using electrostatic attraction and repulsion of the electromagnetic field generated by negative and positive charges of the mass analysers. Figure 1.5A demonstrates a typical layout for a quadrupole (Q) mass spectrometer. The two instruments used in the study are hybrid mass spectrometers where Q3 is substituted with another type of mass analyser.

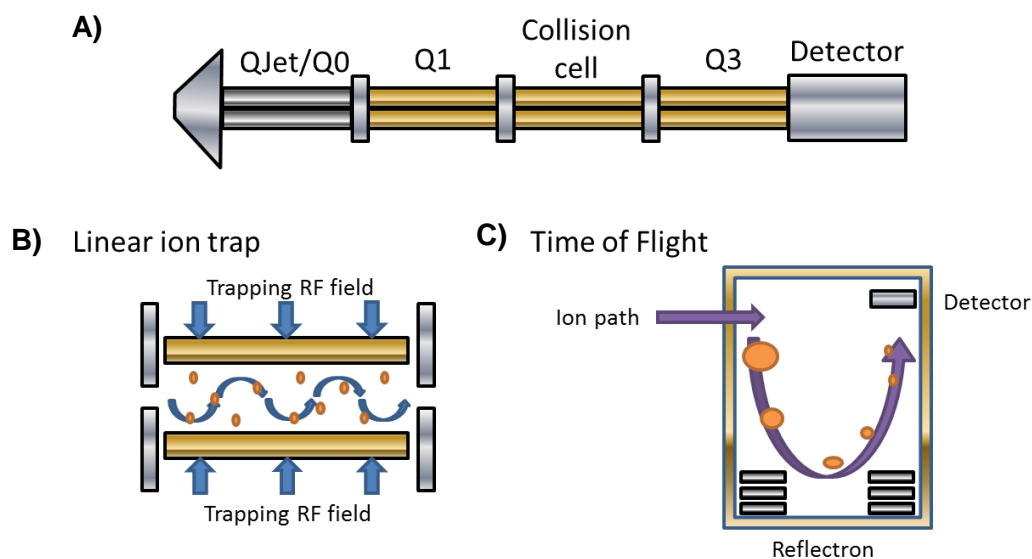


Figure 1.5. Diagram of MS instrument layout and mass analysers. A. Components of MS are labelled detailing the main parts of a quadrupole MS instrument. **B.** Diagram of Linear Ion Trap. **C.** Diagram of the ToF analyser.

1.5.4. Mass analysers

The quadrupole mass filter consists of four parallel gold plated ceramic rods in which opposite rods share polarities. An alternating current (AC) or radio frequency (RF) voltage and constant direct current (DC) is placed to generate an electromagnetic field which separates charged ions on their mass to charge (m/z) ratios. The DC voltage enables ions to move across the quadrupole and the AC or RF voltage causes the ions to spiral resulting in alternative trajectories for the different m/z . Ions with smaller m/z are more influenced by the electromagnetic field whereas ions with larger m/z are influenced less. In both cases the ions can collide with the quadrupole rods neutralising the ion and therefore filter ions of a specific m/z range. Altering the voltages changes the trajectories of the ions and can be used to filter from small to increasingly larger m/z (Miller and Denton, 1986; Steel and Henchman, 1998).

The linear ion trap works in a similar manner to quadrupoles with added trapping capabilities. The linear ion trap uses a two dimensional RF frequency field to trap ions along the axis of the quadrupole ion trap by applying stopping potentials to the entrance and exit of

the electrodes (Fig.1.5B). The three dimensional version is made of three hyperbolic electrodes: a central ring and two endcaps. Alternating polarities draws ions towards the electrodes and repels them to the next avoiding collision of the ions with the electrodes. This generates an RF field which traps the ions and alterations to the RF frequency cause excited ions to eject through the endcaps (Douglas, Frank and Mao, 2004).

In time of flight mass analysers, ions are accelerated into a flight tube in which the time taken to reach the detector is correlated to the m/z of the ion. Both the charge and mass of the ion contribute to speed where a greater charge and low mass will result in faster arrival times. Longer pathways to the detector can also help enhance resolution. Orthogonal ToF analysers pulse packets of ions into the flight tube at 90° (Fig.1.5C). This is then directed at a reflectron which has the same polarity as the ions causing them to be repelled to the detector. The reflectron increases separation by driving ions to travel twice the distance of the flight tube: down the flight tube to the reflectron and then back up to the detector. This lengthens the pathway for the ions with the need of extending the length of the flight tube (Guilhaus, 1995).

1.5.5. MS approaches

There are two main approaches: top-down and bottom up MS. The former provides information on intact proteins while the latter is used for analysis of digested protein/s. MS-based proteomics typically utilises digestion of proteins into peptides for sequence analysis denoted as bottom-up MS. This involves cleavage of proteins into peptides by the use of trypsin which cleaves at the C-termini of arginine and lysine residues. The locations of these sites are important because there is a limit to how big and small the m/z value can be and using the right digestion protein allows peptides to be detectable by fitting between these limits. These limits are dependent on the type of mass spectrometer being employed. Tandem mass spectrometry (MS/MS) methods are employed to measure the m/z of the peptide ion and its fragments generated in the collision cell (Hunt *et al.* 1986). Many mass

spectrometers are hybrids consisting of two quadrupole mass analysers and a third alternate analyser. The 5500 QTRAP and 5600 QToF AB Sciex mass spectrometers used in the study have an ion trap and ToF respectively as their third mass analyser. The first and last mass analysers can either be fixed for ion selection or used to scan ions, depending on the MS/MS method being utilised, and the second analyser acts as the collision cell. The MS/MS methods are categorised either as data independent acquisitions (DIA) in which all ions are analysed and data dependent acquisitions (DDA) which involves the selection of peptide ions for fragmentation. Examples of DIA MS/MS is SWATH and MS^{All} where the former uses windows of increasing m/z to scan all ions in the first mass analyser and the latter utilises a wide m/z window to scan all peptide ions (Simons *et al.* 2012; Gillet *et al.* 2012; Zhu, Chen and Subramanian, 2014). For DDA MS/MS, several semi-targeted and targeted approaches can be employed depending on the type of dataset desired. The most widely used method in the proteomics field is discovery MS/MS which filters the most abundant ions for subsequent fragmentation (Aebersold and Mann, 2003; Dworzanski *et al.* 2004). Semi-targeted methods also include precursor ion scanning, product ion scanning and neutral loss scanning. Precursor ion scanning fixes the last mass analyser to select for fragment ions with a specified m/z and scans for peptide ions that generates these fragments. One study uses the immonium ion fragment of phosphotyrosine at 216 m/z to facilitate identification (Steen *et al.* 2001). Product ion scanning is the reverse of this method and fixes the first analyser with a specified m/z and scans for the fragment ions generated (Hager and Yves Le Blanc, 2003). Multiple reaction monitoring fixes both the first and third analysers for targeted quantitative approaches. This method has been implemented in the quantitation of plasma proteins for the development of assays for biomarker candidacy (Anderson and Hunter, 2006). Neutral loss scanning involves the third mass analyser set to scan with an offset to record peptides with a loss of a mass specific to a trait of the peptide. An example of this application involved scanning for phosphopeptides with a neutral loss of phosphoric acid (Tholey, Reed and Lehmann, 1999). Following tandem mass spectrometry, a MS³ method

can also be utilised by performing a consecutive fragmentation providing additional information about the peptide sequence (Olsen and Mann, 2004).

1.5.6. Fragmentation

In the collision cell inert gas collides with the precursor ions to generate fragment ions resulting in the production of MS/MS spectra. There are different types of fragmentation methods: electron transfer dissociation (ETD), collision induced dissociation (CID) and high energy collisional dissociation (HCD) are most commonly used. This project uses the TripleToF to perform non-targeted tandem mass spectrometry (MS/MS) using CID which typically produces b and y series ions that fragment at the peptide bond. These ions are complementary to one another and are formed from the fragmentation of the peptide bond (Fig. 1.6). Different ions generate a charge on either terminus. A charge generated on the N-terminus is termed as a, b, or c series ions and a charge on the C-terminus is termed as x, y, or z series ions.

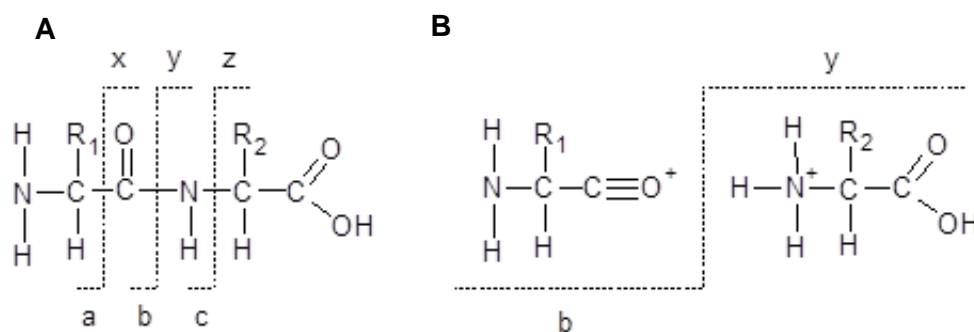


Figure 1.6. y and b ion fragment series. A. Fragmentation at peptide bond. **B.** Fragments formed via y-series and b-series fragmentation.

1.5.7. Data analysis

This project utilised Mascot and PeakView software programmes to convert mass spectra peaks into tables of the peptides analysed with possible modifications depending on the parameters searched within. Mascot is used to translate the mass spectrum peaks into easier understandable data. The peaks, corresponding to ions picked up by the mass

spectrometer, can produce a sequence of peptides present in the sample analysed leading to the identification of the protein of interest where further analysis can be made. Depending on the parameters set, possible modifications can be highlighted due to the probability that mass differences equate to a modified amino acid, which is calculated by the Mascot programme. The likeliness of the modification being present can range from high to low and therefore there is a risk of false positives. This requires confirmation using the second programme PeakView for evidence of the existence of the modifications detected by Mascot.

In PeakView, the data can be displayed as a total ion chromatogram (TIC) or an information dependent acquisition (IDA) spectrum. The total TIC shows the intensity of the ions detected against the time of the acquisition method. MS/MS data of the ions can be displayed showing fragmentation of the precursor ions with changes in intensity and mass differences, which may correspond to a modification. The level of detail gained from the mass spectrometer can show isotopic distribution. Therefore, even peptides with variation in mass due to an extra neutron can be differentiated. An extracted ion chromatogram (XIC) is useful to see where a particular ion mass is most intense during acquisition. Narrow window XIC analysis has been used to generate XICs from MS/MS methods to quantify levels of oxidation (Tveen Jensen *et al.* 2013). In an IDA spectrum, the MS/MS data for individual precursor ions are shown. Using information from Mascot about a peptide that contains a modification, the full MS/MS spectrum is displayed and de novo sequencing can be performed for the removal of false positives. De novo sequencing is required for the validation of peptides assigned to MS/MS spectra and removal of false positive data arising from probability-based software detection. The ease of interpreting MS/MS spectra is dependent on the user's abilities as there are several indicators used to validate a peptide sequence with a modification. For the QToF, the basic validation method is the sequencing of y-series ions as the dominant fragment ions produced during MS/MS. Amino acid mass used for sequencing is the mass of the amino acid with the removal of water (18 Da) to take into account the peptide bonds. As the common enzyme used for digestion is trypsin, the

starting ion is either 147 Da for lysine or 175 Da for arginine. This is because the structure of a y-series ion for any given amino acid is the addition of proton to the amine group [1 Da] (Roepstorff, 1984; Johnson, 1987). Once the starting amino acid is found, which should be the same as the detected modified peptide assigned by the probability-based software, it is simply a case of finding the next ion in the sequence until most of the peptide around the region of the modified residue is assigned to ion peaks in the spectra. In most cases this alone can be used for validation but in some instances using the y-series ions does not help in the sequencing of a peptide. This mainly occurs when the modification is in the high m/z region where fewer ions are detected. These residues are nearer to the amine terminal of the peptide and therefore require sequencing starting from the opposite end. The complementary ion to the y-ion is the b-ion. At this end the starting ion can be any amino acid but with a loss of hydroxide ion from the carboxyl acid group [-17 Da] (Roepstorff, 1984; Johnson, 1987).

Sequencing with y & b ions are good indicators of the presence of a modified residue but there are also diagnostic ions for additional validation. Immonium ions are most commonly used as diagnostic ions for the presence of modifications. They are fragmented ions used as markers for a particular amino acid. Immonium ions are charged amino acids that have lost their carboxylic acid group, however only some amino acids generate high intensity immonium ions: tyrosine, phenylalanine, histidine, and tryptophan. (Falick, 1993; Papayannopoulos, 1995). Some diagnostic immonium ions used include: chlorotyrosine (170 Da) and nitrotyrosine (181 Da) (Tveen Jensen *et al.* 2013). Using mass spectrometry gives a great deal of detailed information on analysed samples and modifications that could lead to a decrease or increase in function. Information acquired can be used as biomarkers for diseased states or further knowledge for the therapeutic drug targets.

1.5.5. High performance liquid chromatography (HPLC)

HPLC is used for prior separation of samples, before entering the mass spectrometer, based on their hydrophobicity. As the study focuses on a mixture of proteins, an isocratic gradient is produced with aqueous and solvent solutions to separate eluting peptides when bound to a C18 hydrocarbon column. This is termed as reversed phase chromatography. Without the prior separation, a mixture of proteins would result in limited information collected to only abundant proteins. Through separation more information can be collected from the different batches of proteins eluted from hydrophilic to hydrophobic over the course of time. Developments in LC-separation are required to reduce sample loading and improve separation of proteins/peptides. Gel-eluted liquid fraction entrapment electrophoresis (GELFrEE) is a technique that integrates gel electrophoresis separation within reverse phase LC. This eliminates the need for prior electrophoresis and sample processing before injection into the LC (Tran and Doucette, 2008). The GELFrEE method has been used in the detection of nitrotyrosine via the increase in hydrophilicity of nitrotyrosine when reduced to aminotyrosine and the aid of diagonal chromatography. The peptide mixture was separated and fractionated by reversed phase HPLC followed by reduction by dithionite and then a secondary separation was performed to collect fractions with the previously described shift. These were analysed with MS to identify nitrotyrosine in the enriched peptide fractions (Ghesquiere *et al.*, 2009). The changes incurred by oxPTMs in peptide/protein elution properties are advantageous when separating modified peptides for analysis.

1.5.6. Digestion into peptides

The gold standard digestion technique for MS is an in-gel trypsin digest. This involves cleaving denatured protein, from gel electrophoresis, at the c-terminal arginine or lysine into peptide fragments enabling the researcher to follow up with standard bottom-up MS techniques. Other methods include; in-solution, on-membrane, on-resin, and on-line digestion and the use of other enzymes/double digestion as well as the use of surfactants.

To improve digestion efficiency MS friendly surfactants such as ProteaseMax (Promega) (Duan *et al.*, 2009; Saveliev *et al.* 2013) and Rapigest (Waters) (Yu *et al.*, 2005) are added and work by further denaturation of proteins to make digestion sites more accessible to aid digestion without disrupting enzyme activity. These MS friendly surfactants degrade over the course of protein digestion.

1.6. Protein oxidation in skeletal muscle

Oxidation in skeletal muscle has been reported for various proteins and for multiple oxPTMs. Some of these reports include detection of carbonyl groups from oxyblot analysis, oxidation of pyruvate dehydrogenase, higher oxidation present in subsarcolemmal mitochondria, and nitrotyrosine detection in carbonic anhydrase to name a few (Sugden, 2000; Vasilaki, 2007; Dalla Libera *et al.* 2010; Crescenzo *et al.* 2014). More specifically many studies have looked at the association of SERCA oxidation to ageing and disease.

1.6.1. Sarco(endo)plasmic reticulum calcium ATPase and changes corresponding to biological ageing

Sarco(endo)plasmic reticulum calcium ATPase (SERCA) is a calcium pump that uses ATP hydrolysis to transport calcium from the extracellular environment into the sarcoplasmic reticulum calcium store (Schoneich, *et al.*, 1999). Vascular relaxation, cardiac and skeletal muscle relaxation, and cell growth and differentiation can all be affected by the regulation of intracellular calcium by SERCA (Strosova, *et al.*, 2009a). The protein is around 1000 amino acid long and around 110kDa. There are three isoforms of SERCA with their own sub-isoforms; SERCA1, SERCA2a/b, and SERCA3a/b/c/d/e/f/g. SERCA1 is expressed in fast-twitch skeletal muscle, SERCA2a is expressed in cardiac and slow-twitch muscle, SERCA2b is expressed in smooth muscle and a variety of other tissues, and SERCA3 is also a non-muscle isoform (Schoneich and Sharov, 2006). In humans SERCA3 has six sub-isoforms, however in mouse there are only the three isoforms a, b and c.

SERCA switches between two conformational forms where the E1 form has its high-affinity calcium binding sites facing the cytoplasm and the E2 form has its low-affinity calcium binding sites facing the endoplasmic reticulum lumen (Vandecaetsbeek, *et al.*, 2009). The high- and low-affinity calcium binding sites are found in the transmembrane domain of SERCA (Voss, *et al.*, 2008). ATP hydrolysis allows the opening and closing of calcium gates in the transmembrane domain of SERCA through conformational changes in the cytosolic domain. The transmembrane region itself contains ten helices (Vandecaetsbeek, *et al.*, 2009). The transmembrane helices anchor SERCA to the lipid bilayer and allow the transport of calcium. Along with the transmembrane domain, SERCA is comprised of the cytoplasmic headpiece and the stalk domain. The cytoplasmic headpiece of the SERCA molecule is exposed on the cytoplasmic surface of the membrane. The phosphorylation and nucleotide binding domains reside in the cytoplasmic headpiece of SERCA along with four other subdomains. The active site of ATP hydrolysis is composed of the phosphorylation domain and the nucleotide binding domain which are structurally and functionally closely related. The remaining stalk domain bridges a connection between the cytoplasmic headpiece and the membrane (Voss, *et al.*, 2008). Figure 1.7A shows the conformational structure of SERCA, labelled with the active site Asp351 and redox regulated Cys674. Figure 1.7B is an approximate schematic of the SERCA structure.

A



B

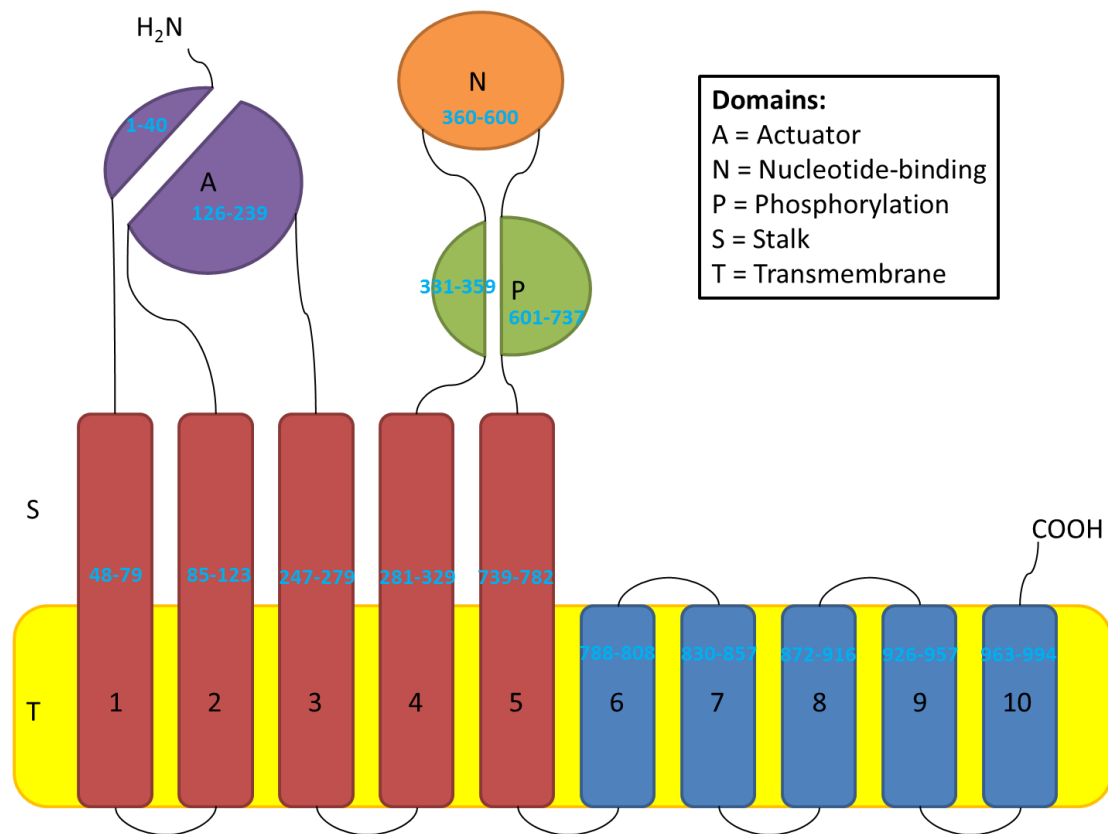


Figure 1.7. 3D crystal structure and approximate schematic of SERCA. A. 3D crystal structure of SERCA with colour coded domains. B. Schematic of SERCA structure with approximate amino acid positions labelled in light blue.

Isoform SERCA2b has a two times higher calcium affinity and lower catalytic turnover rate compared to the other two muscle isoforms SERCA1 and SERCA2a. This is due to SERCA2b's 49 residue lengthened tail at the C-terminus which contains an additional transmembrane helix (TM11) and luminal extension (Vandecaetsbeek, *et al.*, 2009).

Previous studies have shown that when senescent skeletal muscle was compared with young skeletal muscle, it had conformationally changed and its stability had decreased. This was thought to be linked to muscle weakness in ageing and prolonged relaxation times due to decreased calcium uptake by SERCA. The conformational changes were linked to SERCA inactivation, protein unfolding, and aggregation in conditions of mild heating. It had also been noted that particular residues around the nucleotide binding site (Lys515) such as Cys498, Cys525, and Tyr497 would be likely candidates to reduce conformational stability. SERCA2a was found to decrease in activity with age compared to SERCA1. This could be due to the different oxidative modifications that both isoforms undergo and result in slow-twitch muscles being more affected by oxidation compared to fast-twitch muscles (Chen, *et al.*, 1999).

More recent studies have now shown that the more important residues include Cys674 which is the most reactive thiol in SERCA and plays a major role in enzyme activity regulation (Dalle-Donne, *et al.*, 2007), and Tyr122 located on the more accessible region of the cytosolic domain on the N-terminus (Schoneich, 2005).

One study in particular compared the nitration of tyrosine in young adult skeletal muscle and senescent skeletal muscle. When young adult skeletal muscle was compared with senescent skeletal muscle, it showed a 40% decrease in SERCA activity. In young adult skeletal muscle there was a value of around 1 mol of nitrotyrosine per mol of SERCA2a compared to around 3.5mol of nitrotyrosine per mol of SERCA2a that was found in senescent skeletal muscle. The tyrosine residues modified in the young adult SERCA2a were: Tyr122, Tyr130, Tyr497, Tyr586, and Tyr990. In the senescent SERCA2a, the tyrosine residues modified were the same as the ones in the young adult with additional oxidation at Tyr294, Tyr295, and Tyr753. Reduced SERCA activity in ageing was suggested to be

related to the nitration of Tyr294, Tyr295, and Tyr753. Further analysis with SERCA2a from both young adult and senescent skeletal muscle showed that Tyr753 was present in young adult skeletal muscle and Tyr294, Tyr295, and Tyr753 were all present in senescent skeletal muscle. This meant that age-related decrease in SERCA activity were most likely due to Tyr294 and Tyr295. Confirmation of this involved mutating the Tyr753 residue which showed no change to SERCA activity. The study then looked upon the mechanism by which modifications to Tyr294 and Tyr295 affected SERCA activity. It was found that oxidation to these specific tyrosine residues downregulated ATP utilisation by SERCA. Because both tyrosine residues are located on the M4 helix, which is in line with the M5 helix containing the phosphorylation site Asp351, the helix to helix interaction is distorted and disrupts the coupling of calcium transport with ATP-linked phosphorylation resulting in the prevention of optimal rates of active transport (Knyushko, *et al.*, 2005).

1.6.2. Protein oxidation studies in SERCA

In some tissues, HOCl concentrations have been reported to reach 200 μM . One study showed that SERCA activity was inhibited by 50% in the presence of 170 μM HOCl and was completely inhibited by 3mM HOCl. It was found that the 50% inhibition would have approximately oxidised two thiol (SH) groups to disulfides disrupting SERCA's activity. This was further supported by using disulfide reducing agents to recover ATPase activity and Ca^{2+} uptake. 55% of the lost ATPase activity was recovered through this. The partial recovery gained from this treatment indicated that disulfide bonds were formed through HOCl-mediated oxidation. This same study also suggests that oxidation of SH groups by HOCl may be linked to conformational changes to the nucleotide binding site within SERCA. Also the most likely candidate for this alteration is cysteine as it is 100 times more reactive to HOCl compared to the other amino acids (Favero, *et al.*, 1998).

Lysine residues are a major site of reaction of HOCl with many proteins. Chloramine species are produced which decompose to nitrogen-centred protein radicals that induce protein

backbone fragmentation and dimerisation. Low sub-lethal doses of HOCl react with thiols and can initiate apoptosis whereas high concentrations cause rapid necrosis. HOCl decreased SERCA activity by 50% at a 150 $\mu\text{mol/l}$ concentration. Incubation with HOCl also resulted in fragmentation as a new band was formed around 75kDa. Structural alteration of the ATP nucleotide binding site was assessed through the binding of FITC at specific lysine residue Lys515 present in the binding site. The decrease in FITC fluorescence was HOCl concentration dependent (Strosova, *et al.*, 2009b).

Eleven of the thirteen tryptophan residues in SERCA are located in the transmembrane domain of the protein whereas the other two are located in the cytoplasmic domain. It was found that there was no link between the reduction in SERCA activity following HOCl exposure and the conformational changes of the transmembrane domain. However, this is different to other oxidants where hydrogen peroxide (H_2O_2) mediated oxidation showed a link between enzyme activation and conformation changes through tryptophan fluorescence (Strosova, *et al.*, 2009b).

One study showed SERCA activity to be reduced to 50% in the presence of the $\text{Fe}^{2+}/\text{H}_2\text{O}_2/\text{Ascorbic Acid (AA)}$ Fenton reaction. Oxidation of cysteine led to a decrease in thiol groups and the formation of disulphide bonds. Carbonyl formation was also detected and fragmentation occurred possibly due to structural alterations which formed two bands: ~ 50 and $\sim 75\text{kDa}$ (Voss, *et al.*, 2008).

Low levels of nitric oxide can protect ryanodine receptor (RyR) from activation by protein cross-linking whereas higher levels of nitric oxide result in cysteine S-nitrosation occurring which would activate RyR. Nitric oxide's effect is different to other oxidants such as hydrogen peroxide where RyR is inactivated. In comparison to peroxynitrite, nitric oxide is more efficient but less selective in cysteine modification of SERCA. Complete modification of Cys364 results in a 38% decrease of SERCA activity and labelling of Cys344 and Cys364 lead to an inactivation of the enzyme. The most reactive cysteine residues to nitric oxide were: Cys364, Cys670, Cys471, and Cys349. The locations of the cysteine residues were

adjacent to Asp351 phosphorylation site (Cys349 and Cys364), in the nucleotide binding domain (Cys471), and before the hinge domain (Cys670) (Viner, *et al.*, 2000).

Low levels of nitric oxide are also known to be able to activate SERCA through S-glutathiolation at either Cys669 or Cys674 (Strosova, *et al.*, 2009b). However, at higher levels of nitric oxide derived peroxynitrite, SERCA activity is inhibited through irreversible oxidation. Cys674 is oxidised to sulphonic acid where the irreversible oxidation prevents S-glutathiolation and increased activity of SERCA by low levels of nitric oxide or peroxynitrite (Adachi, *et al.*, 2004).

As well as S-glutathiolation, nitric oxide is also able to produce S-nitrosothiol modifications (SNO) on cysteine residues. One study showed SNO-adduct formation when SERCA was exposed to nitric oxide gas and the mass of peptides, which included cysteine residues in their sequence, increased by 29Da (Ying, *et al.*, 2007).

Previous experiments show a comparison of nitrotyrosine oxidative modifications on SERCA2a in old and young rats where the 28 month old rats had 3.5 mols of nitrotyrosine per mol of SERCA2a and the 5 month old young rats had 1.0 mols of nitrotyrosine per mol of SERCA2a. It was also shown that Tyr294 and Tyr295 when nitrated have an effect on the function of SERCA. Both the modified tyrosines in the M4 helix may affect either calcium binding or protein conformation around the Asp351 phosphorylation site. Not only do tyrosine residues become affected by peroxynitrite but both SERCA1 and SERCA2a are shown to have a significant age-dependent loss of reduced cysteine residues. Smooth muscle SERCA2 can be activated through S-glutathiolation of Cys669 and/or Cys674 in the presence of low concentrations of nitric oxide and peroxynitrite. Higher concentrations result in the inactivation of SERCA where the cysteine residues affected most were: Cys614 (~46%), Cys561 (~45%), Cys674/675 (~40%), and Cys498 (~31%) (Schoneich and Sharov, 2006).

One study showed senescent mouse models had around 3.5mol of nitrotyrosine per mol of SERCA2a, and this correlated with a decrease in 40% activity. The tyrosine residues modified to 3-nitrotyrosine are: Tyr122, Tyr130, Tyr294, Tyr295, Tyr497, Tyr586, Tyr753,

and Tyr990. The age-dependent decrease in SERCA activity was shown to be due to nitration of Tyr753, Tyr294 and Tyr295. However, it is Tyr294 and 295 that show to play a major role in the loss of activity of calcium transport. SERCA1 however does not undergo tyrosine nitration and therefore peroxynitrite-mediated protein oxidation results in 1.3mol of cysteine oxidation per mol of SERCA1 with a 17% decrease in activity. This decrease in activity is found to be related to the oxidation of Cys349. Glutathiolation of Cys674 in the presence of low levels of peroxynitrite (10-100 μ M) shows a 25-35% increase in activity. Higher levels of peroxynitrite result in irreversible oxidation of cysteine to sulfonic acid and nitrotyrosine formation which result in a decrease in activity. The location of Tyr294 and Tyr295 is important to the effects on activity as they are located on the luminal end of the membrane-spanning helix (M4) in line with the phosphorylation site Asp351. In order to couple ATP phosphorylation with calcium transport, the M4 helix is relied upon for high-affinity calcium binding and so its structure is important. Distortion of the M4 helix will result in alteration in helix-helix (M4-M5) interactions and affect optimal rates of active transport by SERCA (Knyushko, *et al.*, 2005). In this same study it was also shown that methionine sulphoxide was formed as well as nitrotyrosine. These oxidative modifications occurred on Met126, Met494, Met508, Met598, Met756, and Met979.

Another study showed that SERCA1 oxidation with 3mM peroxynitrite resulted in five cysteine residues modified *in vivo* and *in vitro*: Cys525, Cys674, Cys675, Cys498, and Cys938. Cys364, Cys417, and Cys420 were affected only by peroxynitrite *in vitro* and Cys561, Cys636, Cys614, Cys377, and Cys774 were partially lost during *in vivo* ageing. Loss of SERCA activity was shown to correspond to peroxynitrite oxidation at Cys674/675 and Cys938. It was found that ligand-binding studies showed no significant changes in aged SERCA1 Ca²⁺ or ATP affinity whereas peroxynitrite mediated oxidation inactivated SERCA and resulted in a reduction in Ca²⁺ affinity. This suggested that there were either changes in the calcium-binding domains or domains that regulate high-affinity calcium-binding. It was also found that there was no detection of cysteine residues that had been modified in the vicinity of the high-affinity Ca²⁺ binding sites. This lead to the implication that the effects on

catalytic function by cysteine oxidation could have been caused by a change in protein structure resulting in ATP hydrolysis uncoupling from Ca²⁺ translocation (Sharov, *et al.* 2006a).

When comparing the two isoforms SERCA2a and SERCA1 it was found that *in vitro* tyrosine nitration by peroxynitrite modified different tyrosine residues in each isoform. SERCA1 was predominately nitrated at Tyr122 while SERCA2a was predominately nitrated at Tyr294, Tyr295, and Tyr753. This contrasted *in vivo* detection of nitrated tyrosine residues in SERCA2a as Tyr122 and Tyr130 were the residues that were modified (Schoneich, 2005). Another study showed that Tyr122 modification in skeletal muscle SERCA1 was not detected *in vivo* but had not been detected *in vitro* nitration. Similarly, Tyr122 and Tyr130 were found in SERCA2a *in vitro* peroxynitrite experiments but not *in vivo*. It has been suggested that cellular correction mechanisms might remove the nitrated peptides through degradation or nitrotyrosine to tyrosine enzymatic conversion; however, it is not known yet what really occurs (Knyushko, *et al.*, 2005).

1.7. Aim of project

Many of the previous studies on the effects of oxidation on SERCA have been very specific to a particular amino acid. Exploring a more global analysis of protein oxidation determined susceptibility of residues to particular modifications. While the study had a particular focus on SERCA, other proteins were also analysed. The applications of the MS studies determined the role of oxidation in the aged and obese models and led to comparisons to determine whether protein oxidation affects the models in a similar or different manner.

Therefore, the objectives of the project were as follows:

- To develop mass spectrometry techniques for analysing oxPTMs in mouse muscle.
- To test the MS methodologies developed in muscle tissue from animals with sarcopenia, specifically obesity and aged animals.

Chapter 2

Materials & Methods

2.1. Materials

2.1.1. Animals

Hind legs from 8 months old NMRI (control) and age matched ob/ob (obese) mice were obtained from the Aston University Biomedical facility with permission from the licence holder: Dr Steve Russell, Aston University. Young (9 months) and aged (2 years & 3 months) C57BL/6 gastrocnemius mouse muscle was kindly supplied by Malcom Jackson, University of Liverpool. Experiments were performed under the guidelines of the United Kingdom Home Office in the United Kingdom Animals (Scientific Procedures) Act 1986. The animals were culled by cervical dislocation and the muscles were dissected from the hind legs.

2.1.2. Reagents

PiColorLock Gold kit was obtained from Innova Biosciences, Cambridge, UK. Protease inhibitor cocktail cComplete, EDTA free was purchased from Roche, Welwyn Garden City, UK. MS grade formic acid, sodium hypochlorite (NaOCl), thapsigargin, Laemmli buffer, rabbit polyclonal anti-nitrotyrosine and mouse monoclonal anti-rabbit IgG (γ -chain specific) horse radish peroxidase antibody was also acquired from Sigma-Aldrich, Dorset, UK. MS grade trypsin and ProteaseMax surfactant, trypsin enhancer was sourced from Promega, Southampton, UK. Instant blue Coomassie stain was acquired from Expedeon, Cambridge, UK. Polyvinylidene fluoride (PVDF) membrane and rabbit polyclonal anti-S-Nitroso-Cysteine (SNO-Cys) antibody was attained from Millipore, Watford, UK. Tween 20 was purchased from Fisher Scientific, Loughborough, UK. SuperSignal West Pico Chemiluminescent substrate (ECL reagent) and Pierce Coomassie Plus (Bradford) assay kit was purchased from ThermoFisher Scientific, Loughborough, UK. Goat anti-mouse IgG horse radish peroxidase antibody, mouse anti-SERCA antibody and mouse anti-calnexin antibody were obtained from Santa Cruz, Heidelberg, Germany. All other chemicals were sourced from Sigma-Aldrich and Fisher Scientific.

2.2. Sarcoplasmic reticulum preparation from mouse hind leg skeletal muscle

Sarcoplasmic reticulum (SR) extraction was performed based on a protocol by MacLennan, 1970. Mouse skeletal muscle was acquired from hind legs of the different mice models and was homogenised using an Ultraturrax in 25 mM PIPES containing 0.3 M sucrose with the addition of 1 tablet of the protease inhibitor cocktail per 50 ml buffer. This was centrifuged at 6500g for 30 minutes at 4°C. A sample was taken at this stage and stored at -80°C for analysis of muscle lysate. The supernatant was then further centrifuged at 100,000g for 40 minutes at 4°C. The pellet was resuspended in 10% sucrose in 25 mM PIPES, pH 7.4. This was layered on top of a sucrose gradient made by sequential layers of 2 ml of 40%, 30%, 20% and 10% sucrose in 25 mM PIPES, pH 7.4 and centrifuged at 100,000g for 18 hours at 4°C. The interface between 30% and 40% sucrose was recovered and the sucrose concentration was lowered by the addition of 2 ml of 25 mM PIPES containing 0.4 M KCl. This was centrifuged at 10,000g for 40 minutes at 4°C. The pellet was resuspended in 100 µl of 5 mM HEPES containing 0.4 M sucrose with the addition of 1 tablet of protease inhibitor cocktail per 50 ml of buffer and stored at -80°C. Methionine was added to all buffers to give a final concentration of 5mM, and they were also bubbled with oxygen-free nitrogen gas to reduce the dissolved oxygen.

2.3. Protein concentration determination of sarcoplasmic reticulum

Protein concentration was determined by a Bradford assay kit and read by absorbance spectroscopy at 570 nm. BSA standards ranged from 25 µg/ml to 2 mg/ml. This was carried out by dispensing 10 µl of each standard into a 96 well plate along with the samples from the muscle preps. An addition of 300 µl of Coomassie plus reagent was added to each well and the plate was incubated at 37°C for 30 mins. The absorbance was read and a linear curve was generated from the known concentrations in order to calculate the protein concentration of the samples.

2.4. Assay of SERCA specific activity through free phosphate release

SERCA specific activity was determined using a phosphate release assay using Pi colour lock gold kit and read by absorbance spectroscopy at 630 nm. Thapsigargin, a known, SERCA inhibitor was used to measure function (Lytton, Westlin, and Hanley, 1991). 5 µg of the isolated sarcoplasmic reticulum sample was resuspended in 500 µl of assay buffer. The assay buffer contained 40 mM HEPES (pH 7.2), 0.1 M KCl, 5.1 mM MgSO₄, and 1mM EGTA. SERCA activity was detected in the presence of final concentration 1 mM CaCl₂ and 2.1 mM ATP, with and without a final concentration of 100 nM thapsigargin. The control was the final concentration of 1 mM CaCl₂ and 2.1 mM ATP with the absence of the isolated sarcoplasmic reticulum sample. The activity of SERCA was calculated by subtracting the rate of phosphate release in the presence of thapsigargin from the rate of phosphate release in the absence of thapsigargin. Phosphate (NaH₂PO₄) standards ranged from 100 µM to 2 mM. The activity was expressed in µmol of free phosphate min⁻¹. The specific activity was calculated by dividing the activity by the amount of sample protein used in the assay in mg, to give a value in µmol of free phosphate min⁻¹ mg⁻¹ protein.

2.5. Oxidant treatment of sarcoplasmic reticulum extracted samples

For HOCl treatment, sodium hypochlorite (NaOCl) molarity was determined by reading four different dilutions of the NaOCl stock in 0.1 mM NaOH using absorbance spectroscopy at 290 nm with an extinction coefficient of 350. The dilutions were as follows: 1:1000, 1:2000, 1:2500 and 1:5000. The isolated sarcoplasmic reticulum (5 µg protein) and muscle homogenate (25 µg protein) samples was oxidised with NaOCl in 100 mM phosphate buffer at total volume of 100 µl for 1 hr at 37°C at molar ratio concentrations varying from 1 µM: 10 µM to 1 µM: 1 mM (protein: oxidant). Oxidation was stopped by the addition of 5µl of excess methionine and dried down to around 10 µl by vacuum centrifugation in an Eppendorf concentrator.

2.6. 10% sodium dodecyl sulphate polyacrylamide gel electrophoresis (SDS-PAGE)

10% SDS-PAGE gels were made with acrylamide and bis-acrylamide according to the Laemmli method (Laemmli, 1970). Muscle lysate samples (25 µg protein) and SR samples (5 µg protein) were solubilised in equal volumes of Sigma laemmli buffer, incubated at 100°C for 5 mins, cooled and electrophoresed at a constant 125 V with a pre-stained ladder (Fig.2.1). The gel was stained overnight in 45% methanol, 10% acetic acid, and 0.1% Coomassie blue. It was then destained in the same solution minus the Coomassie blue. Alternatively, the gel was stained with Expedeon Instant blue Coomassie stain. Gels were photographed using a Syngene G-box by selecting automatic imaging and choosing the Coomassie stained protein gel option.



Figure 2.1. Thermo Scientific PageRuler Plus Prestained Protein Ladder, 10 to 250 kDa. Molecular weights are pre-stained and so are visible for the duration of the electrophoretic separation and prior to staining. MW ~70, ~25 and ~10 are coloured differently to allow user to distinguish molecular weights more easily. (Manufacture's image: www.thermofisher.com/order/catalog/product/26619)

2.7. Western blotting using anti-SERCA, anti-calsequestrin, anti-nitrotyrosine and anti-nitrosothiol antibodies

After electrophoresis, the SDS-PAGE gel was sandwiched between western pads, filter papers and PVDF membrane (Fig.2.2). Subsequently, the transfer process took place at a constant 125 V for 1.5 hr. The PVDF membrane was then placed in blocking reagent (5% milk powder in TBST) for 1 hr. Tris buffered saline with Tween 20 (TBST) contained 20 mM Tris, 144 mM NaCl, and 0.1% Tween 20 at pH 7.6. Immunostaining was carried out with the following primary antibodies. Mouse anti-SERCA (1: 1000), mouse anti-calsequestrin (1: 1000), rabbit anti-nitrosothiol (1: 1000), and rabbit anti-nitrotyrosine (1: 1000) were diluted in TBST containing 2.5% milk powder. The membrane was incubated in primary antibody overnight. After washing with TBST, it was transferred to a solution of secondary HRP conjugated goat anti-mouse antibody (1:2000) or mouse anti-rabbit antibody (1: 10000) diluted in PBS pH 7.3, for 3 hours. After washing with TBST, ECL reagent was made by adding equal volumes of the luminol reagent and peroxide reagent to a 1 ml solution and poured onto the membrane. The membrane was scanned using a Syngene G-box by selecting automatic imaging, chemiluminescence ECL and using the default exposure time.

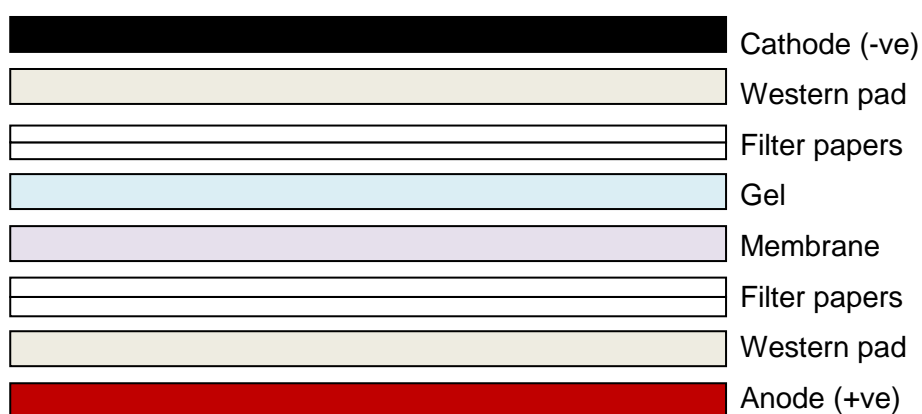


Figure 2.2. Assembly of western sandwich. Using a western blot cassette, usually colour coded with black and red to represent sides of the cathode and anode, the subsequent components were pre-wetted in transfer buffer and layered in the following order: western pad, two filter papers, gel, membrane, additional two filter papers and another western pad from black to red, carefully removing any air bubbles using a roller or pipette tip. The cassette was locked and placed into the tank with transfer buffer. Proteins moved from the gel towards the membrane.

2.8. Oxyblotting using anti-DNP antibody

For oxyblotting, oxidised samples were dried down to 5 μ l by vacuum centrifugation and 12% SDS was added at a 1:1 (v/v). The samples were derivatised by the addition of 10 μ l of 10 mM DNPH in 2M HCl and incubated for 25 minutes at room temperature. They were then neutralised by the addition of 7.5 μ l of 2 M Tris, 30% glycerol and 19% β -mercaptoethanol. Samples were electrophoresed on a 10% SDS-gel and western blotting was carried out as described in section 2.7 but with primary rabbit anti-DNP antibody (1:500) and secondary mouse anti-rabbit IgG antibody (1:1000).

2.9. In-gel tryptic digestion of desired excised bands of SR sample

The desired gel bands were excised from the gel. If the gel was stained with instant blue Coomassie stain and the stain was removed with 30% acetone at 60°C. Gel slices were washed in 100 mM ammonium bicarbonate for 1 hour and then in 1:1 100 mM ammonium bicarbonate : acetonitrile for another hour. The gel slices were reduced by incubation in 100 mM ammonium bicarbonate containing 45 mM DTT and for 30 mins at 60°C and then cooled and left in the dark with the addition of 100 mM iodoacetamide. Gel slices were washed again in 1:1 100 mM ammonium bicarbonate : acetonitrile for 1 hour. Acetonitrile was added and after 10 mins the gel bands were dried in a speed vacuum at 30°C for 15 mins. 2 μ g of MS grade trypsin was added together with 25 mM ammonium bicarbonate and incubated overnight at 37°C. The gel slices were centrifuged at 13,000 g for 5 mins and the liquid was stored in a fresh microcentrifuge tube. 20 μ l of 5% formic acid was added and incubated at 37°C for 20 mins. 40 μ l of acetonitrile was added and further incubated at 37°C for another 20 mins. Once again, the gel bands were centrifuged at 13,000g for 5 mins and the liquid was pooled with the initial extract, and dried in a vacuum centrifuge at 30°C for 45 mins. Alternatively, with the use of ProteaseMax surfactant, trypsin digestion was shortened to 1 hr at 50°C with 1 μ g of trypsin in 0.01% ProteaseMax: 50 mM ammonium bicarbonate.

2.10. Settings for QToF system

2.10.1. NanoHPLC for the QToF system

Eluent A consisted of 98% water, 2% acetonitrile, and 0.1% formic acid and Eluent B contained 98% acetonitrile, 2% water, and 0.1% formic acid. Digested peptides were eluted using a Dionex Ultimate 3000 nano-high performance liquid chromatography (HPLC) 1 hr elution programme. The autosampler was set to take 10 μl of the sample from the sample vial, which was initially retained on a C18 Acclaim 300 μm I.D. x 15 cm trap and then separated on a C18 Acclaim PepMap100 75 μm I.D. x 15 cm 3 μm particle size nanocapillary HPLC column. The HPLC gradient was as follows: from 0-4 min 2% Eluent B, from 4-49 min 45% B, from 49-50 min 90% B, from 50-54 min 90% B, from 54-55 min 2% B, and from 55-65 min 2% B (Fig.2.3). The loading pump was set at a flow rate of 30 $\mu\text{l}/\text{min}$ of Eluent A and the nano pump was set to a flow rate of 0.3 $\mu\text{l}/\text{min}$.

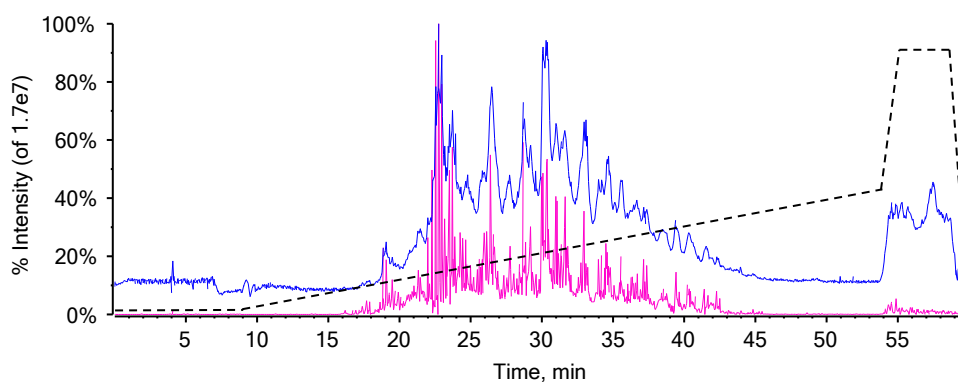


Figure 2.3. Reversed phase elution profile of sample run on nanoHPLC. First 5 min account for dead volume. The rest of the gradient is explained in section 2.10.

2.10.2. Tandem Mass spectrometry on the QTOF system

Digested samples were analysed using 5600 QTOF mass spectrometer (AB SCIEX, Warrington, UK) using electrospray ionisation (ESI). The source temperature was set at 150°C with a curtain gas flow of 25, a source gas of 12, ion spray voltage of 2.5kV and a declustering potential of 50. For the information dependent acquisition (IDA) experiment, survey scans were collected for 0.25 sec in QToF MS positive ion mode for a mass range m/z 350 to 1250. IDA parameters were set to select charge states between 2 to 5 and signals which exceeded 200 cps. Isotopes were excluded within 3 Da with a mass tolerance of 50 ppm, and former target ions were excluded for 12 sec. The maximum number of candidate ions monitored per cycle was 10. For the product ion scans rolling collision energy was enabled with collision energy spread set at 15 and an accumulation time of 0.2 sec in positive ion mode and high sensitivity. The mass range was set to 50 to 2000 Da

2.10.3. Pseudo-Multiple reaction monitoring on the QTOF system

Source settings were the same as above. For MRM, product ion scans were collected with an accumulation time of 0.2 sec in positive ion mode. Mass ranges were set depending on peptides of interest and Skyline software (University of Washington) was used to analyse the data (MacLean *et al.* 2010). This was done with high sensitivity and unit resolution with a declustering potential of 50. Collision energy was calculated using the equation $y=0.044x+5$ for 2+ charge ions and $y=0.05x+4$ for 3+ charge ions. The several variations of the targeted scans are explored in section 3.2.4.

2.11. Settings for QTRAP system

2.11.1. NanoHPLC for the QTRAP system

Eluent A consisted of 98% water, 2% acetonitrile, and 0.1% formic acid and Eluent B contained 98% acetonitrile, 2% water, and 0.1% formic acid. Peptides were eluted using a Dionex Ultimate 3000 high performance liquid chromatography (HPLC) system. The autosampler was set to take 10 μ l of sample from the sample vial which was initially trapped

on a C18 Acclaim 300 μm I.D. x 15 cm trap and then separated on a C18 Acclaim PepMap100 75 μm I.D. x 15 cm 3 μm particle size HPLC column. The HPLC gradient was as follows: from 0-4 min 5% B, from 4-49 min 40% B, from 49-51 min 90% B, from 51-56 min 90% B, from 56-58 min 5% B and from 58-63 min 5% B. Loading pump was set at a flow rate of 30 $\mu\text{l}/\text{min}$ of Eluent A and Micro pump was set to a flow rate of 0.2 $\mu\text{l}/\text{min}$ generated by a 1:1000 flow splitter.

2.11.2. Multiple reaction monitoring settings

Digested samples were analysed with an AB Sciex 5500 Q-TRAP mass spectrometer (AB SCIEX, Warrington, UK) using nanoESI in positive ion mode. Source collision gas was set to high with curtain gas of 20, ion source gas of 13 and ion spray voltage of 2.4kV with a declustering potential of 50, entrance potential of 10, and collision cell exit potential at 12. For the MRM scans, transition masses were set depending on peptides of interest analysed and Skyline software (University of Washington) was used to analyse the data. Resolution for both Q1 and Q3 was set at unit and collision energy was calculated using the equation $y=0.044x+5$ for 2+ charge ions and $y=0.05x+4$ for 3+ charge ions. For Enhanced MS, the mass range was set to between 400 and 1000 Da and scan rate was 10000 Da/sec. Declustering potential was set to 50, entrance potential to 10, collision energy to 10 and dynamic fill time enabled with ion densities set at the instrument default. The Q3 entry barrier was set to 8V.

2.12. Data analysis

Raw data files (.wiff) produced from MS runs were converted by PeakView (AB SCIEX, Warrington, UK) software (.mgf) to run Mascot analysis (Matrix Science, London, UK) (Perkins *et al.* 1999). The spectra generated from MS were matched against the SwissProt database to identify the proteins and modifications within the samples. Each sample file was analysed with the parameters shown in Table 2.1. While not all modifications were run in one search, separate searches with the different combinations of modifications were performed and the results were amalgamated.

Table 2.1. Parameters used for MS/MS analysis with Mascot. All parameters except variable modifications were used as a standard setting for each Mascot run.

Parameter	Setting
Taxonomy	Mus musculus
Database	SwissProt
Enzyme	Trypsin
Max. missed cleavages	1
Peptide charge	2+, 3+, and 4+
Peptide tolerance	0.5 Da
MS/MS tolerance	0.5 Da
Instrument	ESI-QUAD-TOF
Fixed Modifications	Carbomidomethyl (C)
Variable modifications	Oxidation (M), Oxidation (Y), Oxidation (P), Oxidation (HW), Dioxidation (M), Dioxidation (W), Trioxidation (C), Nitro (Y), Chlorination (Y), Allysine (K)

Protein hits were assessed by a Mascot score of over 50 and an ion score of more than 20. Peptides reported as modified were validated by manual *de novo* sequencing using PeakView software (AB SCIEX, Warrington, UK). PeakView software was also used for MRM analysis of raw data files (.wiff) generated from MRM runs.

2.13. Online software

Protein Analysis Through Evolutionary Relationships (PANTHER) is an online tool that was used to categorise proteins upon their biological functions. PANTHER is part of the Gene Ontology Reference Genome Project and is supported by the Thomas Lab at the University of South California (Thomas *et al.* 2003). The list of protein IDs were submitted using a txt. document format to the online tool. Panther then categorised the proteins and displayed the results in a pie chart format. The data was then taken from the online tool to express changes in protein detection by MS/MS.

Development of mass spectrometry methods for the identification and quantification of oxidised proteins in muscle

3.1. Introduction

In order to build a set of methods to explore the effects of oxidative stress to the muscle proteome, a series of developmental procedures were undertaken during the course of the study to generate a workflow best suited to the application of MS technology in oxPTM detection. Many studies in the literature encompass emerging techniques and improvements to the gold standard procedures widely used in the MS field. More specifically, numerous methods have been generated for the assessment of oxidative modifications in both *in vitro* and *in vivo* systems to determine the role of these modifications in diseased and aged models (Berlett & Stadtman, 1997; Sharov, *et al.* 2006a).

3.1.1. Oxidation in muscle

Oxidants in the muscle under healthy circumstances are generally maintained by the body's redox homeostasis. These include adaptive and protective mechanisms most notably including enzymes such as methionine sulphoxide reductase (MSR) to reverse methionine oxidation (Stadtman, Moskovitz and Levine, 2003). Some oxidants even play a role in maintaining redox homeostasis, e.g. nitric oxide has a role in vascular dilation (Joyner and Dietz, 1985). Research has suggested basal levels of oxidation are better for the adaptive system (Yan, 2014). As discussed in the introduction, the imbalance of the redox system can lead to excess oxidant production and damage to surrounding biomolecules. This imbalance has been suggested to occur in diseases and ageing although many would refute the theory that oxidants are the cause of disease or ageing progression.

3.1.2. Methods for detecting oxidative stress

In order to understand what the association is between oxidative stress and these diseases, MS techniques were employed. MS is a quantitative tool used to detect post-translational modifications (PTMs). It uses soft ionisation to charge the peptides of a digested protein and detects these ions that are deflected by an electromagnetic field. The separated peptides

can be further fragmented to produce a fingerprint sequence to determine the position and identification of the PTM. The limiting factor of this method is that the detection is of abundant peptides. Searching for low abundance modifications is difficult. To get around this problem, *in vitro* oxidation was used to generate different levels of modification and possibly increasing abundance of low level modifications to detectable levels.

3.1.4. Aims

This chapter focuses on three aspects of methodology development: optimisation of sample processing methods with focus on sequence coverage and regulation of oxidative artefacts using the control (NMRI mice), preliminary development of MS techniques using *in vitro* oxidised samples, and further optimisation of quantitative MS methods for *in vivo* samples. These three core subjects demonstrated the workflow undertaken to attain methods best suited for the identification and quantitation of oxPTMs of muscular proteins.

The aim of this study was to optimise current MS methods used for the analysis of oxidative modifications of proteins for the application of non-labelling approaches to characterise and quantify oxPTMs in muscle tissue.

3.2. Results

Cleared muscle homogenate and isolated sarcoplasmic reticulum were obtained from the hind leg of the mice models to assess the need for sample purification prior to MS for the identification and quantification of oxPTMs. This allowed investigation of whether MS methods are sensitive enough for characterisation and quantitation in a complex mixture of proteins, such as that in the muscle homogenate, or whether a purified sample is required to lessen competing proteins and increase the abundance of specific proteins within the sample. By isolating the SR, and assuming good purification of the sample, the majority of peptides within the sample should originate from SR proteins. In order to test the limitations of these two types of samples, it is important to produce methods that optimise the efficiency of the MS analysis.

3.2.1. Optimisation of sequence coverage in isolated sarcoplasmic reticulum and cleared muscle homogenate

First and foremost an attempt was made to optimise the sequence coverage of proteins in the control model so that sufficient coverage was attained to maximise the number of modifications detected by MS. The first step in this study was to compare SERCA sequence coverage in both the MH and SR samples through gold standard tryptic digestion (Fig. 3.1). The band at around 100 kDa molecular weight (MW) was excised, proteins were then subjected to tryptic digestion and the resulting peptides from the digestion were submitted to a MS/MS search using the QToF instrument. Higher sequence coverage was found in SR in comparison to MH which was expected as the steps to isolating SR removes proteins and therefore there was a higher abundance of SERCA within the band cut around the 100 kDa MW. With fewer competing proteins the top hits are more likely to include the abundant protein of interest. In this case, more peptides from SERCA were detected as the top abundant ions and selected for fragmentation for MS/MS.

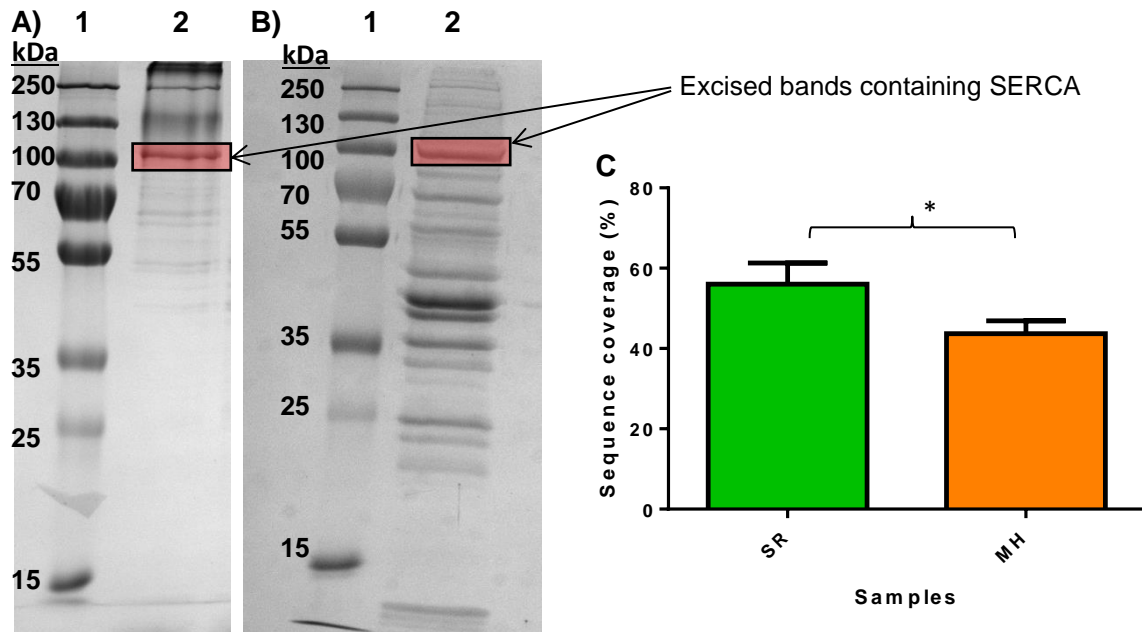


Figure 3.1. SDS-page gel scans of isolated SR and MH and corresponding sequence coverages of SERCA. A. Protein ladder loaded in lane 1 and isolated SR in lane 2. B. Protein ladder in lane 1 and MH in lane 2. The red boxes highlight where SERCA protein resides according to its molecular weight. C. Difference in SERCA sequence coverage for SR and MH samples. * $P < 0.05$ (Unpaired t-test).

Protein: **SERCA1**
Sequence Coverage: **48%**

```

1  MEAAHSKSTE ECLSYFGVSE TTGLTPDQVK RHLEKYGPNE LPAEEGKSLW
51 ELVVEQFEDL LVRILLLAAC ISFVLAWFEE GEETVTAFVE PFVILLILIA
101 NAIVGVWQER NAENAIEALK EYEPENMGKVV RADRKSVQRI KARDIVPGDI
151 VEVAVGDKVP ADIRILSIKS TTLRVDQSIL TGESVSVIKH TDPVPDPRAV
201 NQDKKNMLFS GTNIAAGKAV GIVATTGVST EIGKIRDQMA ATEQDKTPLQ
251 QKLDEFGEQL SKVISLICVA VWLNIGHFN DPVHGGSWFR GAIYYFKIAV
301 ALAVAAIPEG LPAVITTCCLA LGTRRMAKKN AIVRSLPSVE TLGCTSVICS
351 DKTGTLTTNQ MSVCKMFIID KVDGDVCSLN EFSITGSTYA PEGEVLKNDK
401 PVRAGQYDGL VELATICALC NDSSLDNET KGVYEKVEA TETALTTLVE
451 KMNVFNTVR SLSKVERANA CNSVIRQLMK KEFTLEFSRD RKSMSVYCSP
501 AKSSRAAVGN KMFVKGAPEG VIDRCNYVRV GTRRVPLTGP VKEKIMSVIK
551 EWGTGRDTRL CLALATRDTP PKREEMVLDL SAKFMEYEMD LTFVGVVGM
601 DPPRKEVTGS IQLCRDAGIR VIMITGDNKG TATAICRRIG IFSENEEVD
651 RAYTGREFDD LPLAEQREAC RRACCFARVE PSHKS KIVEY LQSYDEITAM
701 TGDGVNDAPA LKKAIEIGIAM GSSTAVAKTA SEMLADDNF STIVAAVEEG
751 RAIYNNMKQF IRYLISNVG EVVCIFLTAA LGLPEALIPV QLLWVNLVTD
801 GLPATALGFN PPDLDIMDRP PRSPKEPLIS GWLFFRYMAI GGYVGAATVG
851 AAAWWFLYAE DGPHVSYHQL THFMQCTEHN PEFDGLDCEV FEAPEPMTMA
901 LSVLVTIEMC NALNSLSENQ SLLRMPPWVN IWLLGSICLS MSLHFLILYV
951 DPLPMIFKLR ALDFTQWLMV LKISLPVIGL DELLKFIARN YLEG

```

Figure 3.2. Representative sequence coverage of SERCA attained by tryptic digestion. Peptides identified by MS are shown in red. Regions highlighted in yellow correspond to transmembrane domains.

Although higher sequence coverage was obtained with SR, there was still around 40% of the protein undetected which mostly covers the hydrophobic regions of the protein (Fig.3.2). According to the ExPASy PeptideMass tool and the parameters set, the maximum sequence coverage that should be attained with tryptic digestion is approximately 68.5% (Supplementary Fig.3.1). The *in silico* digest showed large uncovered areas of SERCA containing very few lysine and arginine residues which represents the transmembrane region of the protein. This is concurrent with the data from Fig.3.2; however, there was approximately 5-10% of the sequence covered by the PeptideMass tool that was not detected in the discovery MS/MS analysis. In an attempt to improve the sequence coverage, ProteaseMax, a surfactant used to expose inaccessible digestion sites, was added to the trypsin reaction incubation to determine whether higher sequence coverage could be gained, but the results showed that any overall increase found was insignificant (Fig. 3.3). Additional means to improve sequence coverage included the use of iodosobenzoic acid which cleaves at tryptophan residues (Fontana *et al.* 1983). Although iodosobenzoic acid resulted in the detection of two peptides within the transmembrane region of the sequence, this was coupled with loss of peptide detection in other areas resulting in no sign of improvement in overall coverage (data not shown). Therefore subsequent experiments were continued with trypsin in the presence of ProteaseMax. Although ProteaseMax did not improve the coverage significantly, it did nevertheless reduce the digestion incubation to one hour, allowing completion of the protocol in one day rather than two, therefore giving a more time-efficient protocol.

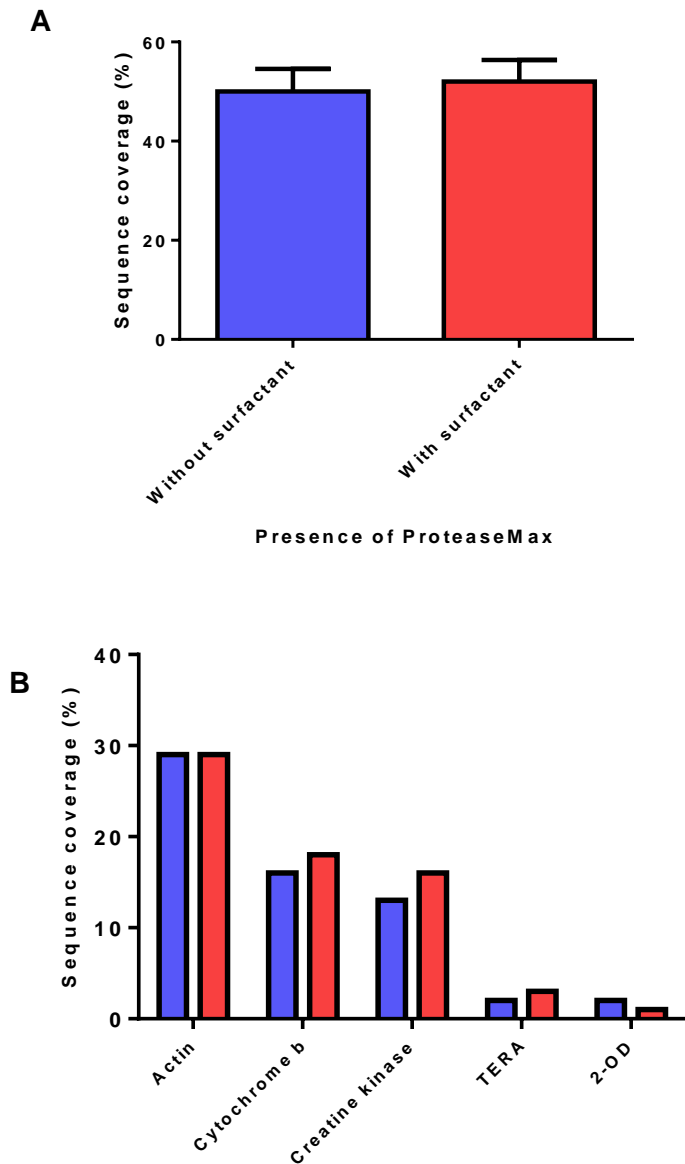


Figure 3.3. Comparison of sequence coverage of SERCA and other proteins in SR samples with and without surfactant. A. Sequence coverage of SERCA with absence of surfactant represented as a purple bar and presence of surfactant represented as a red bar. Unpaired t-test showed data to be insignificant from triplicate values ($P > 0.05$). **B.** Coverage from other proteins: Actin, cytochrome b, creatine kinase, transitional endoplasmic reticulum ATPase (TERA), 2-oxoglutarate dehydrogenase (2-OD). This data is representative of one of the replicates from the triplicates used in the above data (A).

3.2.2. Regulation of oxidation arising from experimental procedures

While it is important to increase the number of modified residues detected during MS, there is also a need to regulate oxidative artefacts that arise from the experimental processing and storage. A number of measures were taken to limit production of these artefacts, including the addition of exogenous methionine to the buffers. As methionine is the most susceptible amino acid to oxidation, theoretically it should act as an antioxidant and reduce oxidation of protein residues within the sample (Levine *et al.* 1996; Hawkins and Davies, 1999). Experiments were carried out to determine how effective the addition of exogenous methionine was at minimising oxidative artefacts. Several residues were quantified using a narrow window XIC approach, discussed earlier in section 1.5, which utilises the data from a discovery MS/MS method and quantifies the intensity of the precursor ion based on the retention time of the peptide without the need for setting up additional targeted experiments. Changes in methionine oxidation (OxM) in SERCA were compared between samples in the presence of the exogenous methionine and the absence of the scavenger (Table 3.1). The results demonstrate that similar residues were oxidised in both sets of sample; however, with the exception of Met452, higher levels of OxM were found in the absence of the methionine scavenger. Furthermore, Met250 from ADP/ATP translocase, Met327 from Actin alpha and Met757 from SERCA show a substantial difference in percentage modification. As the analysis was carried out by narrow window XIC analysis there is a chance that quantitation is influenced by co-eluting peptides with isobaric masses. Accurate determination of the levels of oxidation within the two samples would require MRM analysis where quantitation is based on the product ion intensity generated from the fragmentation of the precursor ion. Nevertheless, the data strongly support the value of methionine as an antioxidant *in vitro*.

Table 3.1. OxM in control SR samples with the presence of an oxidant scavenger (exogenous methionine) and the absence of the scavenger. Table shows peptide of SERCA with modified residue highlighted in red and corresponding percentage modification (\pm S.D.) *Significant difference ($p < 0.05$) between presence and absence of methionine determined by an unpaired t-test ($n=3$).

Residue	Sequence	Percentage modification	
		With Methionine	Without Methionine
SERCA			
Met452	MNVFNTEVR	17.4% \pm 4.4	17.4% \pm 4.8
Met452	M NVFNTEVR		
Met757	AIYNNMKQFIR	54.4% \pm 0.9	80.1% \pm 0.3*
Met757	AIYNN M KQFIR		
Met969	ALDFTQWLMVLK	80.2% \pm 2.1	87.0% \pm 9.2
Met969	ALDFTQWL M VLK		
ADP/ATP translocase 1			
Met250	GADIMYTGLDCWR	34.2% \pm 3.7	47.8% \pm 3.4*
Met250	GAD I MYTGLDCWR		
Actin alpha			
Met327	EITALAPSTMK	19.7% \pm 1.2	79.2% \pm 0.9*
Met327	EITALAPST M K		

3.2.3. *In vitro* oxidation using hypochlorous acid and peroxynitrite

After studies on limitation of oxidative artefacts and optimisation of the sequence coverage, *in vitro* oxidation was performed to generate a database of modifications for oxidised proteins in SR and MH samples for a range of oxidant concentrations. The oxidant concentrations used are given as protein: oxidant molar ratio and have been used to not only determine the susceptibility of residues within proteins but also to facilitate the production of targeted methods for quantitation. Incubating the samples at different concentrations provided an overview on which residues require minimal oxidant concentrations to be modified and at which concentrations a higher oxidative state is achieved. The two oxidants used in the *in vitro* experiments were hypochlorous acid (HOCl) and peroxynitrite (ONOO⁻).

Both oxidants not only oxidise but also have a secondary modifying nature; chlorination and nitration respectively, as explained in section 1.4.

3.2.3.1. Immunoblotting for carbonyl groups within SR and MH oxidised with HOCl and ONOO⁻

To evaluate the effects of HOCl oxidation on SERCA, SR samples were oxidised in a protein: oxidant molar ratio of 1:10, 1:25, 1:50, 1:100, 1:250, 1:500, and 1:1000 along with the control sample in the absence of oxidant. Western blotting with anti-SERCA antibody verified which bands contain SERCA (Fig.3.4A). In all samples, a band was observed above the 100 kDa protein mark where the 110 kDa membrane protein was expected to appear. However, this was not the only band to be identified in the western blot. There were two additional bands present; one band near to the stacking of the polyacrylamide gel in all the samples and the other at 75 kDa, only in the oxidised samples. These two additional bands suggested aggregation and fragmentation of the protein, which means that excising just the band at ~100 kDa would lead to bias selectivity. To avoid limiting detection of modifications to non-aggregated or non-fragmented bands and also leading to inaccurate quantitation, future experiments involved using the GeLC approach as an alternative method where bias selectivity is avoided (Shevchenko *et al.* 2007).

In the OxyBlot, a difference can be seen between the control, 1:10-500, and 1:1000 (protein: oxidant molar ratio) (Fig.3.4B). The carbonyl detection showed increased carbonyl formation in the oxidised samples compared to the control sample; however, carbonyl formation could not be discerned from 1:10-500 (protein: oxidant) treatments. Only the 1:1000 oxidised SERCA showed a distinct difference in protein carbonyl formation to the others. Additionally, there is a band around 60 kDa which is not present in the blot probed with anti-SERCA and therefore indicates carbonyl formation on other proteins. Although carbonyl detection gives an impression of the overall oxidation of the SERCA protein, it does not provide additional information on the characterisation and location of the oxidised residues within the protein.

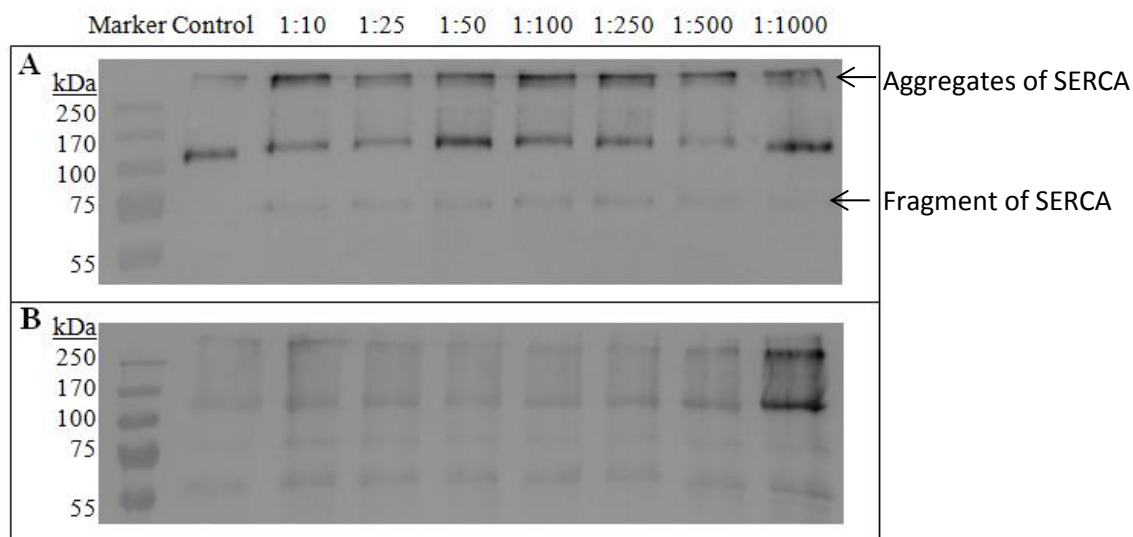


Figure 3.4. Western blot and OxyBlot with increasing protein: oxidant concentrations of HOCl oxidised SERCA from left to right. A. Western blot of HOCl oxidised SERCA with anti-SERCA antibody. **B.** OxyBlot of HOCl oxidised SERCA with anti-DNP antibody.

Similarly, MH was oxidised at the same varying protein: oxidant molar concentrations with the oxidants to demonstrate the effects of the oxidant. Figure 3.5 shows the effects of ONOO^- on carbonyl group production at concentrations between 1:10 - 1:1000. An increased level of carbonyl groups can be seen when comparing concentrations between 1:10 - 1:100 to the control. The major changes occurred at protein: oxidant ratios above 1:100. It can be deduced that oxidant concentrations above 1:100 lead to fragmentation of proteins, which is why a large dense band can be seen at lower molecular weights. Interestingly, very little is present at 1:1000 which could be due to excessive fragmentation and aggregation leading to a substantial loss of protein. To obtain a more quantitative view of the changes in carbonyl formation, the lanes of the oxyblot were quantified using densitometry and the results displayed in a bar chart (Fig. 3.5B). Carbonyl groups increase from the control to 1:250. After this concentration there is a decline in carbonyl groups, which may reflect alternative forms of oxidative modification. The immunoblotting demonstrated increased protein instability at higher concentrations of oxidants and a rough guide to which areas of the gel contained high levels of modification. However, obtaining more detailed information on the characterisation,

location, and relative quantification of oxidised residues required MS/MS as an alternative method for analysing protein oxidation.

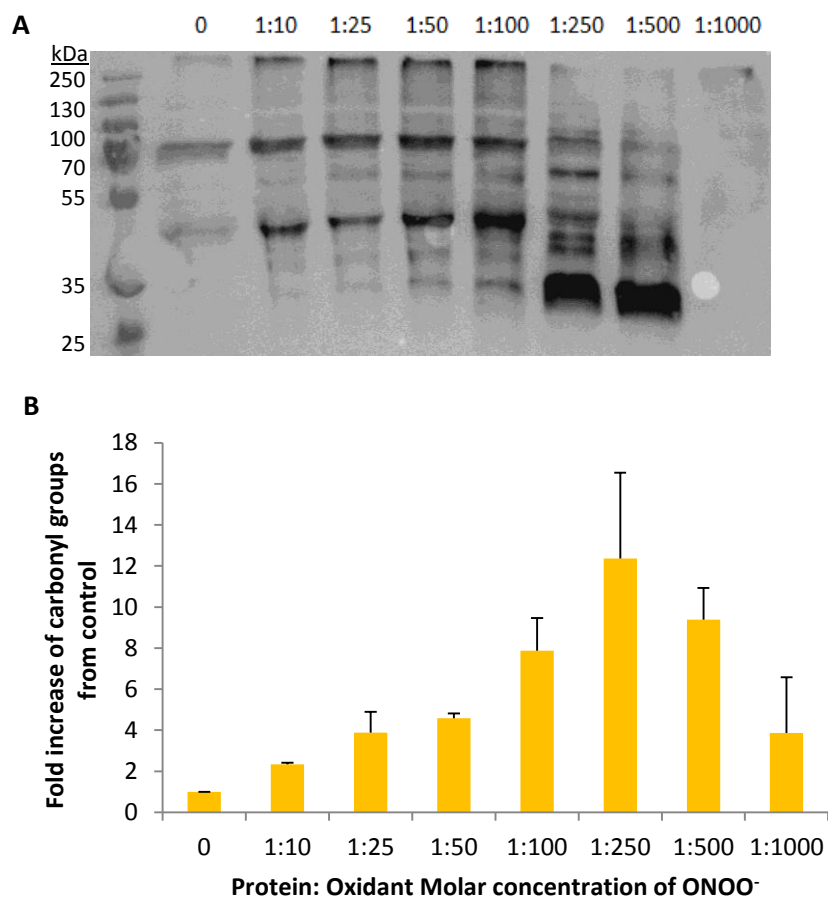


Figure 3.5. Levels of carbonyl groups in MH oxidised with ONOO⁻. **A.** Oxyblot with anti-DNP. **B.** Densitometry of above oxyblot. Error bars displayed as S.E.M (n=3).

3.2.3.2. Characterisation of oxidised residues in HOCl and ONOO⁻ oxidised SR and MH samples

After immunoblotting was performed to determine the levels of oxidation in both the SR and MH samples at varying concentrations, MS/MS analysis was carried out using a QToF instrument to identify oxidative modifications and locate the residues that were modified. Although there have been many publications that have used *in vitro* oxidation to identify oxidative modifications, many of these focus on modifications within a selected protein. This study also mainly focuses on SERCA modifications but modifications in other proteins were also of interest and some were investigated. An advantage of using both SR and MH samples was that an increased number of SERCA peptides could be screened due to higher

sequence coverage in the SR sample, while more modified peptides including abundant non-SR proteins could be detected in MH samples. To illustrate the effects of oxidants on protein detection in MS/MS, a table of the top 10 proteins hits within the GeLC band 1 (area around 250 kDa MW) of MH, excised at MW100-250, for each oxidant treatment and its control was produced (Table 3.2). The top 10 hits are ordered by a Mascot score based on an algorithm combining the sequence coverage and peptide spectral matches to define the highest confidence protein matches (Perkins *et al.* 1999). The increase in oxidant concentrations changes the positioning of the proteins, affecting some proteins more than others. An example of this can be seen when comparing glycogen phosphorylase to SERCA. Glycogen phosphorylase is the top hit for all treatments bar 1:1000; however, the same pattern is not seen with SERCA. For many of the concentrations between the control and 1:100, SERCA is the second highest hit but between concentrations 1:250 and 1:1000 there is a drop in the position of SERCA within the list. When this is coupled to the sequence coverage of the protein, SERCA drops from an average of $29.8 \pm 4.9\%$ ($\leq 1:100$) to an average of $15.7 \pm 9.7\%$ ($\geq 1:250$). On the other hand, glycogen phosphorylase maintains consistently high sequence coverage from 1:250 and 1:500 but drops from an average of $44.6 \pm 4.5\%$ ($\leq 1:500$) to 6% at 1:1000. Another notable difference is the change in Mascot scores throughout the treatments, where a high the Mascot score corresponds to high confidence that the protein is correctly identified. Additionally, creatine kinase is the only protein in the list that maintains a relatively high sequence coverage throughout all the treatments, with sequence coverages fluctuating between 25-39%. In fact, it seems to rise in sequence coverage at higher concentrations of 1:100 and 1:500, unlike the other proteins. These changes could reflect differential susceptibilities of the muscle homogenate proteins to oxidation by HOCl. The changes in Mascot score and sequence coverage demonstrates the effects of oxidation on MS analysis and illustrates the additional challenges of studying protein oxidation.

Table 3.2. Top 10 protein hits of MH oxidised with HOCl at a 1:500 (protein: oxidant molar ratio) with corresponding mascot scores and sequence coverages. Results were taken from a representative sample of GeLC band 1 covering area around 250 kDa MW.

Top 10 hits			Mascot score	Sequence coverage (%)
Band 1 (Control)				
1	Glycogen phosphorylase		1092	37
2	SERCA1		850	24
3	Keratin type I		409	11
4	Creatine kinase		316	25
5	Keratin type II		315	5
6	Glyceraldehyde-3-phosphate dehydrogenase		313	37
7	Filamin C		177	2
8	Fuctose biphosphate adolase A		70	3
9	Xyloside xylosyltransferase 1		43	8
10	Lysozyme g-like protein 2		35	4
Band 1 (1:10)				
1	Glycogen phosphorylase		2493	50
2	SERCA1		1328	37
3	Glyceraldehyde-3-phosphate dehydrogenase		1036	42
4	Creatine kinase		940	37
5	Filamin C		795	12
6	Fuctose biphosphate adolase A		186	11
7	Keratin type II		143	6
8	Keratin type I		123	5
9	L-lactate dehydrogenase A chain		109	12
10	Hemoglobin subunit alpha		107	30
Band 1 (1:25)				
1	Glycogen phosphorylase		2471	46
2	Creatine kinase		1357	37
3	SERCA1		1092	30
4	Glyceraldehyde-3-phosphate dehydrogenase		1029	49
5	Filamin C		834	14

6	Fuctose biphosphate adolase A		266	22
7	Keratin type I		189	7
8	Hemoglobin subunit alpha		186	30
9	Hemoglobin subunit beta		170	44
10	Keratin type II		165	4
Band 1 (1:50)				
1	Glycogen phosphorylase		1822	44
2	SERCA1		1158	27
3	Creatine kinase		989	37
4	Filamin C		613	12
5	Glyceraldehyde-3-phosphate dehydrogenase		600	45
6	Keratin type II		294	9
7	Keratin type I		291	10
8	Fuctose biphosphate adolase A		218	16
9	Glycogen starch synthase		110	7
10	Hemoglobin subunit alpha		100	30
Band 1 (1:100)				
1	Glycogen phosphorylase		2253	41
2	SERCA1		1522	31
3	Creatine kinase		1106	39
4	Filamin C		1093	17
5	Glyceraldehyde-3-phosphate dehydrogenase		703	45
6	Keratin type I		227	7
7	Fuctose biphosphate adolase A		194	15
8	Keratin type II		191	11
9	AMP deaminase 1		157	13
10	Glycogen starch synthase		152	7
Band 1 (1:250)				
1	Glycogen phosphorylase		3220	49
2	Creatine kinase		1988	36
3	Pyruvate kinase		1069	38
4	Beta enolase		807	28

5	SERCA1		659	18
6	Fuctose bisphosphate adolase A		608	31
7	Glyceraldehyde-3-phosphate dehydrogenase		445	30
8	Keratin type II		354	10
9	Keratin type I		305	11
10	Phosphoglycerate mutase 2		233	24
Band 1 (1:500)				
1	Glycogen phosphorylase		2861	45
2	Pyruvate kinase		1445	37
3	Creatine kinase		1140	39
4	SERCA1		878	24
5	Glyceraldehyde-3-phosphate dehydrogenase		666	43
6	Fuctose bisphosphate adolase A		573	32
7	Filamin C		502	10
8	Beta enolase		490	25
9	Keratin type II		416	7
10	Keratin type I		416	11
Band 1 (1:1000)				
1	Creatine kinase		587	25
2	Keratin type I		461	10
3	Pyruvate kinase		367	18
4	Keratin type II		355	11
5	Fuctose bisphosphate adolase A		258	17
6	Glycogen phosphorylase		192	6
7	SERCA1		132	5
8	Glyceraldehyde-3-phosphate dehydrogenase		121	18
9	Dihydropolypyllysine-residue succinyltransferase component of 2-oxoglutarate dehydrogenase complex		98	10
10	Xyloside xylosyltransferase 1		48	2

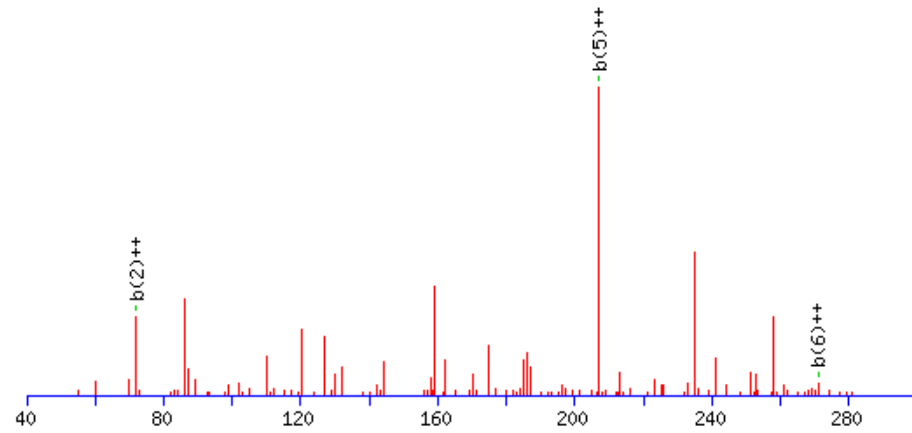
When mining the data retrieved from Mascot on the modifications detected within the samples, it was important that the modifications found were validated using *de novo* sequencing. There are times when using probability based software such as Mascot can result in mistakes. The search engine relies on matching the ions of a MS/MS spectrum to a theoretically generated database and determining the best fit according to the parameter input when submitting the search. When including variable modifications within the search, the software has to determine whether the unknown spectrum originates from a native peptide or modified peptide. To illustrate this, a spectrum of a peptide incorrectly identified as an oxidised peptide from SERCA is shown (Fig.3.6). After manual sequencing, the spectrum was determined to be a native peptide from creatine kinase. The initial step was to sequence the spectrum from the raw data file assuming the peptide identification by Mascot was correct. When the data failed to support the Mascot sequence, it was considered as a false positive, and the following step was to identify what series of amino acids best fit the fragmentation data. When an appropriate number of amino acids had been identified, the sequence was searched in Pubmed BLAST with Swissprot and Mus Musculus as selected for the database and taxonomy, and a list of potential proteins the sequence could have originated from was retrieved. The last step was to find a possible trypsin-digested sequence that matched the *de novo* sequenced spectrum and the precursor ion mass. For this particular example, the peptide was found to be an unmodified peptide, SFLVWVNEEDHLR, from creatine kinase. Other minor mistakes made by Mascot also included ions that were not identified in the MS/MS dataset (Fig 3.7). Overall, *de novo* sequencing has proved to be a valuable technique that users should implement in their workflow to filter out false positive data, especially in proteins containing PTMs. Nevertheless, Mascot is a powerful tool that aids the user in fast and efficient searches of protein and peptide identification that would not be possible on manual sequencing alone.

A) Mascot results

Peptide View

MS/MS Fragmentation of **AAVGNKMFVK**

Found in **AT2A1_MOUSE** in **SwissProt**, Sarcoplasmic/endoplasmic reticulum calcium ATPase 1

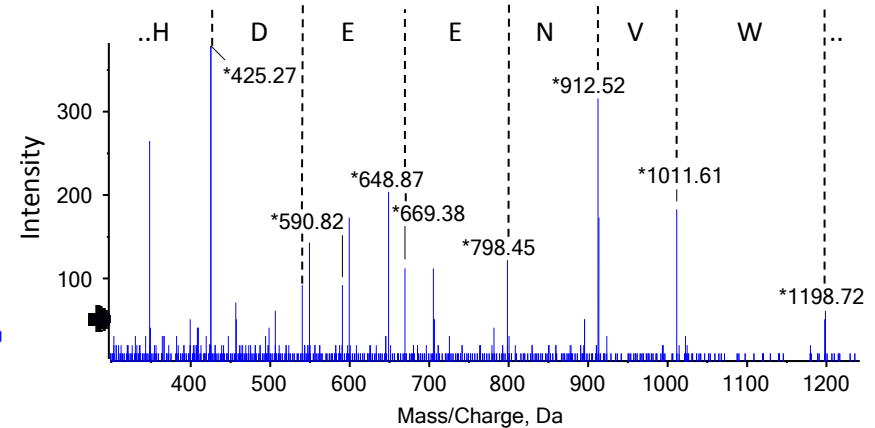


Variable modifications:

M7 : Dioxidation (M)

#	b	b ⁺⁺	b [*]	b ⁺⁺⁺	Seq.	y	y ⁺⁺	y [*]	y ⁺⁺⁺	#
1	72.0444	36.5258			A					10
2	143.0815	72.0444			A	1025.5448	513.2761	1008.5183	504.7628	9
3	242.1499	121.5786			V	954.5077	477.7575	937.4812	469.2442	8
4	299.1714	150.0893			G	855.4393	428.2233	838.4128	419.7100	7
5	413.2143	207.1108	396.1878	198.5975	N	798.4178	399.7126	781.3913	391.1993	6
6	541.3093	271.1583	524.2827	262.6450	K	684.3749	342.6911	667.3484	334.1778	5
7	704.3396	352.6734	687.3130	344.1602	M	556.2799	278.6436	539.2534	270.1303	4
8	851.4080	426.2076	834.3815	417.6944	F	393.2496	197.1285	376.2231	188.6152	3
9	950.4764	475.7418	933.4499	467.2286	V	246.1812	123.5942	229.1547	115.0810	2
10					K	147.1128	74.0600	130.0863	65.5468	1

B) De novo sequencing



C) BLAST results

RecName: Full=Creatine kinase M-type; AltName: Full=Creatine kinase M chain; AltName: Full=M-CK [Mus musculus]
Sequence ID: [splP07310.1|KCRM_MOUSE](#) Length: 381 Number of Matches: 1

Range 1: 228 to 234 [GenPept](#) [Graphics](#) ▼ Next Match ▲ Previous Match

Score	Expect	Identities	Positives	Gaps
29.1 bits(61)	0.014	7/7(100%)	7/7(100%)	0/7(0%)

```

Query 1  WVNEEDH 7
          WVNEEDH
Sbjct 228  WVNEEDH 234

61 vdnpgghpfim tvgcvagdee sytvfkdlfd piiqdrhggv kptdkhktdl nhenlkggdd
121 ldpnyvlssr vrtgrsikgy tlpphcsrge rraveklsve alnsltgefz gkyyplksmt
181 eqeqqqlidd hflfdkpvsp lllasgmard wpdargiwhn dnksflvwvn eedhlrvism
241 ekggnmkevf rrfcvgqlqi eeifkkaghp fmwnehlgv ltcpnslgtg lrggvhvkla
301 nlskhpfee iltrlrqlqr gtggvdtaav gavfdisnad rlgseveqv qlvvdgvklm
361 vemekklekg qsiddmipaq k
    
```

Figure 3.6. Mascot assignment of MS/MS spectrum to incorrect peptide and protein. A. Mascot output of SERCA sequence matched to spectrum. **B.** *De novo* sequenced MS/MS spectrum from raw data file. **C.** BLAST search results with queried peptide highlighted in yellow.

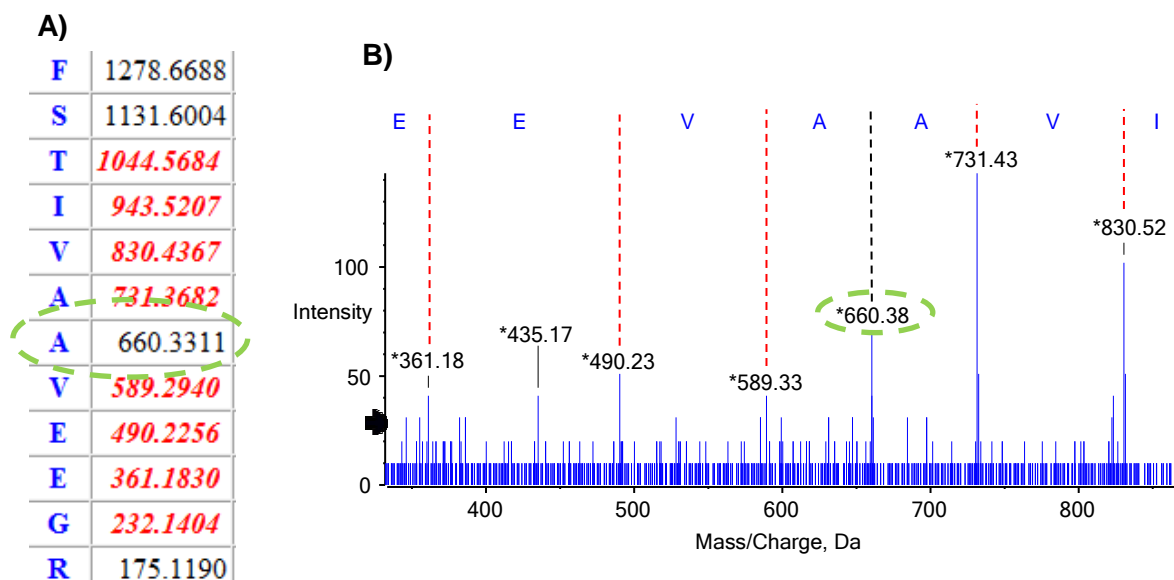


Figure 3.7. Unallocated ion present in raw MS/MS files and highlighted in *de novo* sequenced spectrum. A. Detected ions by Mascot. **B.** *De novo* sequenced peptide showing ion is present in raw data.

As well as filtering out false positive data, there are many sequenced peptides that confirm the presence of modifications (Fig.3.8). The MS/MS spectra of four modified peptides demonstrate the different types of sequencing involved. The types of sequencing included sequencing of a single modification in a peptide (Fig.3.8A&C), multiple modifications within a peptide (Fig.3.8B), and a modification at a terminus of a peptide (Fig.3.8D). Moreover, the detection of immonium ions provides further evidence for the presence of modifications in the samples. Immonium ions are generated when high amounts of collision energy create a charge on the amine group of an amino acid (Falick *et al.*, 1993). In the case of ClTyr, the immonium ion of tyrosine, which is 136 Da, has a further 34 Da added owing to the addition of chlorine (35 Da) and subtraction of hydrogen (1 Da) from the aromatic ring. All four sequenced spectra are examples of the work undertaken to ensure that the modifications presented were correctly identified and provide an accurate representation of residue modifications when analysing samples by MS.

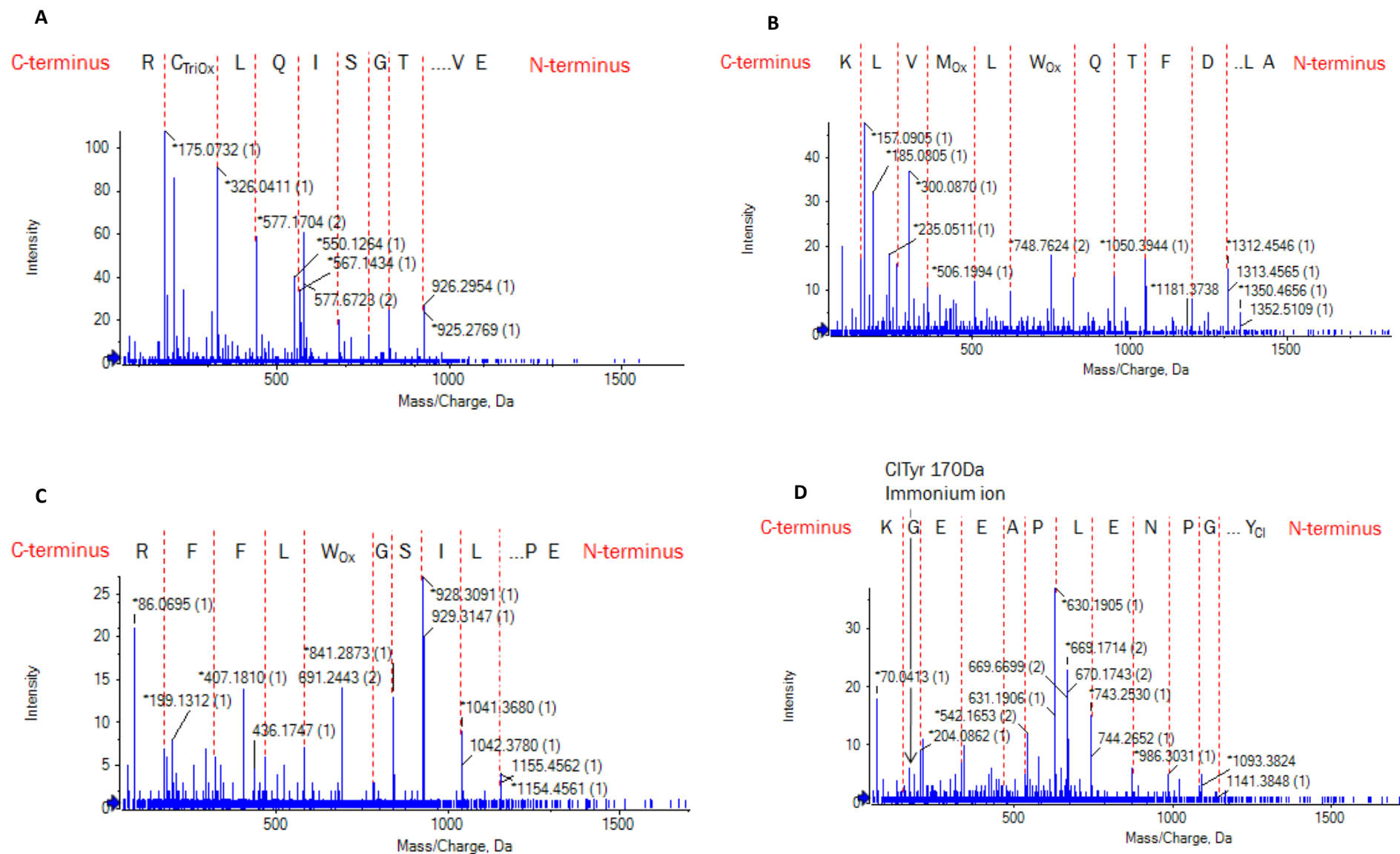


Figure 3.8. De novo sequenced peptides of SERCA from HOCl oxidised SR. Sequenced spectra of **A.** Cysteine trioxidation, **B.** Methioine oxidation and Tryptophan oxidation, **C.** Tryptophan oxidation, and **D.** Chlorotyrosine with labelled immonium ion.

The number of false positives that arose from Mascot vs. correctly identified modified peptides is illustrated by the percentages of false positives, true positives, uncertain and misassigned oxidations for a representative data set, which were as follows: 61%, 13%, 20% and 6% respectively (Supplementary Table 3.1). A total of 19% of oxPTMs were validated and accepted as modifications, whereas the other 81% were false positives or could not be determined from the MS/MS fragmentation spectra. This ~20% result demonstrates how important manual verification is, even though it is a laborious and time consuming process.

For oxPTM discovery MS/MS, SR and MH samples were oxidised with HOCl and ONOO⁻ at protein: oxidant ratios of 1:10, 1:25, 1:50, 1:75, 1:100, 1:250, and 1:500. Oxidative modifications detected using a QToF mass spectrometer were identified and verified using Mascot and PeakView. All modifications with the exception of methionine oxidation were listed. These included methionine dioxidation (DioxM), cysteine trioxidation (TrioxC), tyrosine oxidation (OxY), phenylalanine oxidation (OxF), allysine (Ally), tryptophan oxidation (OxW), tryptophan dioxidation (DioxW), nitrotyrosine (nitroY) and chlorotyrosine (ClY). OxMet residues were excluded from the list because of the numerous amounts detected in all the samples due to the high susceptibility of methionine to oxidation.

Tables 3.3 and 3.4 show validated modifications that were detected using Mascot in SERCA of HOCl- and ONOO⁻-oxidised SR samples respectively. While there were more modifications detected in ONOO⁻ oxidised samples up to 1:500 oxidant concentrations, HOCl shows many more modifications detected in 1:500 sample. Additionally, different modifications can be seen for each of the oxidants; however, this is also seen with the control samples as the control for the HOCl treatments contained a OxY whereas a DioxM was present in the ONOO⁻ control. Although there are common modifications in both treatments, the two differing demonstrates different susceptibilities to the different oxidants. An example of this is EPLISGWLFFR, which first appears in the HOCl treatments at 1:500, but first appears at a 10 times lower concentration of ONOO⁻, specifically at 1:50. While chlorotyrosine was detected following HOCl treatment, demonstrating its chlorinating

potential, ONOO⁻ did not show any of nitrating activity, but this may reflect the reduction in sequence coverage and fewer modifications detected at its highest treatment. Both oxidants caused most modifications in thiol-containing amino acids, which was expected as they are the most susceptible amino acids to oxidation. Interestingly, while OxY is present in HOCl samples, even in the control, the modification was not detected in the ONOO⁻ samples. The OxY modification originates from a single peptide, Tyr694, and the lack of detection in ONOO⁻-treated sample could just be because it was not selected for MS/MS fragmentation during the data-dependent MS/MS routine. The same can be seen in reverse, with C12 present in ONOO⁻ following 1: 100 treatment but not detected at all in the HOCl-oxidised samples. The different modifications seen with the two oxidants provide fragmentation information for a large number of MRM transitions for quantification of oxPTMs in muscle samples.

Table 3.3. Mascot detection of oxidised residues following treatment of SERCA with varying HOCl concentrations. Summary of oxidative modifications detected through searches in Swiss-Prot database with carbamidomethyl as a fixed modification and the variable modifications in the table, as described in Chapter 2. Modified residues are highlighted in red in the peptide sequence.

Protein : Oxidant	Modification	Sequence	Residue
0	TrioxC	EVTGSIQL CR	Cys614
	OxY	IVEYLQSYDEITAMTGDGVNDAPALKK	Tyr694
1:10	OxY	IVEYLQSYDEITAMTGDGVNDAPALKK	Tyr694
	DioxM	AEIGIAMGSGTAVAK	Met720
	TrioxC	TGTLTTNQMSV CK	Cys364
1:50	OxY	IVEYLQSYDEITAMTGDGVNDAPALK	Tyr694
	OxY	IVEYLQSYDEITAMTGDGVNDAPALKK	Tyr694
	DioxM	M NVFNTEVR	Met452
	TrioxC	C LALATR	Cys561
1:100	DioxM	M NVFNTEVR	Met452
	DioxM	AEIGIAMGSGTAVAK	Met720
	DioxM	ALDFTQ W LMVLK	Met969
	TrioxC	C LALATR	Cys561
	DioxW	ALDFTQ W LMVLK	Trp967
	OxF	NML F SGTNIAAGK	Phe209
1:500	DioxW	ALDFTQ W LMVLK	Trp967
	CiTyr	Y GPNELPAEEGK	Tyr36
	TrioxC	C LALATR	Cys561
	TrioxC	KEVTGSIQL CR	Cys614
	TrioxC	EVTGSIQL CR	Cys614
	DioxM	N MLFSGTNIAAGK	Met207
	DioxM	DQ M AATEQDKTPLQQK	Met239
	DioxM	M NVFNTEVR	Met452
	DioxM	IVEYLQSYDEITAMTGDGVNDAPALKK	Met700
	DioxM	AEIGIAMGSGTAVAK	Met720
	OxW	EPLISG W LFFR	Trp831
	OxM & OxW	ALDFTQ W LMVLK	Trp967 & Met969
	DioxW	ALDFTQ W LMVLK	Trp967
	TrioxC	TGTLTTNQMSV CK	Cys364
TrioxC	GTAIA I CR	Cys636	

Table 3.4. Mascot detection of oxidised residues following treatment of SERCA with varying ONOO⁻ concentrations. Summary of oxidative modifications found achieved through searches in Swiss-Prot database with carbamidomethyl as a fixed modification. Modified residues are highlighted in red in the peptide sequence.

Protein : Oxidant	Modification	Sequence	Residue
0	DioxM	TGTLTTNQM S VCK	Met361
	TrioxC	EVTGSIQL C R	Cys614
1:10	DioxM	TGTLTTNQM S VCK	Met361
	Allysine	K EFTLEFSR	Lys481
	TrioxC	EVTGSIQL C R	Cys614
1:50	DioxM	ALDFTQWLM V LK	Met969
	TrioxC	TGTLTTNQM S V C K	Cys364
	TrioxC	EVTGSIQL C R	Cys614
	TrioxC	GTAIAI C R	Cys636
	OxTrp	EPLISGW L FFR	Trp831
1:100	OxM & DioxW	R.ALDFTQWLM V LK.I	Trp967 & Met969
	TrioxC	STEE C LSYFGVSETTGLTPDQVK	Cys12
	DioxM	N MLFSGTNIAAGK	Met207
	TrioxC	SLPSVETLG C TSVICSDK	Cys344
	DioxM & TrioxC	TGTLTTNQM S V C K	Met361 & Cys364
	TrioxC	KEVTGSIQL C R	Cys614
	TrioxC	EVTGSIQL C R	Cys614
	TrioxC	GTAIAI C R	Cys636
	DioxM	R.ALDFTQWLM V LK.I	Met969
OxM & DioxW	R.ALDFTQWLM V LK.I	Trp967 & Met969	
1:500	TrioxC	STEE C LSYFGVSETTGLTPDQVK	Cys12
	OxM & DioxM	F MEYEMDLTFVGVVGM L DPPR	Met585 & Met589
	TrioxC	KEVTGSIQL C R	Cys614
	TrioxC	EVTGSIQL C R	Cys614
	OxM & OxF	TASEM V LADDN F STIVA A VEEGR	Met733 & Phe740

Table 3.5 shows a list of validated modifications from the top 5 protein hits within a band excised around the 100 kDa molecular weight from a gel lane of 1: 250 ONOO⁻ treated oxidised MH. Fewer oxidative modifications were detected in this band in comparison to the increase in nitrations detected. This is seen particularly in glycogen phosphorylase, where 13 nitrotyrosine residues were detected and validated by *de novo* sequencing. An additional difference when comparing modifications detected in SERCA of SR and MH samples is that no modifications were detected in the MH sample, in contrast to 30 found in the SR samples.

This difference shows how purification of an organelle leads to increased discovery of modifications of proteins present in that organelle.

Table 3.5. Mascot detection of oxidised residues in top 5 hit proteins of 1: 250 ONOO-oxidised muscle lysate (excised band MW~100). Summary of oxidative modifications found achieved through searches in Swiss-Prot database with carbamidomethyl as a fixed modification. Modified residues are highlighted in red in the peptide sequence.

Protein ID	Modification	Sequence	Residue
PYGM (Glycogen phosphorylase)	OxW	EIWGV W EPSR	Trp826
	OxM&TrioxC	INMAHL C IAGSHAVNGVAR	Met442&Cys446
	TrioxC	VFADYEEYIK C QDK	Cys784
	NitroY	Y E FGIFNQK	Tyr162
	NitroY	ARPEFTLPVHF Y GR	Tyr204
	NitroY	DFNVGG Y IQAVLDR	Tyr263
	NitroY	VL Y PNDNFFEGK	Tyr281
	NitroY	HLQI Y EINQR	Tyr405
	NitroY	DF Y ELEPHK	Tyr473
	NitroY	IGED Y ISDLQLR	Tyr512
	NitroY	LLS Y VDDEAFIR	Tyr525
	NitroY	FS Y ALER	Tyr549
	NitroY	VIFLEN Y R	Tyr649
	NitroY	GYN Y AQEYDR	Tyr732
	NitroY	GYN Y AQEYDR	Tyr733
NitroY	VFAD Y EEYIK	Tyr781	
KCRM (Creatine kinase)	TrioxC	RF C VGLQK	Cys254
	NitroY	VLTPDL Y NK	Tyr39
	NitroY	GGDDLDPN Y VLSSR	Tyr125
KPYM (Pyruvate kinase)	TrioxC	GIFPVL C K	Cys474
	NitroY	GD Y PLEAVR	Tyr670
	OxM&NitroY	ITLDNA Y MEK	Tyr203&Met204
	TrioxC	NTGI C TIGPASR	Cys49
ENOB Beta-enolase	No modifications observed	N/A	N/A
AT2A1 SERCA	No modifications observed	N/A	N/A

3.2.3.3. MRM quantification

After validation of the modified peptides with Mascot, the data obtained from the MS/MS searches were utilised to generate a list of transitions for subsequent production of MRM methods. Most of the modified peptides chosen for MRM analysis originated from SERCA as it is the primary model protein this research focuses on. In addition to SERCA, glycogen phosphorylase was another protein that peaked interest as it showed high susceptibility to nitration from ONOO⁻ in comparison to other abundant proteins (Table 3.5). The first set of

transitions was produced to test the MRM approach on a QTRAP instrument (Table 3.6). All of the peptides in this transition list contained oxidised methionine, as it is a common modification and has been shown to be present alongside other oxPTMs within a few modified peptides.

Table 3.6. Transition list for methionine oxidation in peptides from SERCA for the QTRAP instrument. Three product ions were used for identification of SERCA peptide. Modified residues highlighted in red.

Peptide	Precursor ion (m/z)	Product ions (m/z)
N M LFSGTNIAAGK	490	346.2 573.4 731.5
NMLFSGTNIAAGK	484.7	204.1 346.2 573.4
M NVFNTEVR	563.4	274.2 618.4 765.5
MNVFNTEVR	555.4	274.2 618.4 765.5
KAEIGIAM M SGTAVAK	507.3	218.1 690.5 837.6
KAEIGIAMSGTAVAK	502	218.1 690.5 821.6
V M ITGDNK	503.3	534.3 647.4 794.5
VIMITGDNK	495.8	261.2 534.3 778.5

Following initial tests on the QTRAP instrument, several other transition lists were generated to begin analysis in *in vitro* oxidised samples. These are shown in Tables 3.7, 3.8 and 3.9, which list transitions for NitroY in glycogen phosphorylase and oxidised residues of SERCA detected in previous discovery MS/MS and nitrotyrosine residues of SERCA from a study by Knyushko *et al.* 2005.

Table 3.7. Transitions list for NitroY in glycogen phosphorylase for the QTRAP instrument. Three product ions were used for identification of glycogen phosphorylase peptide. Modified residues are highlighted in red.

Protein/Residue	Sequence	Precursor ion (m/z)	Product ions (m/z)	Collision energy
Glycogen phosphorylase Y525	LLSYVDDEAFIR	720.9	750.4	37.7
			865.5	
			964.6	
	LLSYVDDEAFIR	743.4	750.4	37.7
			865.5	
			964.6	
Glycogen phosphorylase Y405	HLQIIYEINQR	713.9	659.4	37.4
			822.5	
			935.5	
	HLQIIYEINQR	736.4	659.4	37.4
			867.5	
			980.6	
Glycogen phosphorylase Y281	VLYPNDNFFEGK	721.9	741.4	37.8
			856.5	
			970.5	
	VLYPNDNFFEGK	744.4	741.4	37.8
			856.5	
			970.5	
Glycogen phosphorylase Y263	DFNVGGYIQAVLDR	783.9	701.4	40.5
			814.5	
			977.6	
	DFNVGGYIQAVLDR	806.4	701.4	40.5
			814.6	
			573.3	

Table 3.8. Transitions list for oxidised residues in SERCA for the QTRAP instrument. Three product ions were used for identification of SERCA peptide. Modified residues are highlighted in red.

Modification	Sequence	Precursor ion (m/z)	Product ion (m/z)	Collision energy
TrioxC	EVTGSIQL C R	577.3	326.1	30.4
			439.2	
			925.5	
Unmodified	EVTGSIQLCR	581.8	335.1	30.4
			448.2	
			934.5	
TrioxC	TGTLTTNQMSV C K	716.4	298.1	36.5
			857.5	
			958.5	
Unmodified	TGTLTTNQMSVCK	720.8	307.1	36.5
			866.4	
			967.4	
DioxM	ALDFTQWL M VLK	748.9	522.3	37.9
			635.4	
			821.5	
Unmodified	ALDFTQWLMVLK	732.9	490.3	37.9
			603.4	
			789.5	
OxW & OxM	ALDFTQ W LMVLK	748.9	506.3	37.9
			619.4	
			837.5	
DioxW & OxM	ALDFTQ W LMVLK	756.9	506.3	37.9
			619.4	
			821.5	

Table 3.9. Transitions list for NitroY in SERCA for the QTRAP instrument. Three product ions were used for identification of SERCA peptide as well as measuring the immonium ion marker. Modified residues are highlighted in red.

Modification	Sequence	Precursor ion (m/z)	Product ion (m/z)	Collision energy
Unmodified	GAIYYFK	431.2	457.3	24
			620.3	
			733.4	
NitroY (x2)	GAIYYFK	476.2	502.2	24
			710.3	
			823.4	
Unmodified	EYEPENMGK	491.7	561.3	26.6
			690.3	
			853.4	
NitroY	EYEPENMGK	522.2	577.3	26.6
			706.3	
			914.4	
Unmodified	VDGDVCSLNEFSITGSTYAPEGE VLK	929.8	842.5	50.5
			1005.5	
			1106.6	
NitroY	VDGDVCSLNEFSITGSTYAPEGE VLK	944.8	842.5	50.5
			1050.5	
			1151.6	
Unmodified	GAIYYFK	431.2	136.1	65
			181.1	
			120.1	
NitroY (x2)	GAIYYFK	476.2	136.1	65
			181.1	
			120.1	

Prior to quantitation with MRM, narrow window XIC analysis of NitroY residues in glycogen phosphorylase was carried out, as mentioned in section 1.5 (Fig. 3.9 and 3.10). This method utilises the data set obtained from discovery MS/MS to approximately quantitate modified peptides. Comparing modified peptides in the different ONOO⁻ treatments enables an understanding of how different residues are modified by increasing oxidant concentrations (Fig. 3.9). The most susceptible residue appears to be Tyr281, followed by Tyr263, with Tyr525 being the least susceptible. Additionally, the quantitation follows the pattern seen in the immunoblot and MS/MS sequence coverage results, where there was a decrease after 1:250.

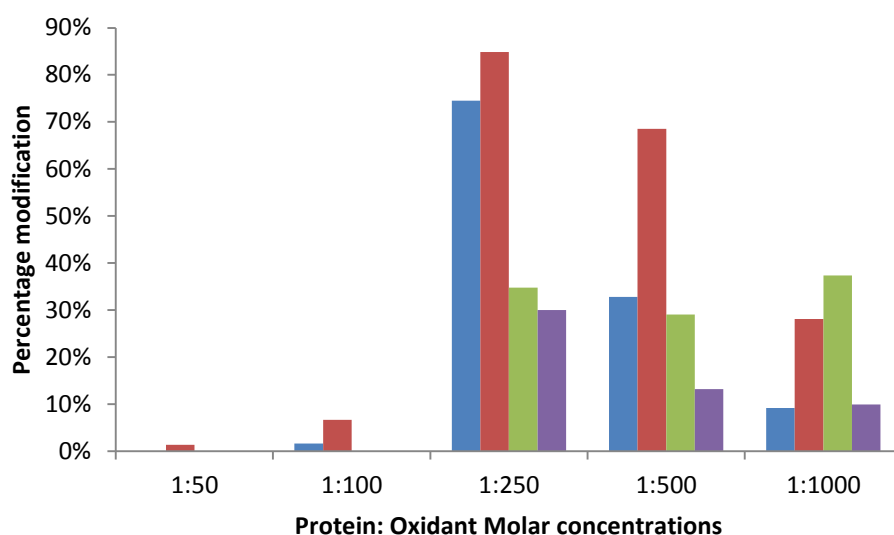


Figure 3.9. Quantification of nitrotyrosine in glycogen phosphorylase with protein: oxidant molar concentrations of ONOO⁻. (From representative sample) Blue: DFNVGGYIQAVLDR (Y263). Red: VLYPNDNFFEGK (Y281). Green: HLQIIYEINQR (Y405). Purple: LLSYVDDEAFIR (Y525). Modified residues are highlighted in red.

XIC analysis with the MS/MS discovery results also showed changes in precursor ion abundancies for each NitroY in their respective peptide populations. By displaying the percentage modification in a graphical format, residue susceptibility is more apparent and demonstrates that not only the type of amino acid governs likeliness to modification, but also other factors, including structural positioning. In the case of glycogen phosphorylase treated

with 1: 250 protein: oxidant molar concentration of ONOO⁻, residues Tyr281, Tyr263, and Tyr473 were found to be modified about 50%, while Tyr512 and Tyr781 were the least modified residues showing less than 10% modification (Fig.3.10).

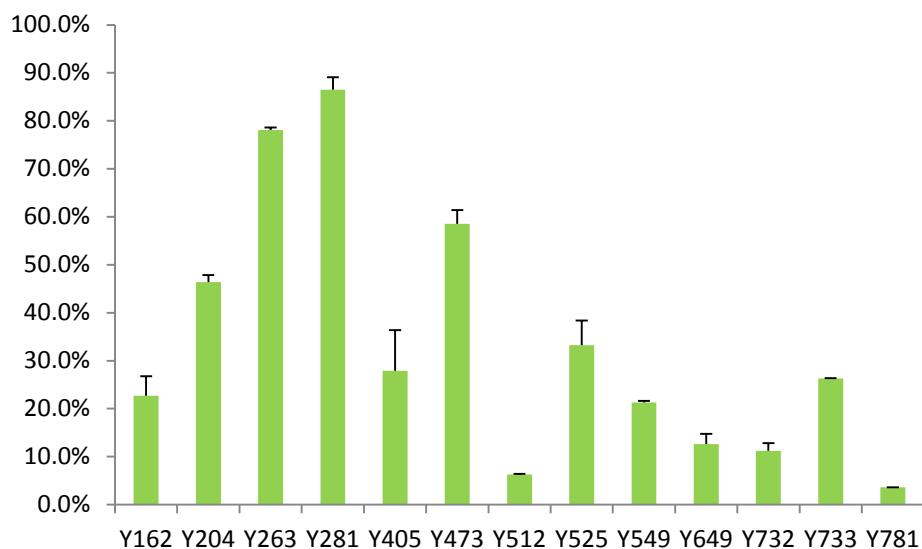


Figure 3.10. Percentage modification of nitrotyrosine residues in 1:250 ONOO⁻ oxidised MH samples using XIC analysis. Error bars of triplicate values displayed as S.E.M.

Although XIC analysis is not necessarily an accurate method of quantifying modified residues due to the presence of isobaric peptides in samples of high complexity, it does provide an overall idea of residue susceptibility and in turn which residues may be best used for subsequent MRM quantitation. Choosing less susceptible modifications may result in them being difficult to quantify, especially if these methods are to be translated into analysis of *in vivo* samples. MRM quantitation of Nitrated Tyr281 of glycogen phosphorylase gave similar results to those obtained by XIC analysis (Fig. 3.11). There was a substantial increase in percentage modification when comparing the range of protein: oxidant molar concentration between 1: 0 and 1: 100 and those between 1: 250 and 1:1000. When comparing the trend seen in the earlier blots in section 3.2.3 to the MRM results, it can be elucidated that the fragmentation and aggregation of 1: 1000 sample is responsible for the drop in percentage modification. Additionally with MRM, NitroY was quantified in samples treated with oxidants at ratios as low as 1: 25, whereas it was not seen during XIC analysis;

however, below this ratio NitroY was not detectable. Whether this modification occurs *in vivo* will require further analysis. The trend observed follows what was seen in the immunoblots, which showed that western blotting and MS are both comparable methods. Only at a protein:oxidant ratio of 1:100 could the nitrated residue be clearly detected, which may mean NitroY will be difficult to measure in biological samples unless the tissue has been subjected to severe stress by high oxidant levels.

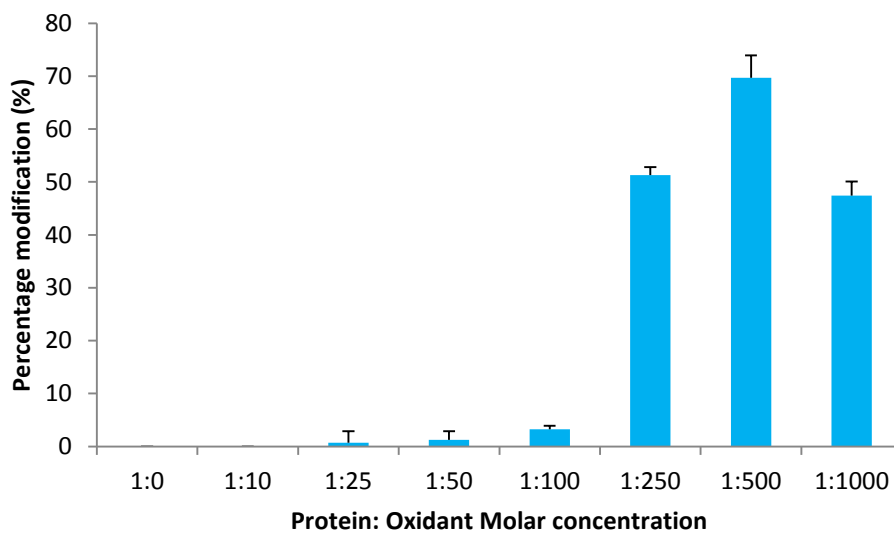


Figure 3.11. MRM quantitation of NitroY (Y281) of glycogen phosphorylase treated with varying concentrations of ONOO⁻. Error bars of triplicate values displayed as S.E.M.

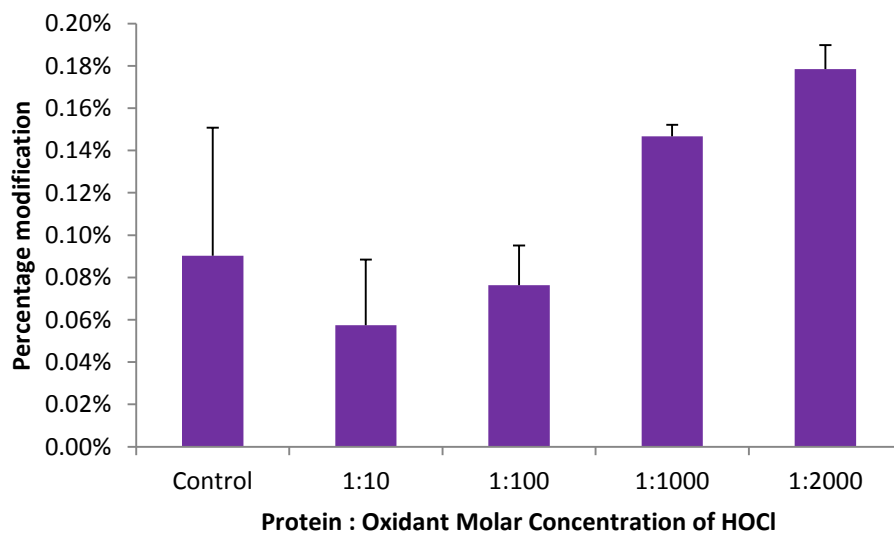


Figure 3.12. MRM quantitation of TrioxC in SERCA peptide CLALATR in samples with varying concentrations of HOCl. Error bars displayed as S.E.M.

Initially, several OxMet modified peptides with their respective unmodified counterparts were analysed using MRM. MRM demonstrates the ability to determine which residues are more susceptible to oxidation. For example, Met720 residues were found to be more modified than Met452. OxM modifications were easier to detect than other modifications, due to methionine's high susceptibility to oxidation. When searching for TrioxC, DioxT, CIY, etc., it proved more difficult to obtain clear, intense and defined transitions because of their low occurrence. Optimisation of the MRM technique will also be required to quantify less susceptible modifications in addition to quantification of OxM.

3.2.4. Comparisons of QToF vs. QTRAP systems in quantification

The QTRAP system is designed to use MRM based techniques, whereas the QToF system required adaption of a product ion scanning mode to analyse selected ranges for pseudo-MRM analysis. This method analyses a range rather than focusing on a particular mass. In order to test the application of these two instruments in quantification of oxPTM in biological samples, obese (*ob/ob*) and aged (C57BL6) mice models were used. This determined the effect the sensitivity and resolution of the instruments had on the quality and ease of quantification, demonstrating the pros and cons of using time of flight and trap-based systems for label-free quantification. More in-depth analysis for these models will be discussed later in chapters 4 and 5. This section discussed these models only to assess the two different instruments in quantification of oxPTMs. To test whether analysis could be performed with MH, several modifications were tested with both the SR and MH samples on the QTRAP (Fig. 3.13). The data show that oxPTMs can be detected in MH and additionally because higher protein concentrations can be obtained with MH, the signals are much higher than SR which, because of sample purification, has 30 times less protein. For all experiments thereafter MH was used for quantitation, instead of SR.

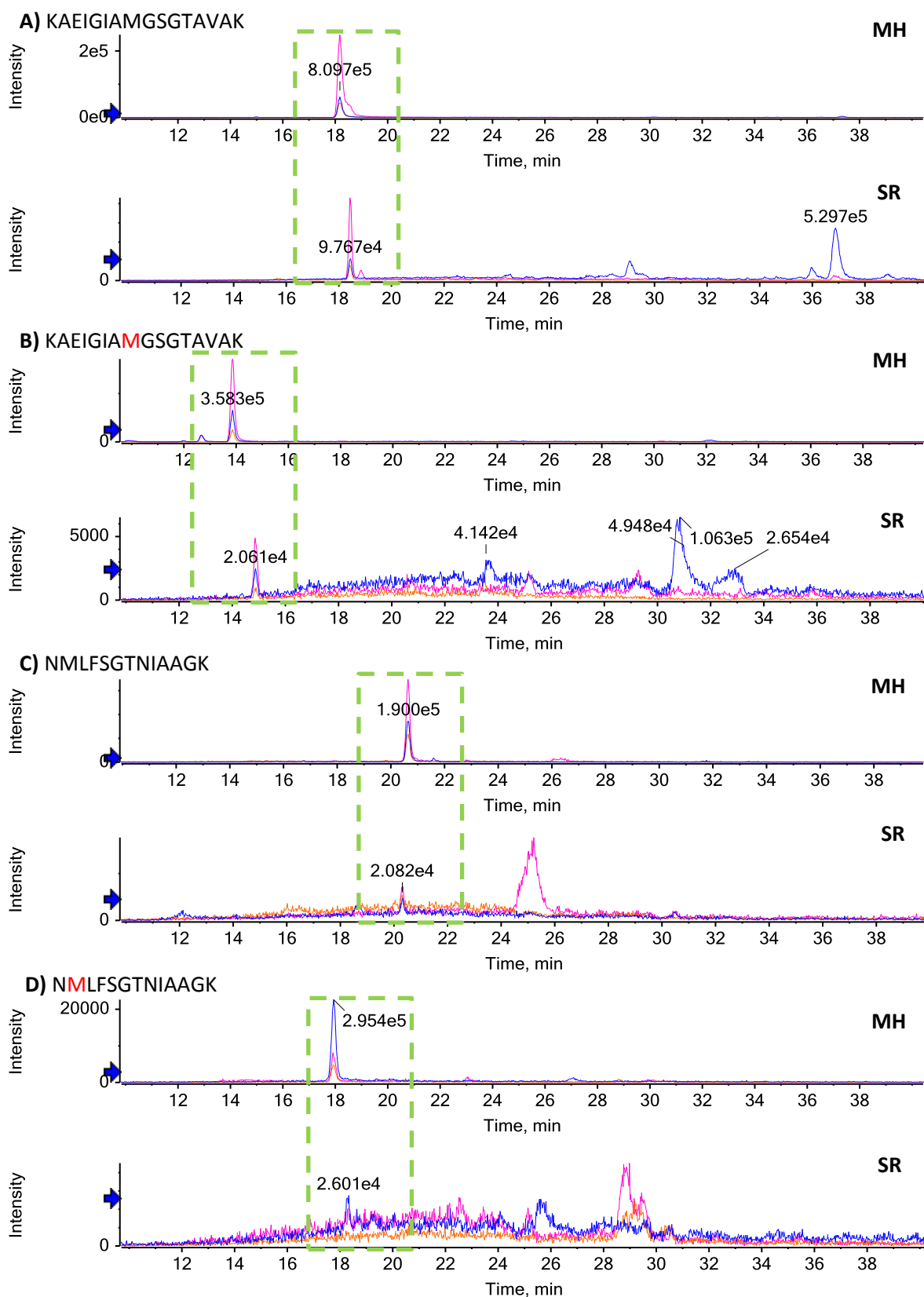


Figure 3.13. Comparison of MH and SR samples for quantitation of OxM residues using the QTRAP. Green boxes highlight transition peaks for oxidised KAEIGIAMGSGTAVAK (B) and NMLFSGTNIAGK (D) and their respective native peptides (A&C).

Additionally, a few specific peptides were compared to determine the limit of detection and accuracy of the QToF system vs the QTRAP system. OxPTMs were compared in both systems and showed a significant difference (Table 3.10). Due to the fact that samples were processed at different times, it is difficult to say whether artefactual oxidation affected the results when comparing quantitation between the QToF and the QTRAP. Met720 has a larger contrast with a 17.7% increase in detection of OxM in the QToF, whereas Met452 only showed a 4.4% increase. This could be due to residue susceptibility, but does indicate that the two instruments cannot be compared based on oxidised residues.

Table 3.10. Comparison of QToF and QTRAP quantitation of OxM modifications of Met452 and Met720 of SERCA. Quantitation was noted for each replicate and an average was calculated. S.E.M. determined for native and oxidised peptides measured by ToF and QTRAP (n=3).

Replicates	QToF		QTRAP	
Met452				
1	Native	81%	Native	87%
	Oxidised	19%	Oxidised	13%
2	Native	87%	Native	91%
	Oxidised	13%	Oxidised	9%
3	Native	82%	Native	85%
	Oxidised	18%	Oxidised	15%
Average	Native	83.3 ± 3.2%	Native	87.7 ± 3.1%
	Oxidised	16.7 ± 3.2%	Oxidised	12.3 ± 3.1%
Met720				
1	Native	70%	Native	88%
	Oxidised	30%	Oxidised	12%
2	Native	76%	Native	83%
	Oxidised	24%	Oxidised	17%
3	Native	61%	Native	89%
	Oxidised	39%	Oxidised	11%
Average	Native	69 ± 7.5%	Native	86.7 ± 3.2%
	Oxidised	31 ± 7.5%	Oxidised	13.3 ± 3.2%

On the other hand, when comparing nitration, there is less risk of artefactual changes in modification through sample storage or handling. The QToF and QTRAP still show differences in quantitation of the oxPTMs (Table 3.11), as well as better signal to noise for the QToF over the QTRAP (Fig. 3.14).

Table 3.11. Comparison of QToF and QTRAP quantitation of NitroY in glycogen phosphorylase. Results are from a representative sample. Modified residue is highlighted in red.

Peptide	Residue	QToF	QTRAP
LLS Y VDDEAFIR	Tyr525	7%	16%
VLY P NDNFFEGK	Tyr281	16%	14%
HLQI Y EINQR	Tyr405	0.34%	- Noise level

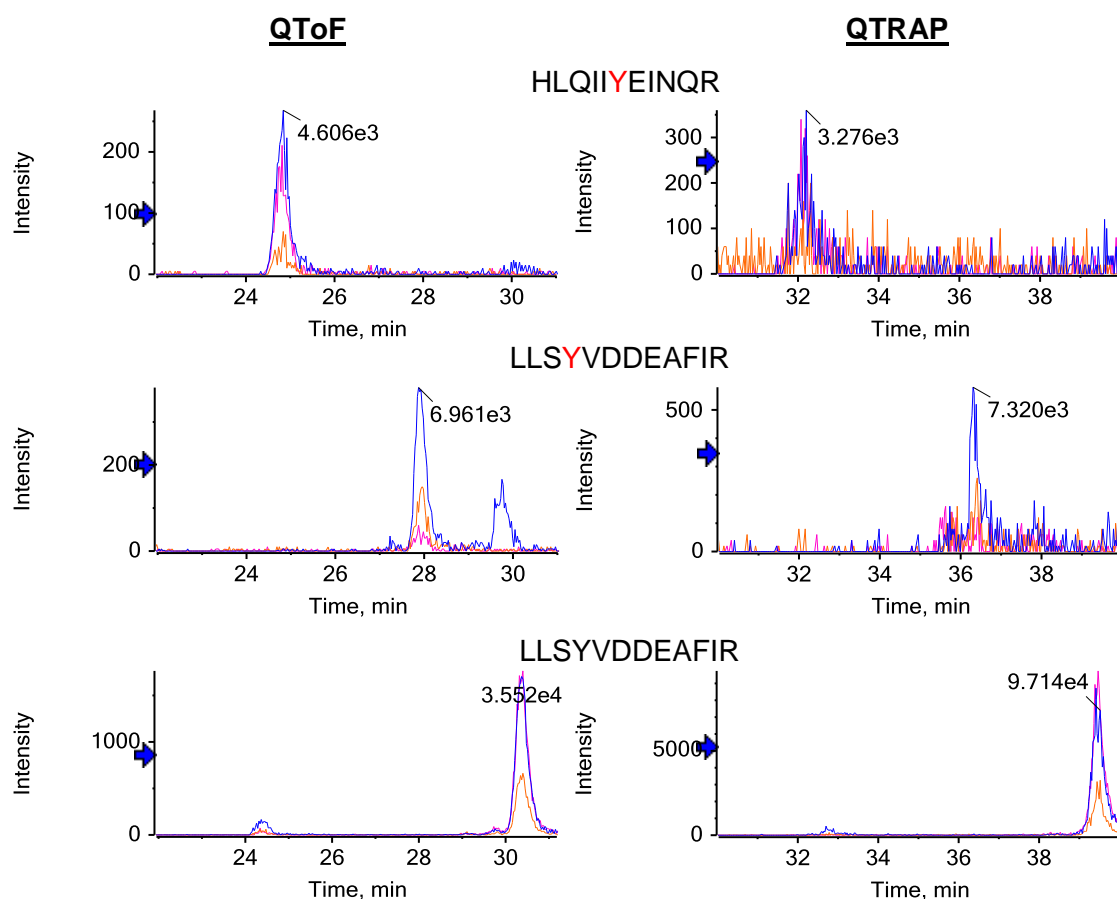


Figure 3.14. Comparison of QToF and QTRAP XIC transitions for NitroY and native peptides from glycogen phosphorylase. Modified residues are highlighted in red.

There were also differences in the false positive peaks detected in both samples. Figure 3.15 shows that an extra peak was detected in the QTRAP data when compared to the same XIC transitions in the QToF. This difference is most likely due to the higher resolution capabilities of a QToF instrument.

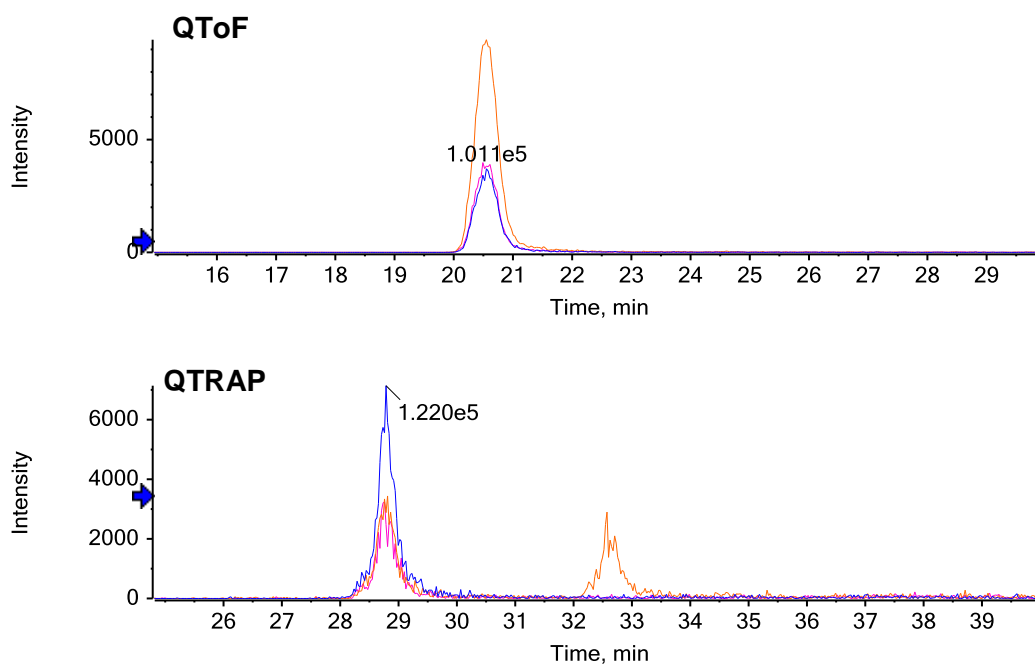


Figure 3.15. Comparisons of QToF and QTRAP XIC of SERCA peptide EVTGSIQLCR. A. XIC transitions for peptide analysed using QToF. B. XIC transitions for peptide analysed using QTRAP.

Higher resolution enables selection of a precursor ion mass window to ensure isobaric peptides are not displayed. This is also seen in Figure 3.16, where there is very little to distinguish the two peptides in a QTRAP spectrum apart from the lack of the third transition, whereas the QToF can differentiate between the two peaks.

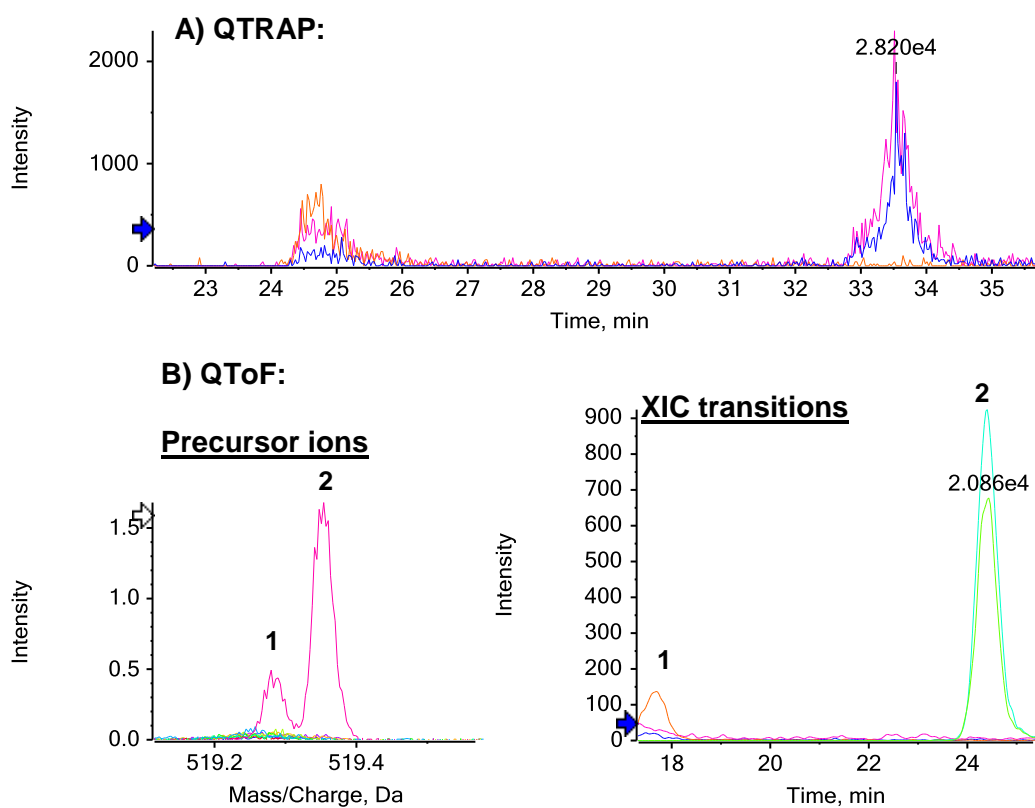


Figure 3.16. Comparison of QTRAP and QToF MRM analysis of SERCA peptide GTAIAICR. **A.** XIC transitions of SERCA peptide measured in QTRAP instrument. **B.** XIC transitions of peptide measured in QToF instrument. XIC transitions generated from peaks labelled as 1 and 2 of different precursor ion peaks.

For the QToF system, three methods were tested: selected product ion monitoring, full product scan and a focused product ion scan. The ToF instrument used in this study required adaptation to the product ion scanning mode to produce methods for quantitation. The mass windows were either narrowed to include a specific product ion mass window or wide enough to analyse a series of product ions generated from a chosen precursor ion mass of interest.

3.2.4.1. Narrow window selected product ion monitoring QTOF analysis

The selected product ion monitoring method involved taking three product ions that appeared consecutively in a sequence and using a narrow mass window scan that included the masses of these three product ions. By doing so, a hybrid MRM-product ion scan method was created and involved the user generating XICs from the list of product ions produced by the precursor ion mass input. Although this method worked well for some peptides, other peptides produced spectra in which false positive peaks could be seen (Fig. 3.17). This also demonstrated the existence of isobaric peptides that generate similar mass fragments. To avoid this, a second method was produced that involved increasing the mass range to search for more transitions per precursor ion. Although this method has a greater similarities to the product ion scan, it still has a targeted approach as the range does not include product ions smaller than 200 Da and cuts off at high masses where MS/MS spectra are predominantly noise. The cut off points reduce the time spent on data collection in unnecessary mass ranges, where little data of importance would be collected.

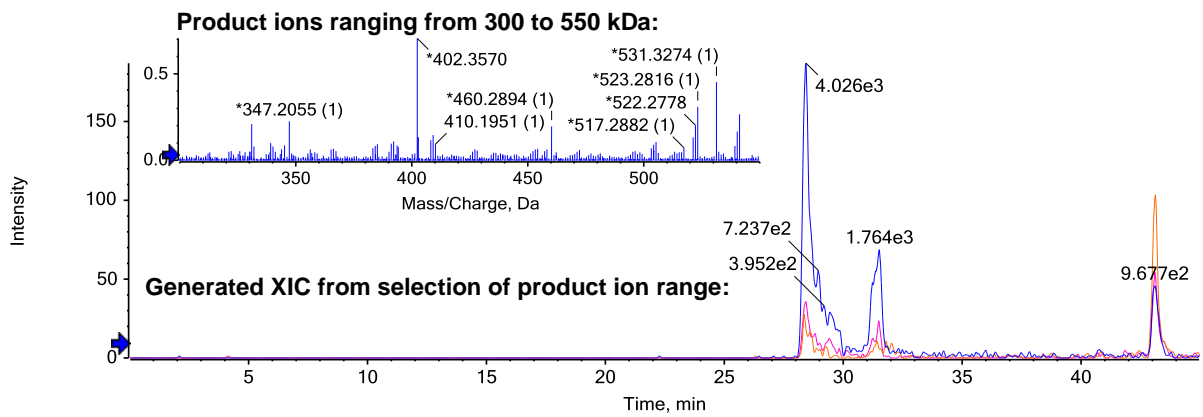


Figure 3.17. Example from selected product ion monitoring method with XICs generated from range between 300-550 kDa. TrioxC of CLALATR SERCA peptide oxidised with 1:100 ONOO⁻. Spectrum has been Gaussian smoothed by 1.5 points.

3.2.4.2. Wide window selected product ion monitoring QTOF analysis

The selected product ion scan method with a wider mass window enables a larger number of transitions of the peptide to be searched and simplifies the choice when deciding which transitions are best suited for subsequent targeted approaches. This method also reduces false positive peak detection which can occur when using a method with limited transitions (Fig. 3.18). Typically, many standard MRM methods use a minimum of three transitions, but when analysing a complex mixture of proteins, the risk of detecting false positives is much greater. Although this method would be a good starting point to find which product ions are best used for subsequent targeted methods, it is time consuming to collect data on a single peptide and leads to fewer scan events within a single method program.

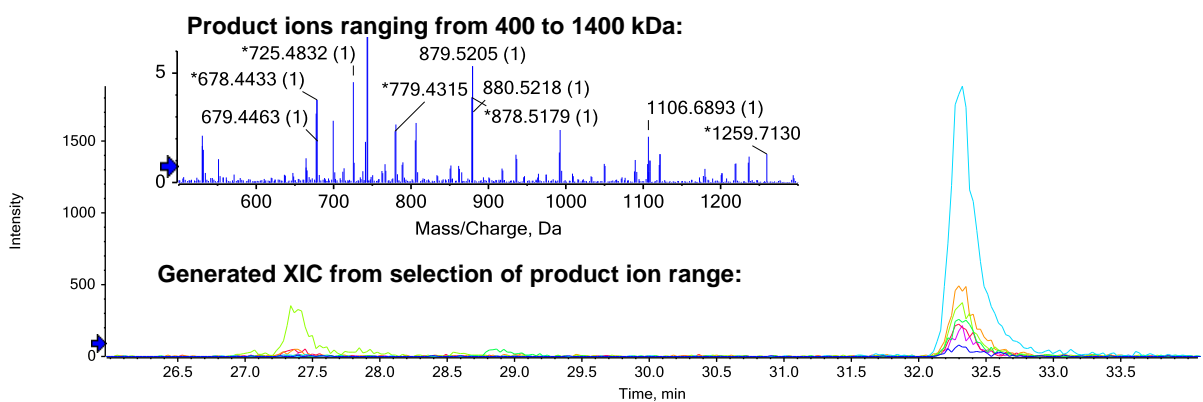


Figure 3.18. Example of product ion scan of nitrotyrosine in glycogen phosphorylase. NitroY525 of LLSYVDDEAFIR in glycogen phosphorylase from 1:500 ONOO⁻ oxidised sample. Scan ranges between 400-1400 kDa.

3.2.4.3. Focused product ion scanning QToF analysis

The third technique developed on the QToF was a highly targeted approach, whereby the transition mass ranges were shortened to a 1 Da mass range around the mass of the selected product ions. The 1 Da mass range was chosen so that the focused QToF method was directly comparable to the QTRAP MRM method. Figure 3.19 shows overlaid spectra from native, OxM and DioxM peptides. With this method a mass shift can be seen with the transitions, as well as changes in intensity between the native and modified peptides. Additionally, utilising a focused scan increases the time spent measuring a selected few transitions as opposed to measuring a larger number of product ions allowing for reduced duty cycles and increased number of peptide quantitation. It also produces a method nearest to typical MRM routines used in quadrupole and TRAP instruments.

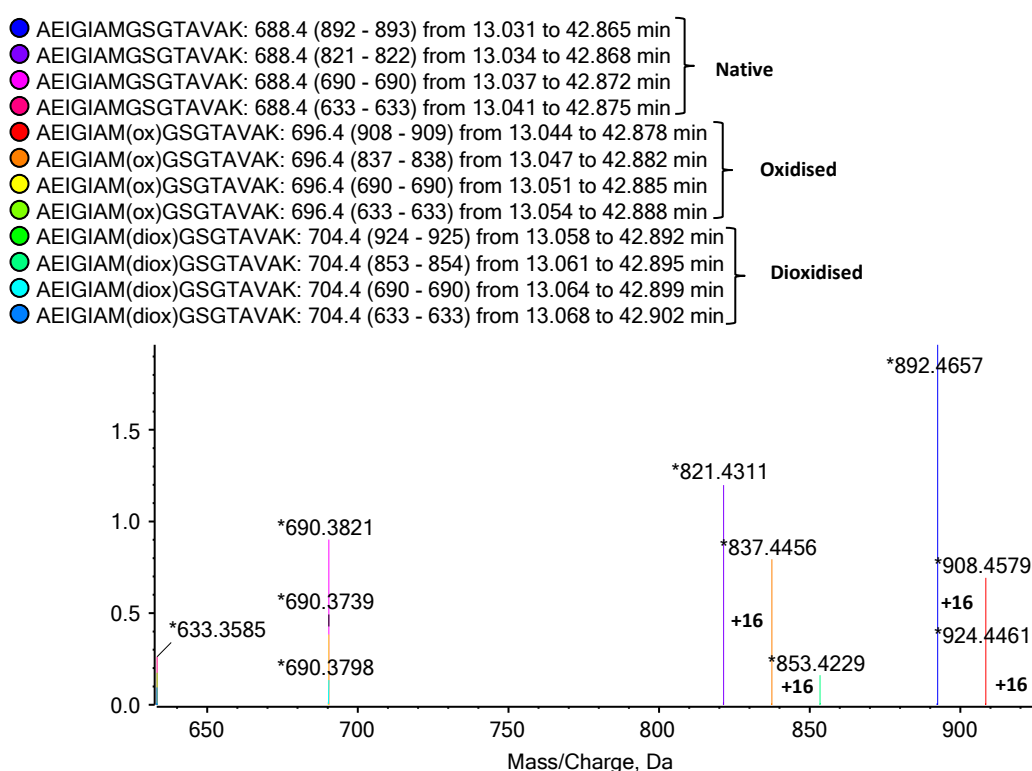


Figure 3.19. Example of targeted MRM method using selected product ions of native, OxM and DioxM from SERCA peptide AEIGIAMGSGTAVAK. Addition of oxygen represented as mass shift of +16. Modified residue is highlighted in red.

In all three methods, the retention time of the peptides is an important factor for distinguishing false positive peaks. As the quantitation is carried out on the same LC-MS system as discovery MS/MS, the retention time of the peaks is expected to be the same. The QTRAP system is at a disadvantage because the different LC set-ups can account for changes in the initial dead volume prior to the start of the LC gradient leading to different retention times exhibited in the two instruments (Fig. 3.14).

The three methods used for quantitation were developed at different time points during the project, as throughout the study there was a continuous focus on developing and optimising methods best suited for the characterisation and quantitation of oxPTMs in muscle.

3.3. Discussion

The aim of this study was to optimise current MS methods used for the analysis of oxidative modifications for the application to muscle tissue and develop these methods for characterisation and quantitation of oxPTMs. This was achieved by the development of non-labelling discovery and quantitative MS methods for the analysis of oxPTMs in muscle proteins that could be used to study occurrence in ageing or disease. Optimisation of sample handling, oxPTM detection and quantitation was explored.

3.3.1. Handling of samples

It was essential to regulate the oxidative artefacts that arise during sample handling. As the focus of the study was to explore the oxidative modifications in muscle, preventing the introduction of adventitious oxidation required the addition of a scavenger (Levine *et al.* 1996; Hawkins and Davies, 1999). These results showed higher levels of oxidised methionine residues when peptides were detected in the absence of exogenous methionine. While some residues demonstrated little to no change, other residues such as Met757 in SERCA and Met327 in actin showed higher susceptibility to oxidation in the absence of a scavenger. Additionally, many of these residues are surface exposed and are more easily accessible to oxidants. In view of the high susceptibility to oxidation, it is essential to minimise oxidation during handling and storage of samples, in order to quantify accurately oxidative modifications induced *in vivo*. The data demonstrated that addition of methionine was able to prevent experimental oxidation artefacts, thus improving data collection for correct understanding of oxidations induced *in vivo* and limitation of false positives. The addition of the scavenger had varied results in the protection of some residues over others which may lead to a greater separation of highly susceptible residues as well as indication of whether conformation plays a role.

Additionally, a different approach was taken to handling gel slices from SDS-PAGE gels. Studies that focus on exploring individual modifications or single proteins will often select

bands to excise when performing in-gel digestion. The results from the immunoblots showed oxidised proteins are susceptible to aggregation and fragmentation which means a protein is not localised to one area on the gel. To refrain from unconscious bias selectivity of bands at the 'correct' molecular weight, the GeLC method was used to analyse the whole gel lane but still utilise electrophoresis for fractionation of the samples. GeLC has been used to analyse complex protein mixtures for downstream mass spectrometry approaches in other studies (Shevchenko *et al.* 2007; Piersma *et al.* 2013; Dzieciatkowska, Hill and Hansen, 2014). By using this method aggregate and fragments of proteins can also be analysed for oxPTMs. In this regard, a GeLC approach has significant advantages over cutting specific bands where the protein should appear on SDS-gel.

3.3.2. *In vitro* oxidation

To assess the suitability of the methods for analysis of oxPTMs in subsequent studies on aged and obese models, *in vitro* oxidation of muscle proteins was used as the starting point for the development of the MS approaches. Using MS techniques for global analysis, oxidations of methionine, cysteine, tyrosine, tryptophan, and phenylalanine and chlorination of tyrosine have been detected within oxidised SERCA. This included the discovery of chlorination to Tyr36, which had not been previously reported. It cannot be said for sure whether these modifications play a major role in disease, but their investigation will lead to a greater understanding of the impact ROS have on proteins in disease and may help in the identification of possible biomarkers.

Western blotting demonstrated the effects of *in vitro* oxidation to the SERCA protein. Both aggregation and fragmentation of the protein could be seen. The additional SERCA band present near the stacking gel could have been caused by inter- and intra-molecular interactions leading to aggregation and oligomerisation. Additionally, this band was denser in the oxidised samples. One possible intermolecular interaction associated with oxidation that could contribute to this is the formation of dityrosine bonds, which are generated through

tyrosyl radical formation (Heinecke *et al.*, 1993). There is a small amount of aggregation/oligomerisation in the control sample which may be due to the hydrophobic nature of the protein. HOCl promotes aggregation/oligomerisation by strong non-covalent interactions by alterations to the structure from the formation of chloramines, oxidations, and carbonyls (Chapman, *et al.* 2003). The detection of fragmented SERCA band after incubation with HOCl has been previously reported (Strosova *et al.* 2009). Peptide bond cleavage has been shown to occur when reactive oxygen species attack glutamyl, aspartyl, and prolyl side chains (Garrison, 1987), where oxidation of proline to pyrrolidone has been reported by Uchida *et al.*, 1990.

Following immunblotting, discovery MS/MS analysis determined the type and location of modifications in SERCA. Oxidised Met720 and Met452, found in the phosphorylation domain and nucleotide binding domain respectively, can be observed in lower protein: oxidant samples. These appeared to be more easily oxidisable than other methionine residues. Met720 in particular may be an important residue, as it is adjacent to Cys674, a key residue involved in redox regulation of SERCA (Adachi *et al.* 2004). The role of this residue may be to act as a scavenger for oxidants to prevent the further oxidation of Cys674 to an irreversible form (Ying *et al.* 2008).

One particular modification of interest identified in 1:500 HOCl oxidised SERCA was Tyr36 chlorination, which is found in the actuator domain. This represents a novel finding as there are no previous reports of ClY in SERCA, despite there being several studies of HOCl-induced stress on SERCA. The detection of this novel modification further supports the importance of global analysis of modifications over focus on specific modifications. ClY in particular is an interesting modification because the chlorination is specific to HOCl. The formation of ClY has been proposed to occur through direct HOCl oxidation and via transfer of chlorine from chloramines (Domigan *et al.*, 1995). Chloramines are produced from the reaction of HOCl with amino groups; $R-NH_2 + HOCl \rightarrow R-NHCl + H_2O$, and are capable of transferring chlorine to other substrates but when other substrates are not available,

chloramines can be stabilised by hydrolysis to aldehydes (Winterbourn, 1985; Hazen *et al.*, 1998). Although Tyr36 chlorination had been detected *in vitro* in this study, it is not known whether this modification occurs *in vivo* and further analysis in disease models is required to determine this. If Tyr36 were to have an effect in the actuator domain, it may influence SERCA's ability to revert back to the E1 state, which has high affinity calcium binding sites near to the cytoplasmic opening resulting in a reduction in calcium uptake (MacLennan *et al.* 1970).

Many publications on tyrosine modifications in SERCA are focused on NitroY formation (Viner *et al.* 1996; Knyushko *et al.* 2005). However, this study has demonstrated the presence of other oxidation states such as chlorination of Tyr36 and the addition of oxygen to Tyr694 *in vitro*. Similarly, Phe209 oxidation was also identified as a modification detected in the SR samples. Like Tyr36, Phe209 is also located in the actuator domain, whereas Tyr694 is located in the phosphorylation domain. The detection of Tyr694 oxidation in the control samples as well as the oxidised samples may be due to its accessibility as an exposed amino acid. The OxW residues detected in the samples are located in the transmembrane domain but there have not been many reports on modifications in this domain and links to activity. However, there has been a report suggesting conformational changes in the transmembrane domain of SERCA are linked to adjuvant arthritis (Strosova *et al.*, 2009b). Whether the oxidised tryptophan residues in the transmembrane domain play a role in the conformational changes is still unknown.

The final type of modification that was detected in the majority of the samples was TrioxC. Four residues with this type of modification were identified and these were Cys364, Cys561, Cys614, and Cys636. Both Cys364 and Cys561 were located in the nucleotide binding domain whereas Cys614 and Cys636 were located in the phosphorylation domain. Cys636, in particular, was found to be adjacent to Cys674 previously mentioned to be involved in redox regulation. This residue may work in the same manner as Met720 as protection from further oxidation.

Additional analysis of other proteins in the muscle led to the discovery of glycogen phosphorylase susceptibility to nitrotyrosine formation when subjected to peroxynitrite treatment. NitroY residues have been reported both *in vitro* and in ageing studies. When comparing the residues identified in a study by Sharov *et al.* 2006b, in which rat skeletal muscle glycogen phosphorylase was nitrated with peroxynitrite, seven of the tyrosine residues were modified at the same position: 204, 263, 281, 405, 473, 732 and 733. The remaining six residues were not seen in the rat study and additionally modifications seen in the rat study were not detected in mouse glycogen phosphorylase. Different sequence coverages could be a factor as to why some different modifications were seen but not others. The thirteen NitroY residues detected in glycogen phosphorylase may be due to the combination of the many surface exposed tyrosine residues and the protein being one of the most abundant proteins within the muscle lysate. The combination of the abundance of glycogen phosphorylase and easily accessible residues could explain why it contains many nitrotyrosine residues in comparison to the other proteins in the sample.

3.3.3. Development of quantitative MS methods

With a list of modifications identified using discovery MS/MS with *in vitro* oxidation, several targeted and non-targeted MS methods were performed to test quantitation of the oxPTMs in muscle proteins. Narrow mass window XIC analysis was performed on the data set obtained from discovery MS/MS. The quantitation of NitroY residues in glycogen phosphorylase demonstrated differences in susceptibility of the different tyrosine residues. Residues Tyr204, Tyr263, Tyr281, and Tyr473, that were also present in the rat study, showed high levels of nitration. Interestingly, neighbouring residues Tyr723 and Tyr733 were also shown to have different susceptibility. In an alternate study by Sharov *et al.* 2009, residues corresponding to Tyr281, Tyr473, Tyr405, Tyr473 and Tyr549 from this study, were shown to exhibit more than 50% nitration after 1 mM peroxynitrite treatment in the glycogen phosphorylase of rabbit muscle. While residues Tyr281 and Tyr473 do show high levels of nitration after peroxynitrite treatment, other residues are shown to have higher nitration than

Tyr405, Tyr473 and Tyr549. Additionally, at high levels of nitration maximum percentage modification of Tyr281 reaches around 90% whereas the study in rabbit muscle glycogen phosphorylase reached nitration levels of up to 99% with relative quantitation with MS/MS. However, quantitation of Tyr281 with MRM in mouse muscle shows a maximum of around 75% nitration. The difference seen from the targeted approach demonstrates the advantages to using MRM as a quantitative tool to more accurately quantify oxidative levels.

In order to develop a quantitative method using a non-labelling approach, MRM on the QTRAP was tested against pseudoMRM methods developed on the QToF instrument. The QTRAP and QToF instruments were sensitive enough to measure *in vitro* oxidised peptides in muscle homogenate which had a higher protein complexity compared with the isolated sarcoplasmic reticulum sample. The analyses of the QTRAP and QToF instruments occurred at different time points of the study and so are not directly comparable. However, the results from the comparisons showed advantages to using different mass analysers for quantitation. When comparing the levels of OxM residues, the QTRAP showed similar detection to the QToF in Met452 but a larger increase in oxidation was shown for Met720. This most likely suggests that although a scavenger was added to the storage buffer of the samples, highly susceptible residue will still be oxidised over time. Quantitation with NitroY in glycogen phosphorylase showed better signal to noise ratio for the QToF system enabling easier quantitation. Additionally, the QToF demonstrated better resolution of transitions. For this study, the QToF was more optimised for the application of oxPTM quantitation in muscle proteins. This is not to say the QToF is a better instrument as studies have shown advantages of different MS in other experiments (Rousu, Herttuainen and Tolonen, 2010).

Moreover, several targeted methods were developed over the course of the study to adapt product scanning feature into a pseudoMRM approach. The three methods have advantages and disadvantages but ultimately show the routes taken to optimise methods for quantitation of oxPTMs in muscle. Similar methods have been reported and demonstrate the tactical

advantages to using semi-targeted and targeted approaches depending on the application (Sherrod *et al.* 2012; Lee, Paull and Person, 2013).

3.3.4. Concluding remarks

From these data it can be concluded that analysis of oxPTMs is not a simple process and requires caution when handling samples to prevent adventitious oxidation as well as unconscious bias towards selecting proteins of the corresponding molecular weight band that may lead to losing additional information about protein modification in aggregates and fragments. By analysing several modifications, novel modifications were detected with *in vitro* oxidation and quantitation of oxidised residues revealed information about residue susceptibility. The development of MS technology could potentially be translated to an analytical tool for detection of biomarkers in clinical samples. Although mass spectrometry is a powerful tool that can be used for detection and quantification of oxidised proteins, there are still limitations to this technique. Further development of these methods is required in order to assess the utility of modifications as potential biomarkers. However the MS techniques developed are applicable to aid the further understanding of the role of protein oxidation in ageing and obesity.

Chapter 4

Identification and quantification of oxPTMs in muscle proteins of an obese model

4.1. Introduction

Obesity is increasingly affecting the world population with a 400% rise in obese individuals reported in England over the past 20 years and £4.2 billion direct costs to the NHS (McCarthy, 2015). One of the major causes of obesity in humans is the increasing resistance to leptin, similar to the resistance to insulin that occurs in diabetes. Leptin is a hormone secreted by adipose tissue and act on receptors in the hypothalamus to suppress appetite (Bates and Myers, 2003). Obese individuals have high levels of leptin circulating in the blood; however, because of insensitivity to leptin the brain does not respond and causes the individuals to overeat. Factors that have been proposed to contribute to leptin resistance include: free fatty acids and impaired transport through the blood brain barrier (Banks, DiPalma and Farrell, 1999; Banks *et al.* 2004).

4.1.1. Obesity and the effects on muscle

Muscle inflammation is reported to arise during obesity which has been linked to muscular dysfunctions (Fink *et al.* 2013; Pellegrinelli *et al.* 2015). Additionally, when coupled to sarcopenia, it is shown that the combination of sarcopenia and obesity increased odds for difficulties in physical performance (Zhong, Chen and Thompson, 2007; Rolland *et al.* 2009). To determine whether oxidative modifications may be involved in muscle performance, oxPTM analysis was used to determine whether higher levels of oxidation exist in obese muscle proteins.

4.1.2. The ob/ob mouse model

Ob/ob mice are leptin deficient and are commonly used as models to study type II diabetes and obesity (Drel *et al.* 2006). Ob/ob mice have a deficiency of leptin, which causes overeating and leads to obesity. While leptin deficiency and leptin insensitivity is not comparable in the progression to obesity, both would eventually lead to obesity associated

problems i.e. diabetes, atherosclerosis, cardiovascular diseases, etc. Therefore ob/ob mice can be used to explore the effects of inflammation on muscular proteins.

4.1.3. Aims

Following on from the previous chapter, the methods developed were applied to the analysis of oxPTMs in biological samples. There is not much reported on oxidative modification to the muscle proteins in ob/ob mice and therefore this study focused on the characterisation and quantification of oxidised proteins in ob/ob mice, mainly using the MS approaches developed in the chapter 3.

4.2. Results

When the muscle from the hind leg of the control and obese mice models was extracted and stripped from the fat, the weight of the muscle prior to homogenisation was recorded (Fig. 4.1A). The average weights for control and obese mice were ~1.5 g and ~1 g respectively and demonstrated a significant drop in muscle weight for the ob/ob model to approximately one third of the control muscle. The muscle was homogenised and both the SR and MH samples were obtained from triplicate mice for both models. After preparation of the samples, the specific activity of SERCA was measured by calculating the difference between total ATP hydrolysis in the presence and absence of thapsigargin: a known SERCA inhibitor (Lytton, Westlin, and Hanley, 1991). The specific activity was measured in μmol of free phosphate $\text{min}^{-1} \text{mg}^{-1}$ of protein and showed a drop in SERCA function (Fig. 4.1B). The reduction in SERCA specific activity elucidates that protein function decreases in the obese model, however, the loss in SERCA activity is non-significant. Nevertheless the loss of muscle mass indicates physiological differences in the models which may be the result of oxidative damage to a different subset of proteins from known oxidised proteins in the ageing model.

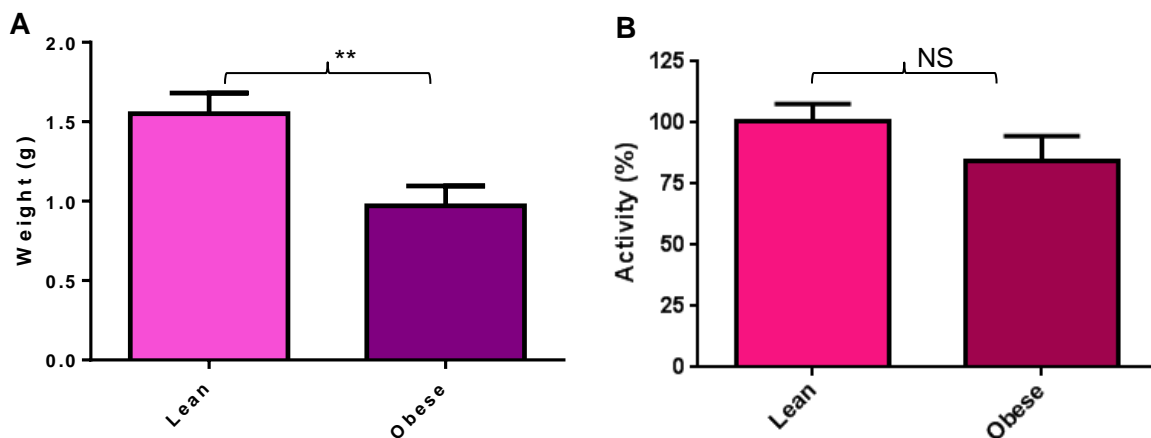


Figure 4.1. Comparisons of muscle weight and SERCA activity in both control and ob/ob models. A. Weight of whole hind mouse legs and **B.** Activity of SERCA normalised to the control. NS = non-significant data ($p > 0.05$), $n = 3$.

4.2.1. Immunoblotting with anti-nitrosothiol (-SNO) and anti-nitrotyrosine

To determine whether the samples contain oxidised proteins, isolated SR and muscle homogenate were electrophoresed on a 10%-SDS gel and subjected to probing with anti-SNO and anti-NitroY antibodies. NitroY was detected in the muscle homogenate of both the control and ob/ob samples; however, there appeared to be higher levels in the ob/ob samples (Fig. 4.2), although this was only apparent in the MH samples as no obvious bands were seen in the SR samples. The bands relating to NitroY detection were most dense in the mid to lower molecular weight region between 55 kDa and just below 25 kDa marker of the molecular weight ladder.

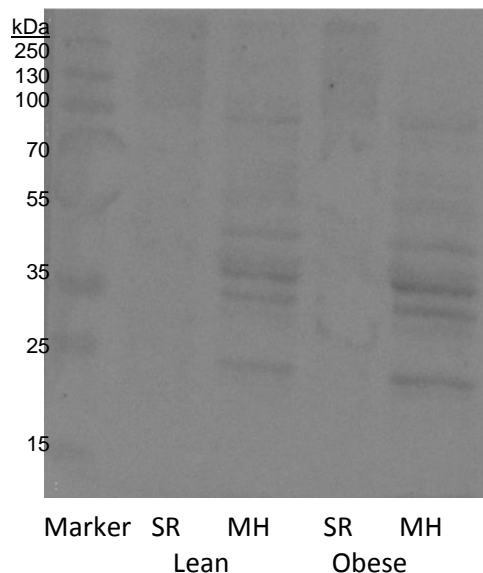


Figure 4.2. NitroY detection in lean & obese mice of isolated SR and muscle homogenate using western blotting. Samples were ran of a 10% SDS-gel and transferred to a PVDF membrane and probed with anti-nitrotyrosine.

Similarly, higher levels of nitrosothiols were detected in ob/ob samples in comparison to the control samples (Fig. 4.3). There were fewer bands present in the SNO immunoblot and the densest bands appear to be just above the 35 kDa marker and just below the 25 kDa marker. To ensure that this was not due to the indiscriminate binding of the secondary antibody, blots of MH samples were probed with the secondary alone and displayed no binding as the resulting blots appeared blank (Supplementary figure 4.1). It also appears that similar bands are shown with the presence of SNO and NitroY modifications.

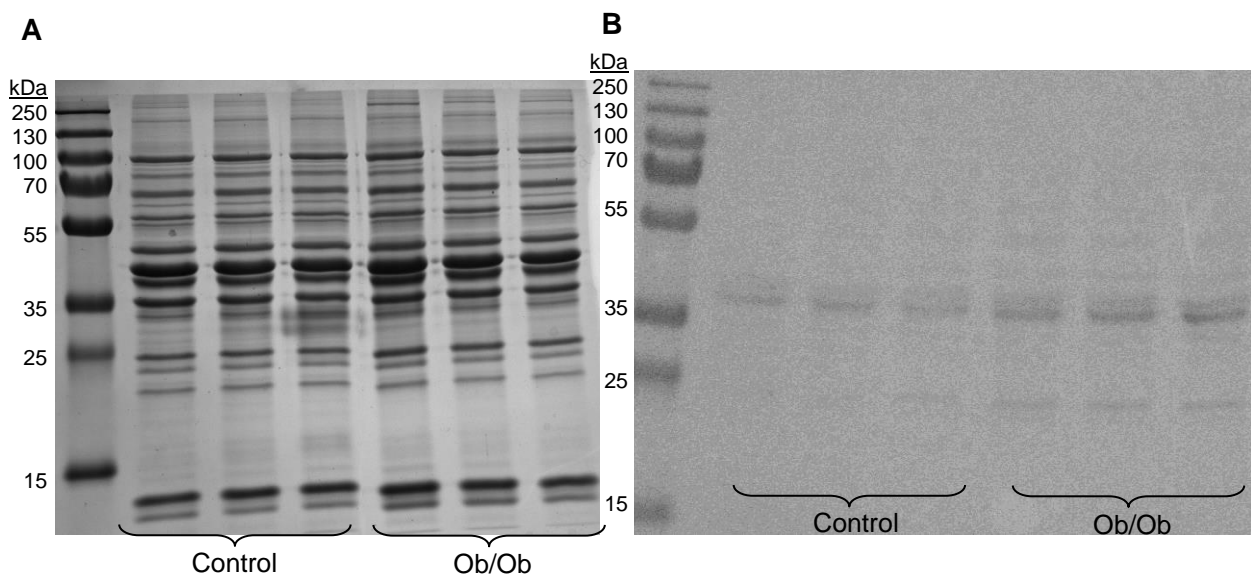


Figure 4.3. SDS-gel and immunoblot of SNOs in control and obese MH. **A.** Expedeon stained SDS-gel of control (lanes 2-4) and ob/ob (lanes 5-7) triplicate MH samples. **B.** Immunoblot probed with anti-SNO in triplicates of control (lanes 2-4) and ob/ob (lanes 5-7) of MH.

Both immunoblots support the presence of the oxidative modifications but from this technique, the identity of the modified proteins cannot be determined using this method. The samples were therefore subjected to MS analysis to characterise and quantify the oxidative modifications present in the samples.

4.2.2. Identification of oxidised residues in the control and ob/ob mice

In a similar manner to the *in vitro* studies, the proteins were digested and subjected to MS analysis to characterise and locate the modifications present in the samples. To accomplish this, the whole gel lane was analysed, termed GeLC-MS/MS (Piersma *et al.* 2013), rather than excising specific bands as in the previous approach. By opting for a non-biased approach during sample processing, there is no selective exclusion of peptides with potential modifications. Multiple modifications on proteins can affect their migration on a SDS-gel and so if modifications cause aggregation of the protein, higher molecular weight bands should not be excluded. The same applies to fragmented proteins, which may be present in lower molecular weight bands. Figure 4.4 shows how both the isolated SR and MH samples were fractionated and subsequent data is associated with the fractions as numbered there. The SR gel was divided into 6 fractions. By dividing the fractions into six parts, there is still some level of increased resolution via the separation of proteins by molecular weight. The gel could be divided into more fractions, increasing the resolution further, but this would lead to too many MS runs and would not be very efficient. On the other hand, the MH gel required more fractions as there was a greater variety of proteins in the whole lysate compared with the purified sample and it required more resolution. In doing so, chances of detecting modifications should increase, which would lead to a better understanding on the effects of oxidation within obese muscle, as well as a longer list of modifications with potential for discovering novel modified residues.

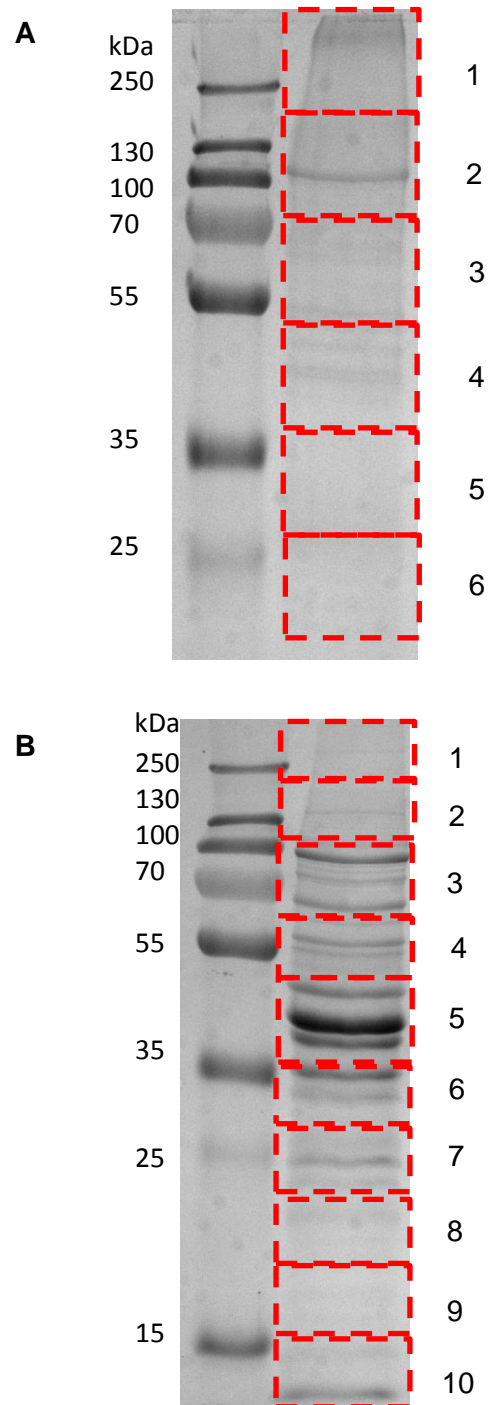


Figure 4.4. Expedeon stained SDS-gel of isolated SR and muscle lysate from obese mouse hind legs. A. Isolated SR. B. Muscle lysate. GeLC fractions of each sample are highlighted in red boxes and numbered.

Table 4.1 lists the top 5 proteins identified in each fraction of isolated SR from muscle of ob/ob mice, with the exclusion of the common contaminant keratin. Although procedures were set in place to minimise contaminating the samples with keratin during processing, it cannot be completely avoided. The table also lists the mascot score, mass of protein and sequence coverage. This data set shows higher Mascot scores were found in the higher molecular weight region of the gel compared to the lower molecular weight region which reflects what is seen in SDS-gel as there is a higher abundance of proteins in the high molecular weight region. The masses for the top hits from GeLC fraction 1 to 6 were as follows: 223.6 kDa, 110.7 kDa, 74.9 kDa, 59.8 kDa, 43.2 kDa, and 33.1 kDa. Although this fits the electrophoretic separation of proteins by mass, SERCA and sarcalumenin were not detected in the expected fractions. Sarcalumenin, a 99 kDa protein, was found in fraction 4, where almost all other proteins ranged from 55-60 kDa. SERCA, a 110 kDa protein, was also found in this fraction, as well as in fractions 1, 2 & 3, suggesting possible aggregation and fragmentation of the proteins. Overall, the sequence coverage for the top 5 hits in all GeLC fractions ranged between 17-68%, with an average sequence coverage of ~39%. This level of sequence coverage was expected to be sufficient to detect a reasonable number of modifications in this protein list.

Table 4.1. List of modifications identified and validated in obese muscle. Top 5 protein hits of isolated SR in each GelC slice with exclusion of keratin. *Although the protein was identified, Mascot displayed an error when accessing protein information.

GeLC fraction	Hit	Protein ID	Protein	Mascot score	Mass (Da)	Sequence coverage
1	1	MYH4	Myosin heavy chain 4, skeletal	11661	223632	54%
	2	AT2A1	SERCA	9905	110723	54%
	3	AT1A2	Na+/K+ transporting ATPase subunit alpha-2	1769	113457	33%
	4	RYR1	Ryanodine receptor 1	1604	570381	19%
	5	DYSF	Dysferlin	653	240040	23%
2	1	AT2A1	SERCA	11317	110723	53%
	2	AT1A2	Na+/K+ transporting ATPase subunit alpha-2	2829	113457	39%
	3	PYGM	Glycogen phosphorylase	1158	97681	37%
	4	ODO1	2-oxoglutarate dehydrogenase, mitochondrial	869	117572	40%
	5	B3AT	Band 3 anion transport protein	283	103412	17%
3	1	CMC1	Calcium binding mitochondrial carrier protein Aralar1	1588	74922	55%
	2	AT2A1	SERCA	1585	110723	33%
	3	ALBU	Serum albumin	1443	70700	49%
	4	DHSA	Succinate dehydrogenase [ubiquinone] flavoprotein subunit, mitochondrial	1088	73623	-
	5	ANXA6	Annexin A6	945	76294	49%
4	1	ATPA	ATP synthase subunit alpha, mitochondrial	3851	59830	54%
	2	SRCA	Sarcalumenin	1000	99522	29%
	3	KPYM	Pyruvate kinase isozymes M1/M2	817	58378	41%
	4	ATPB	ATP synthase subunit beta, mitochondrial	652	56265	51%
	5	AT2A1	SERCA	606	110723	26%
5	1	KCRM	Creatine kinase M-type	2271	43246	46%
	2	ENOB	Beta-enolase	1713	47377	38%
	3	KCRS	Creatine kinase S-type	1020	47899	52%
	4	ACTC	Actin, alpha cardiac muscle 1	963	42334	36%
	5	QCR2	Cytochrome b-c1 complex subunit 2, mitochondrial	820	48262	36%
6	1	ADT1	ADP/ATP translocase 1	846	33111	68%
	2	MYP0	Myelin protein P0	768	27775	23%
	3	SYPL2	Synaptophysin-like protein 2	427	29605	26%
	4	PGAM2	Phosphoglycerate mutase 2	411	28980	37%
	5	AT5F1	ATP synthase subunit b, mitochondrial	280	29044	20%

The Mascot results were exported to XML files and processed through PANTHER (Protein ANalysis THrough Evolutionary Relationships), which classified the protein list into their molecular function (Fig.4.5). When comparing the isolated SR and the muscle homogenate, according to the functional classification of the proteins they appear similar in most categories; however, the proteins that contribute to each category are different between the samples. Also the analysis does not take into account the abundance of a single protein but rather the association of each protein to the biological processes. One visible difference between the two samples is the increased percentage of proteins involved in localisation and the decrease in proteins involved in metabolic processes in the purified SR sample in comparison to muscle homogenate.



Figure 4.5. Classification of ob/ob muscle homogenate and isolated SR proteins into biological processes. Pie chart classifying proteins listed in (A) Isolated SR and (B) Muscle homogenate XML files according to their molecular function using online PANTHER software.

Just as described in the previous chapter, de novo sequencing is important and required for validation of the Mascot results. Fig 4.6 shows two peptides that have been sequenced and validated. OxH and OxW of enolase and lactate dehydrogenase showed the variety of modifications detected as well as the start of exploring the effects of oxidation in other proteins. The two peptides were subsequently used for quantitation in obese muscle.

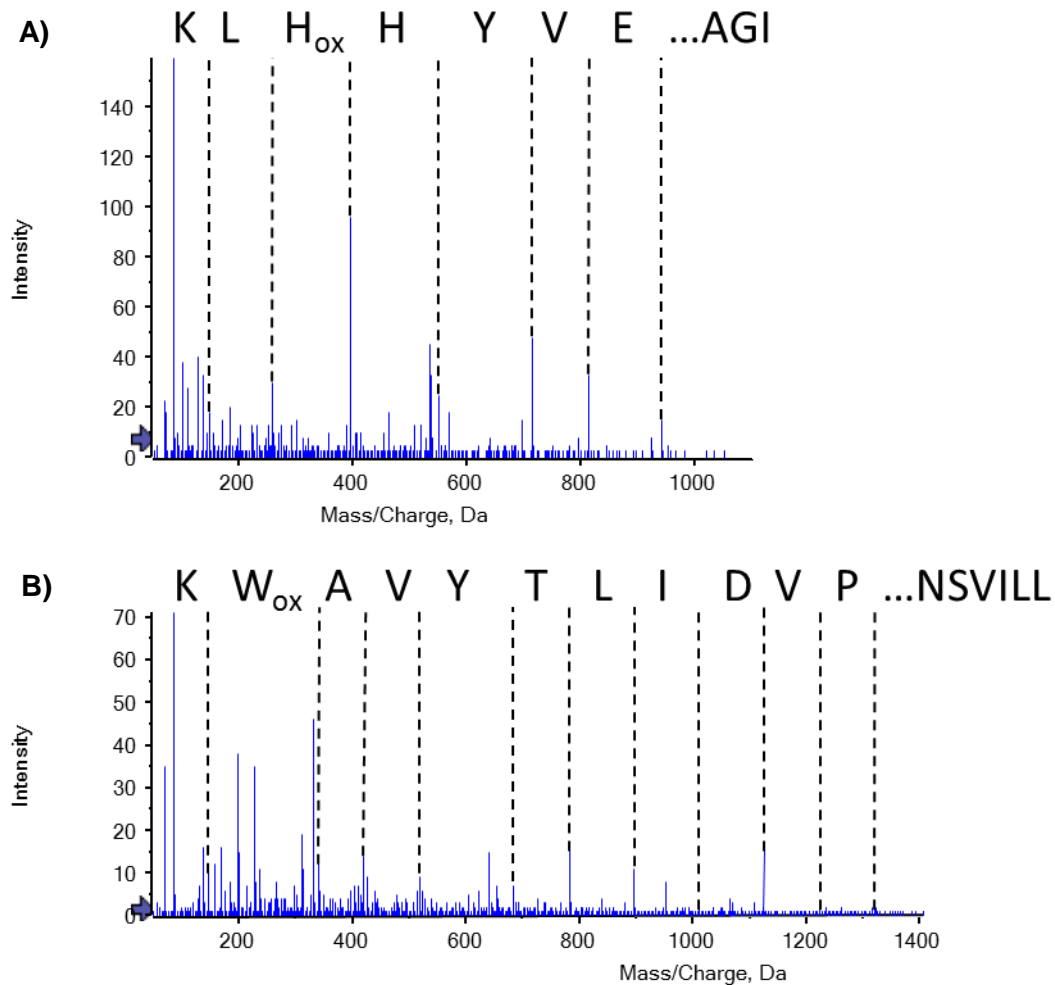


Figure 4.6. De novo sequenced peptides in ob/ob muscle. A. OxH in Beta-enolase 3 (IGAEVYHHoxLK) and **B.** OxW in L-lactate dehydrogenase A chain (LLIVSNPVDILTIVAWoxK).

Figure 4.7 shows the number of modified residues for TrioxC, DioxM and OxM in the control and obese models from the discovery MS/MS data sets for SERCA of SR samples. The presence of all three oxidised residues was significantly more abundant in the obese model, suggesting higher levels of oxidised peptides are present in obesity compared to the lean model. As these modifications were more abundant in muscle from obese animals, they were selected for further investigation by the MRM approach developed in the previous chapter.

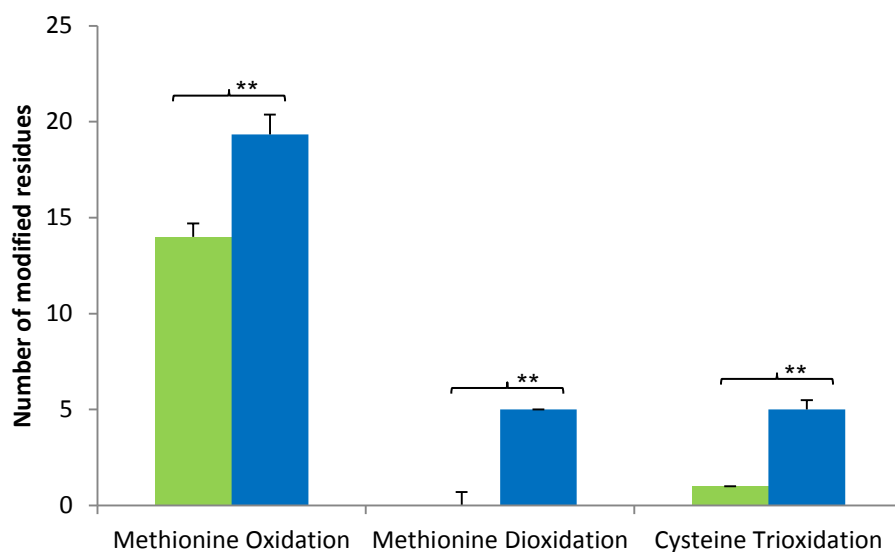


Figure 4.7. Number of modified residues detected in discovery MS/MS of SR samples in control and obese models for SERCA. Green indicates residues counted from control samples and blue indicates residues counted from ob/ob samples. **Statistically significant data ($p < 0.01$) using unpaired t-test, $n=3$.

Following analysis of the proteins and observation of several interesting oxidations, the oxPTMs listed in section 2.12 were set as variable modifications and *de novo sequencing* was performed to verify their occurrence. Table 4.2 presents some of the modifications detected in ob/ob SR samples using discovery MS/MS analysis. Many of the oxPTMs detected were found to be TrioxC, DioxM and OxW modifications. Additional modifications detected include DioxW, OxY and OxH.

Table 4.2. List of modifications detected and validated by de novo sequencing in band 2 of ob/ob SR samples. Summary of oxidative modifications achieved through searches in Swiss-Prot database with carbamidomethyl as a fixed modification and the variable modifications in the table, as described in Chapter 2. Modified residues are highlighted in red in the peptide sequence.

Protein	Modification	Sequence	Residue
SERCA	TrioxC	CLALATR	Cys561
	TrioxC	EVTGSIQLCR	Cys614
	TrioxC	GTAIAICR	Cys636
	OxW	EPLISGWLFFR	Trp832
	DioxW	EPLISGWLFFR	Trp832
	DioxM	AEIGIAMGSGTAVAK	Met720
	DioxM	TGTLTTNQMSVCK	Met361
Na ⁺ /K ⁺ transporting ATPase subunit alpha-2	OxW	SPTWTALSR	Trp416
ADP/ATP translocase 1	OxW	GAWSNVLR	Trp275
Myeloperoxidase	OxW	IQWVGDPDR	Trp101
Pyruvate kinase	OxY and OxM	ITLDNAYMEK	Tyr148&Met149
Creatine kinase M type	TrioxC	RF ^C VGLQK	Cys254
	DioxM	GQSIDDMIPAQK	Met376
Fructose biphosphate aldolase A	DioxM	IGEHTPSALAIMENANVLAR	Met165
	OxW	CPLLKPWALTFSYGR	Trp296
	OxW	ALQASALKAWGGK	Trp314
Glyceraldehyde-3-phosphate dehydrogenase	OxW	LISWYDNEYGYSNR	Trp311
Glycogen phosphorylase	DioxM	MSLVEEGAVK	Met429
	OxW	EIWGVEPSR	Trp826
Pyruvate kinase	TrioxC	NICKVVEVGSK	Cys165
	DioxM	FGVEQDQDVMVFASFIR	Met239
Enolase b	OxH	IGAEVYHHLK	His191
Lactate dehydrogenase	OxW	LLIVSNPVDILTYVAWK	Trp148
Fructose-biphosphate aldolase A	OxW	ALQASALKAWGGK	Trp314

Additionally, oxPTMs were identified in MH samples with additional OxP, Ally and NitroY modifications (Table 4.3). The detection of NitroY in a biological sample suggested that the methods were sufficiently optimised for the analysis of formation of this modification in muscle *in vivo*. While there are similar proteins detected in both the isolated sarcoplasmic reticulum and the muscle homogenate, i.e. creatine kinase and glyceraldehyde-3-phosphate dehydrogenase, the modifications detected differ. Additionally while SERCA modifications are detected in the isolated sarcoplasmic reticulum sample, these are not present in the muscle homogenate alluding to the advantages of using enrichment techniques to unveil modifications of organelle specific proteins.

Table 4.3. Identification of oxPTMs discovered in obese muscle homogenate. All modifications were validated by de novo sequencing and modified residues are highlighted in red. The full table with uncertain and false positive data included is provided in Supplementary Material (Supplementary Table 4.1).

Band	Protein ID	Protein description	Protein mass	Mass/ Charge (m/z)	Peptide score	Peptide expect	Peptide sequence	Modification
1	K1B24_MOUSE	Kallikrein 1-related peptidase b24	29478	407.2217,3+	27.57	0.044	DKSNDLMLLR	Ally; OxM
2	G3P_MOUSE	Glyceraldehyde-3-phosphate dehydrogenase	36072	524.7988,3+	56.22	0.00062	VPTPNVSVVDLTCR	OxP
2	K1B24_MOUSE	Kallikrein 1-related peptidase b24	29478	407.2259,3+	44.11	0.024	DKSNDLMLLR	Ally; OxM
4	SYNJ2_MOUSE	Synaptojanin-2	159578	455.5816,2+	39.24	0.0065	GLPPDHGGK	2 OxP
4	TNR11_MOUSE	Tumor necrosis factor receptor superfamily member 11A	68460	469.2537,2+	27.54	0.047	DSFAGTAPR	OxP
5	G3P_MOUSE	Glyceraldehyde-3-phosphate dehydrogenase	36072	524.7977,3+	39.4	0.0044	VPTPNVSVVDLTCR	OxP
5	K1B24_MOUSE	Kallikrein 1-related peptidase b24	29478	602.3615,2+	50.16	0.003	DKSNDLMLLR	Ally
5	PTPS_MOUSE	6-pyruvoyl tetrahydrobiopterin synthase	16235	509.8174,2+	35.79	0.024	LLPVGALYK	NitroY
6	KCRM_MOUSE	Creatine kinase M-type	43246	539.8088,2+	36.98	0.026	VLTPDLYNK	OxP
6	ALDOA_MOUSE	Fructose-bisphosphate aldolase A	39787	603.3448,3+	34.52	0.0034	CPLLKPWALTFSYGR	Ally
6	G3P_MOUSE	Glyceraldehyde-3-phosphate	36072	599.2975,3+	27.73	0.03	LISWYDNEYGYSNR	OxW

		dehydrogenase						
7	ALDOA_MOUSE	Fructose-bisphosphate aldolase A	39787	1129.621,3+	92.63	0.000002	ALANSLACQGK ^Y TPSGQSGAAA SESLFISNHAY	OxY
7	G3P_MOUSE	Glyceraldehyde-3-phosphate dehydrogenase	36072	524.7943,3+	40	0.033	VPT ^P NVSVVDLTCR	OxP
8	GSTP1_MOUSE	Glutathione S-transferase P 1	23765	608.9556,3+	85.04	4.3E-07	EAAQMD ^M VNDGVEDLR	DioxM
10	HBB1_MOUSE	Hemoglobin subunit beta-1	15944	645.8925,2+	36.88	0.027	LLVVYP ^W TQR	OxW

Although, the Mascot analysis has limited the modifications searched for to twelve, it is possible that modified peptides containing other oxPTMs remained unidentified. However, increasing the number of modifications searched in a single run would increase the complexity of spectral matching with the theoretical database giving rise to more false positives from the searches and also larger datasets would have to be mined. Although the modifications that were searched for are shown in the datasets above, there was an additional potential modification detected in the samples. While performing *de novo* sequencing for validation of a modification, one peptide that Mascot had reported as containing TrioxC was actually found to contain a cysteine that appeared to both alkylated and dioxidised (Fig. 4.8). This strange modification combines the addition of the mass of alkylation (57 Da) with the mass of a dioxidation (32 Da), corresponding to a total of 89 Da and has been reported in another study (Jaeho Jeong, *et al.* 2011). It is important to note that although subsequent quantitation of oxidised residues tried to include other feasible oxidations within the peptide of interest, not all potential modifications could be taken into account. Therefore the quantitation is not absolute but an approximation of the percentage modification based on the current understanding of residue susceptibility to oxidation. For many of the quantified peptides, OxM containing peptides were quantified alongside unmodified forms, owing to their susceptibility to oxidation. Although this is also heavily dependent on the accessibility to the methionine residues in the protein conformation, it is safer to presume that the methionine may be oxidised and always include it as a variable modification.

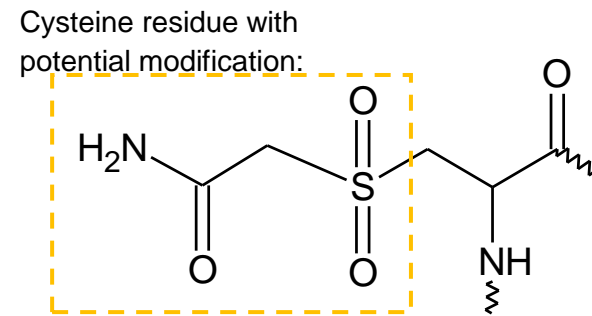
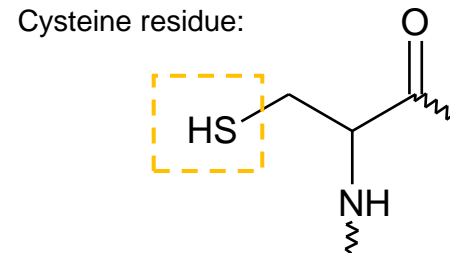
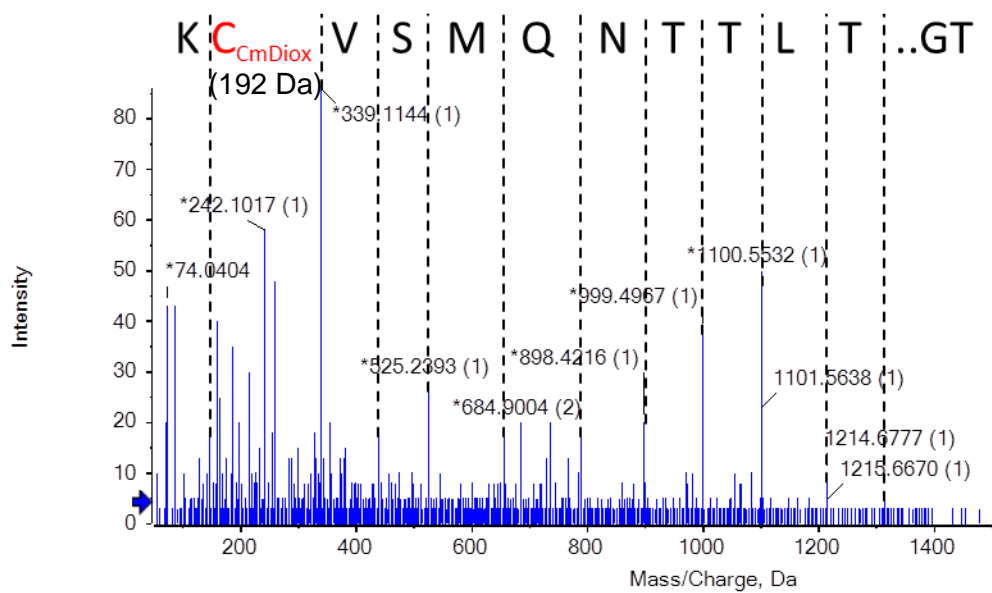


Figure 4.8. Potential unusual modification to a SERCA peptide found in an obese sample. Carbomethylated cysteine + 2 Oxygens (57+32=89) (103+89=192).

4.2.3. Quantification of oxidative modifications by MRM

In addition to previous transitions used for MRM quantitation, a new list was produced incorporating modifications found in other proteins in the discovery MS/MS analysis of obese mouse muscle samples (Table 4.4). These include modified peptides from lactate dehydrogenase, beta-enolase and pyruvate kinase.

Table 4.4. Transition lists for the additional modifications observed in muscle samples from obese mice. Modified residues highlighted in red.

Protein	Sequence/Modification	Precursor ion	Product ions	CE
L-lactate dehydrogenase A chain	LLIVSNPVDILTYVAWoxK	980.6	682.4	48.2
L-lactate dehydrogenase A chain	LLIVSNPVDILTYVAWoxK	980.6	783.4	48.2
L-lactate dehydrogenase A chain	LLIVSNPVDILTYVAWoxK	980.6	896.5	48.2
L-lactate dehydrogenase A chain	LLIVSNPVDILTYVAWK	972.6	666.4	48.2
L-lactate dehydrogenase A chain	LLIVSNPVDILTYVAWK	972.6	767.4	48.2
L-lactate dehydrogenase A chain	LLIVSNPVDILTYVAWK	972.6	880.5	48.2
Beta-enolase 3	IGAENVYHHoxLK	591.8	413.3	31.1
Beta-enolase 4	IGAENVYHHoxLK	591.8	550.3	31.1
Beta-enolase 5	IGAENVYHHoxLK	591.8	713.4	31.1
Beta-enolase 6	IGAENVYHHHLK	583.8	397.3	31.1
Beta-enolase 7	IGAENVYHHHLK	583.8	534.3	31.1
Beta-enolase 8	IGAENVYHHHLK	583.8	697.4	31.1
Glycogen phosphorylase	VLYnitroPNDNFFEGK	744.3	856.4	37.8
Glycogen phosphorylase	VLYnitroPNDNFFEGK	744.3	970.4	37.8
Glycogen phosphorylase	VLYnitroPNDNFFEGK	744.3	1067.5	37.8
Glycogen phosphorylase	VLYPNDNFFEGK	721.9	856.4	37.8
Glycogen phosphorylase	VLYPNDNFFEGK	721.9	970.4	37.8
Glycogen phosphorylase	VLYPNDNFFEGK	721.9	1067.5	37.8
Pyruvate kinase	NICtrioxKVVVEVGSK	612.9	390.2	32.2
Pyruvate kinase	NICtrioxKVVVEVGSK	612.9	519.3	32.2
Pyruvate kinase	NICtrioxKVVVEVGSK	612.9	618.4	32.2
Pyruvate kinase	NICKVVVEVGSK	616.8	390.2	32.2
Pyruvate kinase	NICKVVVEVGSK	616.8	519.3	32.2
Pyruvate kinase	NICKVVVEVGSK	616.8	618.4	32.2

Quantification of the modified peptides with targeted MS methods demonstrated the ability of mass spectrometry as a useful analytical tool for biological samples. Unfortunately, not all modified peptides could be quantified, but the ones that were showed interesting results. Figure 4.10 demonstrates how the percentage modification of a peptide was calculated using the MRM data. Extracted ion chromatograms were used to identify the retention time at which all transitions appeared. This determined which peaks were used for quantification. The area under the peak was calculated for the unmodified and modified peptides to give an overall percentage modification. The highlighted ions show the sequence of the corresponding peak where a mass shift can be seen relating to the addition of one or two oxygen to the peptide when modified.

Not all MRM analyses were successful. Figure 4.9 displays the XIC of the OxW transitions from SERCA in an obese sample that showed signals at noise level. Many modifications gave similarly poor results, which may reflect the limited of sensitivity of the approach and requires further optimisation for the quantitation of oxPTMs that are less susceptible to modification.

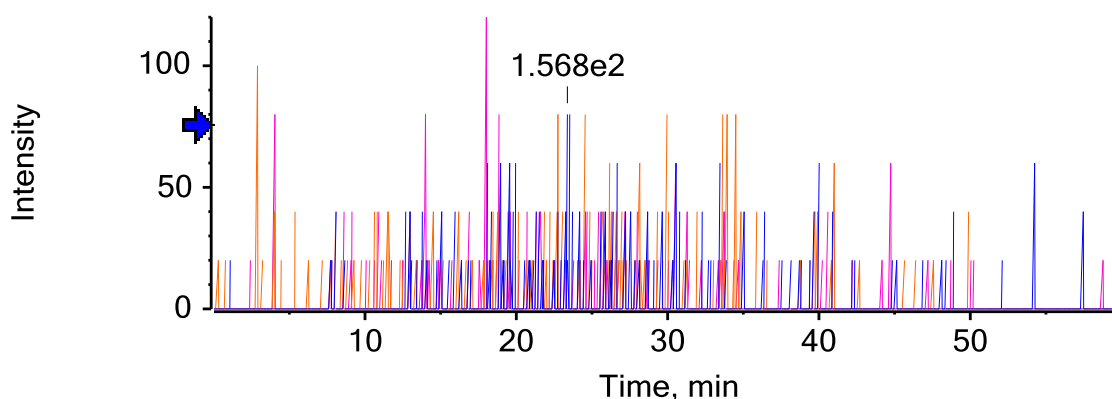
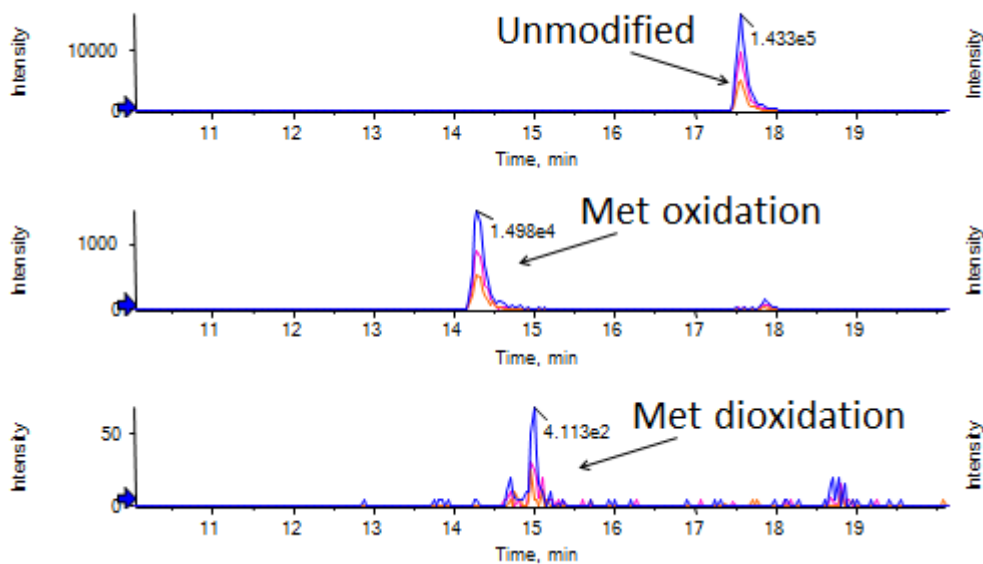


Figure 4.9. MRM spectrum of OxW of SERCA peptide EPLISGWLFFR in obese MH. Transitions coloured blue, orange and pink.

A) Extracted ion chromatograms:



B) Sequenced peptides:

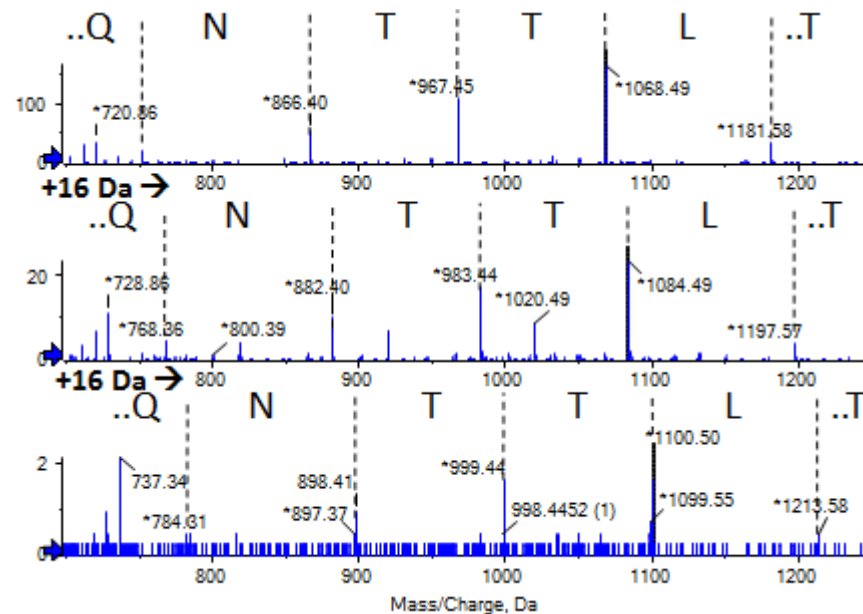


Figure 4.10. MRM spectra of TGLTTNQM^SVCK OxM & DioXM in obese sample. Data are represented as extracted ion chromatograms of product ions (A) and sequenced peptides from MRM (B). +16 Da = Addition of oxygen. → = Mass shift.

From quantification of the raw data, bar charts were produced to represent the difference between ob/ob and control samples (Fig.4.11). All peptides show higher levels of oxidation in the ob/ob samples, but only two showed statistically significant results. The large error bars are due to biological variation and demonstrate the need for many more biological replicates to determine whether ob/ob samples are more oxidised overall than the corresponding controls. Some modifications were shown to be different between the control and obese samples i.e. GTAIAICR with ~6 fold increase and AEIGIAMSGTAVAK with ~1.8 fold increase in obese muscle. As mentioned in the previous chapter, both these peptides are adjacent to Cys674, a key residue involved in the redox regulation of SERCA, and again supports the theory that these two residues play a protective role in order to prevent irreversible modification to Cys674.

Unfortunately, due to limits on MS sensitivity, all of the SERCA peptides successfully quantified contained highly susceptible residues i.e. methionine and cysteine. Although this does provide information on residue susceptibility and possible effects of location of residue to function, there is not enough information to give a complete picture of how oxidants from inflammation, modify muscle proteins in obesity.

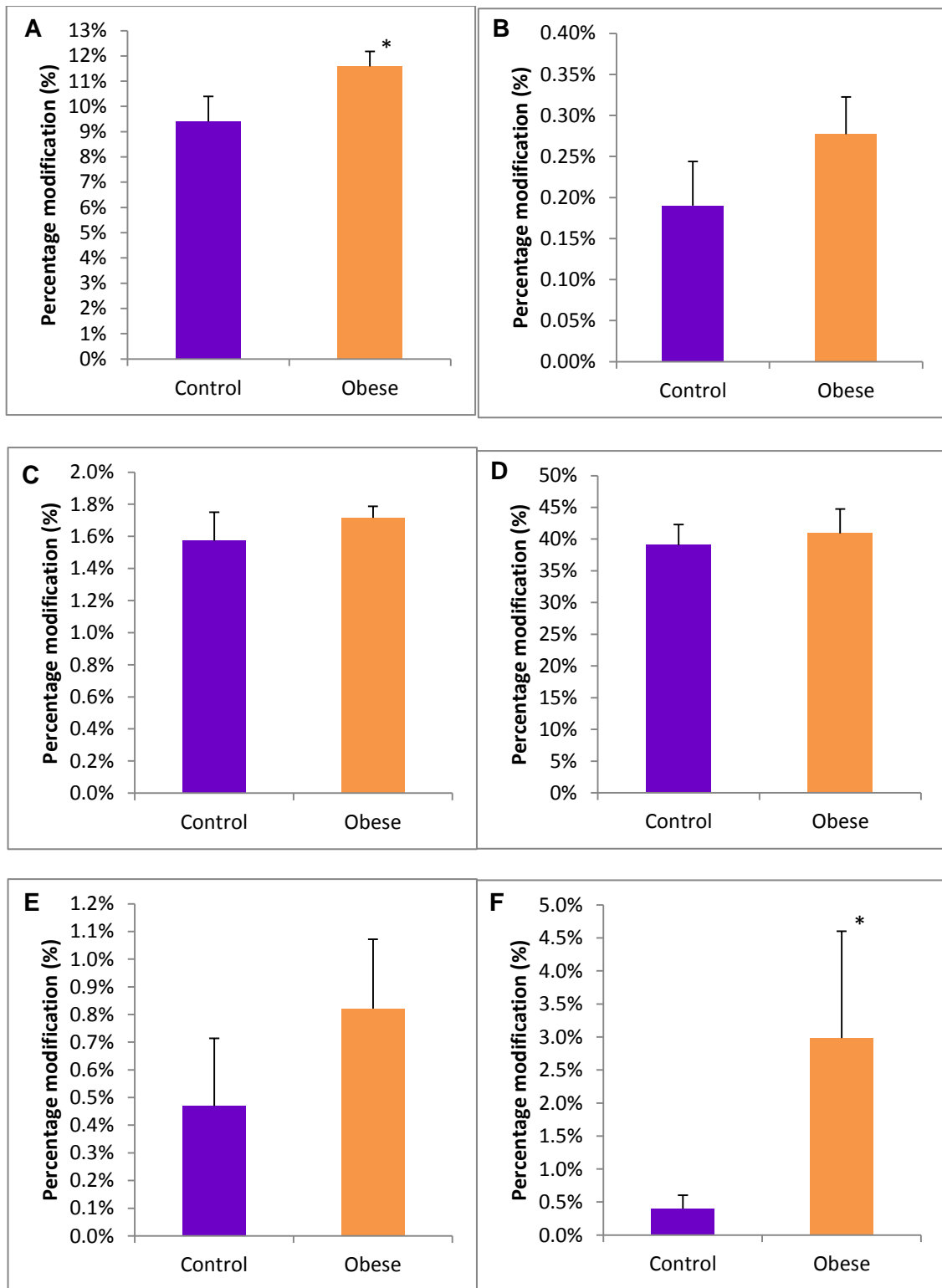


Figure 4.11. Quantitation of SERCA peptides in obese muscle. Percentage modification of OxM (A) and DioxM (B) in TGTLLTNQMSVCK, TrioxC (C) in EVTGSIQLCR, OxM (D) and DioxM (E) in AEIGIAMGSGTAVAK, and TrioxC (F) in GTAIAICR peptides of SERCA. *Statistically significant data (p<0.05), n=3.

4.3. Discussion

4.3.1. Muscle loss and reduction in SERCA activity

Obese mice showed a decrease in muscle mass which suggests that these changes are a result of the obese state of the mouse model. The reduction seen in this study was approximately one third of the control mouse weight and concurs with the evidence from the literature. It is in agreement with a study that found a reduction in muscle mass in ob/ob mice and further reported ~30% decrease in predominant muscle fibre size (Kemp *et al.* 2009). The reduction in muscle mass has been linked to impaired muscle generation brought about by the decrease in macrophage accumulation, activity of myoblasts and angiogenesis (Nguyen, Cheng and Koh, 2011). On the other hand, the specific activity of SERCA was shown to be non-significantly reduced in the ob/ob mice in this study. Studies with SERCA in liver of obese mice have showed decreased activity, alongside reports on muscle changes, which have correlated the impairment of SERCA function with changes in phospholipid composition due to dietary influence (Fu *et al.* 2011; Funai *et al.* 2013). Moreover, literature on SERCA in diabetic models has linked the reduction in activity to the presence of oxPTMs (Ying *et al.* 2008). Although a number of reasons have been suggested for what causes the reduction in SERCA activity, one possible candidate is the effects of oxidative modification on the function of SERCA, which was shown to occur at higher levels than the control in this study.

4.3.2. Increased levels of nitrative modifications in immunoblots

The immunoblots showed higher levels of SNO and NitroY detected in the obese model in comparison to the control. An increased level of NitroY has previously been detected using immunofluorescent histochemistry in the sciatic nerve, spinal cord, dorsal root ganglion of ob/ob mice (Drel *et al.* 2006). NitroY has also been detected in mitochondrial proteins in liver tissue of ob/ob mice (Garcia-Ruiz *et al.* 2006). Both of these studies indicate the presence of

increased NitroY in other tissues and coincide with what has been detected in the skeletal muscle used in this study.

S-nitrosation of insulin receptor beta subunit and protein kinase B/Akt were observed in ob/ob mice (Carvalho-Filho *et al.* 2005), demonstrating the presence of s-nitrosation in muscle and concurring with the results from the immunoblot probed with anti-SNO. The presence of nitrative species in the muscle of ob/ob mice at higher levels is in agreement with the literature and confirms that a higher frequency of proteins in the ob/ob model are present as oxidised biomolecules.

4.3.3. Characterisation of oxPTMs in skeletal muscle proteins of ob/ob mice

In a single band from the SR samples, 12 proteins were shown to contain oxPTMs that were not oxidation of methionine residues: SERCA, Na⁺/K⁺ transporting ATPase subunit alpha-2, ADP/ATP translocase 1, myeloperoxidase, pyruvate kinase, creatine kinase M type, fructose bisphosphate aldolase A, glyceraldehyde-3-phosphate dehydrogenase (GAPDH), glycogen phosphorylase, pyruvate kinase, enolase b, lactate dehydrogenase, and fructose-bisphosphate aldolase A. The majority of these proteins are involved in glucose metabolism and energy production, and while it has been reported that there is increased abundance of GAPDH and aldolase A in obese muscle, it has previously also been reported that these proteins are susceptible to oxidative stress (Shenton and Grant, 2003; England *et al.* 2004; Hittel *et al.* 2005). GAPDH in particular has been reported to be susceptible to cysteine oxidation, resulting to the change in interactors depending on whether GAPDH is present in its oxidised form (Hwang *et al.* 2009). Na⁺/K⁺ transporting ATPase subunit alpha 2 pumps sodium ions out and potassium ions into the cell, and has been shown to be important in maintaining contraction of the skeletal muscle and resisting fatigue that results from the reduced force unable to compensate for the demand (Radzyukevich *et al.* 2013). Myeloperoxidase is found in neutrophils and produces hypochlorous acid as an effective defence mechanism against pathogens (Klebanoff, 1999). In addition to this role,

myeloperoxidase has been reported to have vasoconstricting properties in the skeletal muscle (Csató *et al.* 2015).

SERCA had the highest number of oxPTMs detected: three TrioxC, two DioxM, one OxW and one DioxW, resulting in a total of 7 oxPTMs identified. Met720 and Met361 were found in the phosphorylation domain and nucleotide binding domain of SERCA respectively. Met720 in particular may be an important residue as it is adjacent to Cys674, a key residue involved in redox regulation of SERCA (Adachi *et al.*, 2004). The role of this residue may be to act as a scavenger for oxidants to prevent the further oxidation of Cys674 to an irreversible form. Cys561 was located in the nucleotide binding domain, whereas Cys614 and Cys636 were located in the phosphorylation domain. Cys636, in particular, was also found to be adjacent to Cys674 previously mentioned to be involved in redox regulation. This residue may function in the same manner as Met720, i.e. as an endogenous scavenger to protect cysteine from irreversible oxidation. The last modified residue, Trp832, was found in the transmembrane domain of SERCA. As there is very little on functional studies of these modified residues it is difficult to determine whether these changes have an impact on protein function. However, if these protein functions are affected, it could explain the physical outcomes of lower muscle performance in obesity.

From the muscle homogenate samples, nine proteins were found to be oxidised: kallikrein 1-related peptidase b24, glyceraldehyde-3-phosphate dehydrogenase (GAPDH), synaptotagmin-2, tumor necrosis factor receptor superfamily member 11A, 6-pyruvoyl tetrahydrobiopterin synthase (PTPS), creatine kinase M-type, fructose-bisphosphate aldolase A, glutathione S-transferase P1, and hemoglobin subunit beta-1. Kallikrein 1-related peptidase b24 releases bradykinin which is a vasodilator and is involved in reducing blood pressure (Matsui *et al.* 2005). There are no reports in the literature that show this protein to be modified from Lys119 to Allysine119. GAPDH is involved in glycolysis, but it has also been reported to contribute to modulation of vesicle endocytosis via binding to Pro234 (Robbins, Ward and Oliver, 1995). Substitution of this residue was shown to disrupt endocytosis, however, the

residue that was found to be oxidised in this study was its neighbouring proline residue Pro236. Synaptojanin-2 is involved in membrane trafficking, signal transduction pathways and clathrin mediated endocytosis (Rusk *et al.* 2003). In this study, two neighbouring proline residues were found to be oxidised in the C-terminal, which is proline rich. OxP was also detected in TNF receptor superfamily member 11A at Pro577. The protein is a receptor activator of nuclear factor-kappaB and important for energy metabolism in skeletal muscle as well as suggested candidate for obesity determination (Zhao *et al.* 2006). The enzyme PTPS is involved in the production of tetrahydrobiopterin, which contributes to the conversion of phenylalanine to tyrosine and is involved in production of neurotransmitters (Bonafe *et al.* 2005). PTPS is the only protein with a validated NitroY modification in the current study. Interestingly, this protein was found in the GeLC fraction 5 band, although its native mass is 16 kDa and it was expected to be further down the SDS-gel. When comparing this to the NitroY immunoblot, one of the denser bands is in the same region as the excised GeLC fraction 5 band. Thus not only has NitroY been detected with immunoblotting but also the one of the proteins containing NitroY was identified using MS. Tyr127 is a residue within PTPS that is commonly phosphorylated, and while it is known that phosphorylation to Ser19 is important for maximal activity, additional studies have not yet shown the significance of Tyr127 phosphorylation on activity (Scherer-Oppliger *et al.* 1999; Bian *et al.* 2014). However, nitration of Tyr127 is likely to interfere with its phosphorylation, and potentially its function. Deficiency in tetrahydrobiopterin production could lead to insufficient production of protein due to reduced conversion of phenylalanine to tyrosine. Detection of NitroY and carbonyl groups in creatine kinase have been reported in the literature in aged skeletal muscle (Nuss *et al.* 2009). The protein is important for supplying energy to the muscle and so the group proposed that the nitrotyrosine and carbonyl groups lead to aggregation of the protein and loss of function, which may result in muscle frailty. Haemoglobin subunit beta-1 is important for the transport of oxygen in the blood, and studies involving tryptophan oxidation monitored by fluorescence have suggested that oxidised haemoglobin releases the haem group (Chiu

et al. 1996). One example of a study that looked into oxPTMs in obese mice was the identification of carbonyl groups in adipose tissue, which used mass spectrometry to detect filamin A, eukaryotic elongation factor 1a-1, glutathione peroxidase 1, peroxiredoxin 1, glutathione S-transferase M1 (Grimsrud *et al.* 2007). As this was reported in adipose tissue, the characterisation of the oxidised proteins in the muscle of ob/ob mice could potentially be novel modifications detected in relation to the model. Of the proteins listed, glutathione S-transferase was also detected in the current study; however, the modification identified was methionine dioxidation. Glutathione S-transferase has an important role in protection against oxidative stress via catalysing the reaction of reduced glutathione (Nebert and Vasiliou, 2004).

4.3.4. Quantitation of oxidised muscle proteins

The results from the MRM studies showed successful quantitation of a few oxidised residues in SERCA. From the six quantified peptides, two were considered to have a statistically significant difference when comparing triplicate values from the obese and control muscle. Furthermore only DioxM and TrioxC were quantified using MRM approaches and as these residues are the most susceptible to oxidation, the current methods developed for this study are limited to abundant modifications. While the MRM approach was not particularly successful, it still demonstrated the higher levels of oxidation detected in the ob/ob model. While there does not appear to be previous quantitation of oxPTMs in muscle tissue of ob/ob mice with which to make comparisons, there are alternative studies that do show successful quantitation of oxidised proteins in obesity related models. The effect of antioxidants from green tea was tested on Zucker diabetic fatty (ZDF) rats to determine oxidative changes in plasma proteins by SRM based methods (Madian *et al.* 2011). Proteins containing carbonyl groups were enriched from plasma by biotinylation and subsequently seventeen carbonyl groups were detected and quantified. As these oxidised proteins were identified in plasma samples there were no reports of modified proteins discovered from this muscle study. However, in comparison to the plasma study, the identification of twelve modifications in the

muscle of the ob/ob mice, in which two of the peptides were shown to contain allysine, does demonstrate the advantages and disadvantages of enrichment for specific modifications. While more carbonyl groups were detected in the plasma samples, the opportunity for characterisation and quantitation of other oxPTMs was lost. Nonetheless, the study did show carbonyl group formation on lysine, arginine, proline and threonine residues and demonstrated reduction of oxidation with green tea treatment. Additional differences in the methodology used to quantify the biotinylated enriched carbonyl groups included the fractionation of the plasma samples with a propylsilane (C3) reverse phase column and the use of two transitions for peptide quantitation. This approach increases the concentration of the targeted peptides within a sample injection volume and has a much lower risk of targeting isobaric peptides for MS/MS fragmentation. It also explains the reduced number of peptide transitions used in the study, which would lead overall to reduced cycle times, more peptides quantified in one MS run, and in turn develop high throughput SRM methods. Comparisons to this study indicate the many possible approaches to sample preparation and development of quantitative MS methods when study oxPTMs.

4.3.5. Concluding statement

From these data it can be concluded that enrichment of proteins by isolating SR resulted in characterisation of more oxPTMs, compared to the whole muscle homogenate. On the other hand, the analysis with the muscle homogenate led to the identification of other modifications in proteins that were absent in the isolated SR samples. Thus both types of samples have advantages and disadvantages when identifying oxPTMs using MS/MS approaches. Based on known functions of the proteins described previously in the literature, the consequences of protein oxidation can be suggested; for example, the oxPTMs detected may affect neurosignalling, energy metabolism, protein building, skeletal function and regulation of blood pressure and oxygen transport. Functional studies are required to determine whether the oxPTMs discovered in this study result in functional disruption and in turn lead to the physical traits of obesity. Our current findings have demonstrated detection

of novel modifications, not previously characterised in the muscle of aged model used in this study. The current study reports for the first time the application of pseudoMRM techniques developed to identify Ally, OxP, NitroY, OxW and OxY in the whole muscle homogenate whereas TrioxC, OxW, DioxW, DioxM, OxY and OxH were detected in isolated sarcoplasmic reticulum. The modifications identified in the muscle homogenate have not been previously observed in muscle in obesity and this provides molecular information on which future functional studies of obesity can build an understanding on the role of oxidation in obesity.

Identification and quantification of oxidised proteins in the muscle of aged mice and comparisons to the obese model

5.1. Introduction

Research on ageing has been an ongoing process for many scientists and still has yet to uncover the mechanisms involved in triggering the event that leads to the deterioration of the body through the advancement to death. The peak age at which cognitive abilities, bone mass, muscle strength and athletic performance is at optimum level is 30 years on average (O'Flaherty, 2000; Hughes *et al.* 2001; Rust *et al.* 2012; Hartshorne and Germine, 2015). However, it remains undiscovered as to why this declines after approximately 30 years of the average lifespan. The ageing field encompasses experiments on many theories with various biological systems, tissues and samples to discover what triggers the decline of the body's health and performance after 30. This project specifically investigates the role of oxPTMs in ageing which stems from a theory proposed in 1956 by Denham Harman. Though it is widely debated whether oxidative damage is the cause of the ageing process, early studies demonstrated the presence of oxidation at higher levels in aged tissue. Therefore it was hypothesised that oxidation of biomolecules may be the result of the ageing process and contributes to the deterioration of the body; however to explore this further, preliminary studies were required to understand which oxPTMs were involved and which proteins are inflicted with oxidative damage. This led to a study on the analysis of oxidised proteins in sarcopenia using an aged mouse model.

5.1.1. The sarcopenic model and its association to oxidation

Sarcopenia, the age associated loss of muscle mass and function, inflicts 5% of the elderly population at 65 years and one in two individuals beyond the age of 80 years. (Morley, 2012). The primary focus of this study was on the SERCA protein but analysis of other muscular proteins was carried out. The presence of oxidised proteins has been reported for muscle, with particular focus on SERCA oxidation, in many studies (Viner, *et al.*, 2000; Schoneich and Sharov, 2006; Strosova, *et al.*, 2009b). In addition, ageing studies have shown that there is a slower turnover rate of protein in the muscle, $27 \pm 5\%$ for SERCA,

which could be related to the increased presence of oxidised species in aged tissue (Ferrington, Krainev and Bigelow, 1998). With the diverse studies undertaken on detection of oxidation in muscle, this chapter was set to explore global oxidation within muscle and detect oxPTMs without the need for enrichment for a specific modification.

5.1.2. Analysis of oxPTMs using mass spectrometry

There are a number of ways to detect and measure protein oxidation with both mass spectrometry and non-mass spectrometry methods. Antibodies specific for oxidative modifications, most commonly utilised in immunoblotting, can be used to determine the presence of the modification. Another immunoblotting technique involves the reaction of dinitrophenylhydrazine (DNPH) with protein carbonyls and anti-DNP antibodies to detect the modification (Levine *et al.*, 1994). Although immunoblotting techniques are more sensitive than MS, it lacks the ability to pinpoint the location of the modification or be used in quantitative studies. Mass spectrometry methods involve both labelling and non-labelling methods. With labelling there are different types of tags used: isobaric, isotopic, biotinylated, etc. (Jaffrey *et al.* 2001; Zhou *et al.* 2014). Although the labelling and enrichment strategy reduces the complexity of the sample, the focus is usually on one modification so a lot of information is lost when removing other peptides with different modifications or with a different oxidative state. On the other hand, label-free methods opens up to the detection and quantification of multiple modifications in the same sample. In chapter 3, several quantitation methods were explored and developed for the quantitation of oxPTMs. These MS approaches were then applied in chapter 4 to understand the role of oxidation in an obese model. This chapter outlines the steps that were taken to apply the same MS approaches to an aged model and address similarities and differences between the models.

5.1.3. Aims

The aim of this study was to identify oxPTMs in the muscle of an aged mouse model and determine the percentage of oxidised residues using quantitative MS/MS approaches. In addition to the analysis applied on the ageing skeletal muscle proteome, the work reported in this chapter explored the differences between oxPTMs in ageing and the ob/ob model from the previous set of experiments. This was achieved by discovery tandem mass spectrometry and multiple reaction monitoring.

5.2. Results

Unlike previous experiments, the full muscle of the hind leg was not available. Subsequent experiments were performed on the gastrocnemius muscle kindly provided by Malcolm J. Jackson, University of Liverpool. The lack of tissue available for the study resulted in muscle homogenate samples solely produced and utilised for the analysis of oxidised residues in the aged model. The experiments from the previous chapters have shown successful MS analysis with a complex mixture of proteins.

5.2.1. Muscle weight and SERCA assay in young and aged muscle extracts

Sarcopenia is defined by the loss of muscle mass and function. In order to confirm the sarcopenic properties of the aged model, the weight of the gastrocnemius muscle samples and the specific activity (μmol of free phosphate $\text{min}^{-1} \text{mg}^{-1}$) of an individual protein were assessed. SERCA has been shown to have decreased activity in aged muscle (Xu and Narayanan, 1998; Knyushko *et al.* 2005) and so is a suitable candidate to test the level of functional decrease. As seen in Fig.5.1A, there is a reduction in muscle mass in the aged model when compared to the younger model of approximately 0.08g of muscle. This loss of muscle mass is also coupled with a reduction in SERCA activity of around 30% in Fig.5.1B.

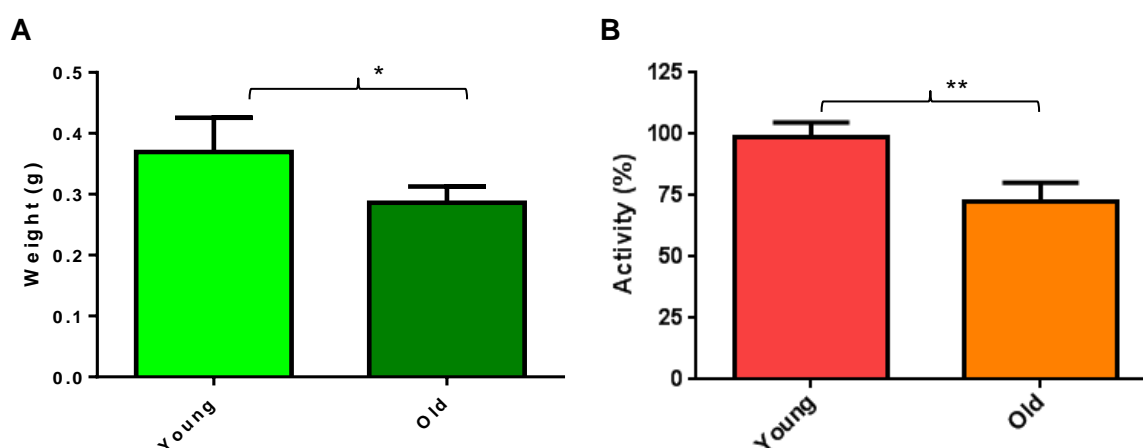


Figure 5.1. Indication of sarcopenia by measurements of the weight of gastrocnemius muscle and functional activity of SERCA. A. Weight of gastrocnemius muscle of control and aged mice; $p < 0.05^*$; $n = 4$ (unpaired t-test). **B.** Activity assay of SERCA (unpaired t-test $p < 0.01^{**}$). Weights of gastrocnemius muscle were provided by Dr Kasia Whysall, University of Liverpool.

These initial results confirm the loss of muscle seen in sarcopenia in addition to the reduced activity of SERCA in the aged model. The next step was to ascertain the global presence of oxidation within the muscle homogenates of both models. This was determined by western blotting with focus on the presence of carbonyl groups and nitrative modifications. These modifications were chosen based on availability of antibodies to these modifications as well as well established methods present in the literature.

5.2.2. Immunoblotting for oxidative modifications of proteins

The carbonyl groups and nitrosothiol were detected using the appropriate antibodies. Carbonyl group detection involved derivatisation with dinitrophenylhydrazine to be detected by anti-DNP. From the first immunoblot, there are not many bands detected in the separated proteins by the electrophoresis (Fig.5.2). The densest band is shown to be just below the wells of the SDS-gel. This may indicate that carbonyl groups, in bands of almost equal density, are present in aggregated proteins in both the young and aged muscle samples. It is not clear whether aggregated proteins were formed *in vivo* or are artefacts but from the loading control there is consistent loading for both samples. Tubulin has a molecular weight of approximately 50 kDa and was used to demonstrate the samples were loaded consistently.

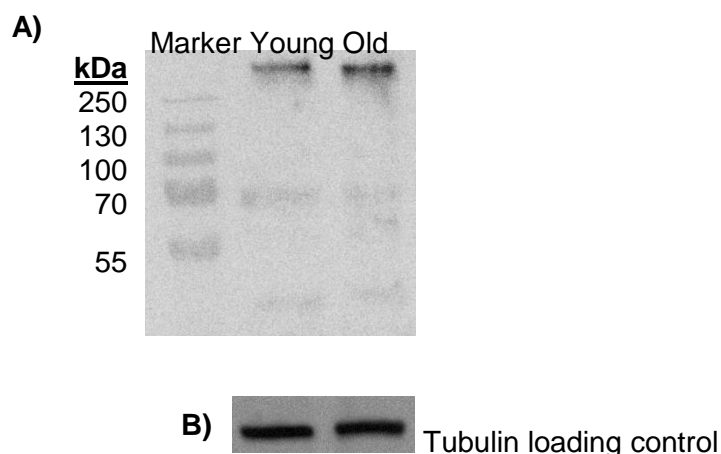


Figure 5.2. Oxyblot of young and aged muscle samples. A. Derivatised carbonyl groups were probed with anti-DNP and **B.** Protein loading was assessed by detection of tubulin.

The second blot, probed with anti-SNO, shows denser bands in the separated proteins but also targeted the same areas of both samples (Fig.5.3). Although this blot seemed to work, there is very little difference seen in the young and aged replicates. From the loading control, there is consistent loading, however, the expected result of an increase in SNO-groups in aged samples was not present. As these are the results achieved and replicates of the blot do not show any additional differences, it can be assumed that there either is no difference in SNO in the models used in this study or resulted from indiscriminate binding of a degrading antibody.

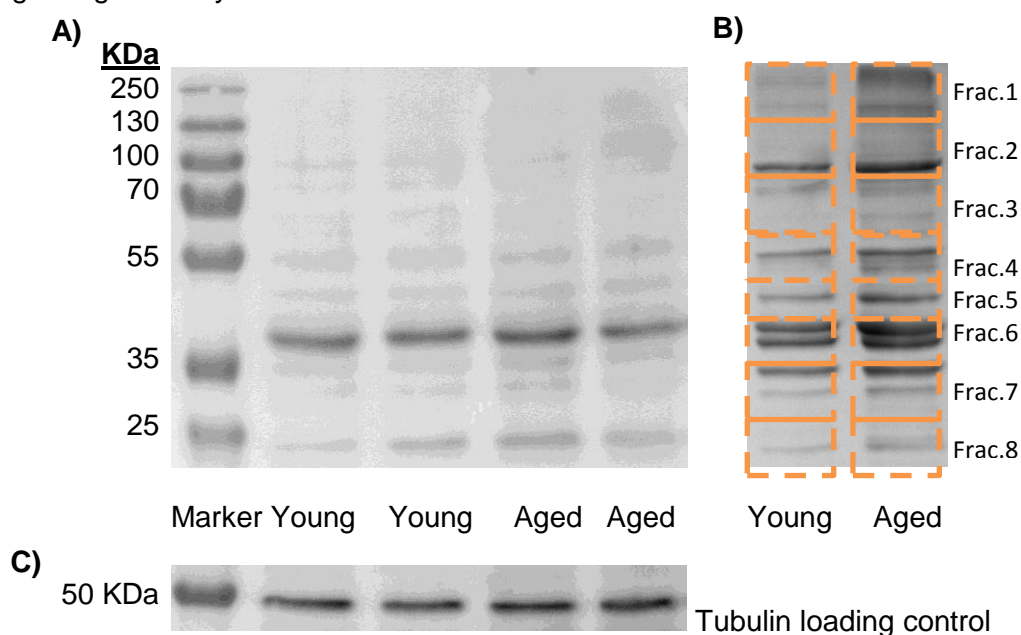


Figure 5.3. Immunoblotting with anti-SNO of young and aged samples in duplicate. A. Immunoblot of young and aged samples probed with anti-SNO. **B.** SDS-PAGE of young and aged samples. Fractions are labelled and outlined with orange boxes. **C.** Loading control assessed with anti-tubulin.

With the current results from the immunoblot, there were no oxPTM differences detected between the two models. This may be due to problems associated with the immunoblotting technique so it was decided that the project would utilise MS analysis to confirm or reject the results obtained from the immunoblots. Several attempts were made to fix the problem but the resulting figures could be down to failure of the antibodies as these sets of experiments were completed much later in comparison to the earlier blots shown in the previous chapters.

5.2.3. Identification of proteins and oxPTMs in young and aged muscle

The next set of experiments involved MS/MS analysis of digested peptides from the muscle homogenate of the young and aged models. The analysis was accomplished by submission of protein IDs to an online gene ontology tool: PANTHER. The gene ontology tool groups proteins into a category that is common to the set of proteins. This was used to group the proteins from the aged muscle into categories of biological processes. The results from the gene ontology study demonstrated that a higher proportion of proteins in the aged model accounted for metabolic processes, biological regulation and response to stimuli while fewer were involved in reproduction, cellular component organisation or biogenesis, and developmental processes (Fig.5.4). However without protein quantitation, it cannot be determined whether proteins from these categories are over or under expressed but does give an indication that the changes in protein abundance may have led to increased or decreased discovery of proteins from the most influenced groups.



Figure 5.4. Gene ontology study on MS discovered proteins in aged gastrocnemius muscle in comparison to proteins from ob/ob whole muscle. Colours represent biological processes colour coded in the key. Pie chart from the previous obesity chapter is shown in top-left box.

Similarly to the previous chapters, the identified modified peptides from Mascot were subjected to *de novo* sequencing to validate whether the identification was a true positive or false positive. Fig.5.5 demonstrates sequencing of a true positive MS/MS spectrum and a false positive. The presence of a proline oxidation in the steryl-sulfatase peptide was confirmed both by Mascot and *de novo* sequencing whereas the peptide from proactivator polypeptide-like shows an alternative sequence from manual sequencing that fits the MS/MS spectrum better than the proposed sequence from Mascot.

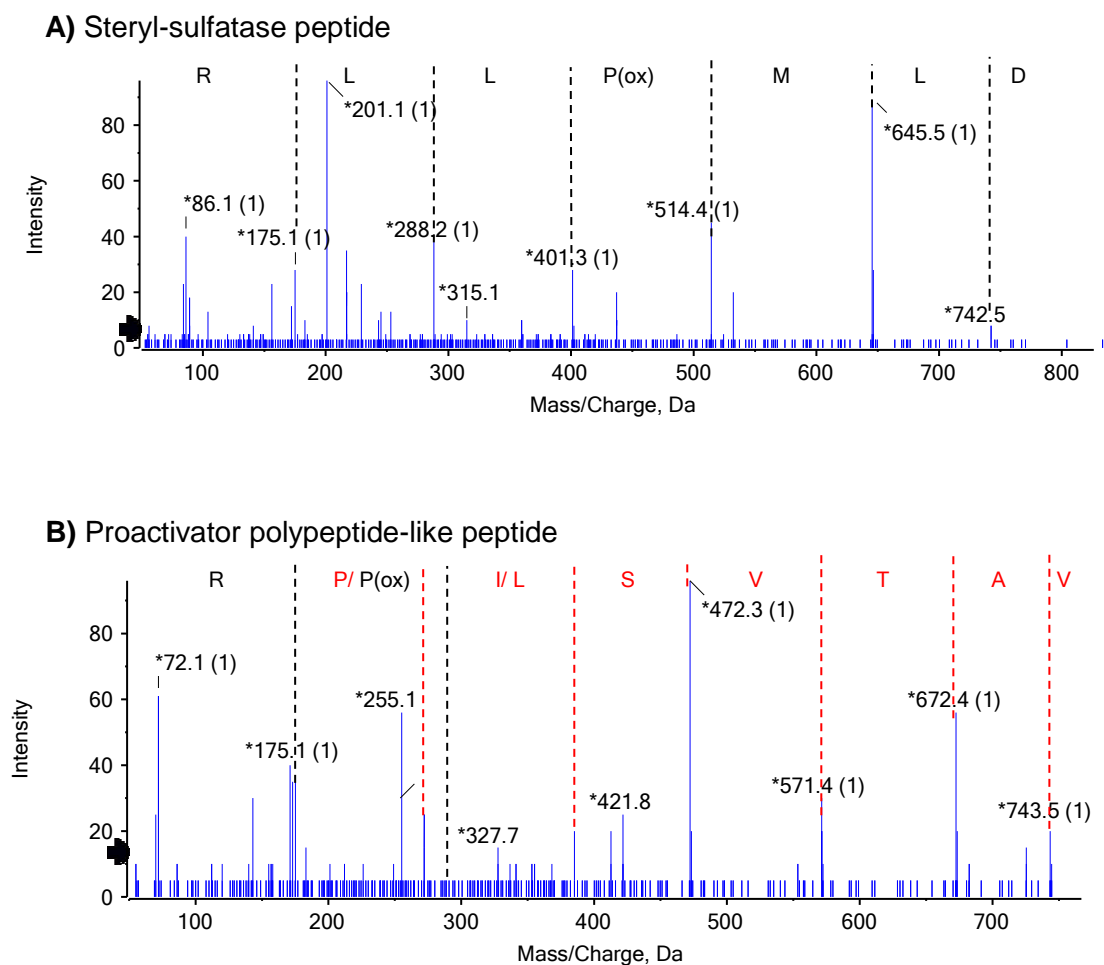


Figure 5.5. *De novo* sequenced oxidised peptides detected by Mascot. A. Spectrum of proline oxidation of Steryl-sulfatase peptide DLMP(ox)LLR validated as true positive result. **B.** Spectrum of oxidised proline of ASPISVP(ox)R peptide from Proactivator polypeptide-like shown to be a false positive result. Mascot detected sequence labelled in black whereas alternative labelling from manual sequencing is highlighted in red.

The results from the aged model could only confidently return 5 verified peptides (Table 5.1). The lack of modifications detected was due to problems with the instrument performance; however, there still was a list of oxPTMs detected from the model. While there were similar protein/peptide identifications when compared to the obese sample, there are also additional ones not previously detected. The differences in oxidised peptide identifications could be due to the observed differences in protein IDs from whole ob/ob muscle and the aged gastrocnemius muscle. With very few modifications detected due to the poorer quality dataset obtained, it is difficult to determine whether there is a substantial difference in oxidation when comparing the control and aged samples. To overcome many of the problems, with additional time, repeated experiments could elucidate whether more modifications could be detected with a second MS/MS run.

Table 5.1. Table of oxidised peptides discovered utilising Mascot. Summary of oxidative modifications achieved through searches in Swiss-Prot database with carbamidomethyl as a fixed modification and the variable modifications in the table, as described in Chapter 2. The results are identified by the protein of origin, modified residue and type of modification as well as the sequence of the oxidised peptide. Residues that were modified in the peptide sequence are highlighted in red.

Protein	Modification & Residue	Sequence
Glycogen phosphorylase	OxY52	DYFFALAHTVR
Glyceraldehyde-3-phosphate dehydrogenase (GAPDH)	OxP236	VPTPNVSVVDLTCR
Acid sphingomyelinase-like phosphodiesterase 3a	DioxM297	DSLMLVLSDK
Steryl-sulfatase	OxP436	DLMPLLR
Phosphoglycerate mutase 2	OxP125	SFDTPPPPMDEK

5.2.4. Quantification of oxPTMs in young and aged muscle

In order to assess the percentage of modified peptides, the aged and young samples were subjected to the same quantitation methods used for the obese sample. Figure 5.6 shows overlaid spectra from native, OxM and DioxM peptide from SERCA. With this method a mass shift can be seen with the transitions as well as changes in intensity between the native and modified peptides. Not only can this be used to quantify oxPTMs but the sequence can also be verified by the differences seen between the transitions.

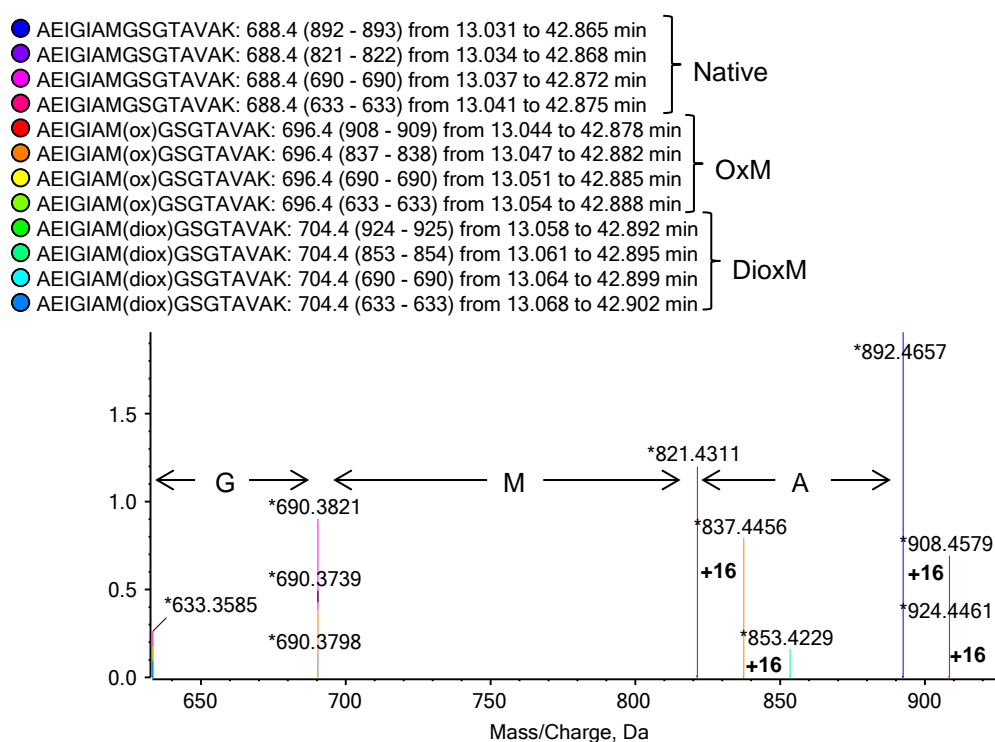


Figure 5.6. Example of targeted MRM method using transitions of native, oxidised and dioxidised product ions from SERCA peptide AEIGIAMGSGTAVAK MS/MS fragmentation. Transitions from native and oxidised peptides are colour coded and labelled to show mass shifts in peptide sequence. The addition of oxygen is labelled as +16,

Using this method, quantitation of the fractions of both the obese study and aged study were compared. Table 5.2 shows quantification in a single peptide from SERCA assessing oxidation of the methionine residue. While there seems to be consistency in the total modification of the aged and obese samples, the controls for each differ with higher levels of methionine dioxidation and lower levels of methionine oxidation found in the young sample

when compared to the lean sample. The control models are from two different mice: NMRI and C57BL/6J. In this data set, there are higher levels of total modification in the obese sample. When separating the two modifications, the obese sample has higher methionine oxidation whereas the aged sample has higher methionine dioxidation. In both sample datasets, there are higher amounts of total modification in the obese and aged samples in comparison to their controls. The data also shows the benefits of quantification with non-biased GeLC fractionation. From the quantification, there are modified and native forms of the peptide detected throughout the gel. The highest level of native peptide is found in the high molecular region where the protein should be present. There are peptides detected at the mid and low MW ranges. For the methionine oxidised peptides, higher levels are detected in the mid to low range whereas the methionine dioxidised seem to be present more in the mid-MW range of the SDS-gel. For many of these cases, it can be assumed that the modifications are more prevalent in aggregated and fragmented forms of the protein.

Table 5.2. MRM quantitation of AEIGIAMGSGTAVAK of SERCA in aged and obese mice. Peak area and percentage modification are displayed in the table. Total modification is highlighted in a darker shade to differentiate between results from individual fractions. Fractions are not the same in the obese and aged sets.

Lean	Frac. 1	Frac. 2	Frac. 3	Frac. 4	Frac. 5	Frac. 6	Frac. 7	Frac. 8	Frac. 9	Frac. 10	Total
Peak area (native)	1.91E+03	1.42E+04	3.12E+03	3.31E+02	3.32E+02	4.18E+02	2.41E+01	1.21E+01	1.21E+01	0.00E+00	2.03E+04
Peak area (OxM)	1.00E+03	4.36E+03	1.73E+03	2.84E+02	2.30E+04	4.47E+03	1.35E+03	1.69E+02	6.03E+01	3.62E+01	3.65E+04
Peak area (DioxM)	0.00E+00	0.00E+00	0.00E+00	0.00E+00	1.46E+02	2.17E+02	6.63E+01	0.00E+00	0.00E+00	0.00E+00	4.30E+02
% Modified (OxM)	34%	24%	36%	46%	98%	88%	94%	93%	83%	100%	64%
% Modified (DioxM)	0%	0%	0%	0%	1%	4%	5%	0%	0%	0%	1%
Obese	Frac. 1	Frac. 2	Frac. 3	Frac. 4	Frac. 5	Frac. 6	Frac. 7	Frac. 8	Frac. 9	Frac. 10	Total
Peak area (native)	2.20E+03	1.64E+04	3.85E+03	4.53E+02	1.01E+03	4.10E+02	4.83E+01	2.41E+01	0.00E+00	0.00E+00	2.44E+04
Peak area (OxM)	1.33E+03	8.19E+03	1.17E+03	1.57E+02	3.21E+04	3.15E+03	9.44E+02	6.03E+01	9.65E+01	3.62E+01	4.72E+04
Peak area (DioxM)	0.00E+00	0.00E+00	0.00E+00	0.00E+00	3.02E+03	9.65E+01	2.41E+01	1.21E+01	0.00E+00	1.21E+01	3.16E+03
% Modified (OxM)	38%	33%	23%	26%	89%	86%	93%	63%	100%	75%	63%
% Modified (DioxM)	0%	0%	0%	0%	8%	3%	2%	12%	0%	25%	4%
Young	Frac. 1	Frac. 2	Frac. 3	Frac. 4	Frac. 5	Frac. 6	Frac. 7	Frac. 8	Total		
Peak area (native)	2.76E+04	1.64E+04	5.19E+02	9.96E+02	2.59E+02	2.41E+01	0.00E+00	0.00E+00	4.58E+04		
Peak area (OxM)	1.29E+04	8.55E+03	4.28E+02	1.08E+04	9.53E+02	1.69E+02	7.24E+01	4.83E+01	3.39E+04		
Peak area (DioxM)	0.00E+00	0.00E+00	0.00E+00	3.22E+03	4.74E+01	0.00E+00	0.00E+00	0.00E+00	3.26E+03		
% Modified (OxM)	32%	34%	45%	72%	76%	87%	100%	100%	41%		
% Modified (DioxM)	0%	0%	0%	21%	4%	0%	0%	0%	4%		
Aged	Frac. 1	Frac. 2	Frac. 3	Frac. 4	Frac. 5	Frac. 6	Frac. 7	Frac. 8	Total		
Peak area (native)	3.49E+04	3.77E+04	2.28E+03	5.77E+03	2.16E+03	9.65E+01	0.00E+00	0.00E+00	8.28E+04		
Peak area (OxM)	3.59E+04	1.46E+04	1.60E+03	3.78E+04	6.05E+03	3.78E+02	3.68E+02	1.15E+02	9.68E+04		
Peak area (DioxM)	2.29E+02	4.83E+01	1.45E+02	7.94E+03	1.17E+02	2.41E+01	0.00E+00	0.00E+00	8.50E+03		
% Modified (OxM)	51%	28%	40%	73%	73%	76%	100%	100%	51%		
% Modified (DioxM)	0%	0%	4%	15%	1%	5%	0%	0%	5%		

MRM quantitation was applied to additional SERCA peptides in order to compare the level of oxPTMs present in aged samples versus the control. From quantification of the raw data, bar charts had been produced to represent the difference between aged and control samples (Fig.5.7). All peptides showed higher levels of oxidation in the aged samples; however, only one result was statistically significant: GTAIAICR. The large error bars were due to biological variation and demonstrate the need for far more biological replicates to determine whether aged samples are overall more oxidised than the controls. The other peptides did appear to have higher levels of oxidation, but owing to the variation between the replicates the differences were not significant. Unfortunately, due to limits on MS sensitivity, all of the successful SERCA peptides quantified contained highly susceptible residues i.e. methionine and cysteine. Though this does provide information on residue susceptible and possible effect of location, there are not enough data to give a complete picture on how oxidants from inflammation, in ageing, modify the protein.

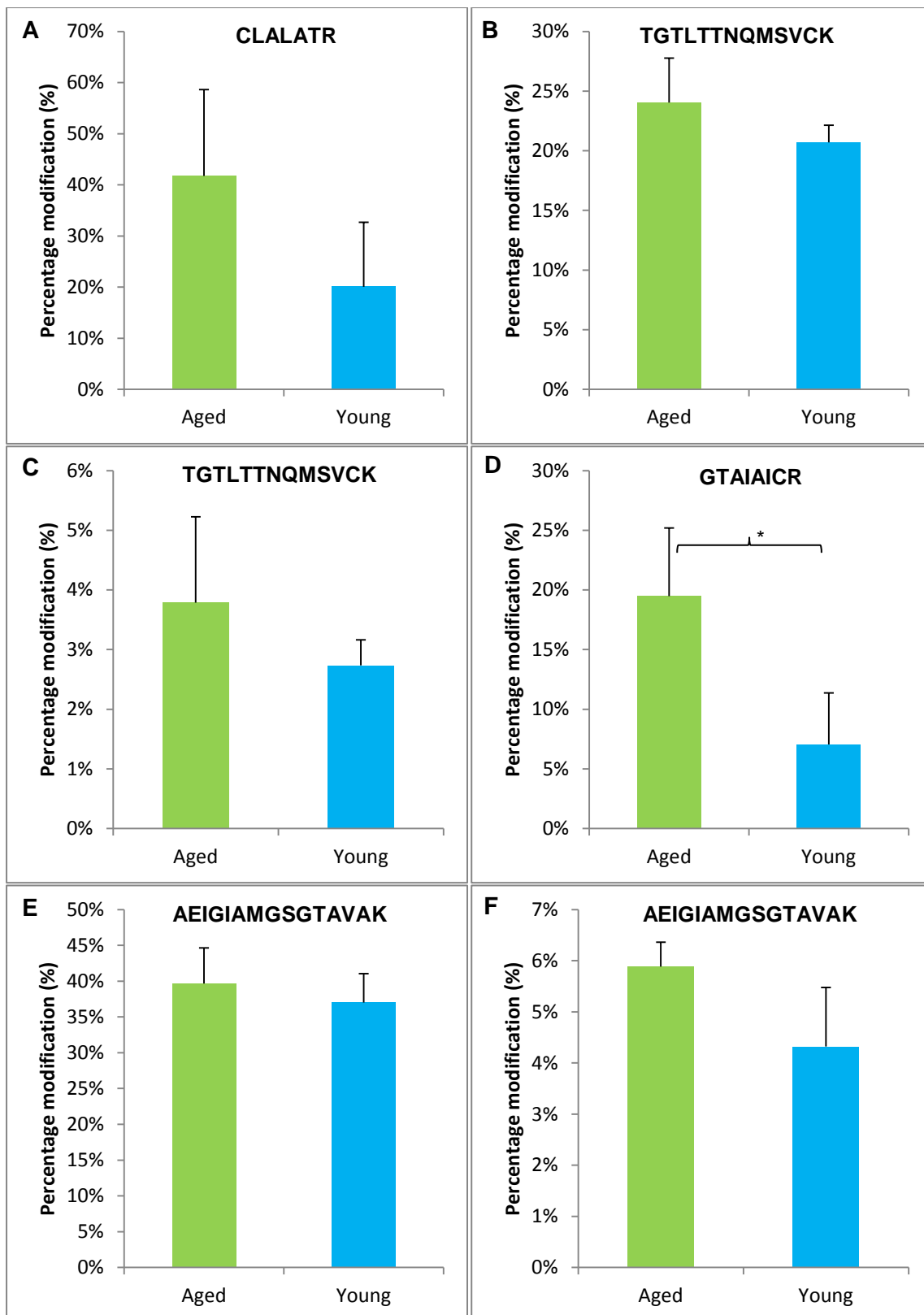


Figure 5.7. Quantification of cysteine and methionine oxidation in SERCA of aged and young samples. Percentage modification of TrioxC (A) in CLALATR, OxM (B) and DioxM (C) in TGLTTNQMSVCK, TrioxC (D) in GTAIAICR, and OxM (E) and DioxM (F) in AEIGIAMGSGTAVAK peptides of SERCA. *Statistically significant data ($p < 0.05$), $n=3$.

5.3. Discussion

5.3.1. Reduction in muscle mass and SERCA activity

The aim of the work described in this chapter was to identify and measure oxidised residues in sarcopenic muscle and compare this both with young animals, and with the results obtained from the analysis of the ob/ob model. As sarcopenia is the loss of muscle mass and function in association with ageing, the aged model was tested to see if it could be characterised as a sarcopenic model. The first part of the analysis involved measuring the difference in muscle weight between young and old muscle tissue. As expected, aged muscle showed a loss of approximately 22% of the control in gastrocnemius muscle weight. A similar loss in mass (around 23%) has been reported previously (Russ *et al.* 2014); however, the same study also showed a 17% reduction in SR calcium release but no change in calcium uptake, which is a result that was not replicated in this study. SERCA activity has been shown to decrease in aged muscle. A few studies have reported a 33% decrease in SERCA function with examples of these studies performed on elderly women and in the aged rat myocardium (Froehlich JP, *et al.* 1978; Hunter SK, *et al.* 1999). A very similar result of approximately 30% decrease in SERCA activity was seen in the aged muscle.

5.3.2. Immunoblotting

The immunoblotting did not give the results anticipated, and suggested some problems with the assays. A number of reasons could have caused this result but by judging the outcome of the Oxyblot and the immunoblot probed with anti-SNO, notable differences can be seen between the 2 procedures were seen. The Oxyblot had dense bands appear near the well which could be the result of the problems at the derivatisation stage leading to aggregation of the protein near the well of the SDS-gel. The anti-SNO blot does not show the same aggregation but rather several bands can be seen in both the control and aged sample with no differences. This could be caused by indiscriminate binding of either the primary or secondary antibody, possibly caused by deterioration through age. While it could be

suggested that the samples stored in the freezer for a substantial amount of time may result in increased aggregation and reduced the discrimination between the oxidative state of the control and aged samples, this appears to conflict with the increase in oxidation shown in the aged samples using the MS approaches.

5.3.3. Gene ontology

The differences in the proteins identified with MS/MS between the aged and obese studies was probably due to the change in the type of muscle sample used for the two studies. While the whole hind leg muscle was used in the obese study, only the gastrocnemius was used in the aged study. The gastrocnemius muscle contains more glycolytic fibres, which have a smaller mitochondrial capacity than oxidative fibres such as those in the soleus muscle (Philippi and Sillau, 1994). Glycolytic fibres have been shown to differ with increased glycolytic enzymes and reduced mitochondrial enzymes when compared to oxidative fibres (Donoghue *et al.* 2007). Ageing muscle has been shown to exhibit a shift from glycolytic to oxidative fibres displaying decreased expression of glycolytic proteins such as enolase and pyruvate kinase, whereas mitochondrial proteins such as NADH dehydrogenase and succinate dehydrogenase are shown to have increased (Gelfi *et al.* 2006; Capitanio *et al.* 2009; O'Connell and Ohlendieck, 2009). However, without quantitative analysis of protein expression in the aged muscle, it cannot be determined whether there is an increase or decrease in the abundance of proteins in the aged muscle in comparison to the control. A group from the Korea Institute of Science and Technology demonstrated upregulation and downregulation of different proteins in aged gastrocnemius muscle when compared to the younger control by MRM analysis of mTRAQ labelled peptides (Hwang *et al.* 2014). mTRAQ is an amine-specific stable isotope labelling method that was utilised in this study to determine the abundance of protein in the aged and young gastrocnemius muscles labelled with light and heavy mTRAQ labels respectively. While the loss of global muscle mass was defined at approximately 10%, the study did report 53 proteins that were differentially expressed of which 20 had reduced expression and 33 had increased expression. The

results from this study elucidate to ageing affecting protein synthesis or degradation, which may explain the increase in expression of some proteins and decreased expression of others.

5.3.4. Identification of oxPTMs in aged gastrocnemius muscle

Five modified residues were identified in glycogen phosphorylase, glyceraldehyde-3-phosphate dehydrogenase (GAPDH), acid sphingomyelinase-like phosphodiesterase 3a, steryl-sulfatase, and phosphoglycerate mutase 2. Glyceraldehyde-3-phosphate dehydrogenase was found to be oxidised at the same proline residue identified in the obesity oxPTM MS/MS discovery experiments from the previous chapter. This suggests that some proteins may be susceptible to oxidation and the susceptibility of these proteins is not disease-specific. Glycogen phosphorylase has been shown to contain oxidised tyrosine at position 52. Tyr52 is in helix 2; a region involved in interactions with adenosine monophosphate (AMP) (Rath *et al.* 2000). It has been reported that there is a SR associated glycogen increase by 30% with ageing (Russ *et al.* 2014). If modifications to glycogen phosphorylase have an effect on the enzyme's conformation, it could in turn disrupt its function and may affect breakdown of glycogen which would lead to an increase in glycogen levels. The function of acid sphingomyelinase-like phosphodiesterase 3a is still being explored. While it was initially thought to be involved in the catabolism of sphingomyelin, a component of the nerve cell membranes, there have been a few reports on alternate possible roles such as a nucleotide phosphodiesterase function (Traini *et al.* 2014). It is unclear whether modifications to this protein would impact on muscle ageing without knowing the exact function of this protein in skeletal muscle. Steryl-sulfatase is involved in the regulation of oestrogen homeostasis but also has been found to regulate energy metabolism and improve insulin sensitivity (Jiang *et al.* 2014). Additionally, this study suggested protective effects by the protein via decreased inflammation in skeletal muscle with the overexpression of steryl-sulfatase. Phosphoglycerate mutase 2 is involved in glycolysis in skeletal muscle and studies in phosphoglycerate mutase deficiency have shown

partial defects to energy metabolism and exercise induced cramps possibly through the increased lactic acid and intracellular acidosis (Argov *et al.* 1987; Oh *et al.* 2006).

5.3.5. Quantitation of oxidised peptides in SERCA

It was reported that aged muscle fibres at rest showed an increase in oxidant production (Palomero *et al.* 2013). The same study also suggests that the increase in oxidation is more likely due to oxidant generation over reduced scavenger capability. Additionally, the paper also refers to research by Muller *et al.* 2007 which discusses the increase in mitochondrial release of hydrogen peroxide in denervated muscle fibres which are also present in aged muscle tissue. These studies indicate there is a higher production of oxidants which would lead to the presence of more oxidised proteins in the aged muscle. This is shown in the quantitative dataset obtained from the research in this chapter; however, the usage of only three replicates meant many of the quantified peptides were insignificant. Even so, the rise in oxidised SERCA residues in the aged gastrocnemius muscle could contribute to the reduction of SERCA activity demonstrated earlier in the chapter.

5.3.6 Summary

In conclusion, the work presented in this chapter has shown that the MS methods for detecting oxPTMs in muscle-derived proteins can be applied to the study of changes in muscle ageing, although with limited success. Only a small number of modifications were identified and quantified, and these were mostly oxidations of the susceptible sulfur-containing residues cysteine and methionine. Nonetheless, the work demonstrates that specific oxidations of a variety of muscle proteins do occur, and interestingly, may be disease or condition-specific, and there were differences between those observed in obese and aged tissue.

Chapter 6

General discussion

The objective of this research was to develop MS methods for the identification and quantification of oxPTMs of muscular proteins within aged C57BL/6 and obese ob/ob mouse models to gain a deeper understanding of the role of oxidative stress in ageing and disease, and to distinguish whether oxidative stress affects the models in a similar manner. As discussed in the background literature, numerous oxidised residues have been characterised and higher levels are reported in aged and diseased models in comparison to their control counterparts. Nevertheless, many of these studies focus on a particular protein, a specific modification, a single oxidant, a type of model, or a combination of the four and therefore lose out information on whether proteins are oxidised at the same sites or if the same modified residues are quantitatively similar when comparing the different models. This study successfully applied non-labelling quantitative MS/MS analysis to measure oxPTMs identified by discovery MS/MS in both isolated sarcoplasmic reticulum and whole muscle lysate. Novel oxPTMs have been detected both in the aged and obese models not previously identified in muscle tissue.

6.1. Summary of findings

6.1.1. Detection and characterisation of oxPTMs in both models

The physiological changes of both models demonstrated loss of muscle mass but only the aged model demonstrated significant reduction in SERCA activity. Additionally, the proteins identified differed based on gene ontology analysis. This was determined to be the result of different muscles used in the experiments. The obesity study utilised the whole muscle which included the soleus, extensor digitorum longus (EDL), and gastrocnemius whereas the ageing study had only utilised the gastrocnemius muscle tissue. The gastrocnemius muscle contains high levels of glycolytic fibres which exhibit increased glycolytic enzymes and reduced mitochondrial enzymes when compared to oxidative fibres (Donoghue *et al.* 2007). The difference in protein expression could also have contributed to the different oxPTMs detected in both studies. The oxidised residues of abundant proteins from whole muscle

homogenate and isolated sarcoplasmic reticulum were characterised in the obese model whereas only the muscle homogenate was analysed for the aged model. This was due to the availability of smaller amounts of muscle tissue in the aged mouse model. Nevertheless, for both models high levels of oxidation were measured when compared to their control counterparts. This was demonstrated both using western blotting techniques and the oxPTMs identified in the obese and aged muscle using discovery MS/MS. The increase in oxidation mimics what is seen in the literature for both models. Increased nitrative modifications, nitrotyrosine and s-nitrosothiols, have been detected in other tissues of ob/ob mice (Carvalho-Filho *et al.* 2005; Drel *et al.* 2006; Garcia-Ruiz *et al.* 2006). Additionally, carbonyl groups and nitrative modifications have been detected in aged tissues (Feng *et al.* 2008; Murakami *et al.* 2012). Preliminary experiments with oxidations generated *in vitro* demonstrated that high sequence coverage was gained by enriching proteins via isolation of the sarcoplasmic reticulum, in comparison to the sequence coverage obtained from the same proteins in the muscle homogenate. While this meant more sequence coverage for particular proteins resulted in detection of additional modifications, the isolation filtered out other proteins with potential modifications of interest. Research groups do adopt pre-enrichment strategies focusing on a particular modification or subset of modification e.g. carbonyl groups and oxidation states of cysteine (Guo *et al.* 2014; Bollineni, Hoffmann and Fedorova, 2014). Nonetheless, the approaches used in this study successfully identified novel different oxPTMs in obese muscle and aged gastrocnemius muscle. The obesity study showed a range of modification identified by Mascot: Ally, OxP, NitroY, OxW and OxY. On the other hand, fewer modifications were identified in the aged gastrocnemius muscle: OxY, OxP and DioxM. This could be due to the differences in muscle fibre types where gastrocnemius contains high levels of glycolytic fibres in comparison to the soleus which contains more oxidative fibres. The higher amounts of mitochondria could lead to oxidative fibres being more susceptible to oxidation than glycolytic fibres.

6.1.2. Quantitation of oxPTMs in both models

In addition to detection, the oxPTMs were quantified using MRM to assess changes in the level of modified peptides for each model. Only a small number of peptides were quantified due to time constraints; however, the data set produced from the peptides demonstrated higher levels of oxidation in the diseased and aged models. This was limited by the number of replicates processed and analysed throughout the study, which resulted in many of the comparisons made being statistically insignificant. Nevertheless, this study has succeeded in producing MS methods for characterisation and quantitation of oxPTMs in muscle for biological material. In addition, the ob/ob model was compared to the aged model with the final findings suggesting that higher levels of oxidative stress is present in aged muscle tissue more so than in obese tissue. Many studies incorporate quantitation and discovery into one MS run decreasing the number of samples processed through MS (Ghesquiere *et al.* 2011; McDonagh *et al.* 2012; Qu *et al.* 2014), however, only ions selected for MS/MS fragmentation would be quantified. This means proteins would need to be abundant which would possibly require enrichment strategies.

6.1.3. Comparison of QToF and QTRAP MS instruments

Another achievement of this study was the comparison of different quantitative methods utilising both the QToF and QTRAP instruments available in the lab. The study demonstrated that both instruments have their advantages and disadvantages in quantifying oxPTMs but also required further fine tuning to develop more suitable methods. While only the standard MRM method was used for the QTRAP, several pseudoMRM methods were developed for the QToF instrument by adapting the product ion scan. These methods have been reported with other instruments but can be adapted to all instruments. A PseudoMRM method was used to measure spiked phosphopeptides in a BSA sample whereby the whole range of product ions were scanned for a targeted precursor ion and quantitation was performed by generating XICs of transitions through manual selection (Sherrod *et al.* 2012).

This method has also been applied to measure cysteine dioxidation and trioxidation detected in nucleoside diphosphate kinase and heat shock 70 kDa protein 8 that was oxidised with varying concentrations of hydrogen peroxide (Lee, Paull and Person, 2013). Targeted methods were developed in this study to demonstrate quantitation of oxPTMs *in vivo* and show that the same instrument used for discovery MS/MS can also be utilised for targeted approaches with the advantages of having the same LC so retention times can be utilised in scheduled MRM methods.

6.2. Future work

6.2.1. Optimising modification searches

Another common modification that should have been included in the Mascot identification of peptides is deamidation (NQ) (Robinson and Robinson, 1991). Deamidation is a process in protein degradation by which the amide containing sides chains of glutamine and asparagine residues are converted to release NH_3 and subsequently produce glutamate and aspartate respectively. It is one of the most common modifications along with the oxidation of methionine and has been shown to increase peptide identification when searching with the deamidation modification as a variable (Jenkins 2007; Yang and Zubarev 2010; Nepomuceno *et al.* 2014). Deamidation has also been reported as an indicator for protein turnover and ageing (Lindner and Helliger, 2001; de la Mora *et al.* 2015). The modification disrupts protein stability and increasing levels indicate the progression towards ageing (Hains and Truscott, 2010). Additionally, it has been reported that oxidation can impact the presence of deamidation in proteins mimicking those present in ageing (Barbariga *et al.* 2014). By adding this modification to the search, there is a higher chance that additional oxPTMs may be discovered by increasing the total number of identified peptide sequences. With multiple modifications in a single peptide, subsequent quantitation will involve measuring more combinations of native, deaminated and oxidised peptides. The extended

list of peptides will increase the time spent on acquiring MRM data. Nevertheless, accurate quantitation requires common modifications to be present so that the data is not skewed.

6.2.2. Additional quantitation of oxPTMs detected in discovery MS/MS

The methods optimised for the study enabled quantitation of highly susceptible residues, cysteine and methionine; however it was difficult to implement these methods on the modifications detected by Mascot of lesser susceptible residues. Given additional time, more optimisation could lead to efficiency of MRM scans and accurate quantitation of oxPTMs in this study's models. With a larger database of quantified modifications, elucidation of how oxidation from the obese and aged models affect the levels of modification would result in a clearer understanding of the role of oxidation and susceptibility of proteins. By increasing the number of residues that were quantified, the susceptibility of residues can be demonstrated as heat maps on proteins with 3D crystal structures. This can then be linked to known functional properties of the domains the residues reside in and understand how oxidation may impact protein function that may result to ageing and inflammatory-related disease.

6.2.3. Increasing number of replicates

Many of the differences observed in the oxidised peptides of SERCA that were quantified for the aged and obese studies were not statistically significant, which may have been the result of the small number of replicates processed during the study. The two peptides that were significant in the obese study were TGTLTTNQM(ox)SVCK and GTAIAIC(triox)R whereas only GTAIAIC(triox)R was found to be significant in the ageing study. While there are studies that address the problems with technical and biological variation (Molloy *et al.* 2003), the deviation between biological replicates is inherent. In order to ascertain the modifications and the relative percentage modification of residues within protein it would require many more replicates. Due to the GeLC fractionation approach used in this study, additional replicates would increase the number of fractionated samples needing to be processed by the LC-MS instruments which in turn would lead to inefficient time spent on collecting

enough data for MRM quantification of oxPTMs. To avoid this problem, alternative approaches would need to be considered. The GeLC method enabled higher resolution and selection of lower abundant peptides for fragmentation in discovery MS/MS. Additionally, the differences detected in the abundance of modified peptides within each fraction translated to how oxidised proteins in the control and obese/aged models ran on a SDS-gel. Nevertheless, there are multiple advances in the MS field that address the challenges of oxPTM detection in biological samples (Verrastro *et al.* 2015)

6.2.4. Scheduled MRM

Standard MRM methods are set up to cycle through and measure targeted product ions from specified precursor ion masses for the total acquisition time of the MS/MS method. An advantage of using LC-MS is obtaining knowledge on the retention times of the targeted modified peptide from discovery MS/MS. By utilising the retention times of the precursor ion, scheduled MRM approaches enables more peptide analysis as it focuses acquisition of transitions of the targeted peptide within the region of the chromatogram at the expected retention time and enables assignment of several time points on the chromatogram to a number of targeted peptides. Early studies have used scheduled MRM to demonstrate measurement of larger peptide and transition lists without compromising sensitivity (Stahl-Zeng *et al.* 2007; Picotti *et al.* 2009) This method has also been employed in studies using MRM to quantify cysteine oxidation called oxMRM (Held *et al.* 2010). The same principle could be applied to measure multiple oxPTMs by increasing the number of peptides quantified within a single run. While additional peptides could be added to the method program, peptides eluting within the same regions of the chromatogram would have to be separated on different MS runs to ensure the duty cycle is not compromised.

6.3. Final conclusions

Our current findings have demonstrated that mass spectrometry is a powerful technique that had enabled detection of novel modifications, not previously characterised in the muscle of the mice models used in this study, and demonstrated quantitation of modifications using non-labelling and non-enrichment based methods on two instruments with different mass analysers. By utilising quantitative MS approaches, heat maps can be generated from 3D crystal structures of the proteins to demonstrate changes in modification. Figure 6.1 shows the percentage increase in oxidation of SERCA residues within the aged and obese models from their respective controls. This enables visual depiction of changes to residues within the protein's 3D conformation and grants further insight to the effect of location on residue susceptibility. As seen in both models, the modified residues are clustered around Asp351 and Cys674; the active site and a residue involved in redox regulated changes in activity. As mentioned before, the modified residues could serve as protection by scavenging oxidants. Additionally, when comparing the increase in oxPTMs in both models, Cys636, Met720 and Cys561 in the ageing model were found to be more oxidised than the obese model. This may explain why we see a significant drop in SERCA activity in the aged muscle and not in the obese muscle. From the data obtained in this study and the research undertaken in other groups, increased oxidation in ageing and obesity is a downstream result of a combination of factors resulting from the rise in oxidant production and the reduction of protein degradation. The proteasome's key role is the degradation of proteins and studies have shown oxidised proteins are degraded at a higher rate particularly for the 20S proteasome and the immunoproteasome (Friguet *et al.* 2000; Jung, Hohn and Grune 2014). However, ageing contributes to the decreased expression of the proteasomes and so it can be suggested that the increased oxidant production coupled with the reduction of proteasome expression explains the increased levels of oxPTMs found in the ageing tissue (Keller, Huang and Markesbery, 2000; Huber *et al.* 2009; Saez and Vilchez 2014). In obesity, higher levels of oxidation and proteasome dysfunction was seen which supports the data shown in this

thesis (Otda *et al.* 2013; Diaz-Ruiz *et al.* 2015). While the methods can still be further optimised to increase the number of modifications detected and expand the types of oxPTMs for quantitation, these current methods can be adapted to assign candidates of oxidative biomarkers for ageing and inflammation related diseases and demonstrate the differences in the role of oxidative damage to muscle proteins.

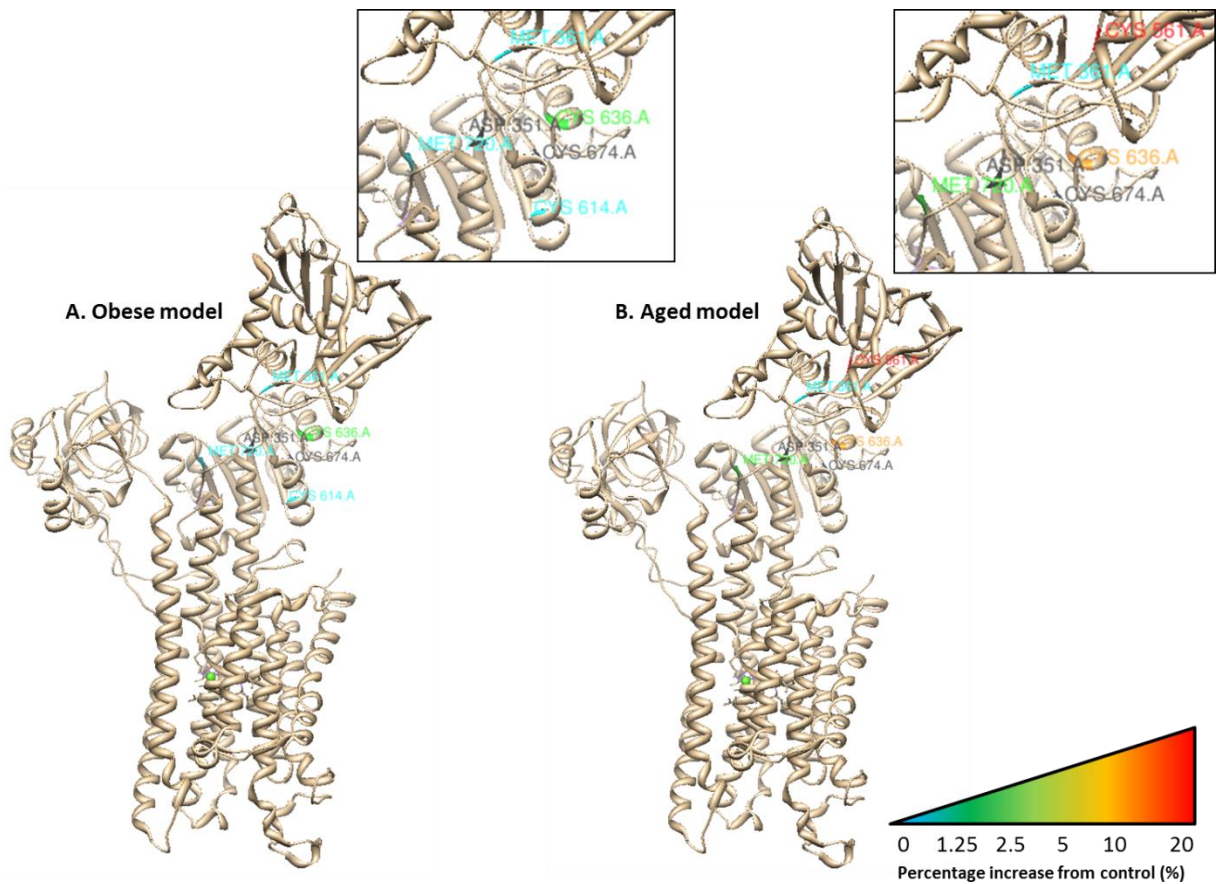


Fig.6.1. Heat map of quantified oxidised residues in SERCA. 3D crystal structures depict percentage increase of oxidation in obese and aged models from respective controls. **A.** Heat map of obese model. **B.** Heat map of ageing model. Residues are highlighted and coloured according to key ranging from 0-20% percentage increase.

Chapter 7

References

1. Adachi, T., Weisbrod, R.M., Pimentel, D.R., Ying, J., Sharov, V.S., Schoneich, C., and Cohen, R.A. (2004). S-glutathiolation by peroxynitrite activates SERCA during arterial relaxation by nitric oxide. *Nature Medicine* **10**, 1200-1207.
2. Aebersold, R., and Mann, M. (2003). Mass spectrometry-based proteomics. *Nature* **422**, 198-207.
3. Alvarez, B., Rubbo, H., Kirk, M., Barnes, S., Freeman, B.A., and Radi, R. (1996). Peroxynitrite-dependent tryptophan nitration. *Chemical Research in Toxicology* **9**(2), 390-396.
4. Amici, A., Levine, R.L., Tsai, L., and Stadtman, E.R. (1989). Conversion of amino acid residues in proteins and amino acid homopolymers to carbonyl derivatives by metal-catalyzed oxidation reactions. *Journal of Biological Chemistry* **264**(6), 3341-3346.
5. Anderson, L., and Hunter, C.L. (2006). Quantitative mass spectrometric multiple reaction monitoring assays for major plasma proteins. *Molecular & Cellular Proteomics* **5**(4), 573-588.
6. Argov Z, Bank WJ, Boden B, Ro Y, Chance B. (1987). Phosphorus Magnetic Resonance Spectroscopy of Partially Blocked Muscle Glycolysis: An *In Vivo* Study of Phosphoglycerate Mutase Deficiency. *Archives of Neurology* **44**(6), 614-617.
7. Banks, W.A., Coon, A.B., Robinson, S.M., Moinuddin, A., Shultz, J.M., Nakaoke, R., and Morley, J.E. (2004). Triglycerides Induce Leptin Resistance at the Blood-Brain Barrier. *Diabetes* **53**(5); 1253-1260.
8. Banks, W.A., DiPalma, C.R., and Farrell, C.L. (1999). Impaired transport of leptin across the blood-brain barrier in obesity. *Peptides* **20**(11); 1341-1345.
9. Barbariga M, Curnis F., Spitaleri, A., Andolfo, A., Zucchelli C., Lazzaro M., Magnani G., Musco G., Corti, A., Alessio M. (2014). Oxidation-induced Structural Changes of Ceruloplasmin Foster NGR Motif Deamidation That Promotes Integrin Binding and Signaling. *Journal of Biological Chemistry* **289**(6); 3736-3748.
10. Bates, S.H. and Myers, M.G. Jr. (2003). The role of leptin receptor signaling in feeding and neuroendocrine function. *Trends in endocrinology and metabolism* **14**(10); 447-452.
11. Bautmans, I., Van Puyvelde, K., and Mets, T. (2009). Sarcopenia and Functional Decline: pathophysiology, prevention and therapy. *Acta Clinica Belgica* **64**(4); 303-316.
12. Beckman, K.B., and Ames, B.N. (1998). The free radical theory of ageing matures. *Physiological reviews* **78**(2), 547-581.
13. Bedard, K., and Krause, K.H. (2007). The NOX family of ROS-generating NADPH oxidases: physiology and pathophysiology. *Physiological Reviews* **87**(1), 245-313.
14. Berlett, B.S., and Stadtman, E.R. (1997). Protein oxidation in ageing, disease, and oxidative stress. *The Journal of Biological Chemistry* **272**(33), 20313-20316.
15. Betz, S.F. (1993). Disulfide bonds and the stability of globular proteins. *Protein Science* **2**(10), 1551-1558.
16. Bian, Y., Song, C., Cheng, K., Dong, M., Wang, F., Huang, J., Sun, D., Wang, L., Ye, M., and Zou, H. (2014). An enzyme assisted RP-RPLC approach for in-depth analysis of human liver phosphoproteome. *Journal of Proteomics* **96**, 253-262.
17. Bodnar, A.G., Ouellette, M., Frolkis, M., Holt, S.E., Chiu, C.P., Morin, G.B., Harley, C.B., Shay, J.W., Lichtsteiner, S., and Wright, W.E. (1998). Extension of life-span by introduction of telomerase into normal human cells. *Science* **279**(5349), 349-352.
18. Bollineni, R.C., Hoffmann, R. and Fedorova, M. (2014) Proteome-wide profiling of carbonylated proteins and carbonylation sites in hela cells under mild oxidative stress conditions. *Free Radical Biology & Medicine* **68**, 186-195.

19. Bonafe, L., Thony, B., Penzien, J.M., Czarnecki, B., and Blau, N. (2001). Mutations in the Sepiapterin Reductase Gene Cause a Novel Tetrahydrobiopterin-Dependent Monoamine-Neurotransmitter Deficiency without Hyperphenylalaninemia. *American Journal of Human Genetics* **69**(2), 269-277.
20. Bonekamp, N.A., Volkl, A., Fahimi, H.D., and Schrader, M. (2009). Reactive oxygen species and peroxisomes: struggling for balance. *Biofactors* **35**(4), 346-355.
21. Borniquel, S., Valle, I., Cadenas, S., Lamas, S., and Monsalve, M. (2006). Nitric oxide regulates mitochondrial oxidative stress via the transcriptional coactivator PGC-1 α . *The FASEB journal* **20**(11), 1889-1891.
22. Capitanio, D., Vasso, M., Fania, C., Moriggi, M., Viganò, A., Procacci, P., Magnaghi, V., and Gelfi, C. (2009). Comparative proteomic profile of rat sciatic nerve and gastrocnemius muscle tissues in ageing by 2-D DIGE. *Proteomics* **9**(7), 2004-2020.
23. Carvalho-Filho, M.A., Ueno, M., Hirabara, S.M., Seabra, A.B., Carnevali, J.B., de Oliveira, M.G., Velloso, L.A., Curi, R., Saad, M.J. (2005). S-Nitrosation of the Insulin Receptor, Insulin Receptor Substrate 1, and Protein Kinase B/Akt: A Novel Mechanism of Insulin Resistance. *Diabetes* **54**(4), 959-967.
24. Chen, B., Jones, T.E., and Bigelow, D.J. (1999). The nucleotide-binding site of the sarcoplasmic reticulum Ca-ATPase is conformationally altered in aged skeletal muscle. *Biochemistry* **38**, 14887-14896.
25. Chiu, D.T., van den Berg, J., Kuypers, F.A., Hung, I.J., Wei, J.S., and Liu, T.Z. (1996). Correlation of membrane lipid peroxidation with oxidation of hemoglobin variants: possibly related to the rates of heme release. *Free Radical Biology & Medicine* **21**(1), 89-95.
26. Crescenzo, R., Bianco, F., Mazzoli, A., Giacco, A. and Liverini, G. (2014). Alterations in proton leak, oxidative status and uncoupling protein 3 content in skeletal muscle subsarcolemmal and intermyofibrillar mitochondria in old rats. *BMC Geriatrics* **17**, 79
27. Cruz-Jentoft, A.J., Baeyens, J.P., Bauer, J.M., Boirie, Y., Cederholm, T., Landi, F., Martin, F.C., Michel, J.P., Rolland, Y., Schneider, S.M., Topinková, E., Vandewoude, M., Zamboni, M.; European Working Group on Sarcopenia in Older People. (2010). Sarcopenia: European consensus on definition and diagnosis: Report of the European Working Group on Sarcopenia in Older People. *Age and Ageing* **39**(4), 412-423.
28. Csató, V., Pető, A., Fülöp, G. Á., Rutkai, I., Pásztor, E. T., Fagyas, M., Kalász, J., Édes, I., Tóth, A. and Papp, Z. (2015). Myeloperoxidase evokes substantial vasomotor responses in isolated skeletal muscle arterioles of the rat. *Acta Physiologica* **214**(1), 109-123.
29. Dalla Libera, L., Ravara, B., Gobbo, V., Betto, D.D., Germinario, E., Angelini, A., Evangelista, S., and Vescovo, G. (2010). Skeletal muscle proteins oxidation in chronic right heart failure in rats: can different beta-blockers prevent it to the same degree? *International Journal of Cardiology* **143**(2), 192-199.
30. Dalle-Donne, I., Rossi, R., Giustarini, D., Colombo, R., and Milzani, A. (2007). S-glutathionylation in protein redox regulation. *Free Radical Biology and Medicine* **43**(6), 883-898.
31. de la Mora-de la Mora, I., Torres-Larios, A., Enríquez-Flores, S., Méndez, S-T., Castillo-Villanueva, A., Gómez-Manzo, S., López-Velázquez, G., Marcial-Quino, J., Torres-Arroyo, A., García-Torres, I., Reyes-Vivas, H., and Oria-Hernández J. (2015). Structural Effects of Protein Aging: Terminal Marking by Deamidation in Human Triosephosphate Isomerase. *PLoS ONE* **10**(4), e0123379.

32. Diaz-Ruiz, A., Guzmán-Ruiz, R., Moreno, N.R., García-Rios, A., Delgado-Casado, N., Membrives, A., Túnez, I., El Bekay, R., Fernández-Real, J.M., Tovar, S., Diéguez, C., Tinahones, F.J., Vázquez-Martínez, R., López-Miranda, J., Malagón, M.M. (2015). Proteasome Dysfunction Associated to Oxidative Stress and Proteotoxicity in Adipocytes Compromises Insulin Sensitivity in Human Obesity. *Antioxidants and Redox Signaling* **23**(7) 597-612.
33. Dilman, V.M., and Dean, W. (1992). The Neuroendocrine Theory of Aging and Degenerative Disease. *The Center for Bio-Gerontology*, Pensacola, Florida.
34. Domigan, N.M., Charlton, T.S., Duncan, M.W., Winterbourn, C.C., and Kettle, A.J. (1995). Chlorination of tyrosyl residues in peptides by myeloperoxidase and human neutrophils. *Journal of Biological Chemistry* **270**, 16542-16548.
35. Domingues, M.R.M., Domingues, P., Reis, A., Fonseca, C., Amado, F.M., and Ferrer-Correia, A.J. (2003). Identification of oxidation products and free radicals of tryptophan by mass spectrometry. *Journal of the American Society for Mass Spectrometry* **14**, 406-416.
36. Donoghue, P., Doran, P., Wynne, K., Pedersen, K., Dunn, M.J., Ohlendieck, K. (2007). Proteomic profiling of chronic low-frequency stimulated fast muscle. *Proteomics* **7**(18), 3417-3430.
37. Douglas, D.J., Frank, A.J. and Mao, D. (2005). Linear ion traps in mass spectrometry. *Mass Spectrometry Reviews* **24**(1), 1-29.
38. Drel, V.R., Mashtalir, N., Ilnytska, O., Shin, J., Li, F., Lyzogubov, V.V., Obrosova, I.G. (2006). The leptin-deficient (ob/ob) mouse: a new animal model of peripheral neuropathy of type 2 diabetes and obesity. *Diabetes* **55**(12), 3335-3343.
39. Duan, X., Young, R., Straubinger, R.M, Page, B., Cao, J., Wang, H., Yu, H., Canty, J.M., and Qu, J. (2009). A straightforward and highly efficient precipitation/on-pellet digestion procedure coupled with a long gradient nano-1c separation and orbitrap mass spectrometry for label-free expression profiling of the swine heart mitochondrial proteome. *Journal of Proteome Research* **8**, 2838-2850.
40. Dworzanski, J.P., Snyder, A.P., Chen, R., Zhang, H., Wishart, D., Li, L. (2004). Identification of Bacteria Using Tandem Mass Spectrometry Combined with a Proteome Database and Statistical Scoring. *Analytical Chemistry* **76**(8), 2355-2366.
41. Edgerton, V.R., Smith, J.L., Simpson, D.R. (1975). Muscle fibre type populations of human leg muscles. *The Histochemical Journal* **7**(3), 259-266.
42. England, K., O'Driscoll, C., and Cotter, T.G. (2004). Carbonylation of glycolytic proteins is a key response to drug-induced oxidative stress and apoptosis. *Cell Death & Differentiation* **11**(3), 252-260.
43. Falick, A. M., Hines, W. M., Medzihradzsky, K. F., Baldwin, M. A., and Gibson, B. W. (1993). Low-mass ions produced from peptides by high-energy collision-induced dissociation in tandem mass spectrometry. *Journal of the American Society for Mass Spectrometry* **4**, 882-893.
44. Fan, X., Zhang, J., Theves, M., Strauch, C., Nemet, I., Liu, X., Qian, J., Giblin, F.J., Monnier, V.M. (2009). Mechanism of Lysine Oxidation in Human Lens Crystallins during Aging and in Diabetes. *The Journal of Biological Chemistry* **284**(50), 34618-34627.
45. Favero, T.G., Colter, D., Hooper, P.F., Abramson, J.J. (1998). Hypochlorous acid inhibits Ca²⁺-ATPase from skeletal muscle sarcoplasmic reticulum. *Journal of Applied Physiology* **84**, 425-430.

46. Feng, J., Navratil, M., Thompson, L.V., and Arriaga, E.A. (2008). Principal component analysis reveals age-related and muscle-type-related differences in protein carbonyl profiles of muscle mitochondria. *The journals of gerontology. Series A, Biological sciences and medical sciences* **63**(12), 1277-1288.
47. Fenn, J.B., Mann, M., Meng, C.K., Wong, S.F., and Whitehouse, C.M. (1989). Electrospray ionisation for mass spectrometry of large biomolecules. *Science* **246**(4926); 64-71.
48. Ferrington, D.A., Krainev, A.G., and Bigelow, D.J. (1998). Altered Turnover of Calcium Regulatory Proteins of the Sarcoplasmic Reticulum in Aged Skeletal Muscle. *The Journal of Biological Chemistry* **273**(10), 5885-5891.
49. Filippin, L.I., Vercelino, R., Marroni, N.P., and Xavier, R.M. (2008). Redox signalling and the inflammatory response in rheumatoid arthritis. *Clinical & Experimental Immunology* **152**(3); 415-422.
50. Fink, L.N., Costford, S.R., Lee, Y.S., Jensen, T.E., Bilan, P.J., Oberbach, A., Blüher, M., Olefsky, J.M., Sams, A., Klip, A. (2014). Pro-Inflammatory macrophages increase in skeletal muscle of high fat-Fed mice and correlate with metabolic risk markers in humans. *Obesity* **22**; 747-757.
51. Finkel, T., and Holbrook, N.J. (2000). Oxidants, oxidative stress and the biology of ageing. *Nature* **408**, 239-247.
52. Fontana, A., Dalzoppo, D., Grandi, C., and Zamboni, M. (1983). Cleavage at tryptophan with o-iodosobenzoic acid. *Methods Enzymology* **91**, 311-318.
53. Friguet, B. (2006). Oxidized protein degradation and repair in ageing and oxidative stress. *FEBS letters* **580**(12), 2910-2916.
54. Friguet, B., Bulteau, A.L., Chondrogianni, N., Conconi, M., Petropoulos, I. (2000). Protein degradation by the proteasome and its implications in aging. *Annals of the New York Academy of Sciences* **908**, 143-154.
55. Froehlich J.P., Lakatta, E.G., Beard, E., Spurgeon, H.A., Weisfeldt, M.L., and Gerstenblith, G. (1978). Studies of sarcoplasmic reticulum function and contraction duration in young adult and aged rat myocardium. *Journal of Molecular and Cellular Cardiology* **10**(5), 427-438.
56. Fu, S., Yang, L., Li, P., Hofmann, O., Dicker, L., Hide, W., Lin, X., Watkins, S.M., Ivanov, A., and Hotamisligil, G.S. (2011). Aberrant lipid metabolism disrupts calcium homeostasis causing liver endoplasmic reticulum stress in obesity. *Nature* **473**(7348), 528-531.
57. Fu, X., Mueller, D.M., and Heinecke, J.W. (2002). Generation of intramolecular and intermolecular sulfenamides, sulfinamides, and sulfonamides by hypochlorous acid: a potential pathway for oxidative cross-linking of low-density lipoprotein by myeloperoxidase. *Biochemistry* **41**(4), 1293-1301.
58. Funai, K., Song, H., Yin, L., Lodhi, I.J., Wei, X., Yoshino, J., Coleman, T., Semenkovich, C.F. (2013). Muscle lipogenesis balances sensitivity and strength through calcium signaling. *The journal of clinical investigation* **123**(3), 1229-1240.
59. García-Ruiz, I., Rodríguez-Juan, C., Díaz-Sanjuan, T., del Hoyo, P., Colina, F., Muñoz-Yagüe, T. and Solís-Herruzo, J. A. (2006). Uric acid and anti-TNF antibody improve mitochondrial dysfunction in ob/ob mice. *Hepatology* **44**(3), 581-591.
60. Gardner, J.P., Kimura, M., Chai, W., Durrani, J.F., Tchakmakjian, L., Cao, X., Lu, X., Li, G., Peppas, A.P., Skurnick, J., Wright, W.E., Shay, J.W., and Aviv, A. (2007). Telomere

- dynamics in macaques and humans. *The Journals of Gerontology: Series A, Biological sciences and Medical sciences* **62**(4), 367-374.
61. Gelfi, C., Viganò, A., Ripamonti, M., Pontoglio, A., Begum, S., Pellegrino, M.A., Grassi, B., Bottinelli, R., Wait, R., Cerretelli, P. (2006). The human muscle proteome in aging. *Journal of Proteome Research* **5**(6), 1344-1353.
 62. Ghesquiere, B., Colaert, N., Helsens, K., Dejager, L., Vanhaute, C., Verleysen, K., Kas, K., Timmerman, E., Goethals, M., Libert, C., *et al.* (2009) *In vitro* and *in vivo* protein-bound tyrosine nitration characterized by diagonal chromatography. *Molecular & Cellular Proteomics* **8**, 2642-2652.
 63. Ghesquiere, B.; Colaert, N.; Helsens, K.; Dejager, L.; Vanhaute, C.; Verleysen, K.; Kas, K.; Timmerman, E.; Goethals, M.; Libert, C., *et al.* (2008) *In vitro* and *in vivo* protein-bound tyrosine nitration characterized by diagonal chromatography. *Molecular & Cellular Proteomics* **8**, 2642-2652.
 64. Gillet, L.C., Navarro, P., Tate, S., Rost, H., Selevsek, N., Reiter, L., Bonner, R., and Aebersold, R. (2012). Targeted Data Extraction of the MS/MS Spectra Generated by Data-independent Acquisition: A New Concept for Consistent and Accurate Proteome Analysis. *Molecular and Cellular Proteomics* **11**(6), O111.016717.
 65. Gregor, M.F. and Hotamisligil, G.S. (2011). Inflammatory mechanisms in obesity. *Annual Review of Immunology* **29**; 415-445.
 66. Griffiths, H. R., Moller, L., Bartosz, G., Blast, A., Bertoni-Freddari, C., Collins, A., Cooke, M., Coolen, S., Haenen, G., Hoberg, A.M., Loft, S., Lunec, J., Olinski, R., Parry, J., Pompella, A., Poulsen, H., Verhagen, H., and Astley, S.B. (2002). Biomarkers. *Molecular Aspects of Medicine* **23**, 101-208.
 67. Grimsrud, P.A., Picklo, M.J. Sr., Griffin, T.J., Bernlohr, D.A. (2007). Carbonylation of adipose proteins in obesity and insulin resistance: identification of adipocyte fatty acid-binding protein as a cellular target of 4-hydroxynonenal. *Molecular and cellular proteomics* **6**, 624-637.
 68. Guilhaus, M. (1995). Principles and Instrumentation in Time-of-Flight Mass Spectrometry. *Journal of Mass Spectrometry* **30**, 1519-1532.
 69. Guo, J., Gaffrey, M.J., Su, D., Liu, T., Camp, D.G, Smith, R.D., Qian, W.J. (2014) Resin-assisted enrichment of thiols as a general strategy for proteomic profiling of cysteine-based reversible modifications. *Nature Protocols* **9**(1), 64-75.
 70. Gutteridge, J.M.C., and Halliwell, B. (2000). Free radicals and antioxidants in the year 2000: a historical look into the future. *Annals of the New York Academy of Sciences* **899**, 136-147.
 71. Hager, J.W., and Yves Le Blanc, J.C. (2003). Product ion scanning using a Q-q-Q linear ion trap (Q TRAP) mass spectrometer. *Rapid Communications in Mass Spectrometry* **17**(10), 1056-1064.
 72. Hains, P.G. and Truscott, R.J.W. (2010). Age-Dependent Deamidation of Lifelong Proteins in the Human Lens. *Investigative ophthalmology and visual science* **51**(6), 3107-3114.
 73. Harman, D. (1956). Aging: a theory based on free radical and radiation chemistry. *Journal of Gerontology* **11**(3), 298-300.
 74. Harman, D. (2003). The free radical theory of ageing. *Antioxidant Redox Signaling*. **5**(5), 557-561.
 75. Harrison, J.E., and Schultz, J. (1976). Studies on the chlorinating activity of myeloperoxidase. *Journal of biological chemistry* **251**, 1371-1374.

76. Hartshorne, J.K. and Germine, L.T. (2015). When Does Cognitive Functioning Peak? The Asynchronous Rise and Fall of Different Cognitive Abilities Across the Life Span. *Psychological Science*, **26**(4), 433-443.
77. Hawkins, C.I., Pattison, D.I., and Davies, M.J. (2003). Hypochlorite-induced oxidation of amino acids, peptides and proteins. *Amino acids* **25**, 259-274.
78. Hawkins, C.L. and Davies, M.J. Generation and propagation of radical reactions on proteins. *Biochimica et Biophysica Acta* **1504**(2-3), 196-219
79. Hayflick, L. and Moorhead, P.S. (1961). The serial cultivation of human diploid cell strains. *Experimental Cell Research* **25**, 585-621.
80. Hazen, S.L., d'Avignon, A., Anderson, M.A., Hsu, F.F., and Heinecke, J.W. (1998). Human neutrophils employ the myeloperoxidase-hydrogen peroxide-chlorine system to oxidize α -amino-acids to a family of reactive aldehydes. *Journal of Biological Chemistry* **273**, 4997-5005.
81. Heinecke, J.W., Li, W., Daehnke, H.L., and Goldstein, J.A. (1993). Dityrosine, a specific marker of oxidation, is synthesized by the myeloperoxidase-hydrogen peroxide system of human neutrophils and macrophages. *The Journal of Biological Chemistry* **268**(6), 4069-4077.
82. Held, J.M., Danielson, S.R., Behring, J.B., Atsriku, C., Britton, D.J., Puckett, R.L., Schilling, B., Campisi, J., Benz, C.C., and Gibson, B.W. (2010). Targeted quantitation of site-specific cysteine oxidation in endogenous proteins using differential alkylation and multiple reaction monitoring mass spectrometry approach. *Molecular & Cellular Proteomics* **9**, 1400-1410.
83. Hittel, D.S., Hathout, Y., Hoffman, E.P., Houmard, J.A. (2005). Proteome analysis of skeletal muscle from obese and morbidly obese women. *Diabetes* **54**(5), 1283-1288.
84. Holmes, C. (2013) Systemic inflammation and Alzheimer's disease. *Neuropathology and Applied Neurobiology* **39**(1); 51–68.
85. Hornsby, P.J. (2007). Telomerase and the ageing process. *Experimental Gerontology* **42**(7), 575-581.
86. Hoskins, J.A., and Davis, L.J. (1998). Analysis of the isomeric tyrosines in mammalian and avian systems using high performance liquid chromatography with fluorescence detection. *Journal of Chromatography* **426**, 155-161.
87. Hu, D., Serrano, F., Oury, T.D., and Klann, E. (2006). Aging-Dependent Alterations in Synaptic Plasticity and Memory in Mice That Overexpress Extracellular Superoxide Dismutase. *The Journal of Neuroscience* **26**(25); 3933-3941.
88. Huber, N., Sakai, N., Eismann, T., Shin, T., Kuboki, S., Blanchard, J., Schuster, R., Edwards, M. J., Wong, H. R. and Lentsch, A. B. (2009). Age-related decrease in proteasome expression contributes to defective nuclear factor- κ B activation during hepatic ischemia/reperfusion. *Hepatology* **49**, 1718-1728.
89. Hughes, V.A., Frontera, W.R., Wood, M., Evans, W.J., Dallal, G.E., Roubenoff, R., and Fiatarone Singh, MA. (2001). Longitudinal muscle strength changes in older adults: influence of muscle mass, physical activity, and health. *The journals of gerontology. Series A, Biological sciences and medical sciences* **56**, 209-217.
90. Hunt, D.F., Yates III, J.R., Shabanowitz, J., Winston, S., and Hauer, C.R. (1986). Protein sequencing by tandem mass spectrometry. *Proceedings of the National Academy of Sciences of the USA* **83**, 6233-6237.
91. Hunter, S.K., Thompson, M.W., Ruell, P.A., Harmer, A.R., Thom, J.M., Gwinn, T.H., and Adams, R.D. (1999). Human skeletal sarcoplasmic reticulum Ca²⁺ uptake and muscle

- function with aging and strength training. *Journal of Applied Physiology* **86**(6), 1858-1865.
92. Hurst, J.K., Barrette Jr., W.C., Michel, B.R., and Rosen, H. (1991). Hypochlorous acid and myeloperoxidase-catalyzed oxidation of iron-sulfur clusters in bacterial respiratory dehydrogenases. *European Journal of Biochemistry* **202**(3), 1275-1282.
 93. Hwang, C.Y., Kim, K., Choi, J.Y., Bahn, Y.J., Lee, S.M., Kim, Y.K., Lee, C., Kwon, K.S. (2014), Quantitative proteome analysis of age-related changes in mouse gastrocnemius muscle using mTRAQ. *Proteomics* **14**(1), 121-132.
 94. Hwang, N.R., Yim, S.H., Kim, Y.M., Jeong, J., Song, E.J., Lee, Y., Lee, J.H., Choi, S., and Lee, K.J. (2009). Oxidative modifications of glyceraldehyde-3-phosphate dehydrogenase play a key role in its multiple cellular functions. *Biochemical Journal* **423**(2), 253-264.
 95. Ishimitsu, S., Fujimoto, S., and Ohara, A. (1984). Hydroxylation of phenylalanine by the hypoxanthine-xanthine oxidase system. *Chemical & Pharmaceutical Bulletin* **32**, 4645-4649.
 96. Jaffrey, S.R. and Snyder, S.H. (2001). The biotin switch method for the detection of s-nitrosylated proteins. *Science's STKE : signal transduction knowledge environment* **2001**, pl1.
 97. Jenkins, N. (2007) Modifications of therapeutic proteins: challenges and prospects. *Cytotechnology* **53**(1-3), 121-125.
 98. Jeong, J., Jung, Y., Na, S., Jeong, J., Lee, E., Kim, M-S., Choi, S., Shin, D-H., Paek, E., Lee, H-Y., and Lee, K-J. (2011). Novel Oxidative Modifications in Redox-Active Cysteine Residues. *Molecular & Cellular Proteomics* **10**(3), M110.000513.
 99. Jiang, H., Ju, Z., and Rudolph, K.L. (2007). Telomere shortening and ageing. *Zeitschrift fur Gerontologie und Geriatrie* **40**(5), 314-324.
 100. Jiang, M., He, J., Kucera, H., Gaikwad, N.W., Zhang, B., Xu, M., O'Doherty, R.M., Selcer, K.W., Xie, W. (2014). Hepatic overexpression of steroid sulfatase ameliorates mouse models of obesity and type 2 diabetes through sex-specific mechanisms. *Journal of Biological Chemistry* **289**(12), 8086-8097.
 101. Jin, K. (2010). Modern biological theories of ageing. *Aging and Disease* **1**(2), 72-74.
 102. Johnson, M.A., Polgar, J., Weightman, D., and Appleton, D. (1973). Data on the distribution of fibre types in thirty-six human muscles. An autopsy study. *Journal of Neurological Sciences* **18**(1), 111-129.
 103. Johnson, R.S., Martin, S.A., Biemann, K., Stults, J.T., Watson, J.T. (1987). Novel fragmentation process of peptides by collision-induced decomposition in a tandem mass spectrometer: differentiation of leucine and isoleucine. *Analytical Chemistry* **59**(21), 2621-2625.
 104. Joyner, M.J., and Dietz, N.M. (1985). Nitric oxide and vasodilation in human limbs. *Journal of Applied Physiology* **83**(6); 1785-1796.
 105. Jung, T., Hohn, A., and Grune, T. (2014). The proteasome and the degradation of oxidized proteins: Part II – protein oxidation and proteasomal degradation. *Redox Biology* **2**, 99-104.
 106. Juránek, I. and Bezek, S. (2005). Controversy of free radical hypothesis: reactive oxygen species – causes or consequence of tissue injury? *General Physiology and Biophysics* **24**, 263-278.

107. Kang, D-K., Jeong, J., Drake, S.K., Wehr, N.B., Rouault, T.A., and Levine, R.L. (2003). Iron regulatory protein 2 as iron sensor: Iron-dependent oxidative modification of cysteine. *Journal of Biological Chemistry* **278**, 14857-14864.
108. Keller, J.N., Huang, F.F., and Markesbery, W.R. (2000). Decreased levels of proteasome activity and proteasome expression in aging spinal cord. *Neuroscience* **98**(1), 149-156.
109. Kemp, J.G., Blazev, R., Stephenson, D.G., Stephenson, G.M. (2009). Morphological and biochemical alterations of skeletal muscles from the genetically obese (ob/ob) mouse. *International Journal of Obesity* **33**, 831-841.
110. Kirkinetzos, I.G., and Moraes, C.T. (2001). Reactive oxygen species and mitochondrial diseases. *Cell and Developmental Biology* **12**, 449-457.
111. Klebanoff, S.J. (1999). Myeloperoxidase. *Proceedings of the Association of American Physicians* **111**(5), 383-389.
112. Knyushko, T.V., Sharov, V.S., Williams, T.D., Schoneich, C., and Bigelow, D.J. (2005). 3-Nitrotyrosine modification of SERCA2a in the ageing heart: a distinct signature of the cellular redox environment. *Biochemistry* **44**, 13071-13081.
113. Laemmli, U. K. (1970). Cleavage of structural proteins during the assembly of the head of the bacteriophage T4. *Nature* **227**, 680-685.
114. Lech, M., and Anders, H-J. (2013). Macrophages and fibrosis: How resident and infiltrating mononuclear phagocytes orchestrate all phases of tissue injury and repair. *Biochimica et Biophysica Acta (BBA) - Molecular Basis of Disease* **1832**(7), 989-997.
115. Lee, C.F., Paull, T.T., Person, M.D. (2013). Proteome-wide detection and quantitative analysis of irreversible cysteine oxidation using long column UPLC-pSRM. *Journal of Proteome Research* **12**(10), 4302-4315.
116. Leeuwenburgh C., Rasmussen, J.E., Hsu, F.F. Mueller, D.M. Pennathur, S. and Heinecke, J.W. 1997. Mass Spectrometric Quantification of Markers for Protein Oxidation by Tyrosyl Radical, Copper, and Hydroxyl Radical in Low Density Lipoprotein Isolated from Human Atherosclerotic Plaques. *The Journal of Biological Chemistry* **272**, 3520-3526.
117. Levine, R. L., Mosoni, L., Berlett, B. S., and Stadtman, E. R. (1996). Methionine residues as endogenous antioxidants in proteins. *Proceedings of the National Academy of Sciences of the USA* **93**(26), 15036-15040.
118. Levine, R.L., Williams, J.A., Stadtman, E.A., and Schacter, E. (1994). Carbonyl assays for determination of oxidatively modified proteins. *Methods in Enzymology* **233**, 346-357.
119. Lindner, H. and Helliger, W. (2001). Age-dependent deamidation of asparagine residues in proteins. *Experimental Gerontology* **36**(09), 1551-1563.
120. Lipman, R.D., Bronson, R.T., Wu, D., Smith, D.E., Prior, R., Cao, G., Han, S.N., Martin, K.R., Meydani, S.N., and Meydani, M. (1998). Disease incidence and longevity are unaltered by dietary antioxidant supplementation initiated during middle age in C57BL/6 mice. *Mechanisms of Ageing and Development* **103**(3), 269-284.
121. Liu, R., Liu, I.Y., Bi, X., Thompson, R.F., Doctrow, S.R., Malfroy, B., and Baudry, M. (2003). Reversal of age-related learning deficits and brain oxidative stress in mice with superoxide dismutase/catalase mimetics. *Proceedings of the National Academy of Sciences of the USA* **100**(14); 8526-8531.
122. Lu, W., Ogasawara, M.A., and Huang, P. (2007). Models of reactive oxygen species in cancer. *Drug Discovery Today: Disease Models* **4**(2); 67-73.

123. Lytton, J., Westlin, M., and Hanley, M.R. (1991). Thapsigargin Inhibits the Sarcoplasmic or Endoplasmic Reticulum Ca-ATPase Family of Calcium Pumps. *The Journal of Biological Chemistry* **266**(26); 17067-17071.
124. MacLean, B. Tomazela, D.M., Shulman, N., Chambers, M., Finney, G.L., Frewen, B., Kern, R., Tabb, D.L., Liebler, D.C., MacCoss, M.J. (2010). Skyline: an open source document editor for creating and analyzing targeted proteomics experiments. *Bioinformatics* **26**(7); 966-968.
125. MacLennan, D. H. (1970). Purification and properties of an adenosine triphosphatase from sarcoplasmic reticulum. *Journal of Biological Chemistry* **245**, 4508-4518.
126. Madian, A.G., Myracle, A.D., Diaz-Maldonado, N., Rochelle, N.S., Janle, E.M., Regnier, F.E. (2011). Determining the effects of antioxidants on oxidative stress induced carbonylation of proteins. *Analytical Chemistry* **83**(24), 9328-9336.
127. Mather, K.A., Jorm, A.F., Parslow, R.A., and Christensen, H. (2011). Is telomere length a biomarker of ageing? A review. *The Journals of Gerontology: Series A, Biological sciences and Medical sciences* **66A**(2), 202-213.
128. Matsui, H., Takano, N., Moriyama, A., and Takahashi, T. (2005). Single-chain tissue-type plasminogen activator is a substrate of mouse glandular kallikrein 24. *Zoological Science* **22**(10), 1105-1111.
129. McDonagh, B., Martínez-Acedo, P., Vázquez, J., Padilla, C.A., Sheehan, D., and Bárcena, J.A. (2012). Application of iTRAQ Reagents to Relatively Quantify the Reversible Redox State of Cysteine Residues. *International Journal of Proteome Research* **2012**(ID 514847), 9.
130. McPherson, P.A. and Turemen, B.T. 2014. 3,4-Dihydroxy-L-phenylalanine as a biomarker of oxidative damage in proteins: improved detection using cloud-point extraction and HPLC. *Biochemical and Biophysical Research Communications* **452**(3), 376-381.
131. Miller, P.E., and Denton, B.M. (1986). The quadrupole mass filter – basic operating concepts. *Journal of Chemical Education* **63**, 617-622.
132. Mirzaei, H. and Regnier, F. (2005). Affinity chromatographic selection of carbonylated proteins followed by identification of oxidation sites using tandem mass spectrometry. *Analytical Chemistry* **77**(8), 2386-2392.
133. Mirzaei, H., Schieler, J.L., Rochet, J-C., and Regnier, F. (2006). Identification of Rotenone-induced modifications in α -Synuclein using affinity pull-down and tandem mass spectrometry. *Analytical Chemistry* **78**(7), 2422-2431.
134. Molloy, M.P. Brzezinski, E.E., Hang, J., McDowell, M.T., VanBogelen, R.A. (2003). Overcoming technical variation and biological variation in quantitative proteomics. *Proteomics* **3**(10), 1912-1919.
135. Moreau, V.H., Castilho, R.F., Ferreira, S.T., and Carvalho-Alves, P.C. (1998). Oxidative damage to sarcoplasmic reticulum Ca²⁺-ATPase at submicromolar iron concentrations: evidence for metal catalyzed oxidation. *Free Radical Biology and Medicine* **25** (4-5), 554-560.
136. Morley, J.E. (2012). Sarcopenia in the elderly. *Family Practice* **29** Suppl 1:i44-i48.
137. Muller, F.L., Song, W., Jang, Y.C., Liu, Y., Sabia, M., Richardson, A., and Van Remmen, H. (2007). Denervation-induced skeletal muscle atrophy is associated with increased mitochondrial ROS production. *American Journal of Physiology* **293**(3), R1159-1168.

138. Murakami, H., Guillet, C., Tardif, N., Salles, J., Migné, C., Boirie, Y., Walrand, S. (2012). Cumulative 3-nitrotyrosine in specific muscle proteins is associated with muscle loss during aging. *Experimental Gerontology* **47**(2), 129-135.
139. Nebert, D.W., and Vasiliou, V. (2004). Analysis of the glutathione S-transferase (GST) gene family. *Human Genomics* **1**(6), 460-464.
140. Nepomuceno, A.I., Gibson, R.J., Randall, S.M., Muddiman, D.C. (2014). Accurate identification of deamidated peptides in global proteomics using a quadrupole orbitrap mass spectrometer. *Journal of Proteome Research* **13**(2), 777-785.
141. Nguyen, M.H., Cheng, M., and Koh, T.J. (2011). Impaired muscle generation in ob/ob and db/db mice. *ScientificWorldJournal* **11**, 1525-1535.
142. Nguyen, T., Nioi, P., and Pickett, C.B. (2009). The Nrf2-antioxidant response element signaling pathway and its activation by oxidative stress. *The Journal of Biological Chemistry* **284**, 13291-13295.
143. Nuss, J. E., Amaning, J. K., Bailey, C. E., DeFord, J. H., Dimayuga, V. L., Rabek, J. P., and Papaconstantinou, J. (2009). Oxidative modification and aggregation of creatine kinase from aged mouse skeletal muscle. *Aging* **1**(6), 557-572.
144. O'Connell, K., and Ohlendieck, K. (2009). Proteomic DIGE analysis of the mitochondria-enriched fraction from aged rat skeletal muscle. *Proteomics* **9**(24), 5509-5524.
145. O'Flaherty, E.J., 2000. Modeling Normal Aging Bone Loss, with Consideration of Bone Loss in Osteoporosis. *Toxicological Sciences* **55**(1), 171-188.
146. Oh, S.J., Park, K.S., Ryan, H.F. Jr, Danon, M.J., Lu, J., Naini, A.B., DiMauro, S. (2006). Exercise-induced cramp, myoglobinuria, and tubular aggregates in phosphoglycerate mutase deficiency. *Muscle & Nerve* **34**(5), 572-576.
147. Olsen, J.V., and Mann, M. (2004). Improved peptide identification in proteomics by two consecutive stages of mass spectrometric fragmentation. *Proceedings of the National Academy of Sciences of the USA* **101**(37), 13417-13422.
148. Otsuda, T., Takamura, T., Misu, H., Ota, T., Murata, S., Hayashi, H., Takayama, H., Kikuchi, A., Kanamori, T., Shima, K.R., Lan, F., Takeda, T., Kurita, S., Ishikura, K., Kita, Y., Iwayama, K., Kato, K., Uno, M., Takeshita, Y., Yamamoto, M., Tokuyama, K., Iseki, S., Tanaka, K., Kaneko S. (2013). Proteasome dysfunction mediates obesity-induced endoplasmic reticulum stress and insulin resistance in the liver. *Diabetes* **62**(3), 811-824.
149. Palomero, J., Vasilaki, A., Pye, D., McArdle, A., Jackson, M.J. (2013). Aging increases the oxidation of dichlorohydrofluorescein in single isolated skeletal muscle fibers at rest, but not during contractions. *American Journal of Physiology Regulatory Integrative and Comparative Physiology* **305**(4), R351-358.
150. Papayannopoulos, I. A. (1995). The interpretation of collision-induced dissociation tandem mass spectra of peptides. *Mass Spectrometry Reviews* **14**, 49-73.
151. Parthasarathy, S., Khan-Merchant, N., Penumetcha, M., Khan, B.V., and Santanam, N. (2001). Did the antioxidant trials fail to validate the oxidation hypothesis? *Current Atherosclerosis Reports* **3**, 392-398.
152. Pattison, D.I., and Davies, M.J. (2005). Kinetic analysis of the role of histidine chloramines in hypochlorous acid mediated protein oxidation. *Biochemistry* **44**, 7378-7387.
153. Pellegrinelli, V., Rouault, C., Rodriguez-Cuenca, S., Albert, V., Edom-Vovard, F., Vidal-Puig, A., Clement, K., Butler-Browne, G.S., and Lacasa, D. (2015). Human

- adipocytes induce inflammation and atrophy in muscle cells during obesity. *Diabetes* **64**; 3121-3134.
154. Perkins, D.N., Pappin, D.J., Creasy, D.M., and Cottrell, J.S. (1999). Probability-based protein identification by searching sequence databases using mass spectrometry data. *Electrophoresis* **20**(18); 3551-3567.
 155. Pfeiffer, S., Schmidt, K., and Mayer, B. (2000). Dityrosine formation outcompetes tyrosine nitration at low steady-state concentrations of peroxynitrite: Implications for tyrosine modification by nitric oxide/superoxide *in vivo*. *Journal of Biological Chemistry* **275**, 6346-6352.
 156. Philippi, M., and Silau, A.H. (1994). Oxidative capacity distribution in skeletal muscle fibers of the rat. *The Journal of Experimental Biology* **189**, 1-11.
 157. Picotti, P., Bodenmiller, B., Mueller, L.N., Domon, B., and Aebersold, R. (2009). Full dynamic range proteome analysis of *S. cerevisiae* by targeted proteomics. *Cell* **138**(4), 795-806.
 158. Pitt, A., and Spickett, C. (2008). Mass spectrometric analysis of HOCl- and free-radical-induced damage to lipids and proteins. *Biochemical Society Transactions* **36**, 1077-1082.
 159. Qu, N., Guo, L.H., and Zhu, B.Z. (2011). An electrochemical biosensor for the detection of tyrosine oxidation induced by Fenton reaction. *Biosensors and Bioelectronics* **26**, 2292-2296.
 160. Radi, R. (2004). Nitric oxide, oxidants, and protein tyrosine nitration. *Proceedings of the National Academy of Sciences of the USA* **101**(12), 4003-4008.
 161. Radzyukevich, T.L., Neumann, J.C., Rindler, T.N., Oshiro, N., Goldhamer, D.J., Lingrel, J.B., and Heiny, J.A. (2013). Tissue Specific Role of the Na,K-ATPase $\alpha 2$ Isozyme in Skeletal Muscle. *The Journal of Biological Chemistry* **288**, 1226-1237.
 162. Rath, V.L., Ammirati, M., LeMotte, P.K., Fennell, K.F., Mansour, M.N., Danley, D.E., Hynes, T.R., Schulte, G.K., Wasilko, D.J., Pandit, J. (2000). Activation of human liver glycogen phosphorylase by alteration of the secondary structure and packing of the catalytic core. *Molecular cell* **6**(1), 139-148.
 163. Robbins, A.R., Ward, R.D., and Oliver, C. (1995). A mutation in glyceraldehyde 3-phosphate dehydrogenase alters endocytosis in CHO cells. *Journal of Cell Biology* **130**(5), 1093-1104.
 164. Robine, J.M and Ritchie, K. (1991). Health life expectancy: evaluation of global indicator of change in population health. *British Medical Journal* **302**(6774); 457-460.
 165. Robinson, A.B. and Robinson, L.R. (1991). Distribution of glutamine and asparagine residues and their near neighbours in peptides and proteins. *Biochemistry* **88**, 8880-8884.
 166. Roepstorff, P. and Fohlman, J. (1984). Proposal for a common nomenclature for sequence ions in mass spectra of peptides. *Biomedical Mass Spectrometry* **11**(11), 601.
 167. Rolland, Y., Lauwers-Cances, V., Cristini, C., Abellan van Kan, G., Janssen, I., Morley, J.E. and Vellas, B. (2009). Difficulties with physical function associated with obesity, sarcopenia, and sarcopenic-obesity in community-dwelling elderly women: the EPIDOS (EPIDemiologie de l'OSteoporose) Study. *The American Journal of Clinical Nutrition* **89**(6); 1895-1900.
 168. Rousu, T., Herttuainen, J., Tolonen, A. (2010). Comparison of triple quadrupole, hybrid linear ion trap triple quadrupole, time-of-flight and LTQ-Orbitrap mass spectrometers in drug discovery phase metabolite screening and identification *in vitro*--

- amitriptyline and verapamil as model compounds. *Rapid Communications in Mass Spectrometry* **24**(7); 939-957.
169. Rusk, N., Le, P.U., Mariggio, S., Guay, G., Lurisci, C., Nabi, I.R., Corda, D., and Symons, M. (2003). Synaptojanin 2 functions at an early step of clathrin-mediated endocytosis. *Current Biology* **13**(8), 659-663.
 170. Russ, D.W., Wills, A.M., Boyd, I.M., and Krause, J. (2014). Weakness, SR function and stress in gastrocnemius muscles of aged male rats. *Experimental Gerontology* **50**, 40-44.
 171. Rust, C.A., Knechtle, B., Knechtle, P., Rosemann, T., and Lepers, R. (2012). Age of peak performance in elite male and female Ironman triathletes competing in Ironman Switzerland, a qualifier for the Ironman world championship, Ironman Hawaii, from 1995 to 2011. *Journal of Sports Medicine* **3**, 175-182.
 172. Ryan, K.C., Johnson, O.E., Cabelli, D.E., Brunold, T.C., and Maroney, M.J. (2010). Nickel superoxide dismutase: structural and functional roles of Cys2 and Cys6. *Journal of Biological Inorganic Chemistry* **15**(5), 795-807.
 173. Saez, I., and Vilchez, D. (2014). The Mechanistic Links Between Proteasome Activity, Aging and Agerelated Diseases. *Current Genomics* **15**(1), 38-51.
 174. Saveliev, S.V., Woodroffe, C.C., Sabat, G., Adams, C.M., Klaubert, D., Wood, K., and Urh, M. (2013). Mass spectrometry compatible surfactant for optimized in-gel protein digestion. *Analytical Chemistry* **85**, 907-914.
 175. Sawyer, D.T., and Valentine, J.S. (1981). How super is superoxide? *Accounts of Chemical Research* **14**, 393-400.
 176. Scherer-Opliger, T., Leimbacher, W., Blau, N., and Thony, B. (1999). Serine 19 of human 6-pyruvoyltetrahydropterin synthase is phosphorylated by cGMP protein kinase II. *The Journal of Biological Chemistry* **274**(44), 31341-31348.
 177. Schmid-Schonbein, G.W. (2006). Analysis of inflammation. *Annual Review of Biomedical Engineering* **8**, 93-151.
 178. Schoneich, C. (2000). Mechanisms of metal-catalyzed oxidation of histidine to 2-oxo-histidine in peptides and proteins. *Journal of Pharmaceutical and Biomedical Analysis* **21**, 1093-1097.
 179. Schoneich, C. (2005). Mass spectrometry in ageing research. *Mass Spectrometry Reviews* **24**, 701-718.
 180. Schoneich, C., and Sharov, V.S. (2006). Mass spectrometry of protein modifications by reactive oxygen and nitrogen species. *Free Radical Biology & Medicine* **41**, 1507-1520.
 181. Schoneich, C., Viner, R.I., Ferrington, D.A., and Bigelow, D.J. (1999). Age-related chemical modification of the skeletal muscle sarcoplasmic reticulum Ca-ATPase of the rat. *Mechanisms of Ageing and Development* **107**, 221-231.
 182. Sharov, V.S., Dremina, E.S., Galeva, N.A., Williams, T.D., and Schoneich, C. (2006a). Quantitative mapping of oxidation-sensitive cysteine residues in SERCA *in vivo* and *in vitro* by HPLC-electrospray-tandem MS: selective protein oxidation during biological ageing. *Journal of Biochemistry* **394**, 605-615.
 183. Sharov, V.S., Galeva, N.A., Dremina, E.S., Williams, T.D., and Schöneich C. (2009). Inactivation of rabbit muscle glycogen phosphorylase b by peroxyxynitrite revisited: does the nitration of Tyr613 in the allosteric inhibition site control enzymatic function? *Archives of Biochemistry and Biophysics* **484**(2); 155-166.

184. Sharov, V.S., Galeva, N.A., Kanski, J., Williams, T.D., and Schöneich C. (2006b). Age-associated tyrosine nitration of rat skeletal muscle glycogen phosphorylase b: characterization by HPLC-nanoelectrospray-tandem mass spectrometry. *Experimental Gerontology* **41**(4); 407-416.
185. Shenton, D. and Grant, C.M. (2003). Protein S-thiolation targets glycolysis and protein synthesis in response to oxidative stress in the yeast *Saccharomyces cerevisiae*. *Biochemical Journal* **374**, 513-519.
186. Sherrod, S.D., Myers, M.V., Li, M., Myers, J.S., Carpenter, K.L., MacLean, B., MacCoss, M.J., Liebler, D.C., and Ham, A.-J.L. (2012). Label-Free Quantitation of Protein Modifications by Pseudo Selected Reaction Monitoring with Internal Reference Peptides. *Journal of Proteome Research* **11**(6), 3467-3479.
187. Shevchenko, A., Tomas, H., Havli, J., Olsen, J.V., and Mann, M. (2007). In-gel digestion for mass spectrometric characterization of proteins and proteomes. *Nature Protocols* **1**, 2856-2860.
188. Simons, B., Kauhanen, D., Sylvanne, T., Tarasov, K., Duchoslav, E., and Ekroos, K. (2012). Shotgun Lipidomics by Sequential Precursor Ion Fragmentation on a Hybrid Quadrupole Time-of-Flight Mass Spectrometer. *Metabolites* **2**(1), 195-213.
189. Sobott, F., Watt, S.J., Smith, J., Edlmann, M.J., Kramer, H.B., Kessler, B.M. (2009). Comparison of CID Versus ETD Based MS/MS Fragmentation for the Analysis of Protein Ubiquitination. *Journal of the American Society for Mass Spectrometry* **20**(9); 1652-1659.
190. Stadtman, E.A., and Berlett, B.S. (1991). Fenton chemistry: amino acid oxidation. *Journal of Biological Chemistry* **266**, 17201-17211.
191. Stadtman, E.R. (1990). Metal ion-catalyzed oxidation of proteins: Biochemical mechanism and biological consequences. *Free Radical Biology and Medicine* **9** (4), 315-325.
192. Stadtman, E.R. (1993). Oxidation of free amino acids and amino acid residues in proteins by radiolysis and by metal-catalyzed reactions. *Annual Reviews Biochemistry* **62**, 797-821.
193. Stadtman, E.R. (2006) Protein oxidation and aging. *Free Radical Research* **40**(12), 1250-1258.
194. Stadtman, E.R., Moskovitz, J. and Levine, R.L. (2003) Oxidation of methionine residues of proteins: biological consequences. *Antioxidants and Redox Signaling* **5**(5), 577-582.
195. Stahl-Zeng, J. Lange, V., Ossola, R., Eckhardt, K., Krek, W., Aebersold, R., Domon, B. (2007). *Molecular & Cellular Proteomics* **6**(10), 1809-1817.
196. Steel, C., and Henchman, M. (1998). Understanding the quadrupole mass filter through computer simulation. *Journal of Chemical Education* **75**, 1049-1054.
197. Steen, H., Kuster, B., Fernandez, M., Pandey, A., Mann, M. (2001). Detection of Tyrosine Phosphorylated Peptides by Precursor Ion Scanning Quadrupole TOF Mass Spectrometry in Positive Ion Mode. *Analytical Chemistry* **73**(7), 1440-1448.
198. Strosova, M., Karlovska, J., Spickett, C.M., Grune, T., Orszagova, Z., and Horkova, L. (2009a). Oxidative injury induced by hypochlorous acid Ca-ATPase from sarcoplasmic reticulum of skeletal muscle and protective effect of trolox. *General Physiology and Biophysics* **28**, 195-209.
199. Strosova, M., Karlovska, J., Spickett, C.M., Orszagova, Z., Ponist, S., Bauerova, K., Mihalova, D., and Horkova, L. (2009b). Modulation of SERCA in the chronic phase of

- adjuvant arthritis as a possible adaptation mechanism of redox imbalance. *Free Radical Research* **43**(9), 852-864.
200. Sugden, M.C., Lall, H.S., Harris, R.A., and Holness, M.J. (2000). Selective modification of the pyruvate dehydrogenase kinase isoform profile in skeletal muscle in hyperthyroidism: implications for the regulatory impact of glucose on fatty acid oxidation. *Journal of Endocrinology* **167**, 339-345.
201. Sykiotis, G.P. and Bohmann, D. (2008). Keap1/Nrf2 signaling regulates oxidative stress tolerance and lifespan in *Drosophila*. *Developmental Cell* **14**(1), 76-85.
202. Sysak, P.K., Foote, C.S., and Ching, T. (1977). Chemistry of singlet oxygen-XXV: Photooxygenation of methionine. *Photochemistry and Photobiology* **26**, 19-27.
203. Taylor, J.M., Main, B.S., and Crack, P.J. (2013). Neuroinflammation and oxidative stress: Co-conspirators in the pathology of Parkinson's disease. *Neurochemistry International* **62**(5), 803-819.
204. Tholey, A., Reed, J., and Lehmann, W.D. (1999). Electrospray tandem mass spectrometric studies of phosphopeptides and phosphopeptide analogues. *Journal of Mass Spectrometry* **34**, 117-123.
205. Thomas, P.D., Campbell, M.J., Kejariwal, A., Mi, H., Karlak, B., Daverman, R., Diemer, K., Muruganujan, A., Narechania, A. (2003). PANTHER: a library of protein families and subfamilies indexed by function. *Genome Research* **13**(9); 2129-2141.
206. Tosato, M., Zamboni, V., Ferrini, A., and Cesari, M. (2007). The ageing process and potential interventions to extend life expectancy. *Clinical Interventions in Ageing* **2**(3), 401-412.
207. Trachootham, D., Lu, W., Ogasawara, M.A., Valle, N. R-D., and Huang, P. (2008). Redox Regulation of Cell Survival. *Antioxidants & Redox Signaling* **10**(8), 1343-1374.
208. Traini, M., Quinn, C.M., Sandoval, C., Johansson, E., Schroder, K., Kockx, M., Meikle, P.J., Jessup, W., and Kritharides, L. (2014). Sphingomyelin phosphodiesterase-like 3A (SMPDL3A) is a novel nucleotide phosphodiesterase regulated by cholesterol in human macrophages. *Journal of Biochemical Chemistry* **289**(47), 32895-32913.
209. Tran, J.C. and Doucette, A.A. (2008) Gel-eluted liquid fraction entrapment electrophoresis: An electrophoretic method for broad molecular weight range proteome separation. *Analytical Chemistry* **80**, 1568-1573
210. Tveen-Jensen, K., Reis, A., Moulis, L., Pitt, A.R., and Spickett, C.M. (2013) Reporter ion-based mass spectrometry approaches for the detection of non-enzymatic protein modifications in biological samples. *Journal of Proteomics* **92**, 71-79.
211. Valko, M., Rhodes, C.J., Moncol, J., Izakovic, M., and Mazur, M. (2006). Free radicals, metals and antioxidants in oxidative stress-induced cancer. *Chemico-Biological Interactions* **160**, 1-40.
212. Van Buskirk, J.J., Kirsch, W.M., Kleyer, D.L., Barkley, R.M., and Koch, T.H. (1984). Aminomalonic acid: identification in *Escherichia coli* and atherosclerotic plaque. *Proceedings of the National Academy of Sciences of the USA* **81**(3), 722-725.
213. Vandecaetsbeek, I., Trekels, M., De Maeyer, M., Ceulemans, H., Lescrinier, E., Raeymaekers, L., Wuytack, F., and Vangheluwe, P. (2009). Structural basis for the high Ca²⁺ affinity of the ubiquitous SERCA2b Ca²⁺ pump. *Proceedings of the National Academy of Sciences of the USA* **106**(44), 18533-18538.
214. Vasilaki, A., Simpson, D., McArdle, F., McLean, L., Beynon, R.J., Van Remmen, H., Richardson, A.G., McArdle, A., Faulkner, J.A., Jackson, M.J. (2007). Formation of 3-

- nitrotyrosines in carbonic anhydrase III is a sensitive marker of oxidative stress in skeletal muscle. *Proteomics Clinical Applications* **1**(4), 362-372.
215. Verrastro, I., Pasha, S., Tveen Jensen, K., Pitt, A.R., and Spickett, C.M. (2015). Mass Spectrometry-Based Methods for Identifying Oxidized Proteins in Disease: Advances and Challenges. *Biomolecules* **5**(2), 378-411.
216. Viner, R.I., Williams, T.D., Schoneich, C. (2000). Nitric oxide-dependent modification of the sarcoplasmic reticulum Ca-ATPase: Localisation of cysteine target sites. *Free Radical Biology & Medicine* **29**(6), 489-496.
217. Voss, P., Engels, M., Strosova, M., Grune, T., and Horakova, L. (2008). Protective effect of antioxidants against sarcoplasmic reticulum (SR) oxidation by Fenton reaction, however without prevention of Ca-pump activity. *Toxicology In Vitro* **22**, 1726-1733.
218. Wellen, K.E. and Hotamisligil, G.S. (2005). Inflammation, stress, and diabetes. *The Journal of Clinical Investigation* **115**(5); 1111-1119.
219. Wellen, K.E., and Hotamisligil, G.S. (2005). Inflammation, stress and diabetes. *The Journal of Clinical Investigation* **115**(5), 1111-1119.
220. Winterbourn, C.C. (1985). Comparative reactivities of various biological compounds with myeloperoxidase-hydrogen peroxide-chloride, and similarity of the oxidant to hypochlorite. *Biochimica Biophysica et Acta* **889**, 277-286.
221. Wong, S.H., and Lord, J.M. (2004). Factors underlying chronic inflammation in rheumatoid arthritis. *Archivum Immunologiae et Therapiae Experimentalis* **52**(6), 379-388.
222. Xu, A., and Narayanan, N. (1998). Effects of aging on sarcoplasmic reticulum Ca²⁺-cycling proteins and their phosphorylation in rat myocardium. *American Journal of Physiology* **275**(6 Pt 2), H2087-2094.
223. Yan, L.J., and Sohal, R.S. (2002). Analysis of oxidative modification of proteins. *Current Protocols in Cell biology* **Chapter 7**, Unit 7.9.
224. Yan, L.J., Orr, W.C. and Sohal, R.S. (1998). Identification of oxidized proteins based on sodium dodecyl sulfate-polyacrylamide gel electrophoresis, immunochemical detection, isoelectric focusing, and microsequencing. *Analytical Biochemistry* **263**, 67-71.
225. Yan, L.-J. (2014). Positive oxidative stress in aging and aging-related disease tolerance. *Redox Biology* **2**; 165-169.
226. Yang, H., and Zubarev, R.A. (2010). Mass spectrometric analysis of asparagine deamidation and aspartate isomerization in polypeptides. *Electrophoresis* **31**(11), 1764-1772.
227. Yarnell, A. (2009). Cysteine oxidation. *Chemical & Engineering News* **87**(40), 38-40.
228. Ying, J., Clavreul, N., Sethuraman, M., Adachi, T., Cohen, R.A. (2007). Thiol oxidation in signalling and response to stress: Detection and quantification of physiological and pathophysiological thiol modifications. *Free Radical Biology & Medicine* **43**(8), 1099-1108.
229. Ying, J., Sharov, V., Xu, S., Jiang, B., Gerrity, R., Schöneich, C., and Cohen, R.A. (2008). Cysteine-674 Oxidation and Degradation of SERCA in Diabetic Pig Aorta. *Free Radical Biology & Medicine* **45**(6), 756-762.
230. Yu, Y.Q., Gilar, M., Kaska, J., and Gebler, J.C. (2005). A rapid sample preparation method for mass spectrometric characterization of n-linked glycans. *Rapid Communications in Mass Spectrometry* **19**, 2331-2336.

231. Zangar, R.C., Davydov, D.R., and Verma, S. (2004). Mechanisms that regulate production of reactive oxygen species by cytochrome p450. *Toxicology and Applied Pharmacology* **199**(3), 316-331.
232. Zhao, L.J., Guo, Y.F., Xiong, D.H., Xiao, P., Recker, R.R., and Deng, H.W. (2006). Is a gene important for bone resorption a candidate for obesity? An association and linkage study on the RANK (receptor activator of nuclear factor-kappaB) gene in a large Caucasian sample. *Human Genetics* **120**(4), 561-570.
233. Zhou, X., Mester, C., Stemmer, P.M., and Reid, G.E. (2014) Oxidation-induced conformational changes in calcineurin determined by covalent labeling and tandem mass spectrometry. *Biochemistry* **53**, 6754-6765.
234. Zhu, Chen and Subramanian, (2014). Comparison of Information-Dependent Acquisition, SWATH, and MSAll Techniques in Metabolite Identification Study Employing Ultrahigh-Performance Liquid Chromatography–Quadrupole Time-of-Flight Mass Spectrometry. *Analytical Chemistry* **86**(2), 1202-1209.

Appendices

Supplementary material

List of Figures

Figure S3.1. Sequence coverage attained by *in silico* digest of SERCA with trypsin and settings including cysteine residues treated with iodoacetamide

Figure S4.1. Blot probed with secondary antibody alone

List of Tables

Table S3.1. Mascot results of modifications detected in top 5 proteins hits in MH treated with HOCl and validated by *de novo* sequencing

Table S4.1. Mascot results of modifications detected in obese sample and validation by *de novo* sequencing

Figure S3.1. Sequence coverage attained by *in silico* digest of SERCA with trypsin and settings including cysteine residues treated with iodoacetamide. Mass of peptide covered ranges from 500-3000 Da.

10	20	30	40	50	60
MEAAHSKSTE	ECLSYFGVSE	TTGLTPDQVK	rHLEKYGPNE	LPAAEEGKSLW	ELVVEQFEDL
70	80	90	100	110	120
LVRillllaac	isfvlawfee	geetvtafve	pfvillilia	naivgvwqer	NAENAIEALK
130	140	150	160	170	180
EYEPKMGKvy	radrksvqri	karDIVPGDI	VEVAVGDKVP	ADIRILSIKS	TTLRVDQSIL
190	200	210	220	230	240
TGESVSVIKH	TDPVPDPRAV	NQDKkNMLFS	GTNIAAGKAV	GIVATTGVST	EIGkirDQMA
250	260	270	280	290	300
ATEQDKTPLQ	QKLDEFGEQL	SKvislicva	vmlinighfn	dpvhggswfr	GAIYYFKIAV
310	320	330	340	350	360
ALAVAAIPEG	LPAVITTCLA	LGTRrmakkN	AIVRSLPSVE	TLGCTSVICS	DKTGTTLTNQ
370	380	390	400	410	420
MSVCKMFIID	KVDGDVCSLN	EFSITGSTYA	PEGEVLKNDK	PVRAGQYDGL	VELATICALC
430	440	450	460	470	480
NDSSLDFNET	KGVYEKVGEA	TETALTTLVE	KMNVFNTQVR	slskverANA	CNSVIRQLMK
490	500	510	520	530	540
kEFTLEFSRd	rkSMSVYCSP	AKssrAAVGN	KMFVKGAPEG	VIDRCNYVRV	GTTRVPLTGP
550	560	570	580	590	600
VKekIMSVIK	EWGTGRDTRL	CLALATRDTP	PKrEEMVLDD	SAKFMEYEMD	LTFVGVVGMML
610	620	630	640	650	660
DPPRkEVTGS	IQLCRDAGIR	VIMITGDNKG	TAIAICRrIG	IFSENEEVD	RAYTGREFDD
670	680	690	700	710	720
LPLAEQReac	rrACCFARVE	PSHKskIVEY	LQSYDEITAM	TGDGVNDAPA	LKkAEIGIAM
730	740	750	760	770	780
GSGTAVAKTA	SEMVLADDNF	STIVAAVEEG	RAIYNNMKQF	IRylissnvg	evvcifltaa
790	800	810	820	830	840
lglpealipv	qllwvnlvtd	glpatalgfn	pplddimdrp	prspkEPLIS	GWLFFRymai
850	860	870	880	890	900
ggyvgaatvg	aaawwflyae	dgphvsyhql	thfmqctehn	pefdgldcev	feapepmtma
910	920	930	940	950	960
lsvlvtiemc	nalnslsenq	sllrmpwvvn	iwllgsicls	mslhflilyv	dplpmifklr
970	980	990			
ALDFTQWLMV	LKISLPVIGL	DELLKFIARN	YLEG		

Figure S4.1. Blot probed with secondary antibody alone. Molecular weight marker present in first lane.

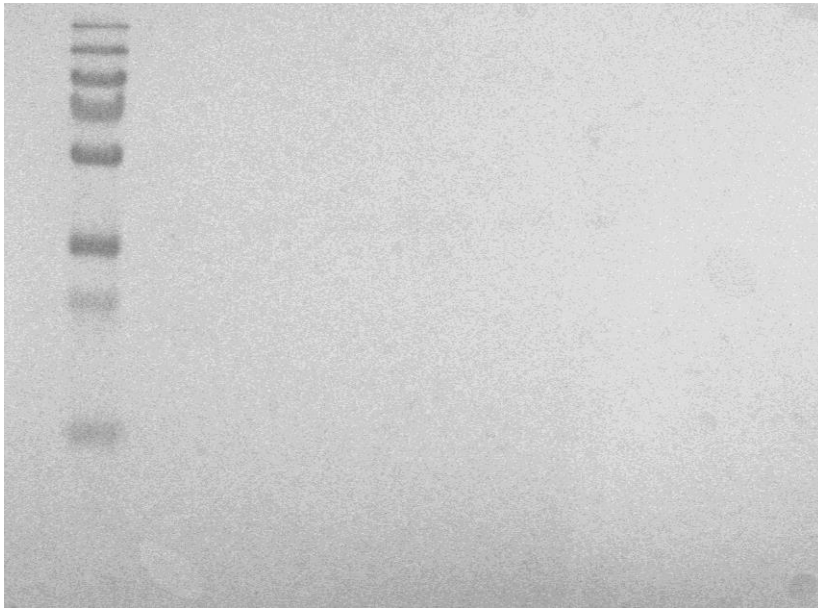


Table S3.1. Mascot results of modifications detected in top 5 proteins hits in MH treated with HOCl and validated by *de novo* sequencing. True positives are green, spectra that could not be sequenced are yellow, false positives that are deemed to be another modification are orange, and absolute false positives are red.

Protein	Modification	Sequence	Residue	Notes
Glycogen phosphorylase	Y ox	DYYFALAHTVR	Y53	Partially sequenced however cannot say if modification is present
	Y Cl	TLQNTMVNLALENACDEATYQLG LDMEELEEIEEDAGLGNGGLGR	Y114	False positive
	Y N C Triox	TLQNTMVNLALENACDEATYQLG LDMEELEEIEEDAGLGNGGLGR	Y114 C109	False positive
	Y N C Triox M ox	TLQNTMVNLALENACDEATYQLG LDMEELEEIEEDAGLGNGGLGR	Y114 C109 M100	False positive
	M ox C Triox Y ox M diox	TLQNTMVNLALENACDEATYQLG LDMEELEEIEEDAGLGNGGLGR	M100 C109 Y114 M120	False positive
	C Triox M diox	LAACFLDSMATLGLAAYGYGIR	C143 M148	False positive
	Y ox Y Cl	LAACFLDSMATLGLAAYGYGIR	Y156 Y158	False positive
	Y Cl	YEFGIFNQKICGGWQMEEADDWLR	Y162	Possibly a ClY?
	Y N K Ally C Triox	YEFGIFNQKICGGWQMEEADDWLR	Y162 K170 C172	Partially sequenced however cannot say if modifications are present
	M Diox	ICGGWQMEEADDWLR	M177	Sequenced and could potentially also be OxM and OxW at W175 and M177
	M Diox C Triox	ICGGWQMEEADDWLR	M177	False positive
	M ox Y N	WVDTQVVLAAMPYDTPVPGYR	M225 Y234	False positive
	M diox	WVDTQVVLAAMPYDTPVPGYR	M225	False positive
	Y ox	WVDTQVVLAAMPYDTPVPGYR	Y227	False positive
	K Ally	LWSAKAPNDFNLK	K248	Possibly an Allysine although MSMS spectra not great

P ox	VAIQLNDTHPSLAIP ELMR	P348	Unsure whether false positive or P ox
M Diox	VAIQLNDTHPSLAIP ELMR	M351	Sequenced and validated
P ox M Diox	VAIQLNDTHPSLAIP ELMR	P343 M351	False positive
C Triox Y ox	T C AYTNHTVLPEALER	C373 Y375	Sequenced from r to t. Possible that this is correct however Tyr immonium ion present with no mod
C Triox Y Cl	T C AYTNHTVLPEALER	C373 Y375	False positive
P ox	WPVHLMETLLPR	P389	Sequenced and validated
P ox M ox	WPVHLMETLLPR	P389 M393	Sequenced and validated (although MSMS of not great quality)
P ox	VAAAFPGDVDR	P420	After sequencing it is found to be Phe oxidation at F419
M Diox	MSLVEEGAVK	M429	Sequenced and validated
C Triox	INMAHLCIAGSHAVNGVAR	C446	Sequenced and validated
M ox C Triox	INMAHLCIAGSHAVNGVAR	M442 C446	Sequenced and validated
M Diox C Triox	INMAHLCIAGSHAVNGVAR	M442 C446	Not great quality MSMS but sequencing shows it may be modified with stated modifications
C Triox	RWLVL C NPGLAEVIAER	C496	Unsure of whether it is modified or not due to MSMS spectrum
P ox	RWLVL C NPGLAEVIAER	P498	False positive
C Triox	WLVL C NPGLAEVIAER	C496	Sequenced and validated
C Triox P ox	WLVL C NPGLAEVIAER	C496 P498	Possibly a false positive due to poor MSMS data
P ox	WLVL C NPGLAEVIAER	P498	Correct peptide but can't find modification
C Triox	QLLN C LHIITLYNR	C581	Sequenced and validated
Y ox	TIMIGGKAAPGYHMAK	Y614	False positive
M Diox Y N M ox P ox	TIMIGGKAAPGYHMAK	M616 Y614 M605 P612	False positive
Y Cl M Diox	AAPGYHMAK	Y614 M616	False positive
M Diox K Ally M ox Y ox	AAPGYHMAKMI IK	M616 K618 M619 Y614	False positive

	P ox	VIPAADLSEQISTAGTEASGTGNM K	P659	False positive
	M Diox	DIVNMLMHHDR	M767	After sequencing it is found to be His dioxidation at H768
	C Triox	VFADYEEYIKCQDK	C784	Sequenced and validated
SERCA	Y ox	STEECLSYFGVSETTGLTPDQVK	Y15	Possible Tyr ox but could also be Phe ox. Could not fully sequence to determine
	Y N P ox	HLEKYGPNELPAEEGK	Y36 P42	False positive
	K Ally Y N M ox P ox Y ox	EYEPENMGKVYR	K130 Y128 M126 P124 Y122	False positive
	Y Cl K Ally M ox C Triox	KSMSVYCSPAK	Y497 K492 M494 C498	False positive
	K Ally K Ally Y N M ox	KSMSVYCSPAK	K492 K502 Y497 M494	False positive
	K Ally M ox P ox C Triox	SMMSVYCSPAK	M494 C498 P500 K502	False positive
	M ox P ox Y ox	SMMSVYCSPAK	M494 Y497 P500	False positive
	K Ally Y N M ox C Triox	SMMSVYCSPAK	M494 Y497 C498 K502	False positive
	M Diox	AAVGNKMFVK	M512	False positive Actually peptide SFLVWVNEEDHLR (3+) from Creatine kinase M-type
	Y Cl	IVEYLQSYDEITAMTGDGVNDAPA LK.K	Y694	Couldn't find presence of ClY but found Met700 to be oxidised

	M Diox	TASEMVLADDNFSTIVAAVEEGR	M733	Cannot sequence to determine is modification is present
Transitional endoplasmic reticulum ATPase (TERA)	P Ox Y N P Ox K Ally	AVEFKVETDPSPYCIVAPDTVIH CEGEPIK	P172 Y173 P178 K190	False positive
	M ox P ox Y Cl C Triox	FGMTPSKGVLFYGPPEGCGK	M508 P510 Y517 C522	False positive
	M ox P ox Y Cl P ox	FGMTPSKGVLFYGPPGCGK	M508 P510 Y517 P520	False positive
	M Diox P ox Y Cl P ox	FGMTPSKGVLFYGPPGCGK	M508 P510 Y517 P520	False positive
	Y Cl P ox P ox	GVLFYGPPEGCGK	Y517 P519 P520	False positive
	Y ox	FPSGNQGGAGPSQGGGGTGG SVYTEDNDDDLYG	Y805	MS/MS spectra of poor quality
	Aconitate hydratase	M ox P ox Y ox	MAPYSLLVTRLQK	M1 P3 Y4
M Diox P ox Y ox		VAMSHFEPSEYIR	M34 P39 Y42	False positive
M ox M ox P ox K Ally		VAMQDATAQMAMLQFISSGLPK	M105 M107 P116 K117	False positive
M ox M ox P ox		VAMQDATAQMAMLQFISSGLPK	M105 M107 P116	False positive
Elongation factor	M ox K Ally	NMSVIAHVDH GKSTLTDSL VCK	M22 K42	False positive

K Ally P ox M ox M Diox M Ox	IKPVLMMNKMDR	K152 P153 M156 M157 M160	False positive
P ox	ALLELQLEPEELYQTFQR	P171	Unsure if Pro oxidation or unmodified Pro
Y N	QFAEMYVAK	Y232	False positive
Y N Y Ox P Ox P Ox M Ox K Ally	YRCELLYEGPPDDEAAMGIK	Y367 Y373 P376 P377 M383 K386	False positive
C Triox K Ally M Ox Y Ox	SCDPKGPLMMYISK	C388 K391 M395 Y397	False positive
K Ally	VFSGVVSTGLKVR	K426	False positive
K Ally	ARPPDGLAEDIDKGEVSAR	K619	False positive

Table S4.1. Mascot results of modifications detected in obese sample and validation by *de novo* sequencing. The table complements Figure 4.3. Full list of validated Mascot results are shown with peptide expect cut off at 0.05. UC = uncertain, FP = false positive, and TP = true positive.

Band	Protein ID	Protein description	Protein mass	Mass/ Charge (m/z)	Peptide score	Peptide expect	Peptide sequence	Modification	Validation
1	G3P_MOUSE	Glyceraldehyde-3-phosphate dehydrogenase	36072	749.0771,3+	45.27	0.0013	VIISAPSADAPMFVM GVNHEK	OxM; OxP	UC – possible Met ox
1	SYNE2_MOUSE	Nesprin-2	787997	421.2712,4+	45.34	0.007	AAKLSAELPADRPAP K	Ally; 3 OxP	FP
1	CB072_MOUSE	Uncharacterized protein C2orf72 homolog	30701	458.9465,4+	36.24	0.037	AQDGGVHIPPDPED TR	2 OxP	FP
1	GNDS_MOUSE	Ral guanine nucleotide dissociation stimulator	95226	406.2507,3+	34.02	0.039	HGASSTLPRMK	OxM; OxP	FP
1	PRKDC_MOUSE	DNA-dependent protein kinase catalytic subunit	476471	565.7887,4+	30.34	0.021	VMHYSLDIKNTCTSV YTK	CIY; DioxM; Ally; NitroY; TrioxC	FP
1	ECM29_MOUSE	Proteasome-associated protein ECM29 homolog	205398	571.9569,4+	26.26	0.047	IKPLGPMLLNGLTKLI NEYK	2 Ally; OxM; OxP	FP
1	ABCA2_MOUSE	ATP-binding cassette sub-family A member 2	272788	641.8777,4+	28.72	0.036	CTCSAQGTGFSCPS SVGGHPPQMR	OxP; 2 TrioxC	FP
1	K1B24_MOUSE	Kallikrein 1-related peptidase b24	29478	407.2217,3+	27.57	0.044	DKSNDLMLLR	Ally; OxM	TP
1	LTBP1_MOUSE	Latent-transforming growth factor beta-	195032	597.8776,4+	26.09	0.024	KQSYHGYYTQMMECL QGYK	Ally; 2 NitroY; 2	FP

		binding protein 1						OxM; OxY	
2	G3P_MOUSE	Glyceraldehyde-3-phosphate dehydrogenase	36072	524.7988,3+	56.22	0.00062	VPTPNVSVVDLTCR	OxP	TP
2	DLGP4_MOUSE	Disks large-associated protein 4	108940	588.3424,2+	51.69	0.005	TSATLDKSLLK	Ally	FP
2	K1B24_MOUSE	Kallikrein 1-related peptidase b24	29478	407.2259,3+	44.11	0.024	DKSNDLMLLR	Ally; OxM	TP
2	ECM29_MOUSE	Proteasome-associated protein ECM29 homolog	205398	571.9564,4+	39.31	0.021	IKPLGPMLLNGLTKLI NEYK	2 Ally; OxM; OxP	FP
2	ODC_MOUSE	Mitochondrial 2-oxodocarboxylate carrier	33322	686.3938,4+	38.32	0.011	LGPGGGVMLLVYEYT YAWLQENW	2 CIY; OxP	FP
2	MIIP_MOUSE	Migration and invasion-inhibitory protein	43428	747.095,2+	32.57	0.034	LFPEPVDPGAPCR	3 OxP; TrioxC	FP
2	CODA1_MOUSE	Collagen alpha-1(XIII) chain	73640	770.4245,3+	32.52	0.025	GKPGDMGPAGPQGP PGKDGPPGMK	DioxM; OxM; 2 OxP	FP
2	IL3_MOUSE	Interleukin-3	18757	965.5369,4+	30.04	0.034	FYMVHLNDLETVLTS RPPQPASGSVSPNR GTVEC	DioxM; NitroY; 2 OxP; TrioxC	FP
2	MARH5_MOUSE	E3 ubiquitin-protein ligase MARCH5	31781	671.3787,4+	29.37	0.032	ADPLFLLIGLPTIPVML ILGKMIR	DioxM; OxM	FP
2	LRTM1_MOUSE	Leucine-rich repeat and transmembrane domain-containing protein 1	39315	971.051,4+	29.03	0.043	MLNEGLCCGAWAMK GTLLLVS SVGLLLPG VGSCPMK	DioxM; OxM; 2 OxP; 2 TrioxC	FP
2	FUBP1_MOUSE	Far upstream element-binding	68668	777.3713,4+	26.36	0.034	KMGQAVPAPAGAPP GGQPDYSAAWAEYY	2 CIY; OxP; OxY	FP

		protein 1					R		
3	PYGB_MOUSE	Glycogen phosphorylase, brain form	97353	676.3401,3+	72.52	9.7E-06	KTCAYTNHTVLPEAL ER	CIY; Ally; TrioxC	UC – could not sequence
3	PYGB_MOUSE	Glycogen phosphorylase, brain form	97353	452.5715,3+	33.61	0.019	DYFFALAHTVR	OxY	FP
3	LECT1_MOUSE	Leukocyte cell-derived chemotaxin 1	37829	531.7884,4+	36.48	0.022	GNDNHIYNVHYSMSI NGK	NitroY; OxM	FP
3	INT7_MOUSE	Integrator complex subunit 7	108048	428.773,2+	39.55	0.031	LALSPSPR	OxP	FP
3	RSMB_MOUSE	Small nuclear ribonucleoprotein-associated protein B	23811	597.8643,4+	36.25	0.022	GTPMGMPPPGMRPP PPGMRGLL	2 DioxM; OxM; 4 OxP	FP
3	UAP1L_MOUSE	UDP-N-acetylhexosamine pyrophosphorylase-like protein 1	57319	515.2413,4+	34.59	0.013	LGVTYPKGMYQVGL PSQK	Ally; NitroY; OxM; 2 OxP	FP
3	CYTSB_MOUSE	Cytospin-B	118713	511.7001,3+	31.42	0.043	VTLEGLKMENGLK	Ally; OxM	FP
3	INT11_MOUSE	Integrator complex subunit 11	68541	744.0636,3+	31.1	0.048	VPIYFSTGLTEKANHY YK	2 CIY; Ally; OxP; OxY	FP
3	CTSRB_MOUSE	Cation channel sperm-associated protein subunit beta	127053	516.7991,4+	29.06	0.046	SVLIPGYSSFLIMNITD K	CIY; OxM; OxP	FP
3	COBA1_MOUSE	Collagen alpha-1(XI) chain	181548	711.4023,3+	26.04	0.036	GEAGPPGAAGPAGIK GPPGDDGPK	Ally; 4 OxP	FP
3	RGS9_MOUSE	Regulator of G-protein signaling 9	77499	614.876,4+	24.86	0.029	HPHRYVLDAAQTHIY MLMK	2 CIY; DioxM; OxM; OxP	FP
3	F262_MOUSE	6-phosphofructo-2-	60458	589.3372,4+	24.65	0.048	IECYKVITYQPLDPDN	CIY; Ally;	FP

		kinase/fructose-2,6-bisphosphatase 2					YDK	NitroY; OxP	
3	PTPRQ_MOUSE	Phosphatidylinositol phosphatase PTPRQ	257878	503.3252,4+	23.59	0.047	GGHTY N ISVYAINSA GAGPK	CIY	FP
3	TAOK1_MOUSE	Serine/threonine-protein kinase TAO1	116434	426.2518,3+	21.02	0.047	MS YSGKQ ST EK	Ally; OxM; OxY	FP
4	KPYM_MOUSE	Pyruvate kinase PKM	58378	836.781,3+	42.2	0.002	AEGSDVANAVLDGA DC IM LSGETAK	Ally; OxM	FP
4	KPYM_MOUSE	Pyruvate kinase PKM	58378	839.4425,3+	27.93	0.048	AEGSDVANAVLDGA DC IM LSGETAK	DioxM; TrioxC	FP
4	ALBU_MOUSE	Serum albumin	70700	956.1642,4+	31.44	0.0068	Y EATLEK CC AEAN PP AC YGTVLA E FQPLVE EPK	2 OxP; 2 OxY; 3 TrioxC	FP
4	SAPL1_MOUSE	Proactivator polypeptide-like 1	58905	421.7683,2+	40.38	0.046	AS P ISVPR	OxP	FP
4	SYNJ2_MOUSE	Synaptojanin-2	159578	455.5816,2+	39.24	0.0065	GL PP DHGGK	2 OxP	TP
4	LEG4_MOUSE	Galectin-4	36405	1120.177,4+	38.92	0.032	A YVP A PGY Q PT Y NPT L PYKR P IPGGLSVGM SV Y I Q GMAK	CIY; Ally; 3 NitroY; 7 OxP; OxY	FP
4	ADGB_MOUSE	Androglobin	189464	1140.19,4+	38.4	0.049	SMES Y P C Y QDEETKL AFADHTVNYAD Q P P NSWFIVFR	CIY; NitroY; 2 OxP; TrioxC	FP
4	SGT1_MOUSE	Protein SGT1 homolog	72064	483.2613,4+	28.98	0.041	Y K P A K GGV P A H MYG M T K	CIY; 3 Ally; 2 OxM; OxP; OxY	FP
4	CO5A1_MOUSE	Collagen alpha-1(V) chain	184248	480.9388,3+	28.9	0.032	E P A P T Q K P VEAAR	Ally; 3 OxP	FP apqvstptlve aar from serum albumin

4	TNR11_MOUSE	Tumor necrosis factor receptor superfamily member 11A	68460	469.2537,2+	27.54	0.047	DSFAGTAPR	OxP	TP
4	SUV3_MOUSE	ATP-dependent RNA helicase SUPV3L1, mitochondrial	87919	509.8125,3+	25.43	0.045	MSLPRCTLLWAR	OxM; OxP; TrioxC	FP
5	ENOA_MOUSE	Alpha-enolase	47453	594.8367,2+	33.56	0.024	IGAEVYHNLK	NitroY	FP
5	KCRS_MOUSE	Creatine kinase S-type, mitochondrial	47899	714.0618,4+	28.17	0.024	MTPSGYTLDQCIQTG VDNPGHPFIK	NitroY; OxM; OxP	UC
5	PGK1_MOUSE	Phosphoglycerate kinase 1	44921	456.2436,3+	33.88	0.016	AHSSMVGVNLPQK	Ally	FP
5	G3P_MOUSE	Glyceraldehyde-3-phosphate dehydrogenase	36072	524.7977,3+	39.4	0.0044	VPTPNVSVVDLTCR	OxP	TP
5	K1B24_MOUSE	Kallikrein 1-related peptidase b24	29478	602.3615,2+	50.16	0.003	DKSNDLMLLR	Ally	TP
5	SRRM2_MOUSE	Serine/arginine repetitive matrix protein	295521	449.779,2+	41.51	0.0062	VKTVISPR	Ally	FP
5	PTPS_MOUSE	6-pyruvoyl tetrahydrobiopterin synthase	16235	509.8174,2+	35.79	0.024	LLPVGALYK	NitroY	TP
5	UGDH_MOUSE	UDP-glucose 6-dehydrogenase	55482	381.7257,2+	32.4	0.034	MVEIKK	Ally; OxM	FP
5	FGD1_MOUSE	FYVE, RhoGEF and PH domain-containing protein 1	107552	504.2508,2+	34.94	0.04	YLILFNDRLLYCVPR	2 CIY; TrioxC	FP
5	ANKY2_MOUSE	Ankyrin repeat and MYND domain-containing protein 2	49712	1042.095,2+	31.29	0.016	CSVCKMVIYCDQTCQ K	DioxM; Ally; 3 TrioxC	FP

5	TMC7_MOUSE	Transmembrane channel-like protein 7	84423	496.7634,2+	30.64	0.048	ITSCGDSTCELCGYN QK	TrioxC	FP
5	PKP4_MOUSE	Plakophilin-4	132268	622.3748,2+	27.44	0.041	GLYPGSSKPSPIYISS YSSPAR	CIY; 2 NitroY; 3 OxP	FP
5	C1QR1_MOUSE	Complement component C1q receptor	71761	446.1723,2+	26.04	0.047	ESTMPPTTEMPSSPS GSK	OxM; OxP	FP
6	KCRM_MOUSE	Creatine kinase M-type	43246	624.3482,2+	40.07	0.0087	DLFDPPIQDR	OxP	UC – could either be oxP or oxF
6	KCRM_MOUSE	Creatine kinase M-type	43246	539.8088,2+	36.98	0.026	VLTPDLYNK	OxP	TP
6	ALDOA_MOUSE	Fructose-bisphosphate aldolase A	39787	603.3448,3+	34.52	0.0034	CPLLKPWALTFSYGR	Ally	TP
6	G3P_MOUSE	Glyceraldehyde-3-phosphate dehydrogenase	36072	898.4677,2+	60.29	0.00002 5	LISWYDNEYGYSNR	OxY	FP
6	G3P_MOUSE	Glyceraldehyde-3-phosphate dehydrogenase	36072	749.0779,3+	66.02	0.00014	VIISAPSADAPMFVM GVNHEK	OxM; OxP	FP
6	G3P_MOUSE	Glyceraldehyde-3-phosphate dehydrogenase	36072	599.2975,3+	27.73	0.03	LISWYDNEYGYSNR	OxY	FP – Correct sequence, wrong modification = oxW
6	KDM5A_MOUSE	Lysine-specific demethylase 5A	194944	520.2762,4+	35.93	0.0047	QGPDSPGQAPPPPF LMSYK	OxM; 3 OxP	FP
6	UBP33_MOUSE	Ubiquitin carboxyl-	104544	1064.627,4+	35.85	0.04	GLTGLKNIGNTCYMN	OxP; 2	FP

		terminal hydrolase 33					AALQALSNCPLTQF FLDCGGLAR	TrioxC	
6	DESP_MOUSE	Desmoplakin	335158	567.3073,2+	35.74	0.029	ALYKAISVPR	OxY	FP
6	TRA2A_MOUSE	Transformer-2 protein homolog alpha	32354	761.3902,4+	35.23	0.049	AHTPTPGIYMGRPTH SGGGGGGGGGGGGG GGGGGGGR	DioxM; 3 OxP	FP
6	MAST1_MOUSE	Microtubule-associated serine/threonine-protein kinase 1	171747	471.2377,4+	33.82	0.015	GLKEPVAQMPLMPD APR	DioxM	FP
6	VAV2_MOUSE	Guanine nucleotide exchange factor VAV2	101163	694.4076,3+	31.71	0.03	WMEQFEMAMSNIKP DK	2 DioxM; OxM; OxP	FP
6	SSRP1_MOUSE	FACT complex subunit SSRP1	81152	441.7799,4+	30.85	0.047	NMSGSLYEMVSRVM K	DioxM	FP
6	ENO4_MOUSE	Enolase-like protein ENO4	68380	862.9738,3+	29.66	0.033	HDQEQPSTFSMPLL MGSVLSCGK	DioxM; Ally; OxM; TrioxC	FP
6	PXDN_MOUSE	Peroxidasin homolog	167621	498.2523,4+	27.87	0.047	SGKPLLPFATGPPE CMR	Ally; OxM; OxP	FP
6	PTC1_MOUSE	Protein patched homolog 1	160711	529.2876,4+	25.81	0.041	VASGYLLMLAYACL MLR	NitroY; 2 OxM; TrioxC	FP
6	ST14_MOUSE	Suppressor of tumorigenicity 14 protein homolog	96875	642.8141,3+	24.88	0.032	CQNGLCLSKGNPEC DGK	OxP; 3 TrioxC	FP
6	MOFA1_MOUSE	MORF4 family-associated protein 1	14185	389.7237,2+	24.43	0.038	IEKSESS	Ally	FP
7	TPIS_MOUSE	Triosephosphate isomerase	32684	809.9998,2+	31.79	0.048	VVLAYPEVWAIGTGK	OxY	FP
7	CAH3_MOUSE	Carbonic anhydrase 3	29633	926.5382,3+	36.7	0.013	SLFSSAENEPVPLV GNWRPPQPVK	2 OxP	FP
7	CAH3_MOUSE	Carbonic	29633	653.6678,3+	32.8	0.019	HDPSLQPWSASYDP	OxP	FP

		anhydrase 3					GS AK		
7	ALDOA_MOUSE	Fructose-bisphosphate aldolase A	39787	1129.621,3+	92.63	0.00000 2	ALANSLACQGKYTPS GQSGAAASESLFISN HAY	OxY	TP
7	ALDOA_MOUSE	Fructose-bisphosphate aldolase A	39787	1129.618,3+	62.03	0.0023	ALANSLACQGKYTPS GQSGAAASESLFISN HAY	Ally; OxY	UC
7	PGAM2_MOUSE	Phosphoglycerate mutase 2	28980	688.8443,2+	58.38	0.00008 8	SFDTPPPPMDEK	OxP	FP
7	G3P_MOUSE	Glyceraldehyde-3-phosphate dehydrogenase	36072	749.0803,3+	47.49	0.0057	VIISAPSADAPMFVM GVNHEK	OxM; OxP	UC
7	G3P_MOUSE	Glyceraldehyde-3-phosphate dehydrogenase	36072	524.7943,3+	40	0.033	VPTPNVSVVDLTCR	OxP	TP
7	LITD1_MOUSE	LINE-1 type transposase domain-containing protein 1	88705	812.9937,4+	42.18	0.0033	IGMPCLTLYLTSPSES LGAGSDGPKSHSCT K	Ally; OxP; 2 TrioxC	FP
7	FR1L4_MOUSE	Fer-1-like protein 4	225120	761.4287,4+	36.4	0.05	AQDFQVGVTVLEAQ KLVGVNINPYVAVR	Ally; OxY	FP
7	FXYD4_MOUSE	FXYD domain-containing ion transport regulator 4	9548	592.8933,4+	35.66	0.048	THKPSSLPGKATPLII PGSANTC	2 Ally; 2 OxP; TrioxC	FP
7	ZEP1_MOUSE	Zinc finger protein 40	291073	494.6153,4+	33.91	0.027	MLSPANSLDIAMEKH QK	DioxM; 2 Ally; OxM; OxP	FP
7	SOX14_MOUSE	Transcription factor SOX-14	26669	454.2667,4+	33.59	0.041	YVFPLPYLGDTDPLK	Ally; NitroY; 2 OxP	FP
7	SSRP1_MOUSE	FACT complex subunit SSRP1	81152	441.7835,4+	33.29	0.04	NMSGSLYEMVSRVM K	DioxM	FP

7	SRRM2_MOUSE	Serine/arginine repetitive matrix protein 2	295521	449.78,2+	29.7	0.045	VKTVISPR	Ally	FP
7	M3K7_MOUSE	Mitogen-activated protein kinase kinase kinase 7	64928	570.3024,4+	31.34	0.017	ESMAVFEQHCKMAQ EYMK	Ally; 2 OxM	FP
7	TET3_MOUSE	Methylcytosine dioxygenase TET3	182147	492.2576,4+	30.72	0.016	KPPTPAGGPVGAEKT TPGIK	Ally; 4 OxP	FP
7	OLA1_MOUSE	Obg-like ATPase 1	44929	542.3251,4+	29.42	0.038	HLFLTSPKPMVYLVNL SEK	CIY; 2 Ally; OxM	FP
7	F262_MOUSE	6-phosphofructo-2-kinase/fructose-2,6-bisphosphatase 2	60458	589.5749,4+	28.86	0.018	IECYKVTYQPLDPDN YDK	CIY; NitroY; OxP	FP
7	CO4A4_MOUSE	Collagen alpha-4(IV) chain	166046	470.5653,4+	26.75	0.045	GAPGPPGGPPGQPGE NGEKGR	4 OxP	FP
7	EPHA3_MOUSE	Ephrin type-A receptor 3	111652	472.2629,3+	26.14	0.041	VVGAGEFGVEVCSGR	TrioxC	FP
7	GOLM1_MOUSE	Golgi membrane protein 1	44470	734.9005,4+	25.77	0.02	GIINVPGSERQSHIL NQVGIHIPQQA	2 OxP	FP
7	CPNE2_MOUSE	Copine-2	61681	799.944,4+	25.08	0.046	ITRPLLLMNDKPAGK GVITIAAQELSDNR	DioxM; 2 Ally; 2 OxP	FP
7	SAHH2_MOUSE	Putative adenosylhomocyste inase 2	59997	512.2607,3+	22.43	0.04	NGPFKPNYYRY	3 CIY; Ally; OxP	FP
8	GSTP1_MOUSE	Glutathione S-transferase P 1	23765	608.9556,3+	85.04	4.3E-07	EAAQMDMVNDGVED LR	DioxM	TP
8	G3P_MOUSE	Glyceraldehyde-3-phosphate dehydrogenase	36072	749.0818,3+	56.93	0.0015	VIISAPSADAPMFVM GVNHEK	OxM; OxP	FP
8	G3P_MOUSE	Glyceraldehyde-3-phosphate dehydrogenase	36072	524.7956,3+	32.72	0.018	VPTPNVSVVDLTCR	OxP	UC – may be a OxThreonin

									e
8	PRDX1_MOUSE	Peroxiredoxin-1	22390	826.9895,2+	38.63	0.0054	QGGLGPMNIPLISDP K	OxP	UC – possible OxM
8	DLGP4_MOUSE	Disks large-associated protein 4	108940	588.3465,2+	40.78	0.021	TSATLDKSLLK	Ally	FP
8	INT7_MOUSE	Integrator complex subunit 7	108048	428.7752,2+	36.78	0.046	LALSPSPR	OxP	FP
8	SRRM2_MOUSE	Serine/arginine repetitive matrix protein 2	295521	449.7827,2+	33.42	0.028	VKTVISPR	Ally	FP
8	NR4A1_MOUSE	Nuclear receptor subfamily 4 group A member 1	66009	366.6475,3+	29.57	0.039	AHLDSGPSTAK	Ally; OxP	FP
8	NPRL3_MOUSE	Nitrogen permease regulator 3-like protein	64148	455.1785,4+	29.26	0.037	RMTENLLASLSEHER	DioxM	FP
8	CMC1_MOUSE	Calcium-binding mitochondrial carrier protein Aralar1	74922	632.367,3+	28.05	0.043	VSALNVLQDLGLFGL YK	NitroY	FP
8	BCL9L_MOUSE	B-cell CLL/lymphoma 9-like protein	156978	478.2504,4+	27.33	0.029	GLSMSMCHPGQMSL LGR	DioxM; OxM	FP
8	SPIT1_MOUSE	Kunitz-type protease inhibitor 1	58322	526.1954,3+	24.63	0.05	CARFTYGGCYGNK	2 OxY; TrioxC	FP
9	PPIA_MOUSE	Peptidyl-prolyl cis-trans isomerase A	18131	674.864,3+	52.22	0.0023	VNPTVFFDITADDEPL GR	OxP	UC
9	GAS8_MOUSE	Growth arrest-specific protein 8	56400	637.3712,2+	44.53	0.0063	AEGTVVMKLAQK	Ally	FP
9	TENA_MOUSE	Tenascin	237304	414.7694,2+	58.19	0.0021	AVDIPGLK	OxP	FP

9	GAS6_MOUSE	Growth arrest-specific protein 6	76500	703.924,4+	41.19	0.0024	GGLKLSPDMDTCEDI LPCVPFSMAK	DioxM	FP
9	RRP5_MOUSE	Protein RRP5 homolog	209302	527.2703,4+	38.93	0.031	GLVPSMHLADIMMKN PEK	2 DioxM; Ally; OxM; OxP	FP
9	SPR2H_MOUSE	Small proline-rich protein 2H	12852	926.4984,3+	38.55	0.043	CPEPCPPPKCTEPCP PPSYQQK	2 Ally; 8 OxP; OxY; 2 TrioxC	FP
9	MIIP_MOUSE	Migration and invasion-inhibitory protein	43428	747.711,2+	36.6	0.022	LFPEPVDPGAPCR	3 OxP; TrioxC	FP
9	INT7_MOUSE	Integrator complex subunit 7	108048	428.7746,2+	36.1	0.047	LALSPSPR	OxP	FP
9	IMPG2_MOUSE	Interphotoreceptor matrix proteoglycan 2	139099	362.1709,4+	33.74	0.037	HPDSLSSVENAMK	DioxM; Ally	FP
9	GFI1B_MOUSE	Zinc finger protein Gfi-1b	38103	417.9292,4+	33.01	0.035	SHSGTRPFACDVCG K	Ally; TrioxC	FP
9	SH2B2_MOUSE	SH2B adapter protein 2	67257	513.2802,4+	29.5	0.031	SSPEPDGGATPKAAE PASEPR	Ally	FP
9	SHRM4_MOUSE	Protein Shroom4	165475	638.3306,4+	28.94	0.02	ASEPVDSLQKEKPG LETVLPPR	Ally; 4 OxP	FP
9	SOCS4_MOUSE	Suppressor of cytokine signaling 4	50855	351.6202,4+	27.97	0.047	NCSGRHSPGLPSK	OxP; TrioxC	FP
9	CRIS2_MOUSE	Cysteine-rich secretory protein 2	28499	962.0521,4+	26.43	0.049	IGCGIAYCPNQDNLK YFYVCHYCPMGNNV MK	2 DioxM; Ally; OxP; OxY; 4 TrioxC	FP
10	HBB1_MOUSE	Hemoglobin subunit beta-1	15944	645.8925,2+	36.88	0.027	LLVVYPWTQR	OxP	Correct sequence, wrong modificatio

									n = OxW
10	HXA4_MOUSE	Homeobox protein Hox-A4	30733	425.5849,3+	46.87	0.001	EPVVYPWMKK	2 Ally	FP
10	FABPH_MOUSE	Fatty acid-binding protein, heart	14810	467.2353,4+	32.99	0.035	NFDDYMKSLGVGFA TR	NitroY	FP
10	SAPL1_MOUSE	Proactivator polypeptide-like 1PE=1 SV=2	58905	421.7665,2+	41.7	0.016	ASPISVPR	OxP	FP
10	PI51A_MOUSE	Phosphatidylinositol 4-phosphate 5-kinase type-1 alpha	60789	454.2575,4+	36.83	0.027	FYGLYCVQAGGKNIR	2 CIY	FP
10	PI51A_MOUSE	Phosphatidylinositol 4-phosphate 5-kinase type-1 alpha	60789	454.2652,4+	36.28	0.034	FYGLYCVQAGGKNIR	CIY; Ally; NitroY; TrioxC	FP
10	K1B24_MOUSE	Kallikrein 1-related peptidase b24	29478	602.3633,2+	39.68	0.036	DKSNLMLLR	Ally	FP
10	SEM3A_MOUSE	Semaphorin-3A	89840	466.7076,4+	38.83	0.019	EMSSSMTPSQKVWY R	DioxM; Ally; OxP	FP
10	SRRM2_MOUSE	Serine/arginine repetitive matrix protein	295521	449.7815,2+	33.48	0.025	VKTVISPR	Ally	FP
10	IRS2_MOUSE	Insulin receptor substrate 2	137876	857.4639,3+	34.12	0.029	SGGPNSCKSDDYMP MSPTSVSAPK	2 OxM; 2 OxP; OxY; TrioxC	FP
10	FAT3_MOUSE	Protocadherin Fat 3	505005	477.7163,3+	32.62	0.0052	IKAYDADSGFNGK	NitroY	FP
10	BCAS1_MOUSE	Breast carcinoma-amplified sequence 1 homolog	67793	486.7292,4+	26.63	0.025	DPSEHGALPVAAAAPG QAPDK	OxP	FP
10	PRRX2_MOUSE	Paired mesoderm homeobox protein 2	26524	788.9577,4+	25.72	0.042	MDSAAAAFALDPPAP GPGPPPAPGDCAQA RK	DioxM; 8 OxP; TrioxC	FP